DISSERTATION

Assessment and Allocation of Operational Flexibility in Power Systems with Distributed Resources

Submitted at the Faculty of Electrical Engineering and Information Technology, Technische Universität Wien in partial fulfillment of the requirements for the degree of Doktor der technischen Wissenschaften (equals Ph.D.)

under supervision of

Prof. Dipl.-Ing. Wolfgang Gawlik
Institut number: E370
Institute of Energy Systems and Electrical Drives
Technische Universität Wien

Co-supervised by

Prof. Dipl.-Ing. Peter Palensky
Department of Electrical Sustainable Energy
Delft University of Technology

by

Sohail Khan
Matr.Nr. 1328699
Längenfeldgasse 22/16, 1120, Vienna, Austria

June, 2016.

Kurzfassung

Das elektrische Energiesystem ist derzeit in einem Übergang begriffen, der durch das Aufkommen von umweltfreundlichen Erzeugungs- und Verbrauchertechnologien gekennzeichnet ist. Wesentlich dabei ist der steigende Anteil erneuerbarer Energien (engl. renewable energy resources, RES), wie beispielsweise Wind- und Solarenergie. Dieser Übergang führt allerdings zu kritischen Situationen im operativen Bereich, in erster Linie aufgrund der Prognoseunsicherheit im Zusammenhang mit Strom aus erneuerbaren Energiequellen. Daher wird eine erhöhte Flexibilität benötigt, um das Ungleichgewicht zwischen Angebot und Nachfrage in Zukunft bewältigen zu können. Ein hoher Anteil dieser RES ist direkt in die elektrischen Verteilnetze eingebunden, was innovative Ansätze in der Netzplanung erforderlich macht. Ansätze basierend auf aktivem Monitoring und Steuerung können die notwendige Unterstützung für den Umgang mit Flexibilität von Ressourcen bieten, um Prognoseunsicherheiten und andere Herausforderungen bewältigen zu können. Solche Ansätze können allgemein in zwei Kategorien eingeteilt werden: Microgrids bieten die Möglichkeit des unabhängigen Systembetriebs, wohingegen Anwendungen, die einen Anschluss an eine höhere Netzebene voraussetzen, als zellbasierte Ansätze klassifiziert werden.

Betreiber von Microgrids führen für die Planung der Reserven eine Beurteilung der Flexibilität durch, bei der unter Zuhilfenahme von modellbasierten Vorhersagen die mit der Gesamtnachfrage verknüpfte Unsicherheit prognostiziert wird. Die vorliegende Arbeit zielt darauf ab, diesen Prozess durch die Modellierung der Unsicherheit, auf Basis ihrer zugrundeliegenden Dynamik, sowohl wirtschaftlich als auch technisch zu erleichtern. Zu diesem Zweck wurden die dynamischen Variablen erster Ordnung berücksichtigt: Leistung, Rampensteigung und Rampendauer. Es wurde festgestellt, dass die Verwendung einer kompakten, geometrischen Hülle für die tatsächlich realisierten Werte dieser Variablen bei der Erstellung einer solchen Bewertung eine Verringerung der Reserveanforderungen gestattet. Das wiederum erlaubt einen wirtschaftlicheren Planungsansatz. In diesem Zusammenhang wurde für die Modellierung des Arbeitsbereichs der Generatoren im Betrieb ein Variablenraum verwendet, der von denselben dynamischen Variablen aufgespannt wird. Mit Hilfe dieser Formulierung wurde der Planungsprozess für die notwendigen Reserven in ein geometrisches Zuordnungsproblem überführt. Um dieses Problem zu lösen wurde ein neuer Algorithmus entwickelt. Abgesehen von den Generatoren können damit potenziell auch andere Ressourcen für die Bereitstellung von Flexibilität herangezogen werden, beispielsweise steuerbare Lasten oder Stromspeicher. Ein vereinheitlichtes Modell für derartige Ressourcen erleichtert deren Aggregation und das Zuteilungsverfahren. Die Flexibilität von Wärmeerzeugern und das Energiespeicherpotential von thermostatisch geregelten Lasten (engl. thermostatically controlled loads, TCL) konnte anhand dieses Modells demonstriert werden. Dabei wurde gezeigt, dass solche TCLs aufgrund ihrer Fähigkeit die Energie im Betrieb vorübergehend zu speichern besonders interessant sind. Das Speicherpotential für TCL-basierte Aggregation wurde mithilfe eines stochastischen Batteriemodells dargestellt und für Frequenzregelung eingesetzt. Analytische Gleichungen wurden abgeleitet, um die entsprechenden Batterieparameter zu berechnen. In zwei Beispielen konnte dargestellt werden, wie nachfrageseitige Flexibilität (engl. demand response) als Reserveressource eingesetzt werden kann. Im ersten Beispiel wurde anhand der Steuerung einer großen Anzahl von TCLs, die in dieser Form typischerweise in Wohngebieten vorzufinden sind (z.B. Klimaanlagen), das Batteriemodell validiert. Im zweiten Beispiel wurden mithilfe eines Ansatzes zur Simulationskopplung die Auswirkungen der Flexibilitätsaktivierung im elektrischen Netzwerk studiert.

Bisherigen Untersuchungen bezüglich der Abschätzung von Flexibilität basierten auf der Verwendung von Intervallen zur Darstellung der Unsicherheit. Die vorliegende Arbeit geht

einen Schritt weiter und verwendet Korrelationen in der Systemdynamik für die Modellierung einer geometrischen Hülle. Dadurch werden die Gesamtreserveanforderungen in Microgrids basierend auf der Prognoseunsicherheit definiert. Die vorgeschlagene Methode für Reserveplanung wurde für Testfälle auf der Mittelspannungsebene durchgeführt, allerdings sind sie auch ohne Beschränkung der Allgemeinheit in anderen Anwendungsgebieten einsetzbar. Die Anforderungen aus der Reserveplanung wurden außerdem in Anwendungen zur Systembetriebsoptimierung (unit commitment, economic dispatch) verwendet. Darüber hinaus wurde ein Ansatz basierend auf evolutionärer Spieltheorie bezüglich der Tauglichkeit im Bereich der Systembetriebsoptimierung (economic dispatch) untersucht. Die potenziellen Vorteile und Grenzen dieses Ansatzes werden in der folgenden Arbeit ebenfalls aufgezeigt.

Abstract

The electric power system of the present era is in transition towards a future characterized by the environment friendly generation and consumption technologies. Among them is the rising share of Renewable Energy Sources (RES) such as wind and solar energy in the electricity network. This transition has resulted in critical operational challenges primarily due to forecast uncertainty associated with the power from RES. As a result, more flexibility shall be required to deal with demand and supply imbalances in the future. A high share of RES is connected to the distribution networks, thus motivating a need to revisit the distribution network planning and operational practices. An active monitoring and control strategy within the distribution system can provide support against forecast uncertainty and network challenges by handling flexibility offered by the distributed resources. Such local control applications can potentially perform resource scheduling in meeting the local flexibility requirements and provide flexibility services to the connected grid. The control approaches can be classified generally into two categories. The "microgrid" based control enables the independent system operation while the applications designed for only grid connected state can be classified as "cell" based approaches.

The microgrid operator performs flexibility assessment by modeling the uncertainty associated with the overall demand and use it to schedule the reserves. The dissertation aimed to facilitate this process both economically and technically by considering the uncertainty dynamics. For this purpose, the first order dynamical variables of power, ramp-rate and ramp duration were considered. A compact envelope enclosing the uncertain net-demand dynamics in microgrid was found as more economic approach than the state of the art interval based method. The dynamic capability of generators was modeled by a space using the same dynamical variables. This formulation transformed the reserve planning process into a space allocation problem. It has been solved by a novel algorithm of flexibility allocation. Along with the generators, the potential flexibility resources can be of diverse types such as controllable loads, electricity storage and others. A common flexibility model for such resources was proposed that aimed to facilitate the flexibility aggregation and allocation processes. It represented both the energy storage potential and the dynamic capability of a resource. The flexibility of thermal generators and energy storage potential of Thermostatically Controlled Loads (TCLs) have been presented using this model. The TCLs propose an interesting potential due to their ability to temporarily store the energy during operation. The energy storage ability of a TCL aggregation was modeled by a stochastic battery and used in the frequency regulation process. Analytic equations have been derived for calculating the battery parameters. Two test cases have been presented exploring the demand side flexibility as a reserve resource. In the former, a control strategy for a large number of residential TCLs validated the proposed battery model, while in later, a combined simulation framework was developed to study the impact of flexibility activation on the distribution network.

Prior research on the flexibility assessment have used an interval based approach to represent the uncertainty dynamics. This dissertation advanced it by modeling the correlation in uncertainty dynamics by an envelope. It defined the reserve requirements in microgrid based on the forecast uncertainty. The methods for reserve planning have been performed for a medium voltage microgrid test case, however, they can be extended to other related applications in power system without loss of generality. The reserve requirements were used in the unit commitment and economic dispatch applications. In addition, an evolutionary game theory based approach has been explored for the unit commitment problem. Its potential benefits and limitations were discussed.

Acknowledgments

I would like to thank my supervisor Wolfgang Gawlik who gave me an opportunity to write this PhD thesis, for his supervision of research work, patience with the manuscripts and his excellent guidance throughout the process.

I am grateful to Austrian Institute of Technology for supporting and providing me with a broad research platform. Specifically, i would like to thank Peter Palensky for allowing me to work at the Complex Energy Systems research group and his guidance. I am heartily thankful to all members of the group, specially to Hadrien Bosetti for his guidance, encouragement and scientific discussions, Edmund Widl and Wolfgang Hribernik for their support. I am glad to mention my peers Jawad Haider Kazmi, Ishtiaq Ahmed, Aadil Latif, Simon Montgomery, Ikramullah, Mohsin Shahzad, Usman Habib and Wolfgang Müller with whom i had interesting discussions and pleasant time. I also like to thank Shahid Iqbal for the memorable time spent in the Austrian alps that refreshed and kept me going.

I like to express heartily gratitude to my family who made the foundations of my career, for their prayers and encouragement. I am glad to mention my life partner for her encouragement and ongoing support.

Table of Contents

List of Figures

List of Tables

List of Acronyms

AGC	Automatic Generation Control
AS	Ancillary Services
BRP	Balance Responsible Party
CAISO	California Independent System Operator
CHP	Combined Heat and Power
CIGRE	International Council on Large Electric Systems
DER	Distributed Energy Resources
DG	Distributed Generator
DMS	Distribution Management System
DNO	Distribution Network Operator
DSM	Demand Side Management
eCDF	empirical Cumulative Distribution Function
ED	Economic Dispatch
EMS	Energy Management System
EPS	Electric Power System
ERWH	Electric Resistance Water Heaters
ESM	Energy Storage Model
EUE	Expected Unserved Energy
EV	Electric Vehicle
FCR	Frequency Containment Reserve
FCU	Feeder Control Unit
FRR	Frequency Restoration Reserve
HPWH	Heat Pump Water Heaters
HV	High Voltage
HVAC	Heating Ventilation and Air Conditioning
HVDC	High Voltage DC
IEEE	Institute of Electrical and Electronics Engineers
LCU	Load Control Unit
LOLE	Loss of Load Expectation
LOLH	Loss of Load Hours
LTC	Load Tap Changing
LV	Low Voltage
MCP	Market Clearing Price
MF	Membership Function

MV	Medium Voltage
NA	Newton's Approach
NERC	National Electric Reliability Corporation
NGC	Net Generation Capacity
OPF	Optimal Power Flow
PDF	Probability Distribution Function
PDIPM	Primal Dual Interior Point Method
PNNL	Pacific Northwest National Laboratory
PV	Photo Voltaic
RAC	Reliable Available Capacity
RCE	Resource Capability Envelope
RCU	Resource Control Unit
RD	Replicator Dynamics
RES	Renewable Energy Sources
RFM	Resource Flexibility Model
RR	Replacement Reserve
SCED	Security Constrained Economic Dispatch
SCUC	Security Constrained Unit Commitment
SDA	Swinging Door Algorithm
SDP	Semi-Definite Programming
SoC	State of Charge
TCL	Thermostatically Controlled Load
TPM	Transition Probability Matrix
TSO	Transmission System Operator
UC	Unit Commitment
UnC	Unavailable Capacity
USEF	Universal Smart Energy Network
VAR	Volt-Ampere Reactive

1 Introduction

Historically, large power generation units are preferred in the power system due to favorable economics. Most of the major power producing units are either fossil fuel based, hydro-power or nuclear power plants. Despite their economic advantages and favored centralized control, the major issues associated are environmental impacts, transmission and distribution cost & losses. Since few decades, there is a global drive to support the environmentally friendly energy production from Renewable Energy Sources (RES) and improving efficiency of electricity consumption. The driving force for this change are the environmental concerns. Other reasons vary for each region and can be the lack of conventional fuel resources, economy and others. There is also a strong interest in improving the reliability of electricity supply in order to decrease the probability for loss of power due to unforeseen events. Various countries and regions have set ambitious targets for increasing share of energy generation from RES like wind and solar, improving efficiency in generation and consumption & de-carbonization. The result of these activities have led to a drastic increase in the power production from RES. In Europe, Germany has the highest share of installed capacity from RES reaching to 61 Gigawatt (GW) in comparison to 12.9 GW in France, 21.3 GW in Italy and 9.3 GW in Great Britain.

Traditionally bulk power generation has been connected to the transmission network at the ultra-high and high voltage levels. The substations at transmission level steps up the voltage that reduces the losses during bulk energy transfer over long distances. The voltage is then stepped down at distribution substations. Service transformers directs the flow of active power from substation to the customer service delivery points. The advent of RES in the power system has impacted upon all voltage levels in the power system operation. An increasing number of on-shore and off-shore wind farms and solar energy sources are connected to the high (ultra-high) voltage levels. Last decades have also experienced a consistent increase in RES based generation at the residential levels. Bulk of RES is connected to the Medium Voltage (MV) and Low Voltage (LV) distribution networks due to the distributed nature of energy source and their relatively smaller ratings [1]. In Germany, approximately 90% of the total renewable energy based generation is connected to the distribution networks [2]. Due to the distributed nature of such resources, they are commonly termed as Distributed Energy Resourcess (DERs) or Distributed Generators (DGs). According Electric Power Research Institute (EPRI), the DGs are defined as smaller wide spread power sources that can be aggregated to support energy demand. The DGs can also include electricity storage, Combined Heat and Power (CHP) and micro-turbines.

The aggregate impact of DGs on the distribution system can be classified into four main areas; protection systems, fault handling services, network voltage and the frequency. The distribution system has been traditionally designed for unidirectional power transfer considering the top-down hierarchy of the energy market. However, the distributed generation has led to the reverse power flows. The traditional DGs had generally led to uni-directional power flow and had been dedicated for serving particular customers. Hence, both the distribution system protection and the Volt/VAR control were not effected. In those systems, the reverse power flow rarely occurred and when it happened it could be predicted and the impact was on small part of feeder. The growing percentage of DGs have led to an increasing number of and high levels of reverse power flows that impacts the operation of classical protection system. The mismatch between demand and supply resulting from the forecast uncertainty is supported by reserve power in the system. The requirement of reserves shall increase with the rise of RES and the failure in their timely activation can leads to the frequency problems. Similarly, when the demand is low and generation from RES in high, the network experiences a rise in the voltage levels, that can violate the voltage limit constraints.

1.1 Motivation

The distribution network challenges have hindered the rise in distributed generation from RES. It has encouraged the need for an active monitoring and control setup for distributed generation. The forecast accuracy of power from distributed generation needs to be improved in order to reduce the load-generation imbalance and hence the reserve requirements. The distributed resources can offer flexibility in providing reserve against the potential imbalances in the system. A mechanism is required to model the flexibility from diverse resource types, deal with their distributed nature and manage their impacts on the network operations. Such planning and control efforts needs to be frequently updated to manage the volatility of generation from RES and changing network conditions. Due to large number of nodes in the distribution network, there is a strong motivation for implementing a local control mechanism. Among its objectives is to maintain reserves for dealing with the voltage and frequency problems. This strategy can potentially decrease the impact of local uncertainty on the power system operation. The local control in the distribution network can potentially provide service to the critical loads in case of disconnection from the network. It will increase the reliability of the system in dealing with emergency situations.

With the increase in reliance on power generation from green energy, reserves shall play a crucial role in ensuring the critical balance of demand and supply. In the power system planning, there exists methods that assess the flexibility requirements and capability of the system in enduring and supporting the uncertain nature of demand and supply. The objective of such methods is to ensure the generation adequacy in the system. Generation adequacy is defined as the ability of power system to meet the demand under all possible loading conditions. The generation adequacy needs to be maintained while satisfying all network constraints. It is ensured by scheduling and operating generators in meeting the changing demand on monthly, daily, hourly and minute basis. The process takes into consideration the fluctuating renewable energy output and unavailability of resources due to faults and maintenance operations.

1.1.1 Generation Adequacy Requirements

The generation adequacy trend can be assessed by the Net Generation Capacity (NGC). It is the total installed capacity that is the sum of Reliable Available Capacity (RAC) and Unavailable

Capacity (UnC). The UnC is composed of capacity unavailable due to maintenance and overhauls, system reserve, outages and non-usable capacity. The part of RAC is allocated to meet the demand and rest of it is reserved to meet the peak loading conditions. For Europe, the NGC is anticipated to increase from 1021 GW in 2016 to 1167 GW in 2025. However, the RAC increases marginally from 602 to 611 GW as can be seen in Figure 1.1. Unavailable capacity is related to RES based generation as the primary source of energy having limited availability. The increase in net generation capacity over the next decade shall be contributed by 94% from unavailable capacity. A greater portion of the UnC is contributed by the un-usable portion of installed capacity from wind and solar power which shall have a dominant share in the new capacity additions over the horizon from 2016 to 2030 in Europe [3]. The improvement towards energy efficiency shall decrease maintenance, overhaul requirements and the likelihood of outages. Figure 1.2 shows a comparative analysis of the unavailable capacity. It can be observed that the major contributors to the unavailable capacity are wind and solar installations [3].

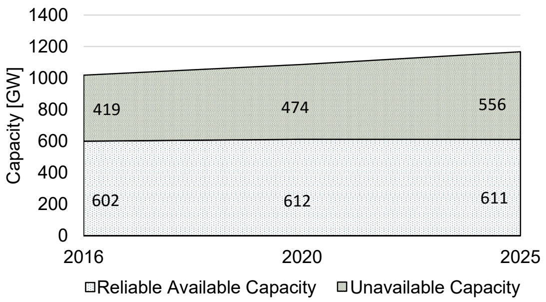

Figure 1.1: Future trends of reliable available and unavailable generation capacity in Europe [3].

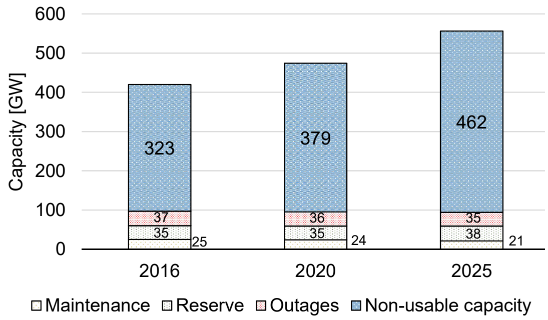

Figure 1.2: Unavailable generation capacity breakdown and the future trends in Europe [3].

1.1.2 Trends in Power Systems

The overall load requirement are anticipated to increase in the future. A comparison of the load requirement and the net generation capacity increase is show in Figure 1.3. In comparison, the evolution of generation mix and its diversity are shown in Figure 1.4. It can be observed that the power from RES shall increase by 44% of the current share in Europe. The generation from fossil fuels and nuclear shall drop due to decommissioning process. Moreover, ongoing hydro power projects shall increase the production capacity by 32% of the current share of RES hydro. The combined share of wind and solar capacity in the generation mix shall increase by 71% of their current share.

Due to increased reliance from RES, new trends are expected to arise in power system impacting the adequacy requirements of the power system. In 2020, Germany shall need to import power during January, February and December months due to extreme conditions [3]. Furthermore, the risks associated with the high share of RES shall require an efficient forecasting methods.

1.1.3 Flexibility and Ancillary Services

The growth of RES shall increase the requirement of ancillary services for maintaining sufficient reserves in the power system. In addition, the decommissioning of coal and nuclear energy

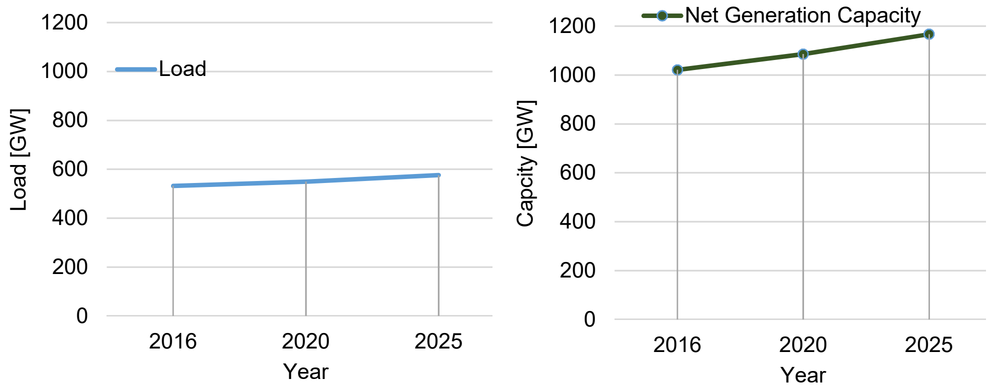

Figure 1.3: Future trends in Europe, where, (a) shows the increase of total load and (b) is the net generation capacity evolution in meeting the demand [3].

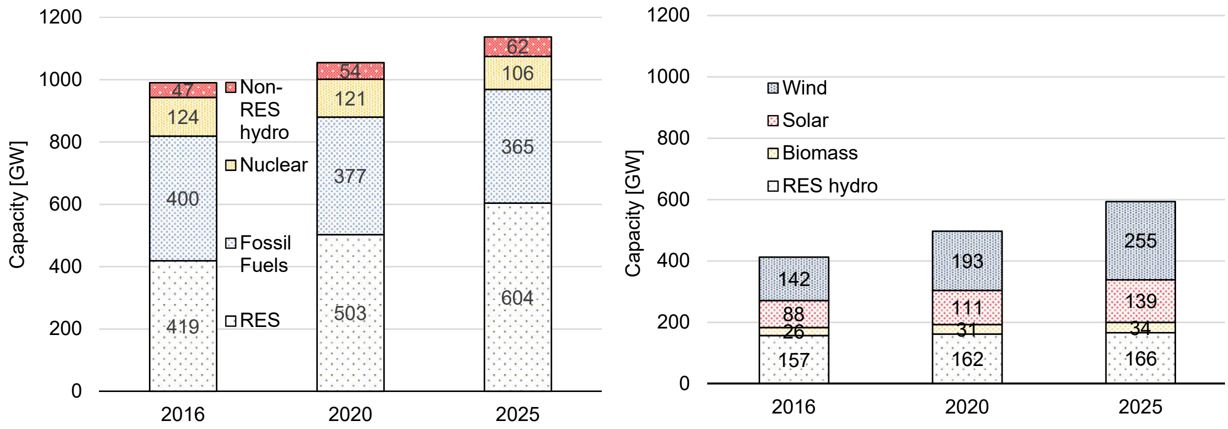

Figure 1.4: Future trends in Europe, where, (a) is the breakdown of net generation capacity and its transition, while (b) shows the evolution for renewable energy sources [3].

based power plants in the future shall make room for other players to participate in the reserve market. Traditionally, reserves have been provided by the bulk power producers as part of their generation bid. However, given the increase of distributed generation, the power system is in transition from the centralized to a distributed control. The decentralized control has been discussed in [4] as, "control centers today are in the transitional stage from the centralized architecture of yesterday to the distributed architecture of tomorrow". The control of distributed generation in the distribution systems shall require a monitoring and control mechanism. Such a mechanism can also provide basis for the flexible loads in providing ancillary services.

An qualitative economic comparison of the potential flexibility resources in providing ancillary services is performed in [5]. The flexibility requirements can be decreased by improving the renewable energy forecasts and performing the sub-hourly scheduling of resources. This is a cost effective approach in comparison with the curtailment of power from RES. To deal with the increased flexibility requirements, it may become important to widen the scope of system operation. It shall require joint market operations and an improved energy market design. The active control of the load can be cost effective solution for providing flexibility. Among this category, the involuntary load shedding is the most expensive option that should only be used in the emergency situations. The commercial and industrial demand response is the least expensive and shall require investments in the communication infrastructure. A direct contributor to the flexibility can be additional generation resources in the network. They are expected to provide high ramp capability in order to meet the variability requirements. In addition, the ramp capability of existing generators can be increased if possible. The renewable energy resources e.g., offshore wind farms are normally distant from the load centers requiring the construction or reinforcement of transmission infrastructure, the expense of which is generally high. The distributed generators providing flexibility shall also require an advance network management. This is relatively an expensive choice in comparison with the demand response programs. Energy storage is technically a favored option for providing flexibility. However, its cost is a major limiting factor for its wide scale deployment. However, with the technological advancements, it may become economically feasible to use it for ancillary services. In addition, the storage can help the Distribution Network Operator (DNO) in increasing the hosting capacity of the network for RES based generation.

The transition of distribution systems towards a more active paradigm has attracted the commissioning of several projects. They are briefly reviewed here in Table 1.1.

Table 1.1: A review of some projects in the field of active distribution networks.

Project	Description
Cell Controller [6]	A distribution area from the 60 kV grid is controlled under a Cell controller for an autonomous operation with a high share of RES. A comprehensive approach for modeling and control of a cell based distribution network with the islanding capability.
evolvDSO [7]	Define future roles of Distribution System Operators (DSOs). The design of future energy markets, regulatory framework, forecasting, scheduling and optimization in distribution grids.
IDE4L [8]	Develop and demonstrate the entire system of distribution network automation, information technology systems and applications for active distribution network management.
DREAM [9]	Lay the foundations for a novel hierarchical management approach in order to integrated distributed RES in a reliable and economic way.
INCREASE [10]	Enabling the RES in MV and LV grid in contributing towards the ancillary services to the DNO and Transmission System Operator (TSO), focusing on the voltage control and reserve services.
DISCERN [11]	Technical and organizational advancements in the European distribution networks to support the smart grid technologies in an intelligent way.
PlanGridEV [12]	Design of planning models and operational practices for supporting the integration of Electric Vehicle (EV) in various configurations of distribution network along with a high share of RES.
EEPOS [13]	Load control mechanism at a neighborhood level in the distribution system leading to better energy management.

The control schemes in an active distribution network can be related to a Virtual Power Plant (VPP), microgrid or a local control based architecture. Such localized solutions shall need to deal with the changing network conditions. In order to localize the impact of uncertainty, an important step is to identify the flexibility requirements locally. The flexibility assessment can lead to insights in the overall demand of a microgrid and associated uncertainty. The local resources can be planned to meet the demand requirements and additionally power can be imported or exported to grid. Such a control platform in the distribution system also facilitate the distribution system resource in providing flexibility bids in energy market. The objectives of a local control mechanism can be divided into planning and operation stages. The planning paradigm aims towards setting a competitive environment where the most economic and environmental friendly technologies contribute towards network resiliency. Network constraints can be limiting factors for resources in delivering their flexibility services. Therefore, these constraints are to be taken into consideration during flexibility planning and operations. Reserve resources are planned in order to deal with the uncertainty associated with the demand. A stochastic framework of optimal reserve scheduling is required that take into consideration the resource availability reflecting the stochastic nature of variables. The controller activates the resources in an economically optimal and operationally viable way. The resources such as demand response and battery storage can also play an effective role in supporting grid operations. The aims of the control mechanism can be to enable such resources in contributing towards demand and ancillary services.

1.2 Problems Addressed

The distribution networks of future anticipate an increasing number of connections from generation sources primarily driven by RES such as wind and Photo Voltaic (PV) systems. The distributed, volatile and uncertain nature of the generation from such sources shall require flexibility from the power system. The generation, storage and responsive loads can provide a suitable compensation for the issues associated from distributed generation. The controllable generation and loads shall require an active monitoring and control mechanism in order to seamlessly operate and participate towards a secure operation of the grid. They are termed as distributed resources and can be thermal generators (e.g., diesel generators), micro hydro power plants, CHP, biomass/wind/solar energy based generators or responsive loads. The planning and operation of the flexibility from such resources at varying time scales shall form the basis for realizing a smart distribution network that ideally enable such technologies. A local control scheme in the form of a microgrid or cell can provide a suitable mechanism for managing these tasks. The objective of such approaches is to localize the uncertainty by prioritizing local resources in meeting the demand. Therefore, the forecasting of generation and consumption shall be required to assess the overall demand/generation and available flexibility. During this process, the control scheme has to deal with the stochastic availability of power from RES and the uncertainty in demand. The flexibility in terms of first order dynamics can be defined by the triad variables of the power, ramp-rate and the ramp duration requirements from the literature [14, 15]. The state of art flexibility assessment methods uses an interval based approach for quantifying the limits on these variables, resulting in a hyper-rectangular model, where vertices of the hyper-rectangle represents worst case scenarios. This approach is useful for the large systems as it reduces the computational burden by evaluating the system only at the vertices. In other words, maximum values of power, corresponding ramp-rate and ramp duration specify the reference values according to which the resources need to be planned. In terms of demand and reserve, it defines the maximum ramp-rate and ramp duration requirements for all demand levels. Maintaining such conservative margins can lead to a safe operation of the system but at a high expense. Furthermore, this approach assumes a uniform likelihood of variables e.g., ramp-rate at all demand values which may not be the case. Consequently, the potential of each generation resource is limited by its ability to offer a fixed ramp-rate at all power levels. This aspect can limit the dynamic potential of the generation resource. For example, a thermal generator or demand response can possess a varying ramp-rate potential as function of the power level. An appropriate model that considers the dynamic ramp-rate limits can improve the situation by enabling the resources bid their true potential, that can result in better resource utilization and economic advantage. A compact geometric model can be a candidate to represent dynamic ramp-rate as function of the demand value. Furthermore, a local control in the distribution system e.g., microgrid has a limited resource thus requires a comprehensive flexibility assessment approach, that can decrease the demand/reserve requirements and improve economics by better resource utilization.

The flexibility requirements are generally obtained by generating a set of scenarios based on the uncertainty models of the variables. Some variables may possess time-series correlations that needs to be modeled. Similarly, the forecast uncertainty can be a function of the its level. Therefore, suitable uncertainty modeling methods are to be selected based on the availability of the historical data and its nature. Secondly, the uncertainty outcomes of each variable needs to be normalized so that they can be combined to yield the lumped uncertainty. The increasing amount of data from the distributed resources shall require data driven approaches that can model the uncertainty from the limited data. An exampling of such a flexibility assessment approach can be the modeling of overall demand in a local control scheme and its uncertainty. Suitable methods are required to represent the uncertainty and its dynamics. This aspect can quantify the impact of increase in distributed generation on the overall system dynamic capability requirements. The results are probabilistic in nature and can be related to the scenarios considered during the planning process. The number of scenarios can be related to the volatility consideration in the forecast and needs to be selected based on a desired probabilistic criteria. Therefore, an emphasis is required to be placed in the selection of sufficient number of scenarios.

The distributed resources shall require to make flexibility bids in an active distribution network. For this purpose, suitable model shall be required to represent the resource potential. The potential resources can be generation (diesel generators, fuel cell, micro-hydro, renewable energy sources), demand (thermal loads, heat pumps, electric vehicles) or storage (pumped-hydro, batteries). A common flexibility model for such diverse type of resources can facilitate the operational management. Recently, a generic approach for a battery based flexibility model has been proposed in [16]. The resources who does not possess the storage capability can also be represented using this model by performing appropriate simplifications of the model. However, a generic model that can represent the dynamic capability in conjunction is lacking in the literature. It should preferably be able to describe the first order dynamic capability of the battery along with the associated response time (if applicable) and cost of service. In other words, a generic model that can be applicable to a diverse range of resources shall form the basis of the flexibility modeling. Once modeled, the flexibility bids can be aggregated in the system. In case of a geometric approach applied to model the resource flexibility, an appropriate mechanism of flexibility aggregation shall be required in relevance.

An important step in generation adequacy planning is to verify that the available flexibility is sufficient to meet the requirements. The demand, ramp-rate and reserve requirements are traditionally allocated using an economic dispatch process. However, in case of an envelope based modeling of flexibility requirements, an advanced mechanism shall be required to allocate it among resources based on their flexibility bids. The flexibility allocation problem is thus transformed to an economic space allocation problem. The selection of flexibility envelope for modeling the demand shall define the computational complexity of the allocation problem. Furthermore, the location of resource and network conditions can limit the flexibility that can be allocated to a resource. Thus the network constraints should be considered during the flexibility allocation process. The flexibility envelope shall also define the reserve requirements at various levels of demand. Reserve requirement is generally probabilistic in nature and can be related to the number of scenarios used to perform flexibility assessment. The consideration of the stochastic reserve requirements for a given demand forecast in the Unit Commitment (UC) and Economic Dispatch (ED) problems can lead to probabilistic confidence in results. The strategic modeling of the resources in distribution network possess an interesting application in such optimization problems. By using Game Theory, the roles of each resource can be defined based on set of strategies that maximized their utility. The approaches that can lead to an equilibrium based on a common signal dispatched to all resources can be of interest as it can potentially decrease communication requirements. This can be particularly relevant if the number of resources in the distribution network under a local control is large. However, the limitation of game theory based schemes needs to be identified for such approaches.

The demand side resources can participate in meeting the flexibility requirement locally and offer the flexibility towards the grid operations. A suitable flexibility model is required to represent the aggregation of the responsive loads in a cell/microgrid based local control scenario. The aggregation of demand responsive loads can represent a stochastic resource that require an elaborate mechanism for assessing the overall capability, availability and the associated cost. Such a model can be defined by a stochastic battery model whose parameters are uncertain and depend on the availability of the resource. A cost effective way is desired to implement such a scheme that requires minimum level of data exchange between a controller and responsive loads. The flexibility model of demand response aggregation needs to be validated for a tracking a realistic reference signal. The impact of the uncertainty and the communication delay needs to be evaluated for assessing the potential of this resource. Furthermore, the utilization of demand side flexibility shall not result in the violation of the network constraints. In the best case, they may support the network operations in addition to providing flexibility in the system.

Overall, a number of research questions are aimed at ranging from assessing the demand and associated uncertainty in a local control scheme to modeling the resource flexibility potential and incorporating it in the planning operations. The local control scheme either implemented as microgrid (if standalone operations in also desired) or cell (if the grid connection is always available) require new methods that aims to increase the operation efficiency, quantify the uncertainty and facilitate the planning and operations by considering a diverse range of resources in the network.

1.3 Methodology and Contributions

The distribution systems are in transition towards a more active paradigm to support the control of power in-feed from RES. The provision of flexibility from distributed resources like demand response and energy storage shall be key players in realizing smart grid future. This necessitates local control approaches in the distribution systems. The aim of such efforts is to increase the hosting capacity of existing distribution networks for renewable energy based intermittent generation and to handle the associated uncertainties. Various approaches in the literature are discussed to enable the DNOs in handling the future challenges of actively managing the network and providing additional services. In the Electra project [17, 18], a distribution network under a DNO is divided into cells as shown in Figure 1.5. A cell is a control area in the distribution network with a well-defined physical boundaries and having a dedicated cell controller. The responsibilities of a cell controller can range from providing additional support service to the DNO to a complete microgrid solution. The cell here is defined as a microgrid if it possesses the property of independent system operation. However, a cell is not essentially a microgrid and can remain indefinitely connected to the distribution network. This thesis builds on the future scenario assumption that the local control either based on cell or microgrid shall play an important role in the future distribution system. The microgrid is a technologically advanced form of the local control in comparison with a cell as it covers both the aspects of grid connected and isolated operation. The proposed methods are developed for the microgrid based control in distribution system. However, they can be be applied for the cell based control as well.

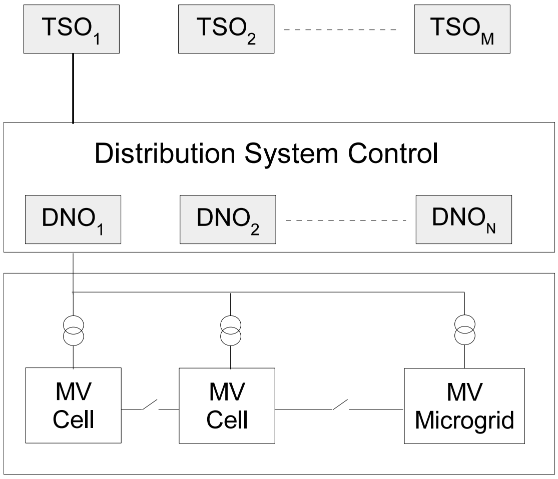

Figure 1.5: A cell based approach for the local control in distribution system.

It is aimed that a comprehensive generation adequacy planning is performed to facilitate the microgrid planner in identifying the local flexibility requirements and assessing the corresponding potential from the distributed resources. In case of microgrid, it can help in planning of local generators and power exchange requirements with the connected grid. The work-flow diagram for the overall flexibility planning process is shown in Figure 1.6. During the whole process, an emphasis is places on the economics of the flexibility assessment and allocation processes. The objectives have been to model the flexibility from a diverse range of resources, aggregate the flexibility potential and allocate the requirements among resources. In addition to the generation sources, the demand side flexibility is assessed and modeled using the proposed flexibility model.

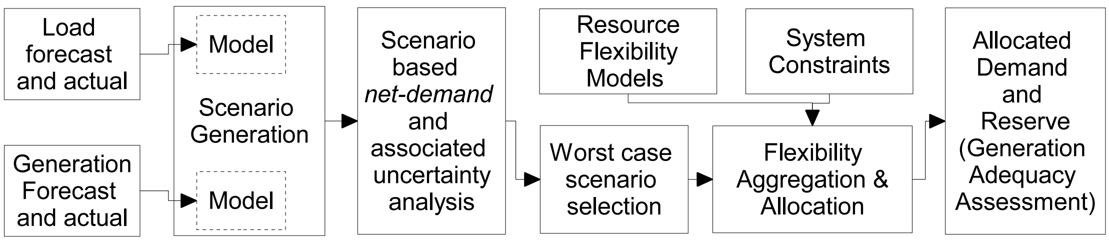

Figure 1.6: In the first stage of flexibility planning, the forecast uncertainty is modeled and used to generate scenarios. From scenarios, the dynamics of the overall uncertainty are evaluated leading to the definition of worst case requirements. Meanwhile, the resource flexibility is modeled. The *net-demand* flexibility is then allocated among resources in the end.

Flexibility assessment. The first part of the process is to perform the flexibility assessment. The energy management system of the microgrid performs the forecasting of power from RES and the anticipated load. These forecasts are used for planning the local resources in various time frames ranging from a day ahead plan to intra-hour schedules. The forecast is accompanied with an uncertainty that needs to be modeled. The forecast uncertainty can be modeled from the probability distribution of the stochastic variables. These distributions can be obtained from the historical data of the prediction and actual values. A suitable model is adopted for each type of uncertainty based on the available historical data and the desired accuracy.

The Markov chain associate a probability of the outcome of an event based on the occurrence of previous events. Thus it is can model the time-series correlation in the data. A Markov chain based approach is used here to model the forecast uncertainty in the load, generation from wind and solar power. The Markov chain and the probabilistic models are used to generate scenarios by performing Monte Carlo sampling. An important aspect is the number of scenarios that are sufficient for modeling the uncertainty. This is defined on the basis of chance constrained optimization theory. It relates the number of scenarios to the desired probability of a constraint violation. The probability is related to likelihood of the uncertain scenarios and confidence in result. The *net-demand* scenarios are created using the sampling process from the individual models. The generated scenarios are used for the flexibility assessment. An appropriate compression algorithm is used to extract dynamics from the scenarios. The flexibility envelope is modeled based on the first order dynamic variables of power, ramp-rate and ramp duration. A novel polytope based method is applied to generate a compact and convex envelope. This leads to more economical assessment in comparison with the state of the art approach of using a hyper-rectangle. Secondly, the proposed approach also considers the correlation between the dynamic variables. The surface of the polytope defines the maximum values of the *net-demand* and associated uncertainty. This step is the starting point for the demand and reserve allocation in the microgrid.

Resource flexibility modeling. Once the flexibility assessment in a microgrid is completed, the next step is to analyze the flexibility from available resources in meeting the demand and reserve requirements. The generation and demand flexibility resources are diverse in the distribution network. Hence, the development of a generic flexibility model that can represent all resources is challenging. Based on a recent generic battery model in [16], a new Resource Flexibility Model (RFM) is proposed in this thesis. The RFM combines the generic battery with a dynamic capability envelope model. The battery model captures the storage potential of the resource while the dynamic capability model allows for a comprehensive modeling of first order dynamic capability and the associated cost. The RFM can contribute to an increase in the flexibility potential of the system and can potentially lead to a better resource utilization. The proposed RFM is demonstrated for a thermal generation unit representing distributed generation and an aggregation of Thermostatically Controlled Loads (TCLs) in the network. This model needs to additionally take into consideration the resource specific constraints. The structure of the methodology used is shown in Figure 1.7. The resource specific constraints can be taken into consideration while generating the flexibility bids at each resource. An alternate approach can be that each resource sends the flexibility potential to the microgrid controller where it is evaluated during flexibility allocation process.

Flexibility aggregation and allocation. The flexibility represented by the RFM for the resources needs to be aggregated for the assessment of overall flexibility potential in the microgrid. A geometric method based on Minkowski's sum is used to perform this aggregation. The flexibility allocation is defined here as a process in which the flexibility requirement envelope is allocated among the Resource Capability Envelope (RCE) of resources. A simple decomposition of the envelopes can be used if the related economics are neglected. However, for a grid connected case of microgrid (cell based scenario) it is important to consider the price of electricity service during

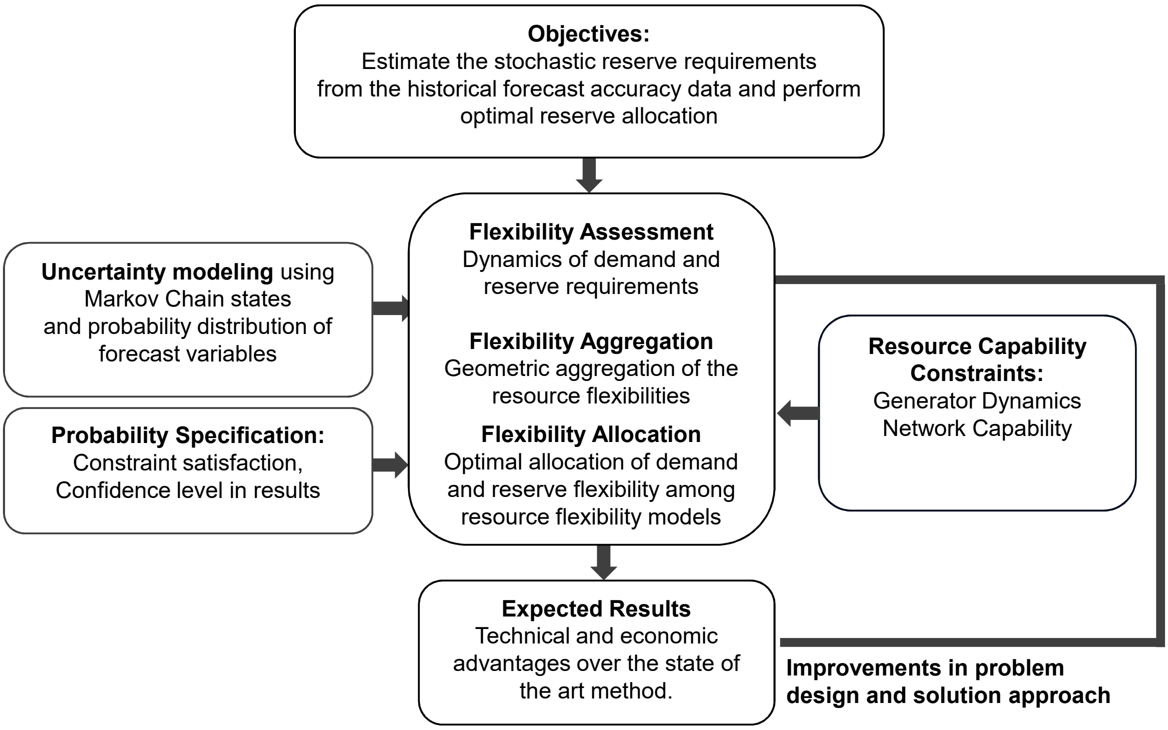

Figure 1.7: Flow diagram of the flexibility assessment, modeling, aggregation and allocation. The flexibility planning is performed while considering the resource capability and network constraints.

resource allocation. Similarly during the island operation of the microgrid, the most economic resources needs the be allocated with priority. The allocation of flexibility should ideally be optimal in terms of generation and maintenance cost to the system. For this purpose, a novel geometric method of polytopic decomposition is proposed. This is a vertex based decomposition method that facilitates the use of existing constraints models found in the common optimization applications. The selection of the envelope model for the flexibility assessment and RCE defines the complexity of the flexibility allocation process. The convex envelope representation is generally preferred from the optimization point of view. The selected polytope approach facilitate the application of the deterministic optimization methods. Figure 1.7 shows the additional considerations during the flexibility allocation process. The network constraints involving the transmission line power ratings and the voltage constraints are taken into consideration while performing the flexibility allocation. This captures the aspect that the location of a resource can be a limiting factor for utilizing its flexibility. The proposed flexibility allocation is demonstrated for a microgrid test case. The required flexibility is allocated between the thermal generators and the main grid. The outcome of the overall process is an economic assessment of resource adequacy based on the available flexibility in the network and can be used to assess the flexibility import/export between the microgrid and the external grid.

Flexibility in operation. The reserve requirements as function of the demand emerges from the flexibility assessment process. In comparison with a fixed reserve which is a normal practice, the consideration of variable reserve as function of demand decreases the reserve cost. This consideration is incorporated for the UC and Security Constrained Economic Dispatch (SCED) problems in microgrid.

Another interesting research direction has been the strategic modeling of the resources. At one end it can facilitate in modeling a strategic model for the resources having multiple strategies in difference scenarios. Such that for a given scenario, the resources can participate with their flexibility bids that aims to maximize their outcomes. The area of game theory presents a theoretical foundation for such a strategic interaction. The case of large number of resources who are modifying their share of flexibility as function of the electricity price or a common signal can lead to a situation that requires less communication infrastructure. The evolutionary game theory is explored for this purpose. A novel application of Replicator Dynamics (RD) method for ED problem is presented. The evolution of the strategies of resources towards an equilibrium are explored. The limitations of the approach are discussed with an emphasis on the RD being a gradient based method. The overall limitations of the game theory based methods for the flexibility allocation problem are discussed.

Demand side flexibility modeling and utilization. The imbalance between demand and supply is reflected on the frequency of electricity in the system. The term frequency regulation stands for the efforts to keep the frequency within the permissible limits. This is achieved by consuming/generating the power to counter the imbalance between demand and supply. The frequency regulation signal can represent the imbalances in the microgrid and/or from the energy market. An overview of the demand side flexibility utilization for the frequency regulation is shown in Figure 1.8.

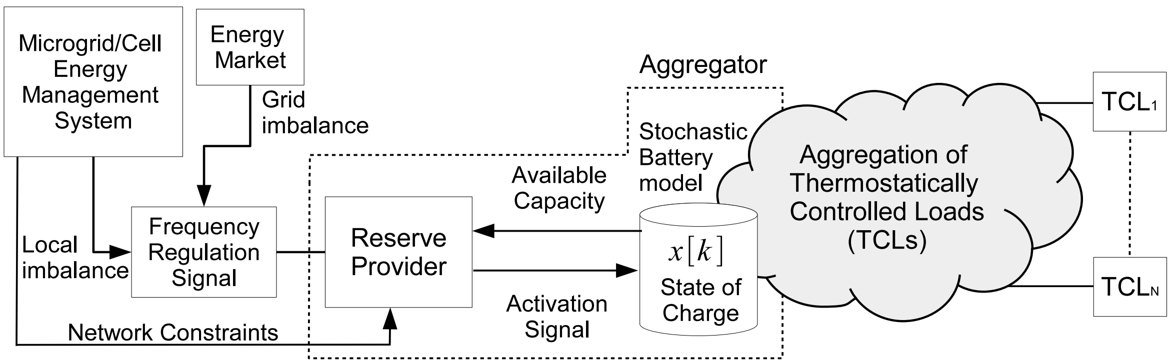

Figure 1.8: Methodology for demand response flexibility from thermostatically controlled loads. An aggregation of such loads is controlled to track reference frequency regulation signal. An aggregator or local controller can act as a reserve provider.

An aggregation of Thermostatically Controlled Loads (TCLs) in the distribution network can provide the frequency regulation flexibility. This thesis presents a novel stochastic battery model is developed to represent the storage potential of TCL aggregation in an active distribution network. During the battery modeling, an emphasis has been placed on the consideration of the availability of resource, decreasing the computational requirements and the sensor requirements. The storage potential of the TCL aggregation operates as a damper for the demand-supply imbalances. This stochastic battery model along with the dynamic capability of TCL aggregation to track a reference frequency regulation signal is modeled by the proposed RFM. A test case for a large number of residential TCLs is used to validate the proposed model.

The demand response service is offered by an aggregator model that can be the part of microgrid or an independent entity. While performing the active demand response, the aggregators needs to ensure that the network constraints are observed. Therefore, the current state of the network is periodically sent to the aggregator. In addition, a combined simulation environment is presented to test the impact of the TCL aggregation based demand response service on the voltage at the critical bus in the network. This consideration aims to cover the operational constraint aspect of flexibility utilization.

1.4 Organization of Thesis

The thesis is organized as follows,

1. **Chapter 2: Control Strategies in Distribution System.**
   This chapter gives an overview of the control strategies in the active distribution networks. The key stakeholders in the control process and prospective flexibility resources are discussed. Aggregator is identified as a key player and a suitable operational model is presented. The control architecture is described from the perspectives of microgrid and cell based approaches. A hierarchical control within a microgrid is explained with emphasis on tertiary level control challenges. Among these challenges, the areas focused in the dissertation are explained.
2. **Chapter 3: Uncertainty Modeling for Flexibility Assessment.**
   This chapter describes the uncertainty modeling methods used for assessing the flexibility requirements in the microgrid. The forecast uncertainty variables are modeled using Markov Chain and empirical Cumulative Distribution Function (eCDF) functions. Monte Carlo sampling is performed on the uncertainty models resulting in the scenarios of the *net-demand* in microgrid. The first order dynamic variables are extracted using a compression algorithm on the scenarios. The analysis leads to the demand and reserve requirements defined as points in space spanned by dynamic variables. A compact and convex envelope approximation is performed to represent the reserve requirements. The stochastic nature of reserve in the optimization problem transforms the deterministic constraints to stochastic variants. A microgrid test case is used to demonstrate the proposed method of the flexibility assessment.
3. **Chapter 4: Resource Flexibility Modeling.**
   This chapter proposes a generic RFM for modeling the flexibility from distributed resources in the power system. The RCE is composed of energy storage model and a capability envelope. The battery model represents the energy storage potential of the resource which can be used to scheduling optimization. While, the capability envelope allows to model the cost of service as function of the power exchange dynamics. Together, they can represent a diverse range of resources. This model has been later used to discuss about the potential flexibility bid structure in the local energy market. The proposed RCE model is applied to a thermal generator and an aggregation of TCLs. These application provides a proof of concept of how the flexibility from generation and consumption side can be formulated using a common model. The RCE based model for thermal generator has been used in Chapter 5, while for TCL aggregation in Chapter 6.
4. **Chapter 5: Flexibility Aggregation and Allocation.**
   This chapter presents the methods for flexibility aggregation and allocation. The desired probabilistic confidence against forecast uncertainty is quantified by the number of scenarios and is represented by the flexibility envelope based on the results in Chapter 3. The thermal generators installed in the distribution network are considered as potential flexibility resources. Their operational capability as discussed in Chapter 4 is aggregated to compare

it with the flexibility requirements. A novel vertex based flexibility allocation algorithm is presented that optimizes for the generation cost. The method is used in the day ahead resource planning problem in microgrid. It gives an insight into demand and reserve contributions from generators and the power import from the grid. The allocated envelopes represent the contribution of resources in terms of their first order dynamics. Based on results, the microgrid can be modeled as a virtual power plant or flexible load. The reserve requirements resulting from the flexibility assessment process are used in the optimization problems of the UC and SCED applications. In the end, a novel application of population game theory based method for the UC problem is discussed.

5. **Chapter 6: Demand Side Flexibility as Frequency Reserve.**
   This chapter discusses an application of RFM based flexibility model representing a TCL aggregation as discussed in Chapter 4 for a secondary frequency reserve application. The TCLs share a common characteristic i.e., they aim to maintain the temperature within certain limits around the set-point called dead-band. The operational state of TCLs can be changed while operating in the dead-band region and hence presents a flexibility potential. This flexibility offered by a large number of TCLs is represented by a stochastic battery model. A central control approach simulates a priority stack based algorithm to track the reference frequency regulation signal. The algorithms for the central control simulating the demand response and for each TCL are presented. The proposed battery model is validated for a test case of a large number of residential TCLs. In addition, a combined simulation platform is proposed to study the impacts of flexibility activation on the network.

6. **Chapter 7: Conclusion and Outlook.**
   This chapter summarizes the contributions from dissertation. The extensions of proposed methods in related topics is presented in the outlook section. Moreover, an approach for flexibility activation from distributed resources (generation and demand) in a distribution network is discussed.

The concept map of the thesis is shown in Figure 1.9.

1.5 Publications

During the course of PhD, following publications have been made,

- S. Khan, W. Gawlik, and P. Palensky, "Reserve Capability Assessment Considering Correlated Uncertainty in Microgrid," *Sustainable Energy, IEEE Transactions on*, vol. 7, no. 2, pp. 637-646, April 2016.
- H. Bosetti, S. Khan, H. Aghaie, and P. Palensky, "Survey, Illustrations and Limits of Game Theory for Cyber-Physical Energy Systems," *at-Automatisierungstechnik*, 62.5, 375-384, 2014.
- S. Khan, H. Bosetti, P. Palensky, and W. Gawlik, "A Replicator Dynamics method for the Unit Commitment problem," in *Workshop on Modeling and Simulation of Cyber-Physical Energy Systems (MSCPES), Berlin*, pp. 1-4, 2014.
- S. Khan, M. Shahzad, U. Habib, W. Gawlik and P. Palensky, "Stochastic battery model for aggregation of thermostatically controlled loads," IEEE International Conference on Industrial Technology (ICIT), Taipei, Taiwan, pp. 570-575, 2016.

- A. Latif, S. Khan, U. Habib, W. Gawlik, and P. Palensky, "Co-simulation Based Platform for Thermostatically Controlled Loads as a Frequency Reserve," in *IEEE workshop on Modeling and Simulation of Cyber-Physical Energy Systems (MSCPES)*, (Accepted), 2016.

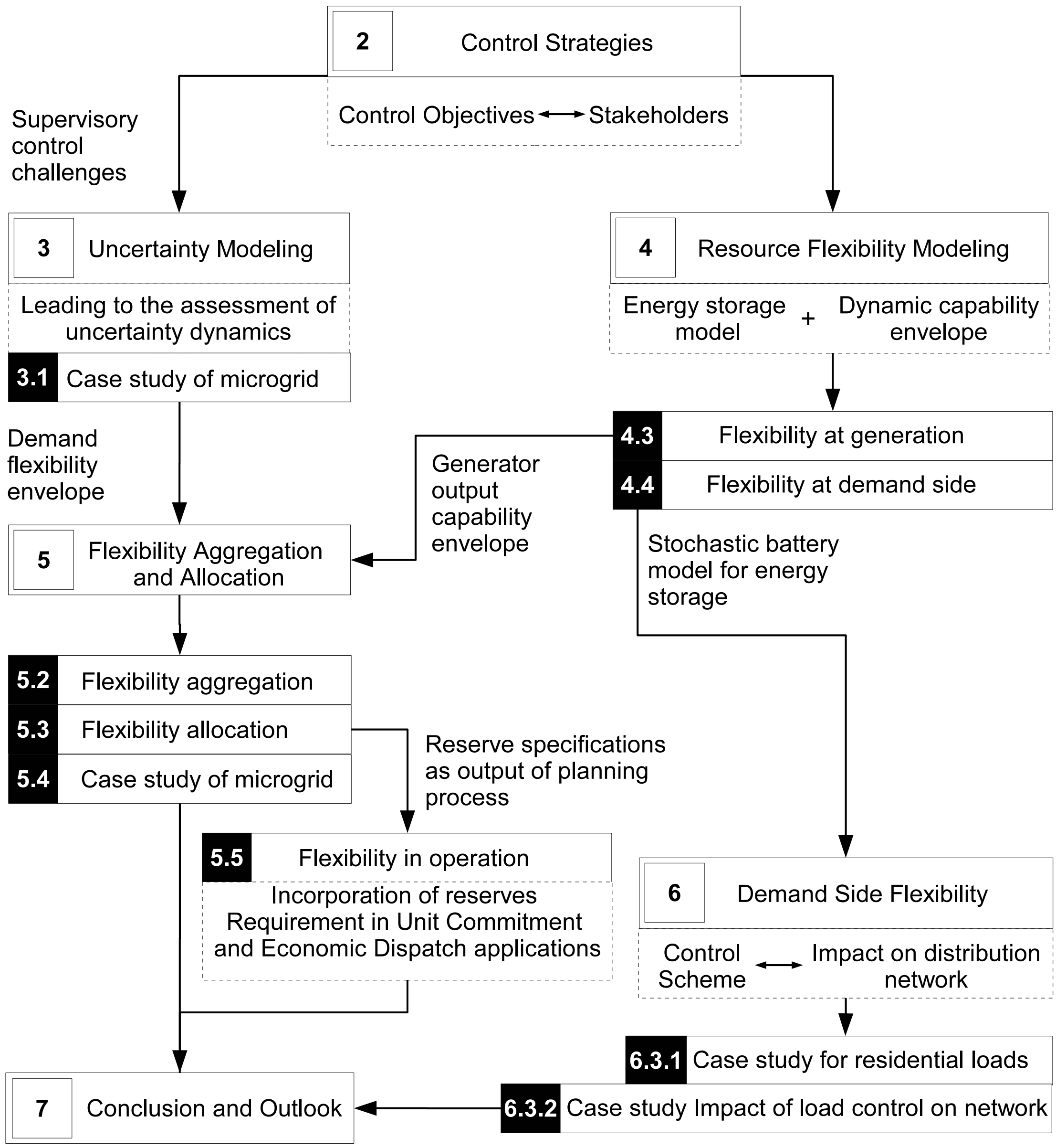

Figure 1.9: Concept map for the thesis contents.

2 Control Strategies in Distribution System

2.1 Introduction

The electric power system represents network composed of a large number of networked sub-systems that aims to meet the energy demand of consumers in a safe, reliable, economic and a sustainable way. The major components of the electric power system are shown in Figure 2.1. The bulk of power is generated by hydro, thermal, nuclear power plants and other generation resources and fed into the transmission network. The power is delivered from the transmission system to sub-transmission and delivered to distribution networks at the distribution substations.

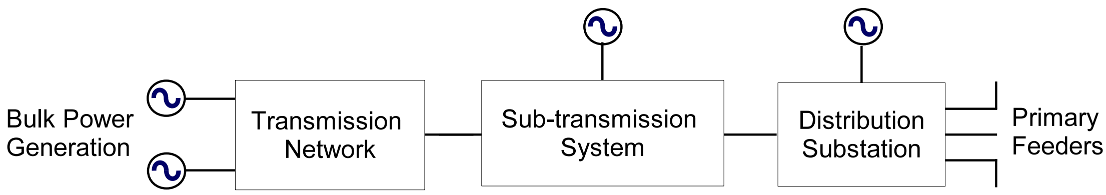

Figure 2.1: Major components of a power system.

The distribution system starts with the distribution substation which is connected mostly to the sub-transmission system and occasionally to the high voltage transmission line. A one line diagram of a typical distribution system is shown in Figure 2.2. At the high-voltage side, the switching is done using simple switch followed by a fuse. While on the low-voltage side of sub-station transformer, the relay/circuit breakers are used [19]. The voltage of the sub-transmission line ranges between 12.47 to 245 kV. The substation transformer steps down the voltage from 4.16 to 34.5 kV. As the energy demand changes the voltage drop between substation and the load varies. Voltage regulators are used to keep the voltage within acceptable limits by the transformer action. Generally, Load Tap Changing (LTC) transformers are used as voltage regulators. They have the variation of typically 10% on the low-voltage side. On the high-voltage side fixed taps are used to adjust the voltage variation. Every substation has a metering arrangement, which can be as simple as ammeter showing the current or a digital recording device that can measure the current, voltage, power, power factor etc. Each distribution substation serves one or more primary feeders. The fuse at the primary feeders provides protection against the short-circuit. The primary feeder typically has a radial structure resembling like branches of tree where the

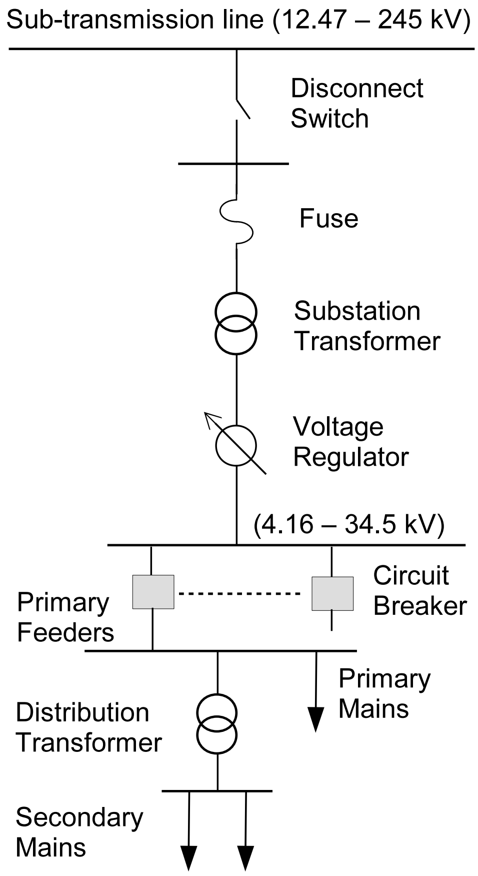

Figure 2.2: One line diagram of a typical distribution system.

distribution transformers are used to further step-down the voltage to the consumers. In some case primary feeders serves the consumers directly through primary mains.

The distribution system has been originally designed to deliver power from the transmission system to the end users in a uni-directional power flow. The rise in the electricity generation at the consumption side is challenging the distribution networks in variety of ways. The principal impact is on the requirement of distribution network to support the power flow in the reverse direction i.e., from the end customers towards the grid. The distribution network comprises of a large number of nodes or buses. This aspect makes the active monitoring and control technically difficult and economically expensive. Thus the distribution systems have been designed to operate with minimum supervision. However, as the share of Renewable Energy Sources (RES) increases in the distribution network, a number of technical issues have been observed. Some of them are related to voltage violating the maximum/minimum limits, congestion in the network due to overloading of lines, false triggering of protection systems and others. It has led to a need of suitable measures that can increase the hosting capacity of the distribution network in incorporating a high share RES. Among these measures is a local control mechanism that can perform active monitoring and control of distributed generation. This has become a necessity for realizing a secure and reliable control of the distribution network in wake of the future scenarios.

Numerous challenges are associated with an active distribution network. The advent of smart meters aims to increase the operational awareness of Distribution Network Operator (DNO). However, the challenge is to handle the data from large number of nodes in the network. Various studies have been done on introducing additional stakeholders e.g., aggregators to manage the Distributed Energy Resources (DER) related activities and their integration in the overall power system operation. Some of the studies have been on the network reinforcements and additional hardware installation to meet the distribution system challenges.

An important step in the transition towards an active distribution network is to determine the maximum hosting capacity in supporting intermittent power from RES. The flexibility from DER can provide valuable support to the network operations and can potentially increase the distribution system hosting capacity. The control and optimization techniques for handling the DER in a Medium Voltage (MV)/Low Voltage (LV) distribution network is an emerging research area that has received significant attention in literature. Various control mechanisms have been presented in the literature spanning from a centralized to distributed and hybrid control approaches. Most of them have proposed a hierarchical approach involving primary, secondary and tertiary level control.

The control mechanisms that can facilitate DER integration in a distribution network are being focused. The flexibility in generation and consumption at the distribution level can play an important role in maintaining the balance between demand and supply. An economic approach is to use the local flexibility of DER in supporting the local demand and reserve requirements within the control area of the distribution network. The first step for this is to assess the flexibility requirements of the local energy demand. Each of DER requires to model its potential as a flexibility resource considering the operational and availability constraints. This thesis discusses the assessment of desired flexibility by modeling the uncertainty. On the other hand the flexibility from the participating distributed resources is modeled. Then the desired flexibility is allocated among resources in an optimal way. The challenges related to the flexibility modeling, assessment, aggregation and allocation are addressed at varying levels.

2.2 Distribution Management System

The state of the art methods in the Distribution Management System (DMS) provides a starting point in the study of the control challenges in the distribution system. A DMS is a collection of applications used by the DNO in order to monitor, control and optimize the distribution system performance. The ultimate goal of the DMS is to enable smart, self-healing, efficient, reliable and economic electricity distribution service. The reliability of the power supply is of paramount importance and is ensured by the planning and operation activities. The time scale of such activities ranges from milliseconds (protection operation) to years (network expansion planning). Figure 2.3 provides a general overview to some applications in the DMS.

DNO monitors the network and the equipment status at the substation. In order to assess the network state, it implements a state estimation algorithm. The output of the state estimator is the core component for the network assessment and optimization applications. The DNO monitors the alarms that may result in triggering of system restoration services. Some restoration services are operated remotely while for other crews are dispatched. The set of tools used for implementing the strategies for the outage management are generally termed as emergency triggered tools. Among such tools is the $N-K$ contingency analysis method. An $N-1$ contingency is a system test if one of the element in the network is not operational. A DMS may deploy $N-1$ and $N-2$ contingency planning as part of reliability assessment. The detailed discussion about the applications in DMS can be found in [20] and [21].

The DNO implements a load forecast estimation based on the historical data and the prediction models. As a result, the *net-demand* forecasts are obtained. The *net-demand* is the subtraction of the local power generation e.g., from renewable energy sources from the demand. The forecast information is used for the reliability support applications.

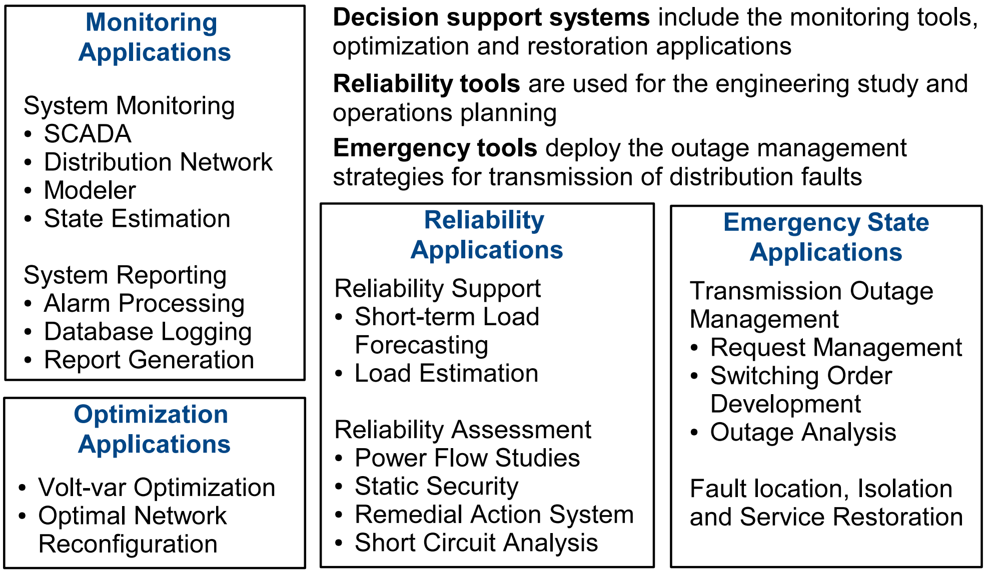

Figure 2.3: Overview of applications in the Distribution Management System.

2.2.1 Distribution System Operational States

A DMS can recognizes up to five operational states as shown in Figure 2.4.

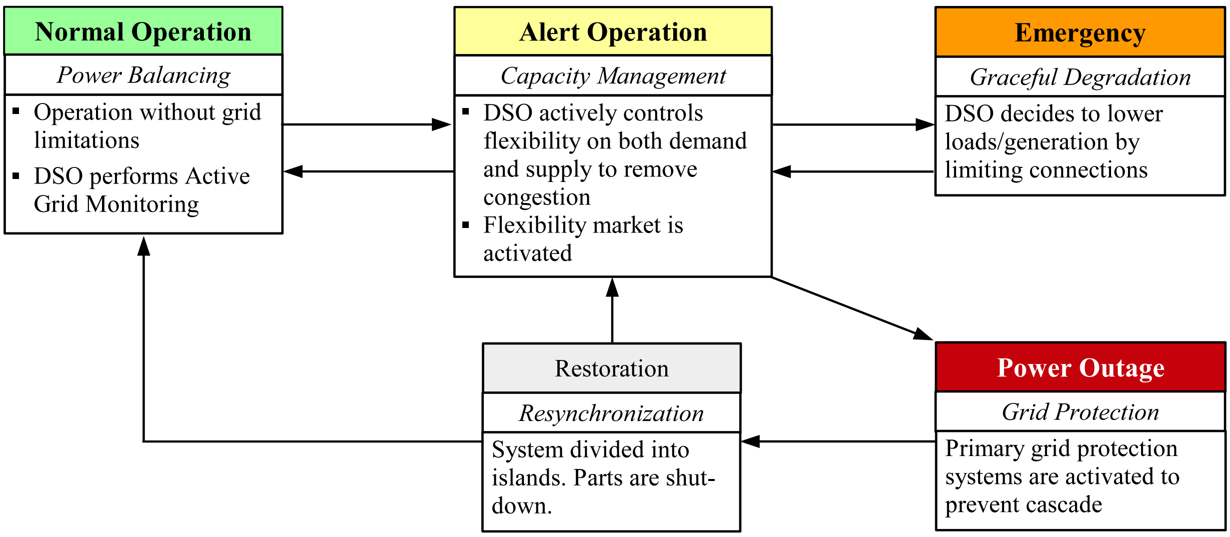

Figure 2.4: Operational modes in the distribution network.

The first mode is called normal mode or green mode. In this mode, DNO performs active grid monitoring and optimization tasks and the system operates as desired. The demand is met with a reasonable accuracy by the scheduled activation of generation resources and the power transfer schedules. The second mode is called alert operation or yellow mode. It is activated when there is a need of active control from DNO in triggering of the reserve flexibility. It can be triggered by a significant forecast error or contingency situation in network. DNO actively controls the loads/generation to remove congestion in this mode. It avoid voltage violations or other limiting constraints causing the alert alarm. The state goes back to the normal if the capacity management solves the problem. The emergency or orange is the third mode of the distribution network. It is activated as a fall back mode when the flexibility available is not able to satisfy the network operational constraints. Graceful degradation is performed in this scheme by limiting the load/generation connections to the distribution network. As soon as the situation normalizes the mode shifts back to the alert mode and subsequently to the normal operation. The fourth mode is called power outage mode. It can be triggered by a major fault at the distribution network or power outage at the transmission side. The DNO implements the emergency response schemes by triggering the protection devices in the network. As the power supply resumes, the distribution system undergoes a restoration phase. The fifth mode is called restoration mode. It is triggered when the power outage situation is resolved. The outage management system is active in this mode. It communicates with the customers to determine the fault location, separate the energized part from the non-energized part and the crews are dispatched to the locations. As the state is restored the system can either go to the alert or normal operation modes. This thesis is related the flexibility utilization from DER during the alert mode operation.

2.2.2 Scenario Assumptions

Based on various reports and outlooks, it is expected that by 2030, between 52% to 89% of electricity production will be generated from RES in Europe [22, 23]. The country specific situation shall vary due to the uneven starting points, policies and availability of RES potential. The overall consequences can be summarized as,

- The growing percentage of renewable based generation in the energy mix requires more reserves in the system in order to handle demand and supply imbalances caused by forecast uncertainties. As the reserves are an expensive resource to maintain during power system operation there is a growing need of load following the generation.
- The reverse direction of power flow in distribution system can cause insecure situations and may trigger the protection systems in an undesired manner. Therefore, appropriate control mechanism or protection reinforcements shall be required.
- The replacement of large synchronous generators by the RES shall result in the reduced inertia against the frequency perturbations in the system. Hence more flexibility shall be required from DER and the importance of demand side participation shall increase.
- Due to the low dispatch capability of RES, the major contributors to the reserves shall be the bulk power producers, flexible loads and storage. Storage is likely to become competitive with the power plants for offering the ancillary services by 2020 [24].
- In order to reduce greenhouse gas emissions, there is a rising need of the electrification of transportation and heating/cooling systems. It is expected that the electricity demand in Europe shall increase by 14% in 2030 as compared to 2012 [25]. The growing demand can burden the network beyond its capacity. Hence the congestion problems are likely to increase in such situations.

- The roll-out of the smart meters and deployment of the sensors shall increase significant potential in monitoring and control applications. However, it shall require special arrangements for handling large data and using it during operations.

The monitoring and control of resources connected to the distribution system can play an important role in providing flexibility that can help in addressing some of the challenges outlined above. For example, if the distribution system is experiencing a congestion problem in an area, the active demand response can decrease the demand. Similarly, reserves at the DER can be activated to maintain energy balance in the network. The dedicated storage and electric vehicles shall also open new directions for flexibility. As more and more resources are actively controlled there is a need of a monitoring mechanism that can inform the DNO about the available flexibility from the distributed resources dynamically. The network impacts of the activation of flexibility from such resources is a critical for a reliable system operation. The distribution network constraints can potential limits the resource potential in the system that may cause voltage, frequency or congestion related problems. Considering the future scenarios, additional control for actively managing the distributed resources shall become a necessity. The objective of this control shall be to provide a holistic mechanism for the seamless assessment, aggregation and allocation of the flexibility on one hand and on the other to address the network constraints in the process.

2.2.3 Stakeholders

It is important to study the role of the key stakeholders in designing the control strategies to tackle the future challenges in the distribution system. In the light of the future challenges, the DNO shall have a key role in communicating with the stakeholders.

Prosumer. The prosumers are traditional consumers but have an ability to contribute their excess production of electricity to the grid. The prosumers are becoming energy aware and motivated to contribute to environmental friendly solution to their energy requirements. The future prosumer can possess an electric vehicle that requires to be charged from preferably using local solar power generated at the prosumer premises. Prosumer may require this service independent of time and place and expect the power system to make it possible. Similarly, the demand response potential of a prosumer can offer valuable flexibility to the system. The energy market is evolving towards a more prosumer friendly setup where the flexibility can be offered and received. However, in order to communicate with large number of prosumers the intermediate control layers or organization shall likely to play a key role.

Supplier (producers, Balance Responsible Party and supplier). The bulk electricity producers, Balance Responsible Party (BRP) and supply companies are considered here as a single category termed as suppliers. The role of the supplier is to provide energy to the consumers whenever it is required. The suppliers may need to communicate with increasing number of prosumers in the future. These prosumers can be large industrial consumers producing part of their electricity demand themselves or the residential consumers. The diversification of the consumer types shall likely to increase in the future. The emerging role of the supplier shall be to fulfill the deficit between the demand and supply of the prosumers instantaneously. A part of this imbalance can be dealt with using flexibility at the prosumers side. Therefore, the supplier of future not only needs to optimize the generation assets but also to take into consideration the flexibility at the prosumers side.

Distribution Network Operator. The DNOs are responsible for the secure flow of the energy between suppliers and consumers. The existing distribution network is designed to be resilient and stable network. However, with the increase in the demand in the form of electric vehicles, heat pumps and due to local renewable generation the network capacity may reach to its limits. Therefore, the role of the distribution network operator shall also be to assess the state of network and communicate with the flexibility service providers to deal with the congestion and the voltage quality problems.

Aggregator. Aggregator can be an independent organization or part of energy supply company. The objective of an aggregator is to accumulate the flexibility from the industrial, commercial and/or residential prosumers. The aggregated flexibility is then traded in the energy market and the bid is customized to meet the stakeholder's requirements. The aggregator is responsible to manage risk of the availability of flexibility e.g., from demand response of prosumers.

Transmission System Operator. The Transmission System Operator (TSO) objective is to ensure that the transmission capacity is available to meet the supply and demand. As the share of renewable increases, the load flow changes dynamically and would require a optimization of resources. The objective of maintaining the sufficient transmission capacity can be challenging. Traditionally, the flexibility is obtained by large power producers to counter the imbalances between supply and demand. As renewables have more share in the energy mix, alternate source of flexibility shall be required to provide the ancillary service flexibility. Thus the TSO shall have an additional responsibility of assessing the reserve requirements and to play a role in energy market for the procurement of the flexibility.

The individual objectives of the stakeholders are an important consideration. The DNO would like to see a flat profile of loads across time to maximize the capacity utilization. The bulk producers of renewable energy would like the demand to follow the generation closely. A prosumer on the other hand would like to have guaranteed availability of energy when required and may prefer to contribute to grid when it is economic. While the aggregator would like accurately compute the available flexibility and activate it as desired. The global objectives of all the stakeholders can only be met as a trade-off and are decided at various levels in the overall topology of the system.

The challenges faced by the distribution system can be broadly classified into two categories, the voltage and the frequency stability. The voltage quality problems are normally attributed to the increase in the load or distributed generation while the frequency problems are due to the imbalances between supply and the demand. Some of the reasons for the imbalance are the uncertainty in the power from renewable energy resources and the load forecasts. The importance of this aspect shall further increase as the percentage of the RES in the energy mix increases. In such a scenario it is preferred that the local resources contribute to the system rescue. In order to facilitate the active role of community, a number of market models are presented in the literature. They aim to include new players like prosumers, aggregators and supplier companies in the decision making process. Among them, the Universal Smart Energy Network (USEF) defines the roles and the operational practices in the new paradigm [26].

2.2.4 Flexibility Resources

The resources in the distribution system that possess the capability of providing the flexibility shall perform a key role in the future. Their roles as flexibility resources is related to the technological advancements and regulatory standards. A general overview of the commonly existing or anticipated resources is discussed here.

Electric vehicles as storage. Recently, there has been improvements in the price performance ratio and the battery technology. It is anticipated that the economic viability of electric vehicles shall increase in the future. Electric vehicles provide unique opportunity to the electric power system for the energy storage. On average, vehicles are parked more than 22 hours a day so the charging process can be scheduled. This storage can play an active role in the peak reduction and as a reserve against imbalances in the grid. When sufficient capacity is available, this resource can be traded in the energy market as well.

Heat pump. The working principle of a heat pump is similar to that of a air conditioner or freezer but in opposite direction. Such that heat pump absorbs the heat from the surrounding cold space and and release it into warmer space. External power is used to transport energy from the heat source to the heat sink. A study has been conducted by Pacific Northwest National Laboratory (PNNL) to assess the demand response potential of the Heat Pump Water Heaters (HPWH) as compared to Electric Resistance Water Heaters (ERWH) [27]. The demand response potential is assessed on the basis of peak reduction and balancing reserves. Both are capable of providing the demand response services. However, it is observed that HPWH is 63% more energy efficient than ERWH. With the anticipated increase in the heat pumps at the distribution system, this resource proposes an interesting potential in the demand response.

Controllable loads. Along with the electric vehicles and heat pumps, additional demand flexibility can be provided by Heating Ventilation and Air Conditioning (HVAC), heating and cooling process of industries and the shift-able loads of the residential consumers. Each of these applications require a specific set of constraints that are to be considered during operation. The shift-able loads introduce inter-temporal constraints and hence the flexibility allocated at one time influences the flexibility available at other times. The internet of things is also an emerging area in which each device can freely exchange information with other. All of these resources can help in maintaining a real time balance between supply and demand.

Distributed Generation. Energy conversion technologies like power to gas and fuel cells are also becoming mature technologies. Power to gas provides opportunity to convert excessive power to gas and even to the liquid. While, fuel cells can perform the reverse process of creating electricity when required. It is possible that in future new value chains combining these aspects arise in the market. The controllable local generation from Combined Heat and Power (CHP), micro-CHP, fuel cells and gas turbines can provide flexibility in the system. A part of their local generation capability can be kept as reserves to provide ancillary services. The variable power generation comes from the RES like wind turbines and Photo Voltaic (PV). Their power in-feed can be curtailed and can be used as a flexibility option. It is generally preferred to use power curtailment as a last resort as it results in the wastage of the renewable energy.

2.3 Role of the Aggregator in the Flexibility Value Chain

The aggregator shall play a central role in the flexibility value chain of the local energy market. The role of the aggregator towards prosumers, distribution system operator, balance responsible party and transmission system operator in the smart grid context is discussed in [26]. An overview of the aggregator role in the distribution system operation is shown in Figure 2.5.

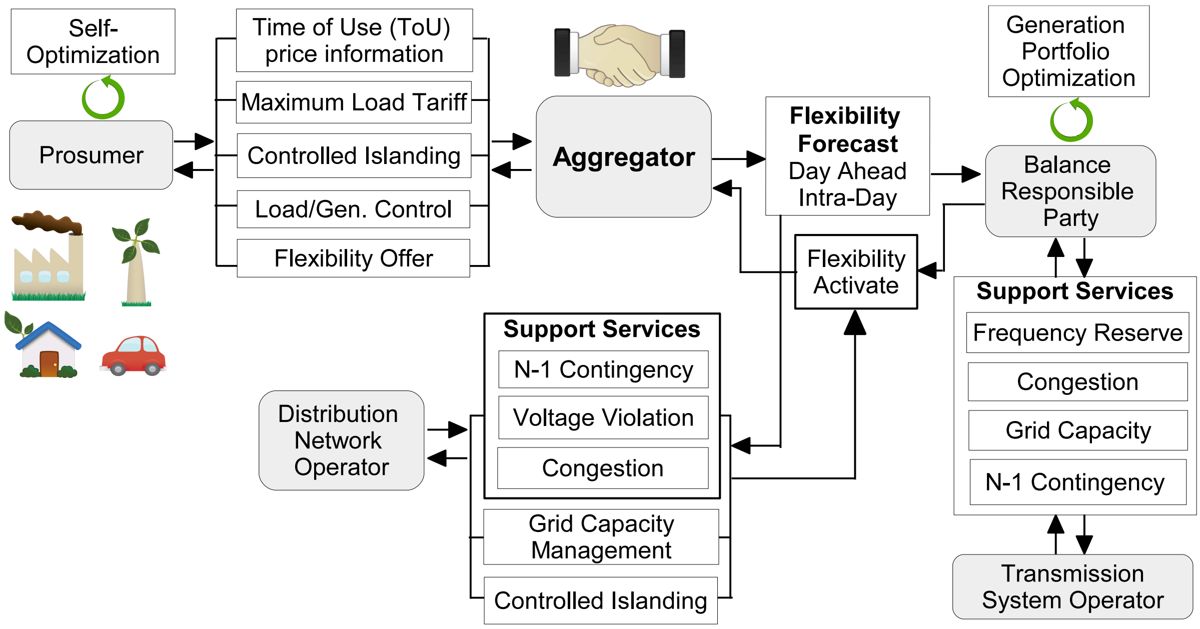

Figure 2.5: Role of the aggregator in flexibility value chain.

2.3.1 Services to Prosumers

The prosumer can represent a residential/industry/commercial customer or a distributed generator. Each prosumer may be implementing a self-optimization based on its preferences and constraints. The flexibility bid by a prosumer can possess a diverse structure that can be contractual with guaranteed availability or a capability that is probabilistic in nature. The role of the aggregator is to accumulate the flexibility bids from prosumers. Aggregator can provide input to this process in terms electricity tariff with respect to time of use. Maximum load tariff provides an incentive to the prosumers to decrease the maximum load by load shifting or load-shedding. The prosumer can save tariff cost and contribute to reducing peaks in demand. It can possess the capability to directly influence the load/generation of a prosumer while utilizing the offered flexibility. For example, the demand side management of Thermostatically Controlled Loads (TCLs) of prosumers can be used to track the reference frequency signal. Aggregator can facilitate the distribution network in case of grid outage by controlling the prosumer based on the agreed upon control schemes.

2.3.2 Services to Balance Responsible Party

Aggregator can facilitate the BRP in the day-ahead, intra-day and shorter time-scale market operations by providing the flexibility forecasts. These forecasts are used by BRP to optimize its generation portfolio and to update the generation/demand schedules dynamically to reduce imbalance charges. The flexibility offered by the aggregator can be committed by the BRP to the

TSO. Primary, secondary and tertiary reserves are activated by the TSO to counter the frequency imbalance caused by the mismatch of demand and supply. The TSO shall have the capability to trigger the flexibility from the aggregator for this purpose. This signal shall be communicated by the TSO to the prosumers through BRP and the aggregator.

There are several applications for which the flexibility can be triggered by the TSO. The congestion is the state of thermal overload of system components due to operating them at their peak ratings. Flexibility can be used to reduce peaks in energy demand/supply and hence relieve congestion in the network. It can be used for the grid capacity management such that to reduce peak load, distribute loads evenly and reduce the losses in the network. In addition, the flexibility reserves can be activated by TSO in case of a contingency.

2.3.3 Services to Distribution Network Operator

The flexibility offered by the aggregator can be used by the DNO to improve the performance and efficiency of the distribution network. It can be used to prevent the possible voltage violations and congestion in the distribution network. Recently, voltage violations have been observed in the distribution networks having high share of PV. This can happen when PV are producing at their peak output and demand is low resulting in the violation of the upper bounds of the voltage. In such situations, DNO can activate the flexibility to relieve the network. This flexibility can come from the demand response, active set-point control of a Distributed Generator (DG) or curtailment of renewable energy in-feed. If a part of distribution system possesses the islanding capability, then a DNO can use the flexibility from the aggregator to control the islanding process.

2.4 Aggregator Workflow

In the USEF market model, a hierarchical model of the future distribution system is presented as shown in the Figure 2.6. Each prosumer has a contract with the supplier about its anticipated power demand and the fixed flexibility offers in this model. The supplier generates a demand forecast based on these contracts and the historical information and provides it to the BRP. The agreed flexibility as per contract is communicated by the supplier to the aggregator. In addition to the contractual flexibility the additional flexibility offer is made by the prosumers via the cell operator to the aggregator. The aggregator is then responsible for accumulating the data about the flexibility and controlling the demand/supply of the prosumers.

Aggregator performs the portfolio optimization along with the BRP resulting in the **A-plan**. BRP uses the net demand information from supplier and the A-plan from aggregator in performing economic dispatch of generators as in the resulting in the **E-program**. The operational schedule is handed over to the TSOs and DNOs. A DNO performs the self-assessment to check whether the network constraints are satisfied considering the planned power transfer. In case of the constraint violations, e.g., distribution transformer overload, DNO can procure the flexibility from the aggregator in order to maintain a reliable operation.

Based on the USEF model, the distribution system can be divided into multiple cells that have well defined boundaries. Each cell corresponds to a control area having a dedicated cell operator. The aggregator broadcasts the current market price forecast to the prosumers via their cell operator. The prosumers optimize their operation with the user defined inputs and provides

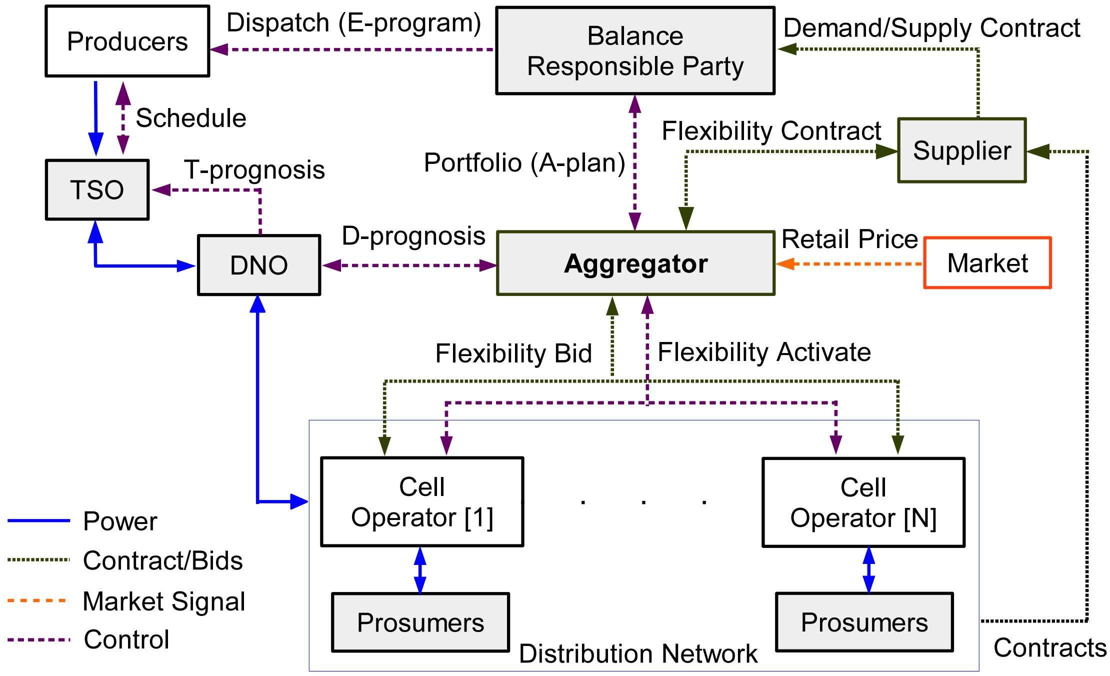

Figure 2.6: Aggregator workflow in the USEF energy market model [26].

updated information to the cell operator about their demand and flexibility. The cell operator bundles the flexibility offers from the prosumers and the associated cost and provides them as a bid to the aggregator. In response to the DNO flexibility request, the aggregator provides the available flexibility offer via **D-prognosis** to DNO and via **T-prognosis** to TSO. The **A-plan** is rescheduled if required and the **E-program** is subsequently updated [28].

The flexibility requires modeling of not only the capacity but also the dynamic capability with which the resources can be made available. It is the function of the capability of the prosumers in reducing/increasing the demand/generation. The key control variables can be active demand response, output of DGs, energy storage and curtailment of renewable energy in-feed. The USEF model provides a mechanism for activating the flexibility at the distribution side. This flexibility can be used to deal with the uncertainty in the forecast variables, particularly the renewable energy generation. A suitable control architecture is required to harness the potential of distributed resources in providing the flexibility.

2.5 Control Architectures in Distribution Network

The power system operation of the present era relies on the centralized generation. However, the increasing decentralized generation shall require new control mechanisms to enable the active monitoring and control. The control strategy primarily aims to maintain voltage and frequency within operational limits while providing additional services. These services are defined by the scope of the control scheme. As discussed in the previous Section, the aggregator shall play an important role in power system operation in future. The control in distribution network aims to enable the aggregator operations while facilitating the DNO. Among the nomenclature used for the control architecture two most common terminologies used are microgrid and cell.

2.5.1 Microgrid and Cell

Microgrid as a term is coined to refer a partially self-controlled area of electric power system that can intentionally island itself. According to Institute of Electrical and Electronics Engineers (IEEE) standard 1547.4, it is referred as distributed resource island system and is defined as , “Distributed resource island systems are parts of Electric Power Systems (EPSs) that have distributed resources and load, have the ability to disconnect from and parallel with the EPS, include the local EPS and may include portions of the area EPS, and are intentional and planned” [29]. International Council on Large Electric Systems (CIGRE) has defined microgrid as, “Microgrids are electricity distribution systems containing loads and distributed energy resources, (such as distributed generators, storage devices, or controllable loads) that can be operated in a controlled, coordinated way either while connected to the main power network or while is landed.” [30].

The concept of cell is presented in a Danish project called “Cell controller” [31, 32]. A cell is a well-defined area in the distribution network that is operating under a cell controller. This controller manages the data communication, measurements and monitoring & control systems. The goal of the cell controller it to enable the active and reactive power control to handle the voltage and frequency within the control area. According to the Cell controller project, the cell can operate in the grid connected and islanded modes. The control enables safe islanding of the cell and re-synchronization with the transmission system. In terms of this definition a cell resembles microgrid. A cell based control architecture is also presented in a European project called Electra [17, 18]. The cell is strictly defined to operating only in the grid connected mode. This definition is selected for the work in this thesis. It classifies the control in the active distribution systems as cell or microgrid based approaches. The cell is referred to having similar capabilities of a microgrid with an exception of services related to the island mode operation. In terms of operational capabilities, the cell is a subset of the microgrid. Therefore, the microgrid based control strategy is selected and discussed here.

2.5.1.1 Advantages of Microgrid

Despite operational and organizations challenges in microgrid implementation in the distribution system, following advantages have been reported in literature [33],

- Microgrid captures a system perspective for customers, utility and society. This system has the capability of achieving the socio-economic objectives. It can contribute to the integration of distributed energy resources in the system.
- Enable the localized control which can be useful in integrating increasing number of distributed generation sources in the distribution network.
- Be a specialized solution for critical or isolated infrastructure. It can also help in application of the backup strategies in emergency situations.
- Microgrid can provide the high power quality to the critical loads in a facility. Thus in case of disconnection from the main grid, the critical loads can continue to operate in a well-managed setup.
- Microgrid capability to withstand independent operation increases the reliability of the overall system.

2.5.1.2 Types of Microgrid

Microgrid can appear in large variety of scales. The important question is that what can be classified as microgrid. It can be answered by looking at the common requirements among the various types of microgrids. A review of various types of the microgrids is presented in [29]. According to it, if a distribution substation possesses the islanding capability then it can be referred as substation island. Similarly, within a substation distribution network, a circuit, lateral (primary or secondary) or a facility can form a microgrid. In [34], the microgrid is categorized in three major scales. The biggest scale is a MV microgrid that can involve multiple feeders (for example rural, residential, commercial). Then is a microgrid having a single LV feeder referred as a LV microgrid. The smallest scale can be a residential house connected to the LV feeder.

The essential ingredients for a microgrid includes on site supply-side(micro-generators) and likely demand-side resources (storage units and controllable loads). It should be capable of handling both normal state (grid-connected) and emergency state (islanded mode) operations. A controlled network area cannot be classified as microgrid if there is absence of load, micro-sources or monitoring and control. In general, a microgrid is a combination of an aggregator for DG, service provider for the network, controller for demand response and can be a regulator for controlling emissions. It is likely to perform all these functions and achieve objectives of economy, resilience and emission reduction simultaneously [34].

2.5.1.3 Microgrid Operational Modes

Microgrid has three operation modes namely, grid connected, transition and island modes [35, 36]. In the **grid connected** mode the voltage and frequency follows the main grid. The central control in the microgrid is responsible for controlling the power flow for optimal cost and reliability. It generates control signals to manage the import/export with the utility grid. During the **transition mode** the central control is responsible for ensuring the quality of voltage and frequency at the point of common coupling. During islanding event the central control may also need to perform emergency demand side management strategy. When the microgrid is re-synchronized with the main grid a number of criteria needs to be satisfied. Among others, primarily the voltage and the frequency difference should be small between the microgrid and the main grid. The **islanded mode** of the microgrid has received perhaps the greatest attention in the literature. As the name implies, microgrid in this mode operates standalone. The local controllable generators are responsible for the maintaining the voltage and frequency in the microgrid. The non-controllable or grid following generators follows the frequency and voltage as set by the controllable generators. From the control perspective there is a significant difference between control in islanded microgrid as compared to grid connected mode. Most notable differences are outlined as,

- In the grid-connected mode, microgrid is connected with the network thus there exists inertia to ensure the frequency regulation during perturbations. But it possesses significantly less inertia when operated in the islanded mode.
- Microgrid is mostly formed at low voltage network. Such networks have a significant resistive part in the network impedance matrix. In this case, the active power through a transmission line also depends on the voltage magnitude as well as the phase. Therefore, there exists coupling between the real and reactive power and they cannot be independently dealt. One of the impact of such scenario is that the fast decoupled method cannot not be used

in computing the load flow for the low voltage network having considerable resistance to reactance ratio.

- Due to relatively high percentage of non-dispatch able renewable energy sources in the generation portfolio, the reliability and security is more of a concern in the islanded mode operation. Thus sophisticated algorithms are required for precise assessment of uncertainty and the corresponding reserve requirement analysis.

2.5.2 Control Architecture

The design of control framework for the microgrid is case specific. However a hierarchical structure is emphasized in the literature [35, 36, 37], and is comprised of three main levels namely, primary, secondary and the tertiary control.

2.5.2.1 Primary Control (Frequency Containment Reserve)

The primary level control is responsible for local voltage control to ensure the proportional load sharing. This control loop is fast and typical response time is in milli-seconds to micro-seconds. The objective of the primary control at a generator is to respond to the transient variations in voltage and frequency by adjustment of its output active and reactive power. This adjustment is done according to a reference curve that relates the active power with frequency (P/f) and reactive power with voltage (Q/V) respectively. This level of control is also sensitive to the nature of the network. If the network is highly inductive, the (P/f) droop control is commonly used. While for a highly resistive network, (P/V) droop control is used to regulate the share of power of the inverter. Such cases are discussed in [38].

The operation of the primary control in the microgrid is demonstrated in Figure 2.7. The frequency deviation from the set-point is first responded by the change in active power set-point of generators. The potential of the primary control in responding to a frequency deviation in a control area is termed as frequency containment reserve.

The increase in inverter based generation from renewable energy sources limits the available inertia in responding to the frequency deviations. Virtual synchronous generators concept can be used to emulate the rotating inertia to damp out the transients in frequency. Various primary control methods have been presented in the literature to target additional objective along with the principal objective. These objectives can be classified as,

- Precise Voltage Regulation (VR).
- Decoupled handling of Active and Reactive Power given by (P/Q).
- Support for Nonlinear Load (NL).
- Robustness towards parameter deviations (RB).
- Simplicity of implementation (S_{imple}).
- Flexibility with respect to line impedance (Z_{flex}).
- Control of Harmonic Distortion (HD).

The approaches in the literature are classified in Table 2.1.

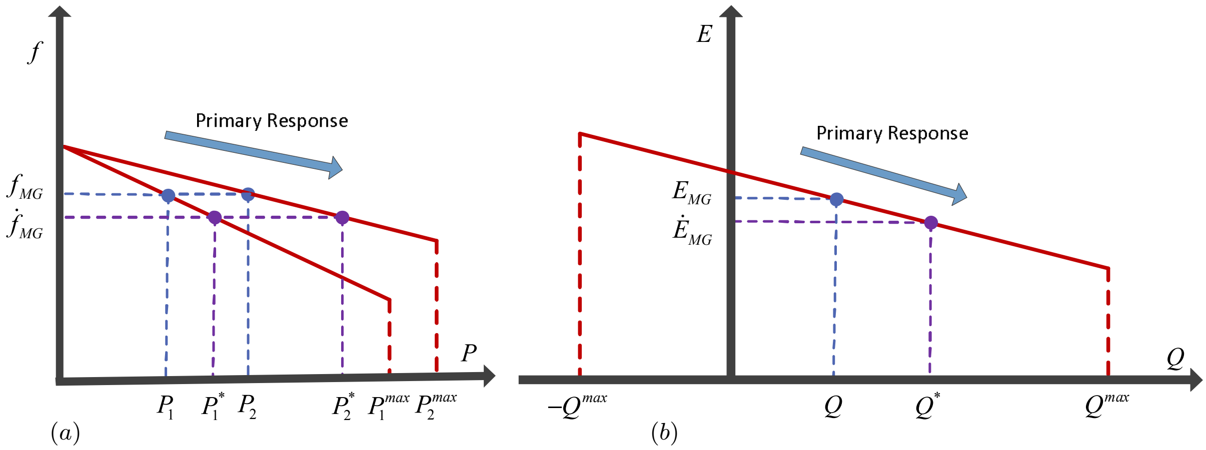

Figure 2.7: Figure (a) shows the droop relationship between the active power P produced by a generator and the output frequency f. Initially, the generators are operating at the nominal frequency f_{MG} (microgrid nominal frequency). The increase in the active load in the network causes the frequency to decrease to f'_{MG}. This droop in frequency is sensed by the generator primary control. The primary control action increases the output power of the generator 1 from P_1 to P_1^* and of the generator 2 from P_2 to P_2^*. Here P_1^{max} and P_2^{max} represents the maximum power ratings of both the generators. Figure (b) shows the droop relationship between the reactive power Q produced by a generator and the output voltage E. Initially, the generator is generating the reactive power Q and the terminal voltage is E_{MG} (microgrid nominal voltage). The increase in the reactive load in the network results in decrease in the voltage. This droop is sensed by the generator and the reactive power is increased to from Q to Q^*. Here, Q^{max} is the maximum reactive power rating of the generator. The $-Q^{max}$ is the maximum power that can be absorbed by the generator.

Table 2.1: Time evolution of primary control techniques in microgrid.

Year	Technique	VR	P/Q	NL	RB	S_{imple}	Z_{flex}	HD
1993	Conventional PF Droop Control [39, 40]					X		
2000	Signal Injection Method [41, 42]			X	X		X	
2005	Adjustable load sharing method [43]	X	X		X			
2006	Voltage P Droop / Freq. Q Boost [44]		X			X		
2010	Adaptive Voltage Droop [45]	X			X		X	
2011	Virtual Frame Transformation [46, 47]		X			X		
2012	Nonlinear Load Sharing [48, 49]			X			X	X
2013	Virtual Output Impedance [50, 51]	X		X	X	X	X	X

2.5.2.2 Secondary Control (Frequency Restoration Reserve)

The general objective of the secondary control loop is to have supervisory control over the primary control. Secondary control has dominantly a centralized structure and relatively slow control loops as compared to primary control. It uses low bandwidth communication to collect measurement data from critical points in the network. It uses this data to estimate the steady state deviations in voltage and frequency caused by the primary control in various parts of the network. The corrective control signals are then sent to the primary control loops as updated set-points [52],[37]. The operation of the secondary control in microgrid is demonstrated in Figure 2.8. The correction control action steers the frequency error towards zero increasing the frequency set-point. The potential of performing the frequency restoration by the adjustment of the reference frequency of generators is termed as frequency restoration reserve.

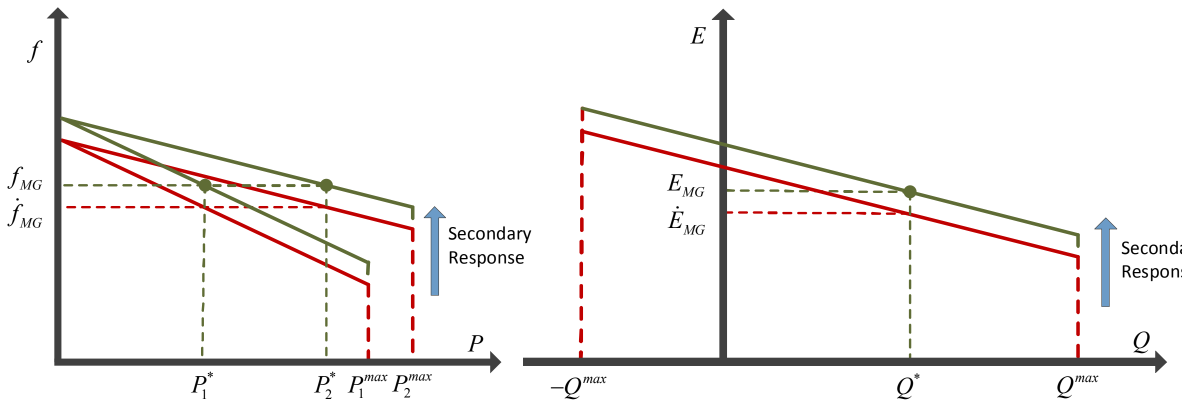

Figure 2.8: Figure (a) shows the secondary control action corresponding to the frequency droop action of primary control. It restores frequency by increasing the frequency reference of each generators to the nominal microgrid frequency f_{MG}.Figure (b) shows the secondary control action of restoring the output voltage of the generator. This is done by changing the internal voltage reference of the generator to the microgrid voltage E_{MG}.

An extensive effort is done recently to improve the performance of secondary control. The objectives like voltage control, harmonic and unbalance compensation is discussed in [53, 54]. The approach used is centralized which raises concerns for single point of failure. A pseudo decentralized scheme inspired from Networked Control Systems (NCS) is proposed in [55]. Authors propose a distributed integral controller based averaging scheme. The reactive power sharing is improved by introducing an additional loop in the local secondary control of each DG. It helps to deal with variable transmission line impedance in the system. A mathematical analysis of the hierarchical control approaches has been discussed in [56]. The important results are that distributed primary and secondary control with properly tuned droop gains (function of proportional power sharing and marginal cost) can be sufficient to perform the economic dispatch minimization. But the work in this paper assumes constant line impedance and do not consider the ramping limits on the generation. A summary of the evolution of secondary control is given in Table 2.2.

Table 2.2: Time evolution of secondary control techniques in microgrid.

Year	Technique
1988	Power deviation method [57]
1989	PLL based parallel operation of inverters [58, 59]
2000	Circular chain control [60]
2004-08	Master slave control [61, 62]
2010	Peak value based current sharing [63]
2010	Angle based droop control [64]
2012	Voltage quality enhancement [54]
2012-13	Distributed secondary control [65, 66, 67]

2.5.2.3 Tertiary Control (Replacement Reserve)

The tertiary level control in the microgrid is related to the economic optimization and overall system monitoring and control tasks. This level also controls the power quality at the point of the common coupling with the main grid particularly during grid transition phases. The dispatch optimization can include technical economic and environmental objectives [68, 69, 70].

The tertiary control activates the replacement reserves that relieves the secondary control and steers the frequency to nominal value. The tertiary reserves generally come from non-spinning generators that are offline and can be made operational generally in 5 to 30 minutes. The time requirements are however application specific. Various other sources can also contribute to this type of reserve. For example, thermal buffering in the loads can be useful. The demand response programs at the load can contribute to primary reserve in a microgrid [71]. The reserve management programs at the load end can be either direct load control or economically driven control. In addition, Electric Vehicle (EV) are envisioned to be an important element in the future distribution system. The storage from the EV can provide the needed reserves as well.

The objectives of the tertiary control spans multiple areas along with the activation of replacement reserves. The major roles of tertiary control are described as [72],

- Voltage and frequency reference dispatch for the secondary control based on the configuration of the microgrid and energy transferred with main grid.
- Issue of voltage/frequency restoration signals during and after transients.
- Sense faults in the system and initiate emergency procedures.
- The power flow control with the main grid/neighboring AC or DC microgrid or both.
- Ensure that critical loads are serviced by the available energy produced in the microgrid
- Performing the active control of loads to implement demand response strategies.
- Ensure that the microgrid satisfy the operational constraints with the utility.
- Consideration for specific requirements/limitations of each DER, including its type, cost of generation, time dependency of the primary source, maintenance intervals, and environmental impacts [73].
- Performing islanding of the microgrid in case of disturbance at manual grid or electricity price based decision.
- Coordinating DGs during black start operation and re-synchronization with the grid.
- Minimize system losses and emissions.
- Maximize the operational efficiency of the DGs.
- Provision to maintain an appropriate level of reserve capacity while rescheduling the operating points of dispatch-able DERs. The objective of the optimization problem can be to control the net power import or export with the connected grid, minimize power losses, maximize the contribution from RES, minimize the generation cost from fuel based generators.

A real time power management and control scheme for a microgrid is presented in [74]. It optimizes multiple objectives including fuel cost, dispatch able loads, emissions, while meeting the power demand and system constraints. The design of microgrid central control as enhanced version of traditional distribution management system has been discussed in [75]. The multi-objective optimization is performed after incorporating the bids from the demand side and generation side controllers. The problem address is of different nature as compared to traditional distribution management systems due to operational mode requirements by microgrid, load side bidding and energy exchanged with the main grid. The reliability indices for campus level microgrid are briefly discussed in [76]. Based on thes indices a systematic model for the supervisory control is presented in [77]. Authors present a model of microgrid consisting of PV, wind turbines, storage units and a central natural gas generation plant.

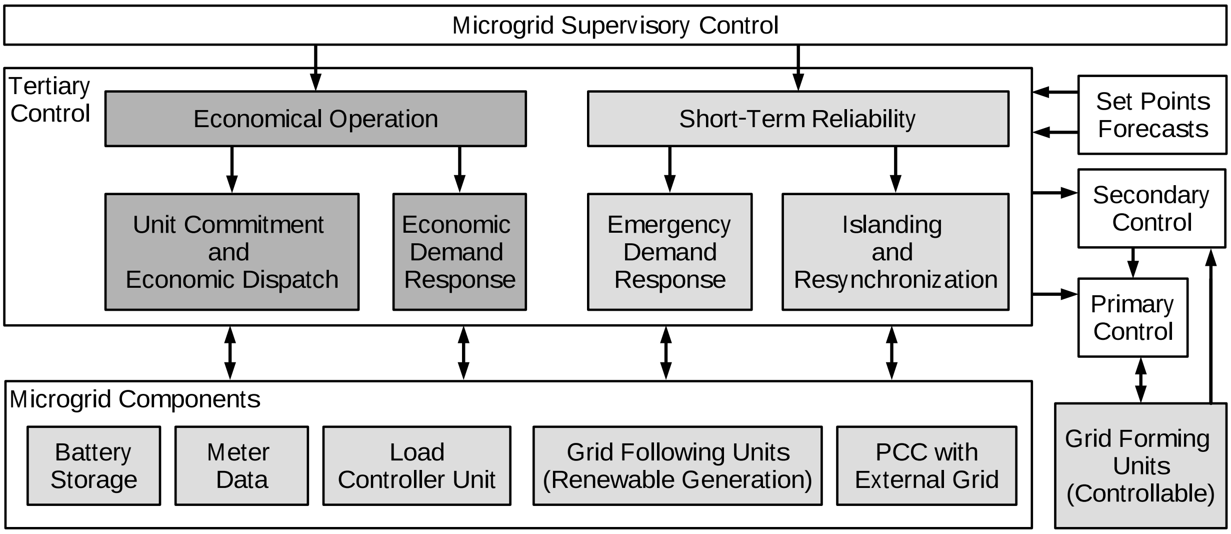

Figure 2.9: Microgrid supervisory control architecture, taken from [77].

An overview of supervisory control architecture from [77] is shown in Figure 2.9. The controllable generators are necessary for the operation of the microgrid in island mode as they play an important role in defining the frequency of the system. Such generators are dispatched in both the short term and day ahead planning similar to the power system operation. They consist of controllable (grid-forming) and non-controllable(grid-following) generators. Grid forming generators can consist of micro-hydro, CHP plants or diesel generators. They are responsible for the frequency regulation in microgrid. While the grid following generators follow the frequency of the grid. They consist of renewable energy resources like wind and solar power plants. The nature of the power produced by them is uncertain and depends on the probabilistic environmental variables. Therefore, the generation forecast is accompanied with the uncertainty. This uncertainty is needed to be incorporated in both short and long term day ahead planning. The two applications used for this purpose are called Unit Commitment (UC) and Economic Dispatch (ED). UC decide about the status (On/Off) of the generators in a day ahead schedule. While ED performs economic optimization of the set point of the active generators considering the operational constraints.

The reserve provision in a microgrid can support to the control and efficiency of overall system when it is connected to the grid. The reserve provided by online generators in case of microgrids may not be enough to deal with low inertia and volatile transients. Hence two types of generation control reserves are introduced in the system. The grid forming reserves are provided by dispatch able generators. They are typically voltage controlled. These generators are directly responsible for the voltage control and power sharing in the system. Their DC side is related to the state of the network. The primary reserve in such systems is incorporated in the rating of such generators i.e. their nominal rating is reduced by the amount of reserve that is required from them. Hence certain amount of reserve is guaranteed to be available all the time. The grid following reserve plays an important role as the grid forming reserve are used. Such type of reserve is realized by active control of non-dispatch able generation sources. These devices are current controlled devices with the reference current generated based on measured terminal voltage and the DC side. The DC side is the function of available energy and the reserve provision will add up to this DC side.

Tertiary control challenges. One of the objectives of microgrid is to provide strong foundation of local control for dealing with the uncertainty. The intermittent power from renewable energy sources and the load forecast variations influences the operation of microgrid. This influence is strong compared to large scale problem dimension due to high share of uncertain variables in generation portfolio and due to the relatively small size of the network. The information about uncertainty based reserve requirement is useful for scheduling the resources ahead of time. This is done in order to deal with the probable deviations from planned activities. The analysis of uncertainty increases the risk awareness for the operator and helps in finding an economic solution for desired confidence.

The uncertainty associated with the transients in the voltage and frequency in the microgrid are dealt at the primary level [36]. The frequency transients are supported by the rotating inertia of the generators that in turn changes the output real power. While the voltage transients are supported by controlling the level of injected reactive power. Both the task are fine-tuned by adjustment of the droop gains of the controllers at the generators. But in case of microgrid the reserve provided by online generators will not be enough to deal with the reserve requirements. Therefore, a certain amount of generation capability needs to be scheduled ahead of time for ensuring safe operation. According to National Electric Reliability Corporation (NERC), the operating reserves are defined as, “Operating reserve is the capability above firm system demand required to provide for regulation, load forecasting error, equipment forced and scheduled outages and local area protection. It consists of spinning and non-spinning reserve.” [78, 79].

The reserves from generators that are operational and synchronized with the grid frequency are called spinning reserves, while the reserve potential from disconnected resources is called non-spinning reserves. A day ahead dispatch in a power system is an optimization task that is performed by the supervisory control authority. It decides the operational schedule of controllable generators considering the forecast variables. In this aspect two algorithms are relevant, the UC and ED. UC is an optimization problem in which binary status of generators is computed for a given energy demand forecast in a time horizon. This problem is subject to generator and network specific constraints. The generator constraints involve the capability constraints of the generators that are diverse and machine specific. The network constraints include constraints like power carrying capability of transmission lines and voltage constraints on buses. The power generated from the renewable energy resources and the anticipated electricity demand are the key variables in this regard. These forecast variables are naturally accompanied by the uncertainty. Therefore, the generators are obliged to offer a certain degree of their production capability as ancillary services. The uncertainty is traditionally encountered by the reserve adjustment approach in the reserve optimization. However, due to relatively strong influence of the forecast variables in the microgrid, it is not sufficient to consider a certain percentage of the load as required reserves. The reserve adjustment approach needs to be made more dynamic and comprehensive. This advancement should be done considering the uncertainty dynamics in the local renewable generation forecast, load forecast and the equipment outage probability. The advent of electric vehicles in the network introduces additional control challenges as well as another control variable in the form of storage [80]. This variable along with the demand side management can also be useful in providing supplementary reserves in the microgrid.

The concept of microgrid was introduced to enable the operation of critical loads in the power system during blackouts and brownouts. In literature microgrid is also advocated in providing local control solution for dealing with the power quality problems arising due to distributed generation in the MV and LV network. Microgrid can also help in implementing the attractive market models to facilitate the increase in renewable energy in the system.

For the remote area applications like vacation houses or distant villages the cost of installation of a transmission line is high. A microgrid in such as scenario can provide energy solutions. The building controller may implement a microgrid scheme in managing the local energy demand and purchase of electricity from main grid. One of the application at a university level has been implemented with good results in [77]. If the microgrid is disconnected from the main grid then the local control can support the critical applications locally.

The application of microgrid as a generic approach in the distribution grid is faced with the regulatory and technical challenges. When a part of distribution system either at MV or LV level is disconnected from the main grid, the current grid code requires that all the distributed generators connected should be disconnected from the network. Assuming that the microgrid is in place and in case of islanded mode the microgrid central controller takes the control of distributed generation, there exists substantial operational challenges due to small inertia and limited generation capability. The operational standards related to the microgrid are also currently in the developing phase.

2.6 Flexibility in Supervisory Control

Among supervisory control applications, the focused areas are shown in the Figure 2.10. The reserve requirements are assessed in the microgrid while considering its dynamics. For this purpose, a number of scenarios of demand, supply and availability are created. The overall demand and reserve requirements in the microgrid are then modeled by an envelope among the first order dynamics variables of power, ramp-rate and ramp duration variables. This leads to an economic flexibility assessment approach in the microgrid that considers the correlation between the dynamics variables. Secondly based on the given demand, the reserve requirements are assessed and allocated among available resources.

In order to model resources in the microgrid, a generic model for a flexibility is presented. The energy storage potential of the resource is modeled with a battery while the operational capability and associated costs are modeled by an envelope. A Polytope is selected as the envelope of choice after comparing the alternatives. The demonstrative example uses this model for Thermostatically Controlled Loads (TCLs). The resources having demand response potential can be described controllable loads. A load controller can have multiple resources e.g., TCLs, EV in its aggregation. The load controller can communicate with the supervisory control and potentially implement a frequency regulation service. The flexibility bid from the load controller should sufficiently represent the energy storage characteristic, stochastic availability and the associated cost. It is desired that when the flexibility from the resources in the network is utilized, it does

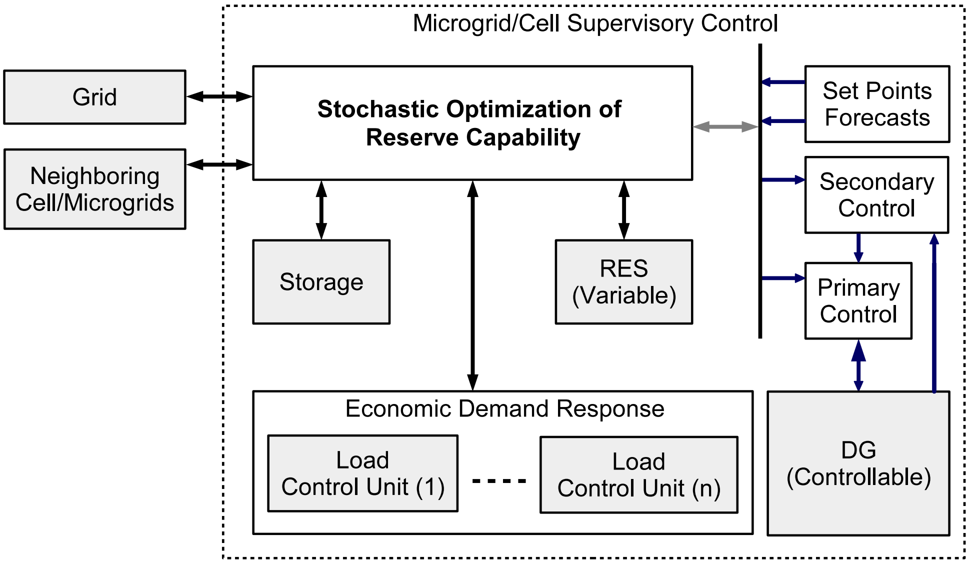

Figure 2.10: This Figure shows the stochastic optimization model for microgrid. This thesis contributes to reserve planning, the results of which are incorporated in UC and ED applications. Moreover, methods are designed to facilitate the demand response potential as the secondary frequency reserve.

not lead to constraint(voltage) violations. This aspect has been considered as a constraint in the demand side management applications.

When a microgrid is connected to the distribution grid the supervisory control is also responsible for the optimizing the value of energy exchanged with the distribution grid. It can be performed by considering the price of local electricity generation in comparison of cost of electricity from distribution grid. This in turn shall also allow to incorporate the available reserve capacity available from distribution grid. The power transfer capacity of the coupling transformer can be considered as a constraint in this regard.

3 Uncertainty Modeling for Flexibility Assessment

3.1 Introduction

Provision of the distribution side resources in providing flexible reserve services can propose a local and cost effective solution to address the uncertain and volatile nature of the power generated from Renewable Energy Sources (RES) [81]. A control mechanism in the distribution system can provide a platform for aggregating the reserve flexibility from the resources and performing their coordinated control for the secure and reliable operation. The microgrid is considered as an attractive choice among various control mechanisms discussed in literature [82]. Among the objectives of microgrid or cell based control in the electric distribution system is to provide a strong foundation of local control for dealing with the increase in uncertainty from generation and consumption of electricity. The forecasts of intermittent power from renewable energy sources and the load variations strongly influence the operation of microgrid. The microgrid is expected to have a high share of uncertain power from RES in its generation portfolio. Furthermore, the advent of electric vehicles shall introduce further uncertainty in the load characteristics. The impact of overall uncertainty in the *net-demand* shall be a significant player in determining the reserve requirements in the microgrid.

The distribution system can be considered pre-dominantly in the steady-state. The steady-state is defined by a "snapshot" of the variables like voltage, power etc. at the buses in the network. Although most of the variables are time varying but the variation is small enough to justify the consideration of power system algebraic model. The set of variables defining the steady-state are load/generation values, switching status and other dynamic variables. A local forecast of the *net-demand* is performed in order to determine the schedule of generation sources to meet the electricity demand and to plan the power import from the grid. The information about uncertainty in forecast variables is important for the scheduling of resources in order to deal with the deviations from planned activities. This information increases the risk awareness for the control entity and helps in finding an economic solution in the stochastic environment that leads to safe and reliable operation of the microgrid.

The resources are scheduled based on the *net-demand* and associated uncertainty forecast. This analysis is obtained by the study of historical information and the probabilistic models of the uncertain variables. From this analysis, the worst case scenarios are obtained that corresponds to the maximum system loading. Following can be the general requirements for determining the worst case scenarios in a microgrid application,

- The probabilistic model of the uncertain variables should preferably capture the *spatial* i.e., variation in level) and *temporal* i.e., variation with time aspects of uncertainty in generation and demand.
- The number of scenarios selected during the resource planning should define a probabilistic guarantee on the results.
- The requirement of flexibility should preferably consider the dynamics along with the level of uncertainty.
- A mechanism for the stochastic constraint formulation is required for a deterministic formulation of the stochastic problem.

These questions are answered by the study of uncertainty type and the associated optimization problem in the active distribution system. This is followed by the model of uncertain *net-demand* for a microgrid test case. The contents of this chapter are partly published in [83].

3.1.1 Uncertainty in Distribution System

The uncertainty in a variable is an unexpected deviation in its status and the goal of uncertainty modeling is to quantitatively represent it. Authors in [84] and [85] provide a general classification of uncertainty. Based on these papers and the general literature in relevance, the uncertainty in distribution system can be broadly classified into three categories,

1. **Forecast uncertainty.** The uncertainty in forecast of power from renewable energy sources, load and market price of electricity.
2. **Uncertainty due to unplanned events.** The contingency (out of service condition) of a line, generation unit or load that leads to unplanned changes in available transmission capacity, generation potential or load requirements. A drastic change in market forces, energy price and other unforeseen interruptions including sensor failure can also be classified in this category.
3. **Modeling uncertainty.** Measurement accuracy of the power system parameters like voltage, power etc. are in this category. These can be due to discretization error and/or faults. The error in state estimation also belong to this category that is influenced by the number of observable values in the distribution system along with the accuracy of the measurements.

3.1.2 Uncertainty Modeling Methods

A rich spectrum of uncertainty modeling methods have been developed in literature and used in practice. The objective of these methods were two folds, firstly, a sufficient representation of the uncertainty and secondly, to assess the impact of uncertainty on the process output. Factor influencing selection of the uncertainty modeling methods are the availability of historical data, accuracy of modeling approach and the support for correlation between uncertain variables. The classification of uncertainty modeling methods is given in Figure 3.1.

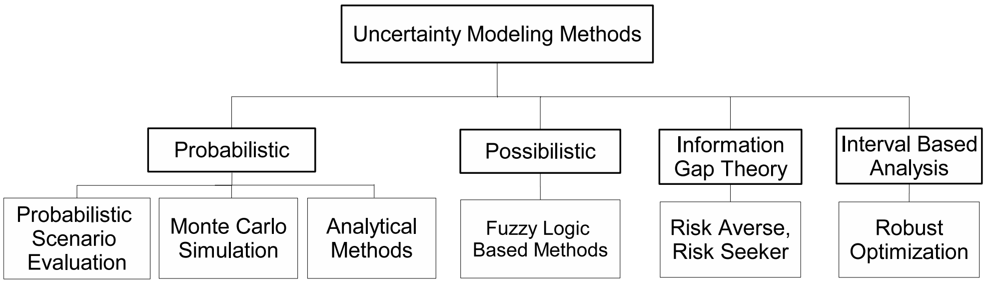

Figure 3.1: Breakdown of the uncertainty modeling approaches.

There are generally two types of uncertainties, the *quantitative uncertainty*[1] and the *qualitative uncertainty*[2] [86]. A review of the modeling methods with the perspective of type of uncertainty, availability of sufficient historical information and problem structure is given in Table 3.1.

Table 3.1: Categorization and methods in the uncertainty modeling.

	Deterministic methods		**Heuristics based methods**	**Set theory based methods**	**Uncertainty boundary based methods**	
					Interval boundaries	Interval boundaries
Method Type	Probabilistic Methods		Possibilistic Methods	Information Gap Decision Theory	Interval Based Analysis	Robust Optimization approach
Uncertainty Modeling	Probability Distribution Function, Cumulative Distribution Function, Markov Chain.		Linguistic definition with fuzzy limits	Uncertainty Sets	Uncertainty Intervals	Uncertainty Sets
Uncertainty Impact Analysis	Numerical Methods	Analytical Methods	α-cut, Defuzzification	Risk Averse, Risk Seeking Methods	Interval Based Analysis Techniques	Adaptive Robust Optimization
	Monte Carlo Simulation	Convolution, Cumulant, Taylor series, Scenario based methods				

The uncertainty modeling methods are briefly discussed here,

Probabilistic methods. The probabilistic methods are applicable when the probability distribution of the uncertain variables can be approximated from the historical data. For example, the wind speed patterns can follow a Weibull Probability Distribution Function (PDF) [87] and load uncertainty in some cases can be modeled by the normal PDF [88]. If the probability distribution is not known then the Markov chain based methods can be used. Once the analytic model of the uncertainty is known, there are two approaches for obtaining the impact on uncertainty of the output. The first approach is numerical and involve Monte Carlo simulations. A scenario set is constructed based on a desired criterion in this process. The uncertain variables are sampled from their respective distributions or models to create this scenario set. The system output is evaluated for each case in the scenario set. This method is relevant when the system is complex and a relationship between output and input uncertainty is analytically difficult to obtain [84]. In [89], sequential Monte Carlo was used to evaluate the impact of wind on the power distribution system. The second approach is to evaluate the output of stochastic process analytically. For

[1]The uncertainty associated with numerical terms quantified by a mathematical function with deterministic parameters.

[2]The uncertainty expressed initially as linguistic non-numeric value such as “near to” or “in between”.

example, convolution based method is one of the analytical approach that can be used to obtain the PDF of output based on the PDFs of input variables [90]. Other analytical methods like cumulant, taylor series and others are reviewed in [84]. A cumulant based method is proposed in [91] for the stochastic optimal reactive power planning in the distribution system having high share of wind power.

Possibilistic methods. The possibilistic methods were first introduced in [92]. In this method, the uncertain parameters are characterized by linguistic categories having fuzzy limits. Here, the Membership Function (MF) describes possibilistic uncertain variable. Methods like $\alpha-$cut are used to find the MF of output if the input MFs are known. The possibilistic methods are useful in case when appropriate PDF of the uncertain variable is not known due to inadequacy or imprecision of the data. These methods also facilitate in modeling the impact of an external parameter on the system. Possibilistic methods in the distribution network have been used for multi-objective planning with fuzzy economics and level of reliability in [93]. A fuzzy evaluation tool was proposed in [94] for analyzing the impact of investment and operation of Distributed Generator (DG) on active power loss and the adequacy of the load supply capability in distribution system.

Information gap theory. Information gap theory can be applied if the PDF or MF of the uncertain variable is not known. There are two major methods used in this theory. Risk averse method is used to set the decision variables in order to avoid the risks. The objective is to make robust decisions while considering the maximum radius of uncertainty. The other method is called risk seeker in which the decisions are set in a way to maximize the impact of perturbation in the uncertain variable hence defining the boundaries of possible outcomes. The information gap theory has been discussed in [95] to help the Distribution Network Operator (DNO) in selection of supply resource for meeting the demand of customers. The volatility of High Voltage DC (HVDC) connected wind power generation was studied using this theory in [96].

Interval based analysis. The upper and lower bounds for the uncertain variables are defined in the interval based analysis method. These intervals can be used in the robust optimization to find the interval limits on the output variables. This method is applicable if the variables are un-correlated. The uncertainty in load demand is studied by an interval arithmetic approach based on probabilistic distributions [97]. In this paper, the interval arithmetic approach is used to consider the load uncertainty in the radial distribution system.

Robust optimization approach. This method is relatively new in solving optimization problems having uncertainty in variables. In the robust optimization, it is assumed that PDF is not available for the uncertain parameter X. It is defined by the uncertainty set $X \in U(X)$, where U is the set from which X can be taken. The robust optimization seeks to optimize the objective while ensuring that the result is valid with high probability for the values of X in set $U(X)$. A two-stage adaptive robust model is presented in [98] for the security constrained Unit Commitment (UC) problem. An adaptive robust optimization model for a multi-period Economic Dispatch (ED) is proposed in [99].

3.2 Stochastic Optimization in Control

State estimator is the base of control applications implemented in Distribution Management System (DMS). The state estimator implements the power flow algorithm that aims to determine the real and reactive power flows in each transmission line. Input to this process is the active & reactive power and voltage information at each bus in the network. A detailed power flow formulation can be consulted from [100]. The power flow model represents the distribution network under a microgrid by a system of non-linear equations. In particular, the state (magnitude and angle) of the bus voltage $\mathbf{X}$ and the apparent power (active and reactive power flow in each branch) $\mathbf{Z}$ can be calculated for a set of inputs. The inputs are active and reactive power injection at each bus $\mathbf{Y}$ according to Equation 3.1,

$$\mathbf{Y} = g(\mathbf{X}), \quad \mathbf{Z} = h(\mathbf{X}) \ . \tag{3.1}$$

3.2.1 Stochastic Optimization Applications

The common optimization applications that can be relevant for an active distribution system are optimal power flow, economic dispatch, unit commitment and Volt-Ampere Reactive (VAR) optimization with uncertain reactive load. The uncertainty in variables leads to a stochastic formulation of these deterministic problems.

Power flow analysis. The steady state power flow analysis assumes the deterministic values of input variables where the associated uncertainty factor is not considered. However, for a highly dynamic scenario i.e., in case of a distribution system having a volatile renewable based generation, neglecting the uncertainty can result in an unrealistic output of the power flow process. This limitation can be overcome by a probabilistic power flow formulation of the problem. It was first presented in [101] and it models the input data like uncertain loads and generation using probabilistic models and calculate PDFs of the line flows. The mathematical treatment of this problem is discussed in [102].

Optimal power flow. The goal of Optimal Power Flow (OPF) is to find the optimal settings of the controllable parameters in the power network in order to optimize the objective function. The objective function can be among minimization of the electricity generation cost, system losses, bus voltage deviation, minimization of the emissions from generators, load shedding, system security and equipment operating limits [102]. The control variables can include generator output power and voltage, transformer tap settings, phase shifters, switchable capacitors/reactors and others. The OPF problem is composed of the system of equations from the general power flow combined with selected constraints and desired objectives. The probabilistic OPF methods allow the consideration of the probability distribution of uncertain variables. One of such methods is a two-point estimate method. It considers the interval uncertainty and evaluate the deterministic OPF for the limits of each uncertain variable.

Economic Dispatch. ED is an OPF problem in which the objective is the minimization of generation fuel cost. The classic ED problem does not consider the transmission line capacity constraints. The consideration of network security constraints makes it as security constrained ED problem. The stochastic factors effecting ED are the uncertain loads and inaccurate fuel cost function along with the uncertainty in the network elements. Stochastic model [103] and fuzzy ED methods [104] aims to solve the probabilistic ED problem.

Unit Commitment. UC is an optimization problem in which binary status of generation units is optimized for a given energy demand forecast. The objective of this problem is minimizing operational cost and satisfying system demand, reserve requirements and generators start-up/shut-down constraints. The uncertainty in this problem depends on the time scale under consideration. The time scale are long term regulation (1 to 2 years), intermediate term (6 month to 1 year) and short term dispatch (1 day to 1 week) [102]. The factors influencing are the uncertainty in load, unit availability and resource availability. In literature the approaches used are the robust and chance constrained UC methods.

VAR optimization with uncertain reactive load problem. The VAR optimization is an OPF problem in which the objective is minimization of real power loss in distribution system and improving the voltage profile by the dispatch of reactive power from generators. The uncertain reactive load and the potential of generators make it a stochastic problem. The reactive load uncertainty is considered using fuzzy sets in [105]. A heuristic method is applied using sensitivities with the objective of minimizing the adjustments in control variables.

3.2.2 Stochastic Optimization Methods

The classic way of incorporating uncertainty in an optimization process is by the consideration of worst case scenarios. It can lead to a robust result but at the high price associated with the conservative margins. Other approaches have been to intentionally tighten constraints that can reflects the confidence against uncertainty. However, as the level of uncertainty increases, there is a strong need of approaches that can model the uncertainty during optimization process. The stochastic optimization methods can be classified into three categories, scenario based, robust and chance constrained optimization.

Scenario-based optimization. The scenario tree based approach formulates the uncertainty instances as deterministic branches of a tree. Thus the key benefits are that the resulting problem is a large scale deterministic optimization problem. In [106] and [107], authors have discussed the impact of uncertainty in wind forecasts on the generation dispatch problem. The scenario based approach is performed after the first stage of UC optimization has been performed. The scenarios are then included by considering a known distribution in correspondence with the volatility of wind. Benders decomposition is used to accommodate the changes from the base case in an iterative manner till the problem becomes feasible. According to [108] the scenario based approaches have two drawbacks. Firstly, it is assumed that the probability distribution of the forecast uncertainty is already known. Secondly, a large number of scenario samples is required to obtain a reasonably high confidence in results.

The scenario-based optimization defines a scenario tree that emerges from uncertainty instances. Consideration of the high number of possible scenarios results in a large problem size. The authors in [106] and [107] have proposed the scenario based approach for incorporating the uncertainty in wind power. The volatility of wind forecast is modeled by a uncertainty distribution that is sampled to generate scenarios. The base case is defined based on the UC results. Changes from this base case corresponding to the uncertainty scenarios is incorporated using benders decomposition method. It is an iterative process that converges to a feasible solution. The drawbacks of scenario based approach are discussed in [108]. Firstly, the probability distribution of the uncertainty is to be knows and secondly, the large number of scenarios needs to be generated and addressed in order to ensure sufficient confidence in results.

Robust optimization. In this approach, the deterministic algorithm includes an uncertainty set that consists of worst case scenarios which are to be avoided. So the solution is searched in a reduced search space. However, this often leads to over-conservative solutions as the worst cases are dealt irrespective of their probability. In [109], the approach is to add a budget to uncertainty in order to adjust the degree of protection from the adverse situations. But the modeling this approach is non-trivial.

In the robust optimization, only the worst case scenarios are considered. The deterministic optimization problem is evaluated for these scenarios and a reduced search space is searched for solution. The consideration of worst case scenarios irrespective of the occurrence probability leads to over conservative results. The uncertainty has been quantified in [109], where it defines the degree of confidence against uncertainty.

Chance constrained optimization. The chance constrained optimization aims at to trade-off between cost and robustness with uncertainty consideration. In this method, a probability is associated with violation of a constraint involving the uncertainty. This probability is used to define sufficient number of scenarios. The worst cast in the scenarios are considered in the deterministic formulation of the optimization problem. Hence, chance constrained optimization combines the benefits of scenario based methods and robust optimization. The uncertainty scenario set is associated with the probability of uncertain events and the confidence in results. Such an approach of defining uncertainty sets in the reserve allocation problem has been presented in [110]. The approach used is for the single time intervals and hence can be termed as Independent Chance Constrained Optimization (ICCO). The consideration of multiple time periods can improve the results in case of time dependent variables. Such an approach is referred to Joint Chance Constrained Optimization (JCCO). The JCCO requires generation of scenarios considering the time correlation of the uncertainty and hence is computationally intensive. The formulation of uncertainty sets have been discussed in [111] and can be considered for ICCO/JCCO problems. A JCCO solution has been proposed in [112] to the hydro thermal system having probabilistic constraints. The approach is inspired from [113] that prioritize the inequalities to reduce the problem size. The ICCO had been used for modeling the uncertainty in demand and generation from RES in this thesis. The time correlation was considered by modeling the uncertain variables using the Markov chain.

3.2.3 Reserves Against Uncertainty

Among the various optimization approaches effected by the uncertainty, this thesis focus on two applications, the stochastic UC and ED. In these problems, resources are scheduled to meet the energy demand while considering the uncertainty. The uncertainty in forecast of power from renewable energy sources like Photo Voltaic (PV) and wind along with fluctuating demand makes it essential to address them during resource planning and allocation. The uncertainty in these processes are traditionally handled by a reserve adjustment approach. A part of generation potential is reserved in this approach, and is ready to be supplied in order to balance the supply and demand. This type of reserve is usually a percentage of the nominal power of generator. The control system in an active distribution network shall also need to plan resources against an outage of a generator, line or load. This reserve can be obtained from the grid or using local resources. Such type of reserves is called contingency reserves. The classification of reserve types and their roles are different for countries and regions. A comprehensive review of the reserve types can be found in [114]. An overview of the reserve types is shown in Figure 3.2.

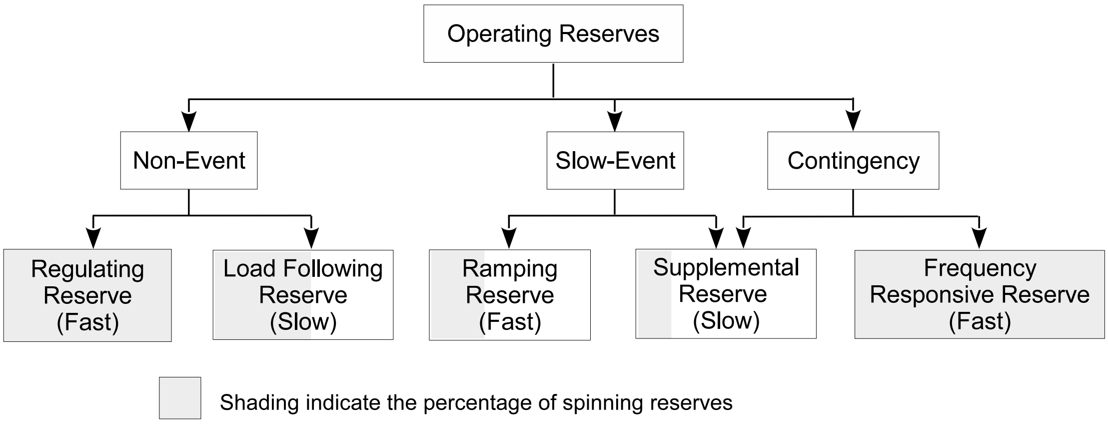

Figure 3.2: Reserve types and their contribution to spinning reserves [114].

Regulating reserve is the available on-line generation capacity margin to cater for the forecast errors. This type of reserves is activated by the Automatic Generation Control (AGC) action and aims to maintain balance between supply and demand. The imbalance is reflected as change in frequency. Hence, the regulating reserves can also be termed as primary frequency reserve. Part of demand that is responsive to frequency deviation can also contribute to the regulating reserves. The load following reserve consists of a combination of spinning and non-spinning reserves. They can also be termed as secondary frequency reserves. This type of reserve is slow as compare to regulating reserves.

The slow event is an event that takes a time duration during which resources can be made operational. For example, a sharp decrease in power from the wind farm shall require the generation resources to ramp-up quickly. Therefore, the ramp-up potential of the resources should be able to meet the requirements in real-time. If this requirement is not met, then the supplemental reserves can be activated. The resources that can participate as supplemental reserves can be off-line generators, load-shedding schemes, emergency demand response and others.

The contingency reserve is the amount of spinning and non-spinning reserve that is available to be deployed by balancing authority to meet the requirements in case of component outages. The component can be a generator, line, bus or any other significantly impacting element in network. According to [115], at least half of the contingency reserve must be spinning reserves. While the additional requirements can be met on a relatively slow activation time using supplemental reserves.

A tentative value of the spinning reserve is defined a-prior to the optimization process of resource scheduling. This value is defined as an addition to the *net-demand*, which is the aggregate demand in the network. The reserves planned against the uncertainty in *net-demand* aims to cover the maximum possible value of error considering the historical record. The interval based approach for defining the capacity, ramp-rate and ramp duration of the *net-demand* has been discussed in [14]. This approach can be used for defining the spinning reserve capacity and ramp-rate requirements. However, during studies it is found that using this approach in the smart distribution system can lead to conservative requirements that can result in high cost. This situation can arise due to relatively small value of *net-demand* (kW to few MW) and high share of uncertain variables in the power balance. Therefore, an elaborate mechanism of uncertainty specification is required that can improve the economics in the reserve allocation process. The contributions in here aims towards,

- An economic specification of spinning reserve requirements due to the forecast uncertainty. It aims towards the modeling of regulating and ramping reserve.
- The modeling of demand response in the distribution system to operate as load following reserve in order to contribute as a load following reserve resource.

3.2.4 Stochastic Constraint Formulation

This section discusses how the probabilistic power balance constraint in the microgrid can be handled using chance constrained optimization theory. The forecast uncertainty in the variables of load, wind and PV power was combined together to model the lumped uncertainty in microgrid. The approach can be extended to other sources of uncertainty as well. The power balance in the microgrid and associated uncertainty is given as,

$$\Delta P^t = \Delta P_D^t - \left(\Delta P_w^t + \Delta P_{PV}^t\right) \quad . \tag{3.2}$$

Here, ΔP_w^t, ΔP_{PV}^t and ΔP_D^t are the wind, PV power and demand uncertainties. The lumped uncertainty in the *net-demand* is given by ΔP^t during t^{th} hour. The power balance equation is given as,

$$\sum_{i=1}^{N} P_i^t = P_D^t - \left(P_w^t + P_{PV}^t\right) + P_{\text{loss}} \quad , \tag{3.3}$$

where, the power generated by the i^{th} generator is given by P_i^t. The active power limits of i^{th} generator are given as,

$$\underline{P_i} \leq P_i^t \leq \overline{P}_i \quad , \tag{3.4}$$

here, the maximum and minimum power ratings of a generator are given by $\overline{P}_i$ and $\underline{P_i}$. A sufficient amount of reserves should be contributed by each generator to meet the overall reserve requirements. The constraint modeling this aspect is given as,

$$SR_i^t \;\leq\; \overline{P}_i - P_i^t \quad , \tag{3.5}$$

$$\sum_{i=1}^{N} SR_i^t \;\geq\; \Delta P^t \quad . \tag{3.6}$$

The reserve contribution by each generator should satisfy its ratings and is given by Equation 3.5. While, the sum of flexibility contributions should be sufficient to meet the overall reserve requirements as given in Equation 3.6.

The reserve requirements in Equation 3.6 are stochastic and hence results in a probabilistic constraint formulation. A generic form of such a formulation as part of optimization problem can be given as,

$$\begin{aligned} &\min_{x\in\mathbb{R}^{n_x}} \; J\left(x\right) \quad , \\ &\text{s.t.:}\; \mathbb{P}\left(\delta\in\Delta \mid \max_{s=1,\ldots,M} g_s(x,\delta)\leq 0\right)\geq(1-\epsilon) \quad . \end{aligned} \tag{3.7}$$

The objective function is a mapping that is given as $J\colon \mathbb{R}^{n_x}\to\mathbb{R}$, while the inequality constraint function is $g_s\colon \mathbb{R}^{n_x}\times\Delta\to\mathbb{R}$. The inequality constraint function involves the uncertainty given as $\delta\in\Delta\subseteq\mathbb{R}^{n_\delta}$. Here, the uncertainty scenarios were sampled from the envelope defined by Δ. The constraint satisfying Equation 3.7 can be referred to as ϵ level feasible solution [116], where, the ϵ defines the probability of constraint violation. It decides the number of sufficient scenarios (S) that results in the uncertainty envelope Δ. The decrease in desired probability of constraint violation increases the number of scenarios and hence the likelihood of rare event occurrence. This approach stems from the chance constrained optimization theory that prevents the requirement of probabilistic distribution of uncertain variables. It also avoids modeling complexity for handling the correlation between such variables. This being a scenario based approach associates the constraint satisfaction probability $(1-\epsilon)$ and the confidence in results $(1-\beta)$ with the number of scenarios S [116],

$$S \geq \frac{1}{\epsilon}\left(\frac{e}{e-1}\right)\left(\ln\left(\frac{1}{\beta}\right) + 2 * n_\delta - 1\right) \ . \tag{3.8}$$

Here, e is the Euler constant and n_δ is the number of uncertain variables. Probabilistic parameters of $(1-\epsilon)$ and $(1-\beta)$ are in the range of $(0,1)$. Such an approach quantifies the probability with the number of scenarios and can be scaled for a given problem.

The interval based approach can be used to define the uncertainty limits in case of un-correlated variables. In such a case, Δ is a bounding box defined as, $B^* := \times_{u=1}^{n_\delta}\left[\underline{\delta_u}, \bar{\delta_u}\right]$. The vertices of B^* defines the reference points for the uncertainty [116]. The Equation 3.7 for such a case is given as,

$$\begin{aligned} \min_{x\in\mathbb{R}^{n_x}} \quad & J(x) \ , \\ \text{s.t.:} \quad & \max_{s=1,\dots,M} \quad \max_{\delta\in B^*\cap\Delta} \ g_s(x,\delta) \leq 0 \ . \end{aligned} \tag{3.9}$$

The inequality constraints are considered at the vertices of B^* as representative of δ [14]. However, if the correlation between uncertain variables exits then the interval based approach cannot be used. An geometric based approach can be used to define the uncertainty envelope, resulting in a general formulation given as,

$$\begin{aligned} \min_{x\in\mathbb{R}^{n_x}} \quad & J(x) \ , \\ \text{s.t.:} \quad & \max_{s=1,\dots,M} \quad \max_{\delta\in\Delta} \ g_s(x,\delta) \leq 0 \ . \end{aligned} \tag{3.10}$$

Here, the inequality constraint needs to be satisfied for the uncertainty instances (δ) within the envelope (Δ). The Equation 3.8 is probabilistic as it is based on the uncertainty envelope. Equation 3.6 transforms to,

$$\mathbb{P}\left(\sum_{i=1}^{N} SR_i^t \geq \Delta P^t\right) \geq (1-\epsilon) \ . \tag{3.11}$$

Equation 3.11 states that the reserve allocated should be sufficient to cover the uncertainty envelope characterized by Δ. Hence the reserve requirements can be related to the probability of constraint satisfaction, given as $(1-\epsilon)$.

The forecasting methods can be classified as linear/nonlinear regression, probabilistic time series and neural networks based methods. This thesis focuses on probabilistic time series based methods. A Markov chain based approach has been used in [117] to model the time series correlation of the uncertainty. This captures the *temporal* aspect of forecast uncertainty. The *spatial* aspect of the uncertainty can be related to the probabilistic model of the variable. If historical information about the uncertainty is related to the forecast level, then appropriate clustering methods are required.

While modeling the forecast uncertainty in the *net-demand* of microgrid, it was observed that the uncertainty is related to the forecast value. Therefore, a binning strategy was used to classify the uncertainty based on the forecast magnitude. The aim had been to model both the *spatial* and *temporal* aspects of uncertainty. The number of scenarios were selected using chance constrained optimization theory [116] for given probability specifications.

3.3 Flexibility Assessment in Microgrid

This section discusses the methodology for modeling the forecast uncertainty in microgrid. It lead to an assessment of required flexibility in terms of demand and reserves requirements. The result was a probabilistic envelope among the variables of *net-demand* values, associated ramp-rate and ramp duration variables.

3.3.1 Scenario Generation

The measurement of uncertainty in a forecast variable needs to be generalized in order to combine the uncertainty from various variables. Therefore, it is taken as the percentage deviation from the forecast value. The analysis of historical data leads to an observation that the percentage error is related to the forecast level. Such that low forecast levels experience high percentage error as compared to high level. Therefore, using a single probabilistic model for the range of the forecast values may not be appropriate. The uncertainty values are clustered based on the forecast levels using a binning structure. Equidistant levels of the forecast data are considered for this purpose. The probability distribution of uncertainty in each forecast cluster may not be know and hence the application of a non-parametric probability density approach is preferred. Here, the empirical Cumulative Distribution Function (eCDF) from [14] was used to model uncertainty in each forecast cluster.

Markov chain based approach was used to capture the correlation between time-series data of uncertainty. The Markov chain defines the probability of occurrence of an event given the occurrence of previous events. A second order Markov chain had been used here. It is represented by a Transition Probability Matrix (TPM) [117]. Algorithm 3.1 models the *spatio-temporal* aspects of the uncertainty. This model had been used to generate the *net-demand* scenarios in microgrid.

The dynamics of scenarios can be represented by the flexibility metrics. A metric based on the first order dynamics i.e., power, ramp-rate and ramp duration had been discussed in [14] and [15]. An interval based approach is used to model the variation across these variables. This approach results in a hyper-rectangular model among the three variables. The vertices of the rectangle represent the requirements in terms of demand and reserve. It is well suited for power system applications with large number of variables as the computational burden is only limited to the vertices. However, the approach is conservative as it considers a uniform ramp-rate requirement for all demand values. Similarly, maximum ramp duration requirement is associated with all demand and ramp-rate values. Such an approach can lead to a safe operation of the system but at a high expense. The situation is different for a microgrid or a local control in the distribution system. A microgrid is likely to have limited resources in terms of generation. Using the interval based approach for the demand and reserve assessment can result in a high cost. Another aspect is that the ramp-rate and ramp duration requirements are correlated with

Algorithm 3.1: Uncertainty modeling algorithm.

The forecast data is clustered among F clusters based on the magnitude;
The forecast error is modeled using eCDF for each cluster;
for $f := 1 \cdots F$ **do** *(Forecast error limit loop)*
    The eCDF of f^{th} cluster is sampled S times;
    The boundary values of uncertainty in each forecast cluster is obtained as L_f;
end
The time series correlation in the uncertainty is modeled using a TPM for second order Markov chain;
for $s := 1 \cdots S$ **do** *(Forecast realizations loop)*
    The initial error states are assumed at $t = 1, 2$;
    for $t := 3 \cdots T$ **do** *(Time periods loop)*
        A probability value is generated using a uniform random generator;
        The t^{th} state of uncertainty is sampled from TPM based on the probability and the occurrence of previous two error states;
        The outcome is bounded by the limits $L_{h(t)}$ of the corresponding forecast cluster $h(t)$;
    end
end

the demand values. Thus a suitable geometric model is required that can compactly represent the requirements while preserving the correlation. Such models have been discussed with much interest in the recent literature. Available transfer capacity in the power system has been modeled using a geometric approach in [118]. Similarly, the real time dispatch problem is discussed in [119], where a polyhedral approach is used. This has further encouraged to study the compact geometric models for this problem.

3.3.2 Uncertainty Envelope Modeling

The uncertain *net-demand* scenarios are to be represented using the selected flexibility metric. In literature, various compression algorithms have been discussed that can be used to extract the dynamics of a curve. Several algorithms such as box-car, averaging and Swinging Door Algorithm (SDA) are discussed in [120]. Based on work in [14], SDA had been selected for the dynamics extraction. The working principle of SDA is explained in Figure 3.3. The SDA is applied on the *net-demand* scenarios resulting in pivot points characterized by the triad variables. The sensitivity parameter ($\epsilon_{\Delta P}$) can be related to minimum ramp-rate limit of the participating generators.

After the identification of pivot-points, the next step is to model an envelope enclosing them. One of the envelope modeling approach is the ellipsoidal model. Authors in [121] have used it to model the uncertainty. The ellipse is of interest as it can be represented by few parameters. However, in order to complete the ellipsoidal structure additional uncertain area may be included in the process. Using this approach for the problem under consideration resulted in enclosing the negative ramp duration region, which is a non-negative value. A possible solution can be to intersect the ellipse with a half space extending towards the positive ramp duration axis. Such an application results in the polyhedral structure of the envelope. It shall require more data for representation and thus the advantage of using an ellipse does not apply. In comparison, a polytope based model provides a compare representation enclosing the pivot point and leads to a convex model. The advantages of the convexity property shall become evident with the discussion

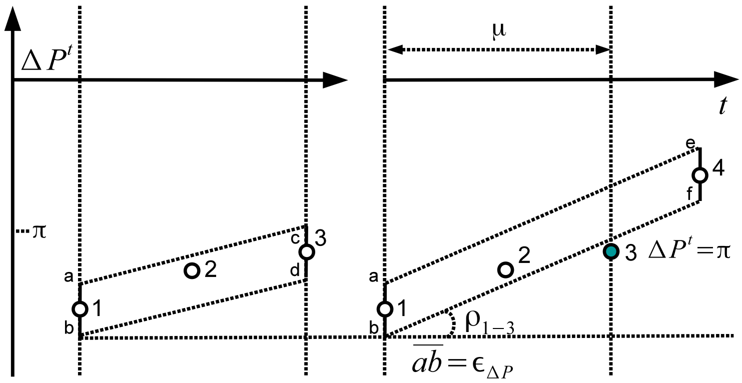

Figure 3.3: The figure shows working principle of swinging door algorithm that is used to extract the first order dynamics. The scenario curve as a representative of lumped uncertainty ΔP^t in microgrid is shown by the points $1 - 4$. A sensitivity parameter ($\epsilon_{\Delta P}$) is set at each point that describes desired ramp-rate resolution. The parallelogram is checked to contain previous points, which in case of *abcd* is true. However, at $t = 4$ the point 3 lies outside $abef$, where 3 is termed as a pivot point. It is represented by magnitude (π), ramp-rate (ρ_{1-3}) and the ramp duration (μ).

of optimization problems in later Chapters. After comparing approaches for uncertainty modeling, the polytope was selected for the representation of the uncertain demand in microgrid. The demand scenarios were generated with a probability associated with number of scenarios from Equation 3.8. The envelope modeling approach extends this probability to the surface of the polytope. The uncertainty envelope Δ as discussed in Equation 3.11 is represented here by the polytope. This consideration results in the satisfaction of the probabilistic constraint while considering the uncertainty dynamics.

A polytope is a convex representation of the intersection of finite number of closed half-spaces. Mathematically, it can be defined by a hyper-plane $\mathcal{H}$ definition given as,

$$\mathcal{P} = \{x \in \mathbb{R} \mid P^x x \leq P^c\} \quad . \tag{3.12}$$

The polytope can also be defined using vertices $\mathcal{V}$ definition, [122],

$$\mathcal{P} = \left[x \in \mathbb{R} \mid x = \sum_{i=1}^{\upsilon_P} m_i V_P^i, m \in [0,1], \sum_{i=1}^{\upsilon_P} m_i = 1 \right] \tag{3.13}$$

Here, $V_P^{(i)}$ is the i^{th} vertex of $\mathcal{P}$ and υ_P is the total number of vertices or pivot-points. The polytope ($\mathcal{P}$) can be sub-divided into two polytopes based on the magnitude being positive and negative. The sub-polytope that includes the non-negative value of power represent demand and associated uncertainty. The other sub-polytope represents the dynamics of power exported to the grid. Here, the demand polytope was focused and it was allocated among the microgrid resources.

The vertices of the demand polytope (Δ) defines the reference points for the resource planning. However, the limited number of them may not be sufficient during resources allocation process. An mechanism performing polytope sectioning is proposed in Algorithm 3.2. It is used to identify the desired number of points on the surface of Δ. The process section the Δ into C sub-polytopes along the demand axis.

The sub-polytope coordinates are given as $[x_j \;\; y_j^k \;\; z_j^k]$. Where, x_j is the j^{th} capacity/power among C capacity values and (y_j^k, z_j^k) is the k^{th} vertex among V_j vertices. V_j are vertices of the

Algorithm 3.2: Sectioning of polytope (Δ).

Compute the bounding box around Δ;
Divide the power axis interval in C number of equidistant points (x_j);
for $j := 1 \cdots C$ **do** *(Polytope sectioning loop)*
  Define an orthogonal hyper-plane for each x_j;
  Intersect Δ with the hyper-plane leading to polygon $S_j(\Delta)$;
end

sub-polytope ($S_j(\Delta)$). It represents the maximum ramp-rate and ramp duration values for the demand x_j.

The polytope (Δ) models the maximum ramp-rate and ramp duration for the demand values. It is to be noted that it does not capture the time information of the forecast. The demand polytope was used for planning the generation resources to possess the capability of support the reserve dynamics requirements. During operation, the operational schedule shall follow the classic economic dispatch approach. The information about the demand dynamics can be used for determining the reserve requirements. The real power axis of the polytope defines the capacity requirements in microgrid, while, the ramp-rate and ramp duration axes provides information about the associated dynamics in the aggregate demand.

3.4 Microgrid Test Case for Flexibility Assessment

The flexibility assessment is performed for a microgrid test case based on International Council on Large Electric Systems (CIGRE) Medium Voltage (MV) benchmark [123, 124], European configuration. The RES like wind and solar energy were included in the microgrid to represent the future scenario of high renewable penetration. Figure 3.4 shows the network configuration.

A wind farm comprising seven wind turbines is connected to the MV network using a tie-line as shown in Figure 3.5. The wind turbines are required to operate with minimum power factor 0.9. The ratings of each wind turbine is 2.78 MVA. All wind turbines are connected to the 20 kV bus by the step-up transformers of equal rating. A capacitor bank is centrally installed to improve the power factor. The wind farm has a controller that allocates the reactive power contribution between wind turbines based on the overall active power generation and the voltage at the tie-line. Algorithm 3.1 is used to generate the wind output data for the wind farm using the historical information.

The nominal load data and transmission line parameters for the MV network are obtained from Appendix C of [125]. A number of load buses in the MV network are equipped with the PV power sources as shown in Figure 3.4. The nominal ratings of the PV apparent power and their bus connection information is given in Table 3.2. The historical data for the wind power output was obtained from [126] and for the load from [127]. It had been normalized and scaled to meet the use-case ratings.

Two thermal generators are connected to bus 8 and 12. They are operated by natural gas and provide necessary backup during the islanded mode operation of the microgrid. In the grid-connected mode of microgrid, they contribute to the demand and ancillary services. The thermal

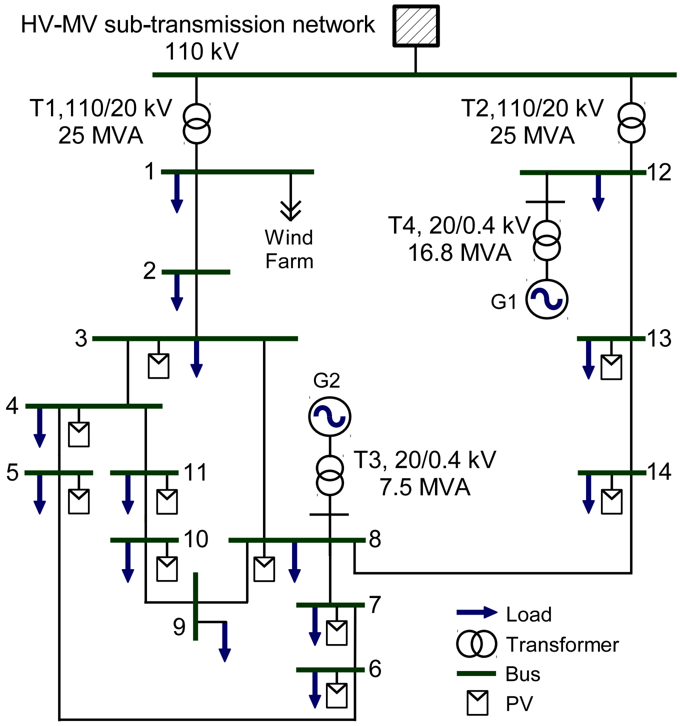

Figure 3.4: CIGRE MV distribution network from [123] modified as microgrid.

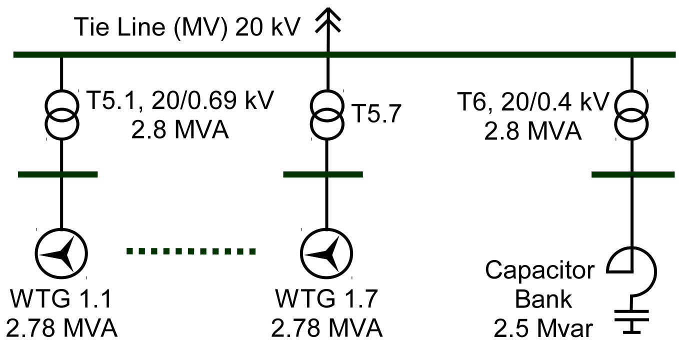

Figure 3.5: Wind farm model.

generation cost (T) is selected as 3.45 [\$/MMbtu]. The generation cost can be given as,

$$\mathrm{Cost}(P_i) = \text{Heat rate}(P_i) \times T \ , \tag{3.14a}$$

$$\text{Heat rate}(P) = a_i P_i + b_i P_i^2 \ . \tag{3.14b}$$

The cost coefficients (a_i, b_i) are derived by fitting a second order polynomial to the historical data of the generator output power vs. heat rate. The generator specifications are given in Table 3.3.

The ramp-rate limits of generators are obtained using the approach from Section 4.3.1. The power exchange with the sub-transmission network have static ramp-rate limits. The peak values $[P_{\min} \ \ P_{\max}]$ for the demand are [10 41], power from the wind-farm [6 17] and PV [0 7] in MW. This data is used to develop the uncertainty model for the renewable energy and demand forecast using Algorithm 3.1.

Table 3.2: Data for PVs in the microgrid test case (S_{nom} [kVA], power factor = 0.8).

Bus	S_{nom}	Bus	S_{nom}	Bus	S_{nom}	Bus	S_{nom}
1	3103	5	113.7	8	91.8	12	3129.4
3	78.5	6	85.7	10	174.67	13	5.32
4	69.6	7	12.0	11	51.6	14	84.4

Table 3.3: System data for the microgrid test case.

		Gen. 1	Gen. 2	Grid
Incremental operating cost	b_i [\$ / kWh^2]	0.04	0.038	0.1
	a_i [\$ / kWh]	10	13	18
$\overline{P_i}$ [MW]		10	5	35
$\underline{P_i}$ [MW]		1	0.5	0
Temperature power slope (k_i) [°F/kW]		0.068	0.2066	-
Thermal stress up limit (H_i) [°F]		200	250	-
Thermal stress down limit (L_i) [°F]		-210	-270	-
Thermal time constant (τ_i) [min]		50	30	-
Maximum ramp-up rate (UR_i) [MW/h]		5.05	2.80	20
Maximum ramp-down rate (LR_i) [MW/h]		5.30	3.02	20

3.4.1 Uncertainty Modeling: Spatial

The spatial aspect of uncertainty describes the value of forecast error. It is observed that the percentage forecast uncertainty can be related to the forecast level. Hence, a binning strategy is used to classify the forecast value in the clusters. The bins here are equally spaced values sampled between minimum and maximum forecast level. Figure 3.6 shows the percentage error in the forecast for the load, wind and PV power in each bin. A significant variation in error can be observed for difference forecast levels. The forecast error in each cluster is modeled using an eCDF function. It is sampled S times using Equation 3.8. The sampling process results in the identification of maximum and minimum limits on the error outcomes of each cluster.

The output of the sampling process for the wind power, PV generation and load forecasts is given in Figure 3.7, 3.8 and 3.9. The results are used to define the interval limits for each cluster. These interval limits have the probability of $(1-\epsilon)$ and is related to the selection of the N. It is selected using Equation 3.8 with the parameters $\beta = 10^{-4}, \epsilon = 0.1$ and $n_\delta = 1$. This set of data yields $S = 162$ scenarios.

Spatial diversity of uncertainty in the power balance is shown in Figure 3.10. Here, various levels of uncertainty define the percentage deviation from the forecast value. The 20% deviation takes significant portion of the permissible deviation region. Subsequently the possibility of deviating higher percentage of the maximum deviation is less probable to occur. In addition, the uncertainty variation along the day is influenced by the renewable energy contribution. Furthermore, the holidays and seasonal patterns also influences the demand patters and can be modeled without loss of generality.

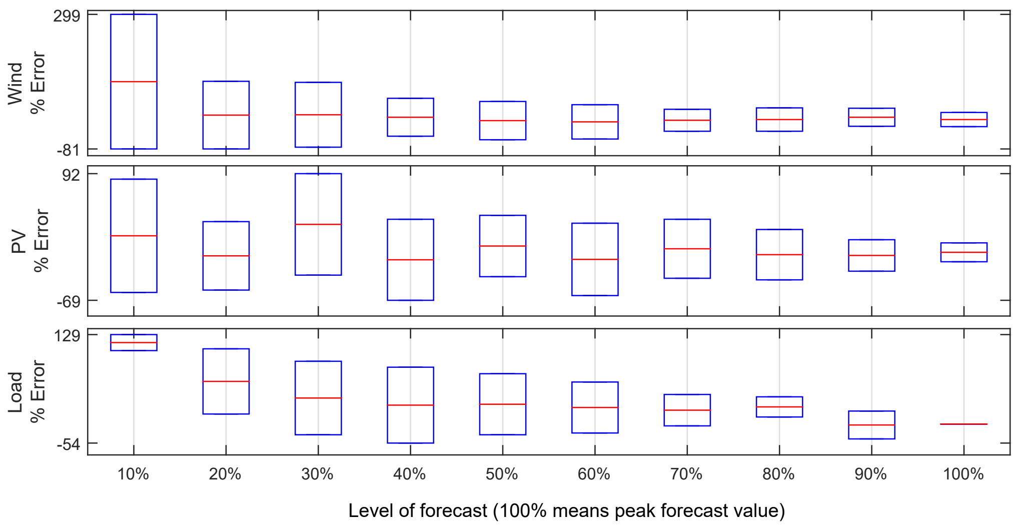

Figure 3.6: Percentage error variation as function of the forecast level, where, the range is divided into 10 levels. The figure shows the percentage error bounds obtained by sampling the eCDF of each forecast cluster S times. The percentage error varies widely for the corresponding forecast level, thus validating the clustering approach adopted in Algorithm 3.1.

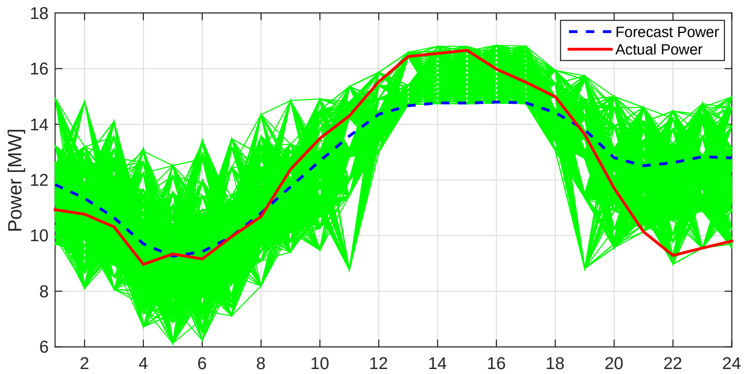

Figure 3.7: Spatial dynamics of the day ahead wind power forecast error.

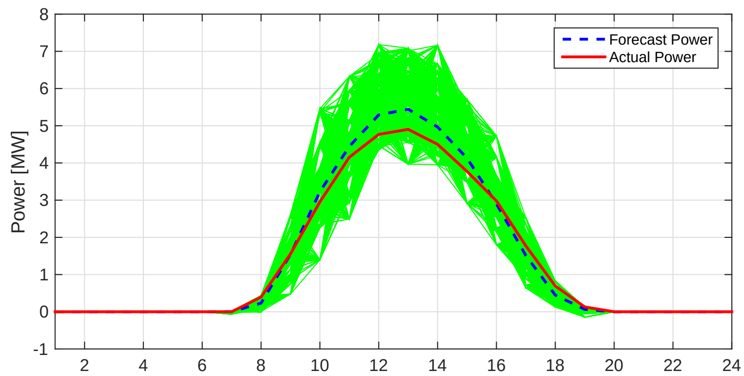

Figure 3.8: Spatial dynamics of the day ahead PV power forecast error.

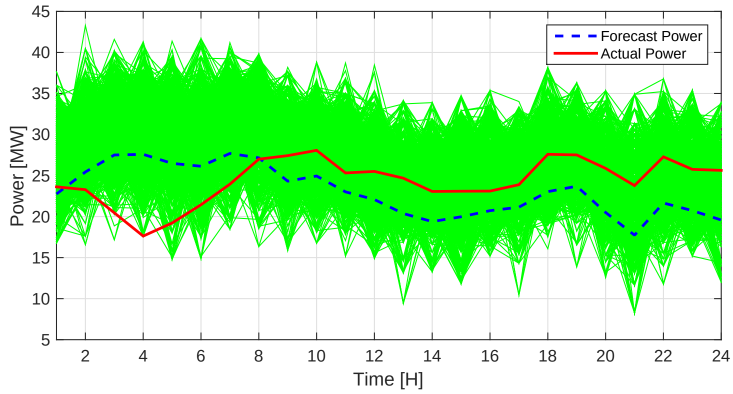

Figure 3.9: Spatial dynamics of the day ahead load forecast error.

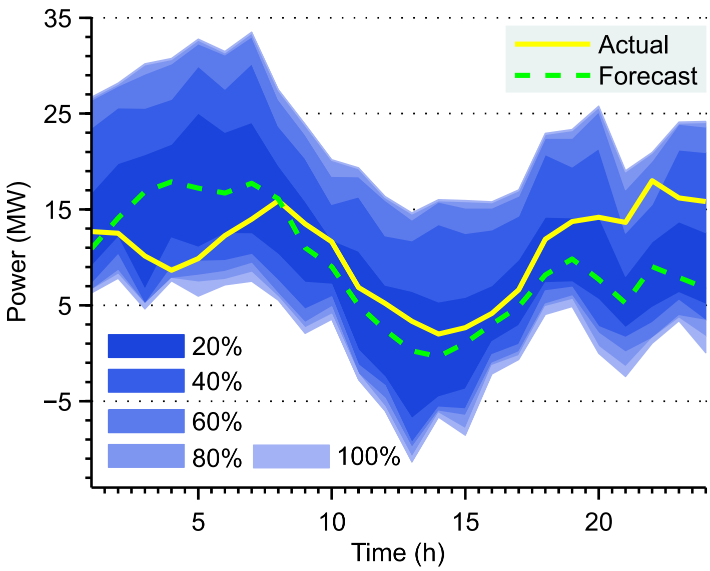

Figure 3.10: The percentage deviation from the day ahead forecast is shown by the density of the shaded area. Higher width of the area indicates more probability of occurrence. Such that lower deviation has large probability and thus more width. The results are obtained by the Monte Carlo sample of the uncertainty models.

3.4.2 Uncertainty Modeling: Spatio-temporal Correlation

The second order Markov chain models the time-series forecast error data by a TPM. The probability of a state is influenced by the occurrence of previous two error states. States can be defined as equidistant points along the percentage deviation. A higher state number reflects more accuracy in the sampling process. Here, 200 transition states were used while formulating TPM. Some of the percentage error states might not receive any entry from the scenario data. This shall decrease the number of transition states. The density map of TPM is shown in Figure 3.11. Where the higher level of curves shows more probability of occurrence. It can be observed that there is a strong correlation along the diagonal. This behavior shows that if the error is sampled in a state the next value of error will most likely be close to the current error state.

A generic diagram of the *temporal* correlation as performed using second order Markov chain is shown in Figure 3.12. The Markov chain captures the time correlation of the uncertainty.

Such that the actual curve shall follow one of the possible state transition trajectories with a probability $(1-\epsilon)$. The *spatio-temporal* characteristics of the forecast uncertainty for the wind, PV and load forecasts are given in Figure 3.13, 3.14 and 3.15. While comparing these results, it can be observed that the PV power forecast uncertainty deviation is least turbulent. It is howe ables are c

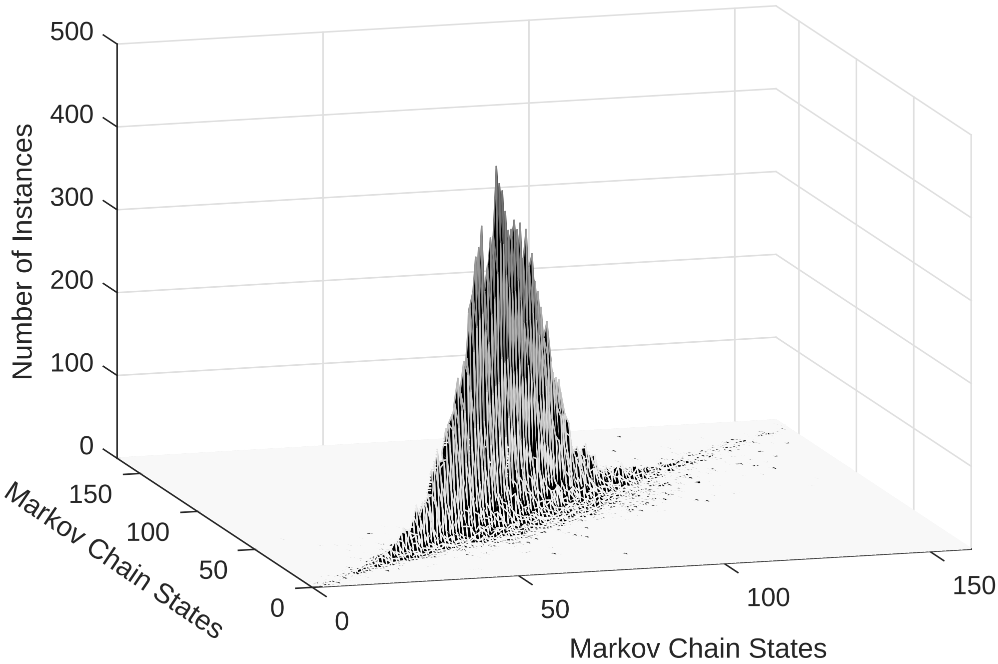

Figure 3.11: TPM of the load forecast error obtained using historical data of one year.

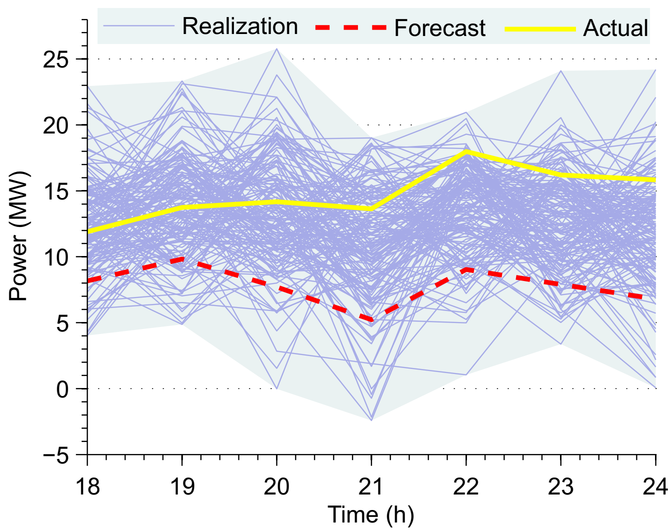

Figure 3.12: The graph shows horizontal correlation between the power balance states as obtained by second order Markov chain. The actual curve is likely to follow the forecast trends with a probability $(1-\epsilon)$ that is the function of S and the order of Markov chain.

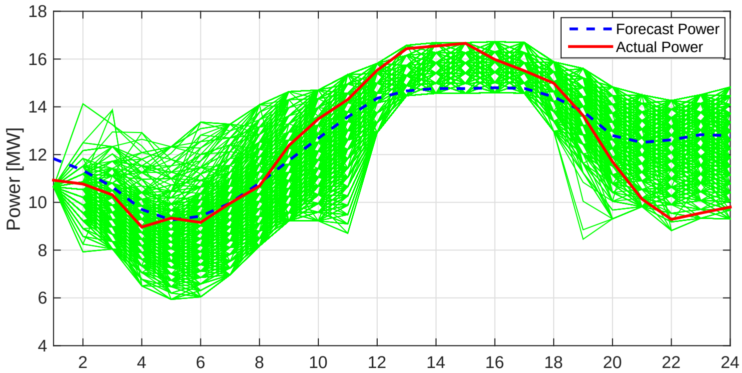

Figure 3.13: Spatio-temporal dynamics of the day ahead wind power forecast error.

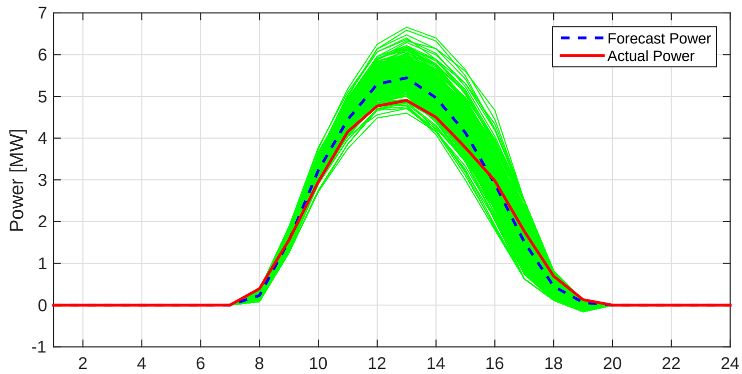

Figure 3.14: Spatio-temporal dynamics of the day ahead PV power forecast error.

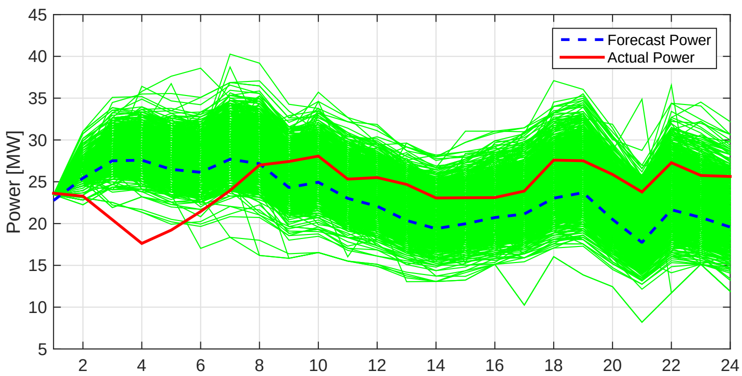

Figure 3.15: Spatio-temporal dynamics of the day ahead load forecast error.

3.4.3 Polytope Formulation

This section applies the SDA from Section 3.3.2 to the scenarios of the *net-demand* obtained using the previous section. The polytope is modeled to enclose the pivot points and is shown in Figure 3.16. While, Figure 3.17 insights into the projections of polytope.

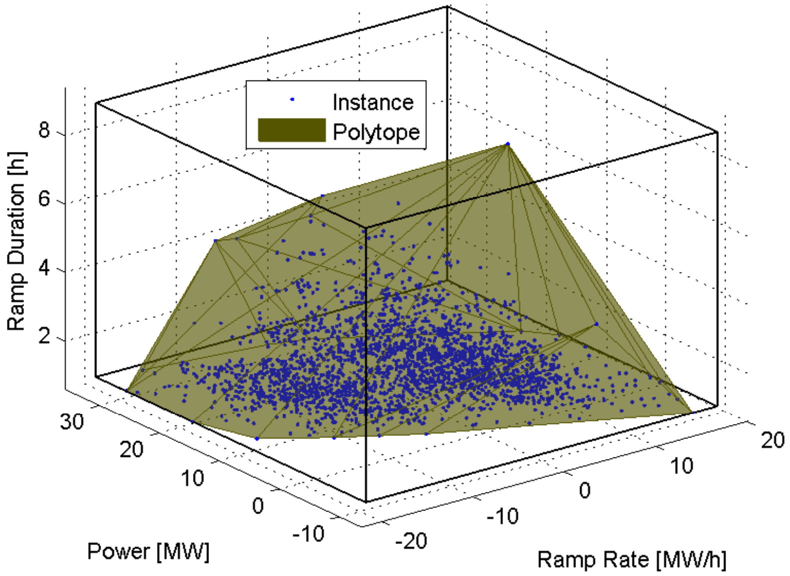

Figure 3.16: A polytope enclosing the pivot-points defines the *net-demand* requirements in terms of first order dynamic variables. The surface of the polytope defines the maximum requirements. A comparison is made with the rectangular box envelope that stems from interval based approach. It shows that the proposed approach can potentially decrease the uncertainty region considerably.

Dvorkin *et al.* have proposed a hyper-rectangular or bounding box representation in [15]. The comparison of the proposed polytope based with the bounding box approach shows that substantial volume of the uncertainty associated with the *net-demand* can be saved. In the case of this test case the volume of the polytope had been 73.53% less than that of the bounding box. It is notable that the projections of the polytope cannot be used for comparing the two approach. The is due to the projections obtained while viewing the polytope from the perpendicular axes.

The rectangular or bounding box approach stems from interval based analysis and leads to define maximum ramp-rate and ramp duration requirements for all power levels. This can lead to conservative results. The comparison shows that the tighter approximation can result in defining the uncertainty precisely while maintaining the probabilistic guarantees associated with the sampling process. The confidence against uncertainty can be increased by decreasing the values of ϵ and β. This shall result in more number scenarios and increase the likelihood of rare events. The analysis of which shall lead to increase in the size of the bounding polytope. The demand polytope Δ is obtained by intersecting the polytope from Figure 3.16 with the hyper-space extending along the positive power axis. It is then sectioned using Algorithm 3.2 leading to a polygon $S_j(\Delta)$ for each demand value x_j along the power axis. The points on the surface of the polytope where it is sectioned are shown in Figure 3.18.

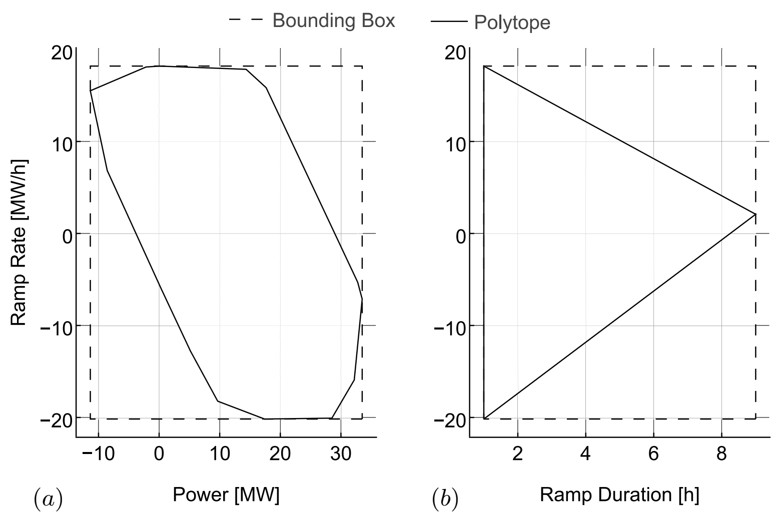

Figure 3.17: This figure shows the projections of polytope and bounding box on $(x-y)$ and $(y-z)$ axes. (a) It shows the plausibility of the ramp-rate as function of the power level. The lower demand experiences a high ramp-up rate in relation with the higher demand values. (b) This graph shows a relationship between the ramp-rate and ramp duration. The small ramp-rate values are likely to be experienced for more duration than high ramping events.

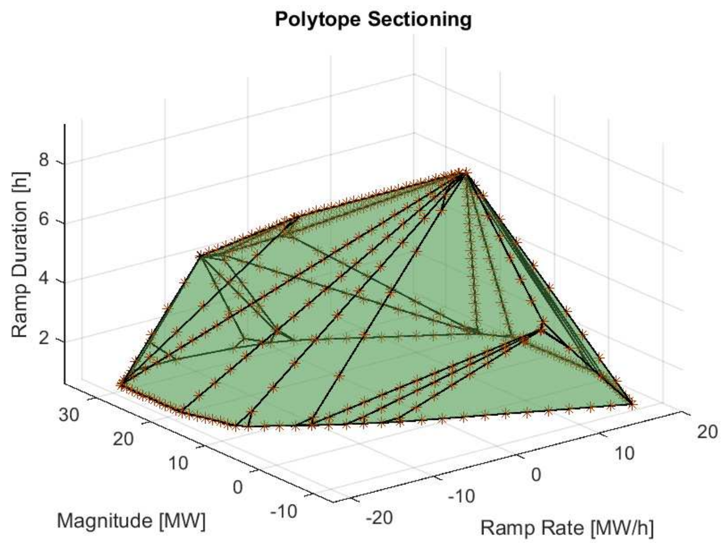

Figure 3.18: Polytope sectioning performed on the surface of the uncertain *net-demand* polytope. It is sectioned at these points leading to 2-dimensional polygons. The result had been used during flexibility allocation process.

4 Resource Flexibility Modeling

4.1 Introduction

In Europe, it is aimed to increase the percentage of renewable energy more than 50% of the total generation capacity by 2050 [128]. The higher magnitude of the renewable energy shall result in more forecast uncertainty, thus requiring more flexibility from the conventional generation resources. A sample case study has been conducted by California Independent System Operator (CAISO) in [129]. This study assesses the flexibility requirements considering the *net-demand* scenarios for each day from 2012 till 2020. The results for one of the day and the scenarios for different years is shown in Figure 4.1. It can be observed from the graph that the net load curve decreases from 8 am on-wards due to the solar power generation and as sun sets, it increases sharply. This steep ramp decreases in the evening hours as the demand decrease. Figure 4.1 also shows that the grid conditions in future shall change by a significant margin during day as compared to the present scenario. The variation shall require resources that can be turned On and Off multiple times in a day and possess a high ramp-up/down capability. The ramp requirements shall vary throughout the year depending on the availability of renewable energy and the demand patterns.

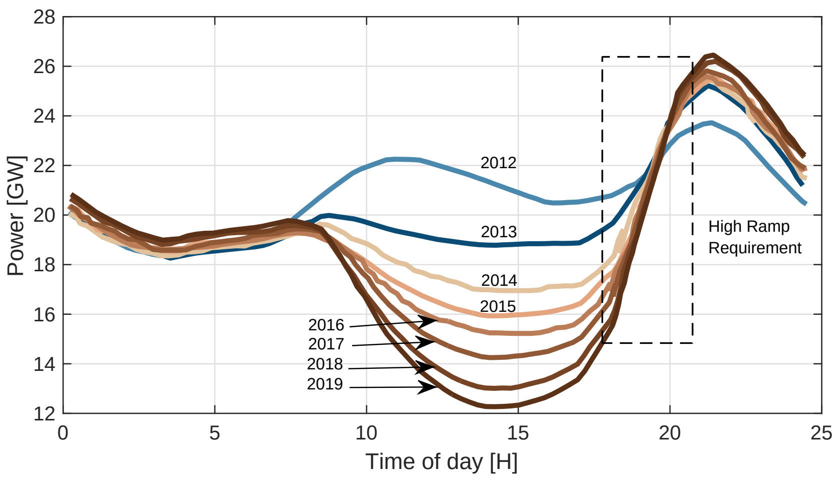

Figure 4.1: The *net-demand* curves by CAISO for the 31^{st} March for years 2012 through 2020, taken from [129].

The steep ramp mentioned with "increased ramp" in the Figure accounts for 12 GW over 3 hours (approximately 67 MW/min). The ramp-rate is expressed in MW per minute at which a resource can change its output. Most of the industrial gas turbines have an average ramp-rate of 25 MW/min [130]. The thermal generators alone may be incapable of meeting such requirements. It has motivated the operation of the grid at shorter (intra-hour) time frames. This step has decreased the impact of forecast uncertainty. However, the spinning reserve requirements shall continue to encourage the participation of local resources. The active distribution network approaches aim to enable the resources like controllable loads, community energy storage and coordinated control of distributed generation in providing grid support. The flexibility from distributed resources can come from thermal loads, heat pumps, electric vehicles, Heating Ventilation and Air Conditionings (HVACs), refrigeration, energy storage, Renewable Energy Sources (RES), Distributed Generators (DGs) and others. A common model that can represent the flexibility at resources shall facilitate the local energy market operations. It can form basis for the flexibility bids that can be used for scheduling problems. This chapter discusses a generic modeling framework termed as Resource Flexibility Model (RFM), that can be used to represent the flexibility offered by distributed resources. The contents are partly published in [83] and [131].

Flexibility specification. A common flexibility modeling framework can facilitate the characterization of distributed resource potential and can be useful during the design of control strategies. Following are the flexibility specifications that can be associated with such a model [118],

- Some of the resources e.g., an aggregate load of a house can act as a generation resource if locally produced electricity is more than the demand of house. Therefore, it is desired that the nature of a distributed resource (demand/generation) can be modeled and changed conveniently when desired.
- It can be tailored to meet the specifications of the diverse types of resources like storage devices, concentrated solar power plants or demand response. Thus a single model may be a representative of a resource when the parameters are customized to represent it.
- It should be able to model the energy storage characteristic to represent resources like pumped-hydro, thermal loads and others. This should not hinder the modeling of no-storage resources.
- The resource specific constraints relating to the dynamic capability of power generation or consumption can be specified. This capability can be the ramp-rate, availability, energy constraints and others.
- The response time of a distributed resource against a control signal can be modeled. This can facilitate to model the resource availability aspect before the use.
- Cost of service can be expressed in terms of the dynamic capability offered. Such that it can be related to the operating point, ramp-rate, response time, time of use or a combination of these variables.

The flexibility definitions have been presented in [132], where it discusses the concept of flex-offer in a Danish project, TotalFlex. This projects models the combined effects of time and energy on the flex-offer. The flexibility interval is divided into time-slices of 1 hour in which the controllable level of energy is defined. It is a sequence optimization problem and can be useful for modeling a large number of resources like residential shift-able loads. However, it cannot capture other desired characteristics as mentioned in Section 4.1 e.g., energy storage. A taxonomy for modeling the flexibility in smart grids is discussed in [16]. Based on this taxonomy, authors have provided a review of the existing flexibility modeling approaches. The flexibility models are classified as namely Bucket, Battery and Bakery models. Among them, a Bucket is a constrained energy and power integrator. The behavior is similar to that of a bucket i.e., the power consumed increases the state of energy in the model. The second model resemble the behavior of battery and hence named as Battery model. It is based on the Bucket model with an additional time constraint associated with the State of Charge (SoC). For example, an electric vehicle may be required to possess certain level of charge in the morning. The Bakery model is based on the Bucket model with additional constraint that the process must run in the continuous stretch for specified amount of time at a fixed power consumption.

A power node modeling framework has been presented in [133]. It represents the power system components using a generic power node. The model describes dynamics of the state-of-charge by a first order differential equation. Its relevance to the mentioned flexibility specifications makes it a suitable choice. Moreover, the proposed model should facilitate the consideration of resource specific constraints described in [16]. The model discussed in [133] has been be termed as a battery model, but it is a Bucket model in the taxonomy from [16].

4.2 Resource Flexibility Model

The Resource Flexibility Model (RFM) consists of two parts, the energy storage model and the resource capability envelope. The first model aims to provide a mathematical representation of the resource energy storage potential. While, the second model characterize the dynamic capability of a resource in providing generation or consumption flexibility.

4.2.1 Energy Storage Model

The SoC dynamics of the energy storage model are given as [133],

$$Cx'[k] = \eta_L \overline{P_L}[k] - \frac{1}{\eta_G}\overline{P_G}[k] + \xi[k] - \upsilon[k] - \omega[k] \ . \tag{4.1}$$

Where, the parameters are,

- η_L and η_G is load and generator efficiency,
- C is the capacity of battery [kWh],
- $x[k] \in (0, 1)$ is the SoC of battery,
- $\overline{P_L}$ and $\overline{P_G}$ are the resource maximum power consumption/generation ratings,
- $P_L = \eta_L \overline{P_L}$ and $P_G = 1/\eta_G \overline{P_L}$ is the net power seen from the grid,
- ξ is the primary in-feed/out-feed of power,
- ω is the power curtailed,
- υ is the battery loss.

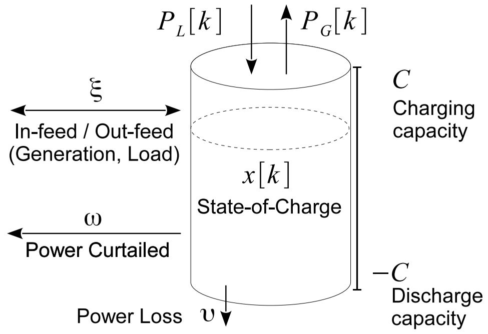

Figure 4.2: Resource flexibility, battery model.

The constraints associated can be defined as,

$$\begin{aligned}&(1)\ \ 0 \le x[k] \le 1\ \ ,\ (2)\ \ 0 \le \underline{P_L} \le P_L \le \overline{P_L}\ \ ,\ (3)\ \ 0 \le \underline{P_G} \le P_G \le \overline{P_G}\ \ ,\\&(4)\ \ \underline{R^+} \le R^+ \le \overline{R^+}\ \ ,\ (5)\ \ \underline{R^-} \le R^- \le \overline{R^-}\ \ ,\ (6)\ \ \xi \cdot \omega \ge 0\ \ ,\\&(7)\ \ |\xi| - |\omega| \ge 0\ \ ,\ (9)\ \ \upsilon \ge 0\ \ ,\end{aligned}$$

where,

- (1) enforces a normalized value for the SoC,
- (2-3) describes that power generated or consumed is positive and is bound by the maximum limits,
- (4-5) defines the ramp-up and ramp-down rate limits for generation or consumption,
- (6) says that the sign of curtailed power should be same as of primary out-feed/in-feed of the power. For example, if power is consumed then the power curtailed is taken positive in relevance to Equation 4.1,
- (7) defines that the curtailment of power cannot exceed the power itself, and
- (8) constrains the storage losses to be a non-negative value.

The model can be customized to represent the characteristics specific to a resource. For example, the power conversion efficiency of the battery model can be the function of its SoC $\eta_G(x[k])$. Similarly, the capacity of battery can be a dynamic variable given as $C[t]$. It and be made a function of the resource availability and its specifications. Such a model facilitates constraint handling in the diverse situations.

Charge state constraint. The constraint of possessing an energy state at a specific time can be modeled as,

$$Cx[0] = C_0\ \ ,\quad Cx[T_{\text{end}}] = C_{\text{end}}\ \ . \tag{4.2}$$

Where, $T_{\text{end}} \in \mathbb{N}$ and C_0, C_{end} is required capacity at time 0 and T_{end}.

Energy constraint. Some resources may possess a constraint that requires a continuous operation at nominal ratings from time a to d in order to meet specific energy requirements. Such a constraint for the generator can be modeled as,

$$\sum_{k=a}^{d} \overline{P_G} x[k] = E \ , \quad 0 \le x[k] \le m \tag{4.3}$$

Where, m is the maximum admissible value of the normalized power. Equation 4.3 is satisfied if,

$$\sum_{k=a}^{d} x[k] \ge (d-a)\,(x[d]-x[a]) \tag{4.4}$$

Continuous operation constraint. A resource can require a continuous operation for T_{run} time to complete a task requiring an energy E. In this case, the battery should be capable of providing this service at each time $[k]$. The constraint can be modeled as,

$$\sum_{k=a}^{a+T_{\text{run}}-1} x[k] \ge T_{\text{run}}\,(x[k]-x[k-1]) \tag{4.5}$$

4.2.2 Resource Capability Envelope

The dynamics of a resource and its operational limits influences its capability of generation/consumption of energy. This capability can be conveniently represented using a geometrical formulation. For example, a polytope can be used to represent the dynamic ramp-rate capability as function of the output power. The energy limits can be incorporated by considering the ramp duration variable. Surface of such a polytope can define the capability limits of the resource as shown in Figure 4.3.

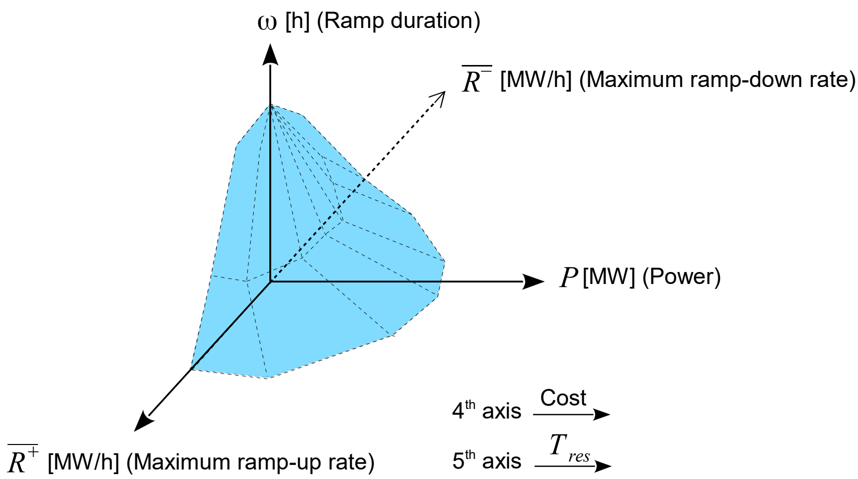

Figure 4.3: Resource Capability Envelope (RCE) as part of Resource Flexibility Model (RFM) representing the dynamic capability of a resource.

Some of the resource like controllable thermal loads can have a response time (delay) in responding to a control signal. This delay can be the function of the operational state of the resource. Hence, it can useful to associate a fourth axis of response time in the polytopic model. The fifth axis from the Figure shows the operational cost than can modeled as a function of any single or combination of other variables.

Operational cost. The operating cost of a resource e.g., generator is the function of power output and is generally given by Equation 4.6,

$$C_F = \sum_{i=0}^{N} \sum_{t=0}^{T} \left(a_i \left(p_{g,i} \right) + b_i \left(p_{g,i} \right)^2 \right) \quad . \tag{4.6}$$

The proposed capability envelope can be used to associating the cost as function of the ramp-rate. Where the ramp-rate can be have fixed nominal ratings or a function of the SoC from the battery model. This approach can be useful if some resources permit the *over-drive* operation. The *over-drive* operations is when a resource operates beyond the nominal ratings. Such an operates generally results in additional costs that can be due to maintenance requirements or reduction in the life expectancy of the equipment. The additional ramp costs can be associated with the ramp-rate and ramp duration variables and can be given as,

$$C_T = \sum_{i=0}^{N} \sum_{t=0}^{T} \left(a_i \left(p_{g,i} \right) + b_i \left(p_{g,i} \right)^2 + C_{OD} \right) \quad . \tag{4.7}$$

Where, $C_{OD} = f(R_i, P_i, T_{\mathrm{dur,i}})$ if $R_i > \overline{R}_i$.

Here,the RFM for a thermal generation unit and the aggregation of thermostatically controlled loads in the active distribution network are explored.

4.3 Flexibility at Generation

Since last two decades, the evolving economic and regulatory environment has resulted in the increase of small scale generation units connected to the distribution network. According to International Energy Agency (IEA), there are five major reasons driving this change [134],

- Advancement in small scale generation technology.
- Economic constraints in the construction of new transmission lines that may be required for the dispatch of bulk power production.
- Increase in the customer demand for reliable electricity.
- The liberalization of electricity market encouraging the participation of small scale generation companies.
- The drive towards environmental friendly generation from renewable energy sources like solar and wind.

The DGs can be classified into controllable or non-controllable types. The output of controllable DGs can be regulated by adjusting the supply of the primary energy source. This category can include internal combustion engine, small gas turbines, Combined Heat and Power (CHP), micro-turbines, small hydro power plants, bio-mass, geo-thermal power plants, fuel cells and others. Non-controllable DGs as the name implies are not actively controlled by the operators and hence their availability cannot be guaranteed. They can include power from wind turbines, Photo Voltaic (PV) and other renewable energy based generation.

Distributed generation in an active distribution network can be modeled using the proposed RFM. The control aspect of the primary energy in-feed can be controlled by the constraints on ξ parameter. Similarly, the capability of a DG can be modeled using the resource capability envelope as discussed in Section 4.2.2. If the DG has fixed nominal ratings for the ramp-rate then the capability can be defined by a simple hyper rectangular structure. The model also facilitates modeling of the dynamic ramp-rate potential of the DG. Authors in [135] and [136] have discussed the dynamic ramp-rate model for a generator. These papers have discussed the economic advantage of defining ramp-rate potential as a function of thermal stress on the rotor. The study reveals that the ramp-rate of a generator can be defined as a dynamic value without causing additional costs when operated within its thermal limits. The costs can be considered if the generator is allowed to operate beyond the elastic thermal limits. The term "elastic" refers to the dynamic range of the limits as compared to the fixed values. In such a case it can be referred as *over-drive* cost. Here, the capability envelope of the thermal generation unit with the dynamic ramp-rate limits is discussed.

4.3.1 Thermal Generation Unit

The thermal generator ramp-rate potential can be modeled as a function of the rotor thermal stress limits. Generally, the generator manufacturer provides fatigue curves that relates the thermal stress of the machine to ramp-rate values. It can be used to associate the ramp capability with the thermal limits. The thermal state of a generator has been modeled in [136] as a combination of previous thermal state (decaying term) and temperature increase due to the ramp process (growth term) . However, the fatigue curve data generally assumes a thermal equilibrium and a constant ramp-rate [135]. Therefore, the decay term can be neglected. The resulting equation for thermal stress can be given as,

$$S_i^t = k_i \tau_i \left(1 - e^{-w/\tau_i}\right) [P_i(t) - P_i(t-1)]/w \ . \tag{4.8}$$

The shift in power output of the machine as resulting of ramping process is given as,

$$P_i(t) - P_i(t-1) = wR_i^+ \ , \tag{4.9}$$

Hence the thermal state of a generator can be given as,

$$S_i = k_i \tau_i R_i^+ \left(1 - e^{-w/\tau_i}\right) \ . \tag{4.10}$$

The thermal limits of the stress are in both directions such that ramping up/down. The Equation 4.10 can be defined in terms of ramp-down rate (R_i^-) as well in a similar way. The thermal stress limits of the machine can be described as,

$$-L_i \leq S_i \leq H_i, \quad i = 1 \cdots M \ . \tag{4.11}$$

The per-hour maximum ramp-up and ramp-down rate ($\overline{R_i^+}$, $\overline{R_i^-}$) are obtained by solving Equation 4.10 for thermal limits and for a ramp duration of 60 minutes (w = 60 min). It is given as,

$$H_i = k_i \tau_i \overline{R_i^+} \left(1 - e^{-60/\tau_i}\right) \ , \tag{4.12}$$

$$L_i = k_i \tau_i \overline{R_i^-} \left(1 - e^{-60/\tau_i}\right) \ . \tag{4.13}$$

Equidistant point of the power (P_i^d), ramp-up ($R_{i,m}^+$) and ramp-down rate ($R_{i,n}^-$) can be taken from the intervals,

$$\underline{P}_i \leq P_i^d \leq \left(\overline{P}_i - \overline{R_i^+}\right), \quad 0 \leq R_{i,m}^+ \leq \overline{R_i^+} \ , \tag{4.14}$$

$$\overline{P}_i \geq P_i^d \geq (\underline{P}_i + \overline{R_i^-}), \quad 0 \leq R_{i,n}^- \leq \overline{R_i^-} \ . \tag{4.15}$$

Equation 4.14 describes the power and ramp-up rate values that can be assigned to i^{th} generator. Similarly, Equation 4.15 describes the interval for the ramp-down rate. Maximum ramp duration (w) can be calculated for each pair of power (P_i^d) and ramp-up rate ($R_{i,m}^+$) values by solving,

$$\max \quad w \ , \tag{4.16a}$$

$$\text{s.t.}: \quad k_i \tau_i R_{i,m}^+ \left(1 - e^{-w/\tau_i}\right) \leq H_i \ , \tag{4.16b}$$

$$\left(R_{i,m}^+ w + P_i^d\right) \leq \overline{P}_i \ . \tag{4.16c}$$

The point $[P_i^d \ R_{i,m}^+ \ w]$ defines a boundary instance in generator envelope for the positive ramp domain. Similarly maximum ramp duration can be obtained for each pair of the power (P_i^d) and ramp-down rate ($R_{i,n}^-$) values by solving,

$$\max \quad w \ , \tag{4.17a}$$

$$\text{s.t.}: \quad k_i \tau_i R_{i,n}^- \left(1 - e^{-w/\tau_i}\right) \geq L_i \ , \tag{4.17b}$$

$$\left(P_i^d - R_{i,n}^- w\right) \geq \underline{P}_i \ . \tag{4.17c}$$

The process was repeated for all pairs of capacity and ramp-up/down values leading to points in the space. A convex envelope (Δ_i) had been used to enclose these points defining the i^{th} generator capability limits.

4.3.2 Resource Capability Envelope for a Generator

The ramp-rate limits of a generator have been assessed based on the thermal limits. It defines the dynamic capability of the generator in terms of the first order dynamics variables (power, ramp-rate and ramp duration). A typical generator data is given in Table 4.1. The capability of generator can be assessed by solving problems in Equation 4.16 and 4.17. The result are the maximum ramp duration (w) values that can be sustained while operating within elastic thermal limits ($H_i, \ L_i$). A convex envelope enclosing the points in space determines the generator capability envelope. Figure 4.4 shows the variation in ramp duration capability as a function of the power and ramp-rate values. The projections of the polytope are shown in Figure 4.5. It is to be noted that the convex envelope approximates the actual capability of the generator which is a non-convex envelope. The convex formulation facilitates in implementing deterministic optimization algorithms that are discussed in the later chapters.

The cost of thermal generation is normally taken as a quadratic or linear function of power produced. However, if the generator is allowed to operate beyond its rated values, it shall incur additional costs. These cost are associated with maintenance, wear of the machines and reduction in its life span. They are attributed to the turbine thermal stress that happens as the ramp-rate

Table 4.1: A typical generator ratings for capability assessment.

Property	Symbol	Value	Unit
Maximum output power	$\overline{P_i}$	10	MW
Minimum output power	$\underline{P_i}$	1	MW
Temperature power slope	k_i	0.068	$^\circ F/kW$
Thermal time constant	τ_i	50	min
Thermal stress up limit	$\boldsymbol{H_i}$	200	$^\circ F$
Thermal stress down limit	$\boldsymbol{L_i}$	-200	$^\circ F$
Elastic thermal stress up limit	H_i	120	$^\circ F$
Elastic thermal stress down limit	L_i	-120	$^\circ F$
Elastic strain cost coefficient	d_i	1	$\$/(^\circ F)^2$

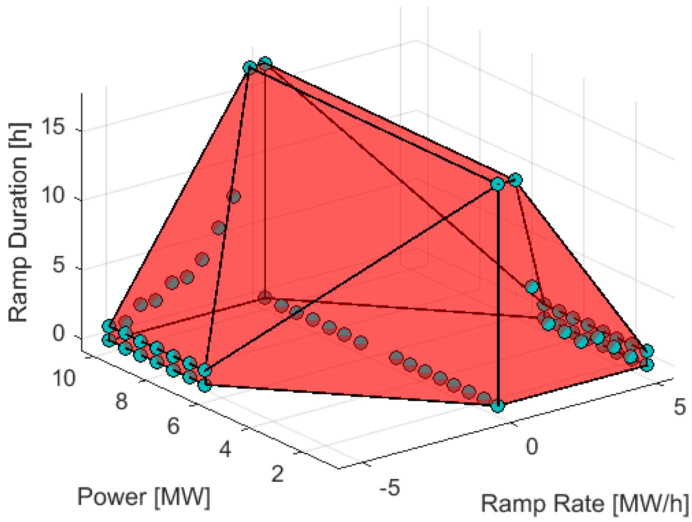

Figure 4.4: Dynamic capability model for a thermal generator.

goes beyond the rated values. The cost of generation from Equation 4.7 has been modified for the case of generator and is given in Equation 4.18,

$$C_{\text{gen}} = \sum_{i=0}^{N} \sum_{t=0}^{T} \left(a_i \left(p_{g,i}\right) + b_i \left(p_{g,i}\right)^2 + C_{h,i} + C_{s,i} \right) \quad . \tag{4.18}$$

Where, $C_{s,i}$ is the start-up cost and $C_{h,i}$ is the *over-drive* cost. The *over-drive* cost is incurred in both cases of violating the upper and lower elastic thermal stress limits (H_i, L_i). In case of violating the upper elastic thermal stress limits, the cost incurred are as [136],

$$C_{h,i} = d_i \left(S_i(t) - H_i\right) \quad . \tag{4.19}$$

Here, $S_i(t)$ is the thermal state after the generator power is ramped by R_i, starting at a power level P_i and for a duration of w. It can be obtained using Equation 4.8. The *over-drive* cost as function of the triad variables is given in Figure 4.6.

The projections on the axes are shown in 4.7. From the figures it can be observed that the elastic thermal constraints are violated for higher ramp-rate limits and for lower values of power. The

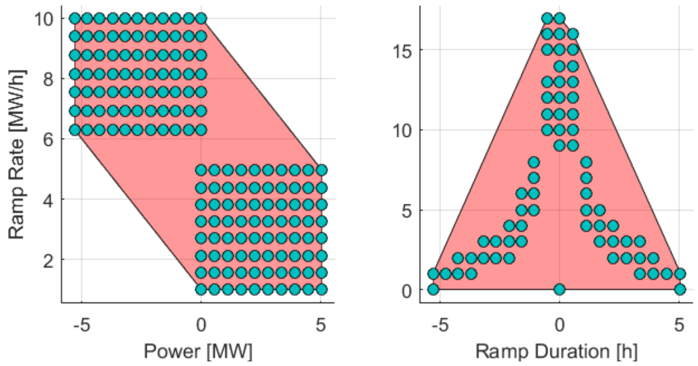

Figure 4.5: Projections of the generator capability envelope.

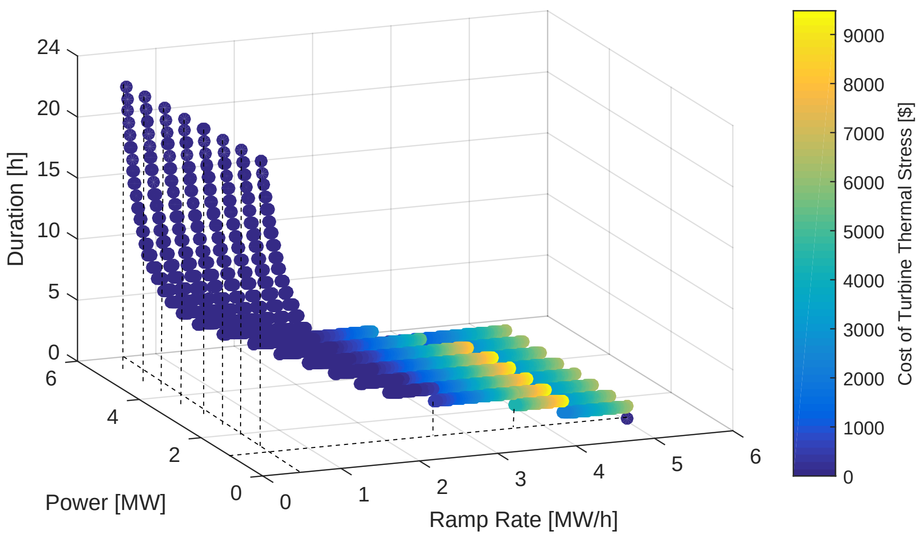

Figure 4.6: *Over-drive* cost of operating the generator beyond its thermal stress limits.

former behavior is due to the higher ramp-rate, that if sustained for less duration can result in elastic thermal stress limit violation and increase the costs. The behavior in the later case for lower values of the power and is due to higher likelihood of sustained ramping resulting in the thermal limit violations.

4.3.3 Energy Storage Model for a Generator

In some cases, it may be necessary to take into consideration the availability of fuel while considering a potential of a generator. For example, the operating limits of generator at a hydro-storage lake are the function of stored potential energy in water. This energy can be represented by a normalized value $x[k]$. The potential energy can be defined as equivalent electrical energy potential C [kWh]. While, $P_{g,i}[k]$ is the power generated at time k. The primary source of in-feed in the form of water/fuel input is represented by ξ and the curtailed power (ω) can be related to the spilled water volume. Both of these parameters needs to be modeled in contributing to SoC, $x[k]$. The variable ramp-rate of the generator connected to the turbine can also be modeled as

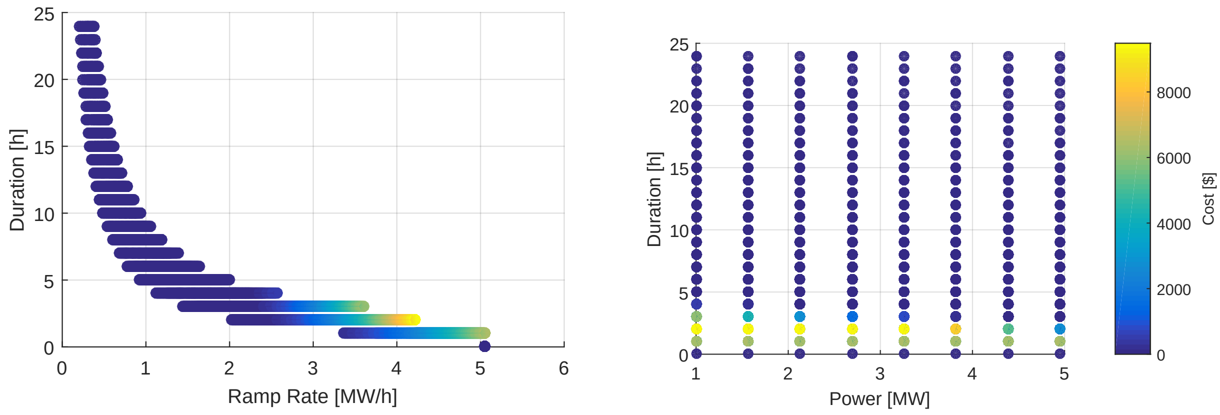

Figure 4.7: Projections of the *over-drive* cost of the generator as function of power, ramp-rate and ramp duration values.

function of energy storage potential along with thermal limits. This modeling shall determine the shape of resulting capability envelope.

Response time. The response of a thermal (diesel) generator to a change in the set-point depends on the inertia of rotor and governor. While assessing the demand/reserve requirements, it is essential to specify the desired response time for the possible values of the ramp-rate. This enables the consideration of generator response time during the resource allocation process. The response of a thermal generator to the change in set-point can be the function of the delay in governor response, engine delay and generator inertia. As a starting point, the work in [137] can be referred. This paper models the engine delay based on the time taken by the governor and inertia in responding to the change in set-point.

4.4 Flexibility at Demand

Demand response is a term used for loads responsive that can change their energy consumption behavior in response to the control signals. It enables the loads to participate in the ramp-rate effort as discussed in Section 4.1. Demand response can be performed on the diverse time scales ranging from real-time frequency responsive loads to the load scheduling. The demand response applications are designed for desirable response time and activation schedules. Among such applications is the secondary frequency reserve. It is used for maintaining the balance between demand and supply in the steady state. The response time for this type of reserve in power system ranges from seconds to minutes and thus limits the maximum admissible delay from the participating resources. The anticipated increase in the renewable energy (30% by 2020 in CAISO) shall increase the reserve requirement significantly (0.6 GW to 1.4GW in CAISO) [138]. Demand response as potential resource has attracted a growing interest recently. The advancements in metering and control infrastructure shall pave the way for implementation of demand response schemes. The demand response programs can be broadly classified into incentive and price based applications [139]. An overview of various demand response approaches is given in Figure 4.8. The details about each category and the corresponding market models can be found in [140]. The shaded regions in Figure 4.8 are the areas that are being focused in this thesis. The flexibility bid structures based on the proposed RFM are discussed while a direct control based scheme is used by the Thermostatically Controlled Load (TCL) aggregation for performing frequency regulation.

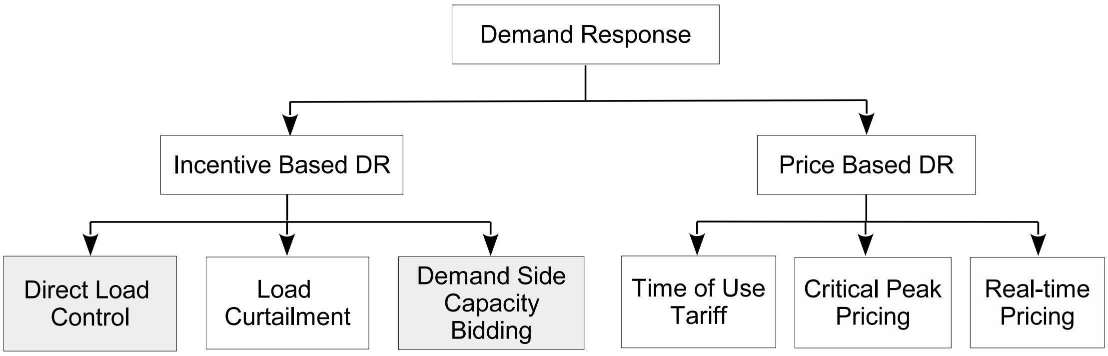

Figure 4.8: Overview of the demand response programs and the shaded focused areas.

4.4.1 Thermostatically Controlled Loads

TCLs such as air conditioners and heating units forms a major part of the total load at demand side. These loads have an ability to store energy temporarily. This characteristic can be used for the demand response service, where it can damp the demand and supply imbalances by charging and discharging when required. The objective of such loads is to maintain their temperature around a set point value. The width of this interval is called the dead-band. The TCL undergoes a cycling process between On and Off states that aims to maintain the average temperature within the dead-band. The On/Off duration is function of the effectiveness of TCL in maintaining temperature within limits and also the environment temperature. TCLs have been explored in the literature with much interest due to their vast numbers at the demand side and their energy storage potential [141]. The aggregation of TCLs can be represented by an equivalent battery model. Such an approach has been used for the frequency regulation service in [142, 143]. Another study in [144] aimed to model the aggregation of TCLs using a state space model. The uncertainty associated with the parameters of state space model has been the focus of [145], where a state queuing model has been used.

A number of studies have been done on improving the equivalent battery model. It has been discussed in [144], but it lacks an insight on the quality of solution. This model has been improved in [146] by introducing an energy dissipation term. The mechanism of using the battery model (representing the flexibility of TCLs) in the energy market has been proposed in [147]. This paper presents a mechanism design based approach to encourage the market participation of the TCLs. Although most of the studies have focused on the spinning reserve potential of TCLs in the energy market. However, in [148], a mechanism is proposed where the TCLs participate as a contingency reserve. Authors present a set theoretic based approach in [149] that aimed to define control trajectories and associated them with the battery parameters. A comprehensive discussion on the necessary and sufficient battery models have been presented in [149]. The "necessary model" proposed by this paper is selected in this thesis. It is used to develop a stochastic representation of the equivalent battery model. The emphasis has been to develop mathematical formulation of the battery parameters that has a comparatively simpler structure for a real time application.

4.4.1.1 System Model

The frequency regulation signal ($r[k]$) as received by a central control from the energy market. It represents the instantaneous imbalance between demand and supply. The central control is responsible for maintaining the battery model as a representative of the TCL aggregation in the network. The central control communicates with the TCLs and control their operational states. Each TCL sends its available flexibility information to the central control. It consists of the status $u^i[k]$, availability $\lambda^i[k]$ and temperature distance to the switching boundary $\pi^i[k]$. The central control models it using a stochastic battery and identifies sufficient number of TCLs to turn On/Off in order to track the reference signal ($r[k]$). The error in the tracking signal is sent back for the monitoring purpose.

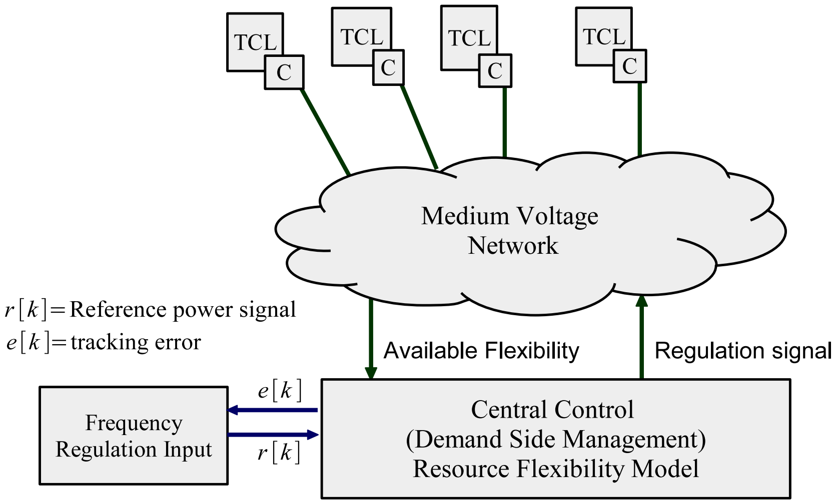

Figure 4.9: Overview of the control mechanism for an aggregation of TCLs.

4.4.1.2 TCL Model

TCLs possess flexibility termed as dead-band around the user defined set-points. The TCL temperature dynamics are shown in Figure 4.10, A non-disruptive operation can be achieved by controlling the operational state of the TCL within dead-band between θ_+ and θ_- [144]. In case of the air-conditioning load the sum of the heating T_h and cooling T_c times is called cycling duration.

In order to simulate the aggregation of TCL, a simplified first order model has been reported widely in the literature [150, 144, 151]. It is given by a stochastic hybrid discrete time difference equation given as,

$$\theta^i(t+1) = g^i\theta^i(t) + (1-g^i)(\theta^i_a(t) - \delta^i(t)\theta^i_g) + \epsilon^i(t) \ , \tag{4.20}$$

here, $g^i = e^{-\tau/(C^iR^i)}$ (τ is the sampling time of the TCL), $\theta^i_g = R^iP^i\eta^i$ and $\theta^i_a(t)$ is the ambient temperature measurement at i^{th} TCL. The first term represents the decaying influence of the temperature from previous time step, while the second term is the temperature gain/loss as TCL is switched On or Off. The parameter ϵ^i represents the measurement error of the i^{th} TCL. The

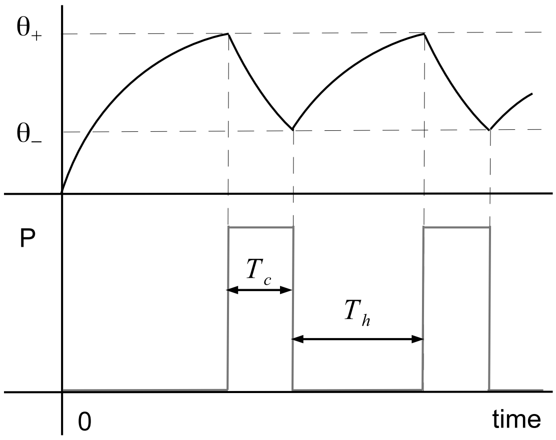

Figure 4.10: TCL temperature dynamics.

rated power of a TCL is given by P^i. It is positive in case of the air-conditioning load and negative for the heaters.

The state transition conditions for a TCL can be given as [144],

$$\delta^i(t+1) = \begin{cases} 1 & \theta^i(t+1) > \theta^i_{\text{ref}} + \Delta^i \\ 0 & \theta^i(t+1) < \theta^i_{\text{ref}} - \Delta^i \\ \delta^i(t) & otherwise \end{cases} \quad . \tag{4.21}$$

Where, Δ^i defines the dead-band around the set-point θ^i_{ref}. The TCL is considered non-controllable when operated outside the dead-band. Control of a TCL in its controllable region results in a non-disruptive interference. Such that it can momentarily suspend the normal operation without effecting the temperature crossing the dead-band limits. The local control of a TCL enforces the natural cycling process as the temperature crosses limits, during which the TCL is not available [144].

In the steady state it is assumed that $\theta^i = \theta^i_{\text{ref}}$. The corresponding power consumption can be obtained by solving the continuous power model from [149], leading to,

$$P^o_i(t) = \frac{\theta^i_a(t) - \theta^i_r}{\eta^i R^i} \quad . \tag{4.22}$$

The baseline power consumption ($P_{\text{base}}(t)$) can be considered as the average power consumed by a TCL operating in the steady state [144]. It can be given as,

$$P_{\text{base}}(t) = \sum_i P^i_o \quad . \tag{4.23}$$

The instantaneous active power consumption at t is the sum of rated power from all active TCLs and is given as,

$$P_{\text{agg}}(t) = \sum_i \delta^i(t) P^i \quad . \tag{4.24}$$

The difference between aggregate and baseline power consumption is given as,

$$\psi(t) = P_{\text{agg}}(t) - P_{\text{base}}(t) \quad . \tag{4.25}$$

This study considers the air-conditioning TCLs. Thus, $\psi(t) > 0$ when the average temperature of the TCL is below the set-point. It indicates the natural phenomenon of temperature decrease when TCL (air-conditioning) is active. In order to use TCLs as a frequency reserve, the reference power imbalance signal ($r(t)$) must be followed in real-time. This can be achieved by controlling the number of active TCLs in the aggregation in real-time. The TCLs can be collectively modeled by as a battery, where the reference signal can charge or discharge if $r(t) > \psi(t)$ or $r(t) < \psi(t)$, respectively. Maximum charging the battery shall turn Off all the TCLs, while the discharge process shall force On state of TCLs.

4.4.2 Energy Storage Model for TCL aggregation

A stochastic battery model has been proposed in [149]. It models the capacity and maximum charge/discharge rates of the battery. According to it, the battery parameters are,

$$\begin{aligned} C' &= \sum_i \left(1 + \left|1 - \frac{a_i}{\alpha}\right|\right) \frac{\Delta_i}{b_i} \\ R'_+ &= \sum_i (P_i - P_i^o) \\ R'_- &= \sum_i P_i^o \end{aligned} \quad , \tag{4.26}$$

here, $a_i = 1/(R_i C_i)$, $b_i = \eta_i / C_i$ and $d = 1/N \sum_i 1/(R_i C_i)$. The parameters are thermal resistance (R), capacitance (C), efficiency (η) and number of TCLs (N). This formulation enables the calculation of the maximum capacity (kWh) available in the system as a stochastic variable. The availability of TCL is a limiting factor in this regard.

The consideration of TCL availability results in a dynamic stochastic model of the battery. The parameters for which are given as,

$$\begin{aligned} C &= \sum_i \lambda^i(t) \left(1 + \left|1 - \frac{a_i}{\alpha}\right|\right) \frac{\Delta_i}{b_i} \\ R_+ &= R'_+ - \sum_i (1 - \lambda^i(t)) P_i \\ R_- &= R'_- + \sum_i (1 - \lambda^i(t)) P_i \end{aligned} \quad , \tag{4.27}$$

where, the $\lambda^i(t)$ is the availability of i^{th} TCL given as,

$$\lambda^i(t) = \begin{cases} 1 & \rho^i(t) > \overline{\rho^i} \ \& \ \underline{\theta^i} \leq \theta^i(t) \leq \overline{\theta^i} \\ 0 & \text{otherwise} \end{cases} \quad . \tag{4.28}$$

The stochastic ramp limit constraint on the reference signal can be considered as,

$$R_- \leq r(t) \leq R_+ \quad . \tag{4.29}$$

While the SoC constraint is incorporated as,

$$-C \leq \left(\sum_i \left[\frac{\theta^i_{\text{ref}} - \theta^i(t)}{b_i} \right] \right) \leq C \quad . \tag{4.30}$$

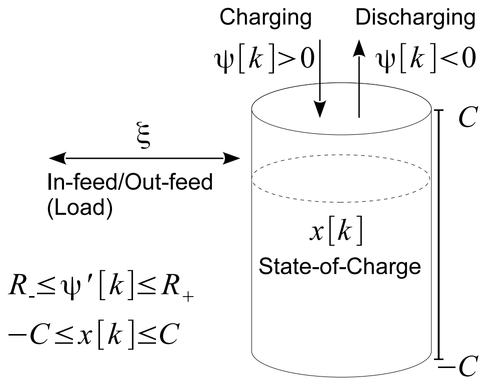

Figure 4.11: Stochastic battery model for the TCL aggregation.

Note: The temperature difference $(\theta^i_{ref} - \theta^i(t))$ in Equation 4.30 represents the temperature decrease when the air-conditioning is On, it represents the charging of the battery.

Stochastic battery model is shown in Figure 4.11. The dynamics of the variables are bounded by the stochastic limits and are given as,

$$\dot{x}(t) = -dx(t) - p(t),\ x(0) = 0,\ |x(t)| \leq C \quad , \tag{4.31}$$

where, the dissipation rate (d) is given as,

$$d = \frac{1}{N} \sum_{k=1}^{N} \frac{1}{R_i C_i} \quad . \tag{4.32}$$

4.4.3 Resource Capability Envelope for TCL aggregation

The dynamic capability of the TCL aggregation is characterized by the ramp-rate and the state-of-charge limits. Based on different values of the $x[k]$, the values of the ramp-rate and ramp duration can easily be obtained while satisfying the following constraints,

$$-C \leq R \times T_{dur} \leq C \ . \tag{4.33}$$

$$\underline{R^-} \leq R \leq \overline{R^+} \ . \tag{4.34}$$

The response time of the TCL aggregation can be modeled using the time delay in the communication and its response time against change in set-point. This delay can be proportional to the load, by assuming a direct relationship with inertia. The cost of service can be modeled as a function of the load change, price in the energy market and customer preferences. The proposed capability envelope as part of RFM can be used to define the resource specific constraints.

5 Flexibility Aggregation and Allocation

5.1 Introduction

Flexibility from distributed resources shall play an important role in supporting the high ramp-rate requirements of future power systems [3, 130]. The activation of flexibility from distributed resources such as generation, load or storage shall require an energy market at the distribution side of the power system. The organizational measures of local market design can pave the way for the flexibility aggregation and fast dispatch of resources. It can potentially improve the local generation forecasts, implement the demand response programs and smart grid technologies based on smart meters and others [5]. Microgrid as a key enabler for the activation of flexibility can support the Distributed Generators (DGs) with higher ramp-rate capability, active demand response from thermal loads, charging control of electric vehicles, network expansion and enhancement, electricity storage using pumped hydro, thermal storage and as a last option active power curtailment from renewables. The flexibility defined by Resource Flexibility Model (RFM) in Chapter 4 can be used to model the flexibility potential of distributed resources in the microgrid. This chapter aims at presenting methods that can be used to aggregate and allocate the flexibility while performing the reserve planning in a day ahead scenario. The allocated reserve capacities have been used in the Unit Commitment (UC) and Security Constrained Economic Dispatch (SCED) applications. They provide a mechanism for incorporating the reserve requirements obtained by the flexibility allocation process in practice. The contents of this chapter are partly published in [83], [152] and [153].

5.2 Flexibility Assessment and Aggregation

The flexibility assessment is an important phase in the operational planning of the microgrid. It aims to predict the demand patterns of consumers and model the associated uncertainty. This section defines a general approach for the demand and reserve requirements in microgrid based on the results from Chapter 3. The reserve margins are generally defined based on the standard reliability metrics. The metric called reliability indexes defines reserve requirements for the system. Here, a distribution feeder is studied to observe the ramp-rate variations in the *net-demand* as function of time of day and month. It is observed the worst case demand and reserve ramp-rate requirements can be an expensive approach during the resource planning process. Thus the proposed approach for modeling the uncertain demand discussed in Section 3.3.2 is relevant for assessing the demand and reserve requirements. The variation of the envelope size for the different levels of probabilistic confidence in results is discussed.

5.2.1 Reserve Flexibility Margins

The objective of operational flexibility planning is to define the demand and reserve requirements in the system. It is necessary to maintain a resource adequacy level. It is a probability that the level of installed capacity is available to serve the demand at all times. Resource adequacy is enforced by implementing the reserve margins in the system. It is a percentage of the installed capacity exceeding the peak demand. It can be set for a specific level of Loss of Load Probability (LOLP). LOLP can be described as a projected value of how much time, in the long run, the load is expected to be more than the capacity of generation resources. The LOLP criteria based metrics includes,

- Loss of Load Expectation (LOLE), measured in number of loss of load events/year,
- Expected Unserved Energy (EUE), measured as percentage of the net energy requirements not served,
- Loss of Load Hours (LOLH), which is number of hours of unserved load.

LOLE and LOLH are based on power loss event expectancy while EUE is about the level of energy not served. A comparison of these metrics is shown in Figure 5.1.

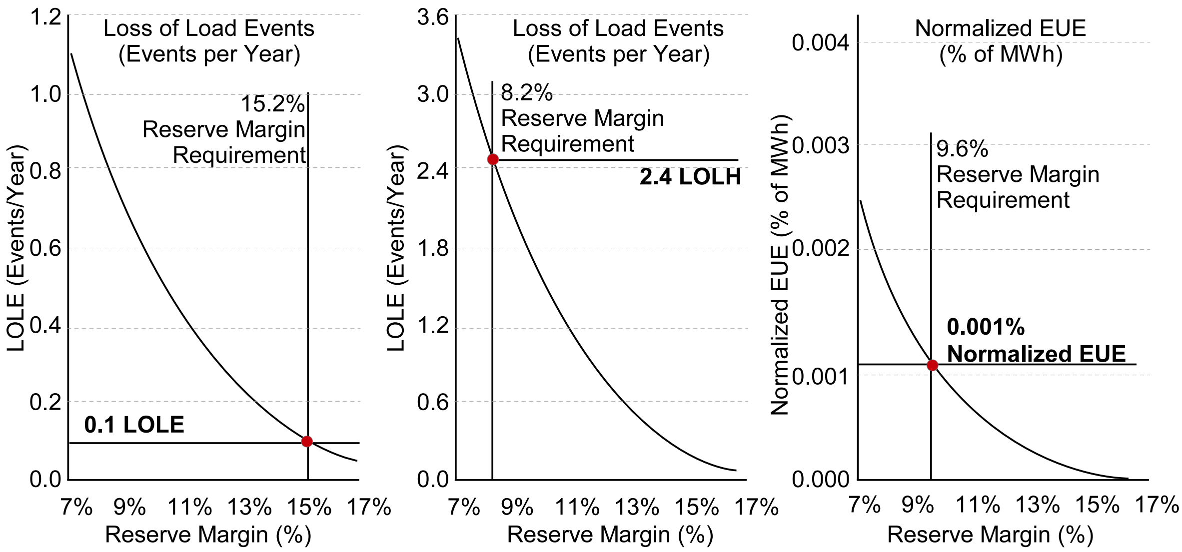

Figure 5.1: Reliability indices representing the reserve requirements, where, LOLH of 2.4 hours per year and LOLE of 0.1 event per year leads to different reserve specifications in United States. The 0.001% normalized EUE is standard in some energy markets [154].

Extensive bench marking is required to determine the level of LOLH that corresponds to a certain LOLE reliability level e.g., 0.1 events per year [155]. Additional discussion about the selection of reserve margins can be found for National Electric Reliability Corporation (NERC) in [156] and the capacity value studies of wind power [157] and solar power [158]. As the load increase the Loss of Load Expectation also increase. A contribution from a resource in sharing the load decreases

LOLE by a margin called Effective Load Carrying Capability (ELCC) or capacity credit. It is of interest to analyze the contribution of resources towards the required capacity credit in order to achieve a specific level of LOLE.

These reliability metrics can be used to define the reserve levels critical for reliable operation in a microgrid. In literature, various studies have discussed the reserve requirements in relevance. An overview of the control and reserve management strategies in microgrid is discussed in [159]. While in [160], a stochastic energy and reserve scheduling method is proposed considering the demand response in the microgrid. Authors in [161] have used artificial neural networks for the forecasting and used the results for the reserve quantification in microgrid. These studies focus on an interval based approach for the reserve allocation. However, this thesis takes a more holistic approach by modeling the uncertain demand dynamics. This consideration leads to the assessment of required reserve capability and is used as a reference during resource allocation.

5.2.2 Demand Dynamics at a Distribution Feeder

The impact of variable generation on the *net-demand* at a feeder for one week duration is shown in Figure 5.2. The data for the analysis is taken from [162]. It can be observed that the penetration of renewables has resulted in steeper ramps. Secondly, deep turn-downs and high peaks are most likely to occur. The generation resources required in future for meeting the demand and providing ancillary services should have high ramp-rate capability and small start-up times.

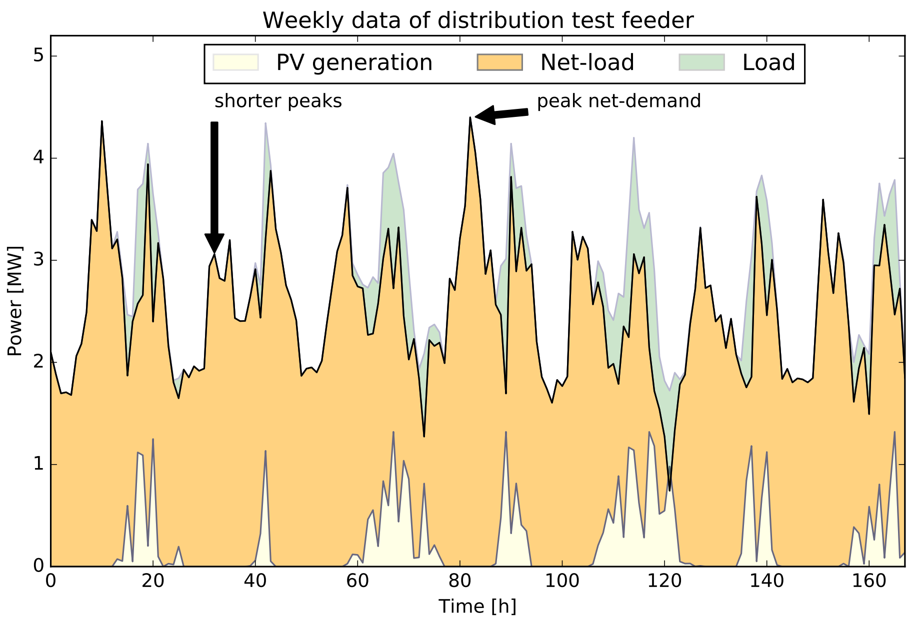

Figure 5.2: Effect of the power generation from Photo Voltaics (PVs) on the *net-demand* at a distribution feeder. It impacts in steep ramps, deeper turn-down and high peaks in the *net-demand*.

Figure 5.3 shows how the ramping intensity varies for each month for the load connected to the distribution feeder. The month of June experiences ramp-up rate ratio of $[0.42 - 0.53]$ during 35% of days in the month. While observing the *net-demand* statistics, it can be observed that renewable energy increases the ramp-up rate requirement for all months. The month of March experiences the least occurrence of high ramp-up ratio.

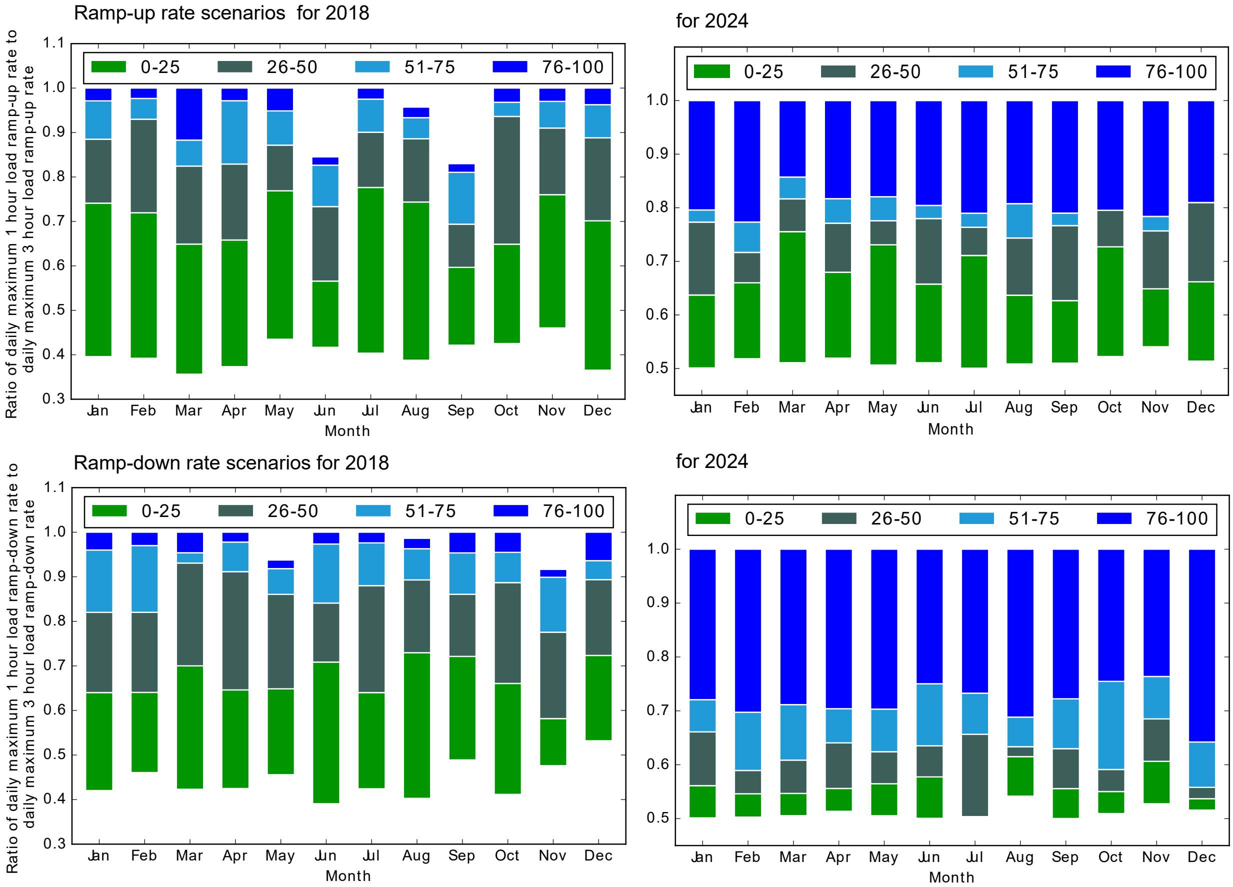

Figure 5.3: Comparing the results in each graph shows monthly variations in the ramp-up/down rates, where each bar represents the ramp intensity contributions. This value is defined as a ratio between 1-hour vs 3-hour ramp excursion. For the top-left graph, the maximum value of this ratio is minimum for months of July and September. While comparing the graphs from the left with right, it can be observed that both ramp-up and ramp-down rates increases for all months. This is due to high share of renewables expected in 2024.

From the analysis, it can be observed that the distribution network shall face high ramp-rates in future. Therefore, the supporting flexibility resources whether DGs or demand response are desired to possess the relevant dynamic capability. This signifies the approach undertaken in this research, that emphasis on the economic modeling of the reserve dynamics that can potentially yield to effective flexibility management strategies.

5.2.3 Flexibility Envelope Modeling

In order to meet the local demand and reserve requirements, the controller in the active distribution network shall play a central role in dispatch of the resources. In order to capture the uncertainty in the *net-demand*, the historical data of the forecast uncertainty was used to develop a probabilistic model. This model captured the spatio-temporal nature of the uncertainty and was used to generate scenarios for a given forecast level. The methodology has been described in

Section 3.4.3. The first order dynamics had been obtained by the application of the compression algorithm on the scenario curves. As the variables of ramp-rate and ramp duration are correlated with the power values, an envelope is modeled to enclose the set of points. The envelope in case of *net-demand* represents the demand and the uncertainty dynamics. The difference between demand and the uncertain *net-demand* envelope determine the reserve flexibility requirements. Furthermore, the size of flexibility envelope is determined by the boundary points enclosed. This size increases with the rise in number of scenarios primarily due to the occurrence of events having less probability. The number of scenarios N is the function of desired probability of constraints satisfaction $(1-\epsilon)$ and confidence in results $(1-\beta)$ as discussed in Equation 3.8. Figure 5.4 shows a the flexibility requirement for various levels of $(1-\epsilon)$. The number of scenarios that are used to generate the envelopes are given in Table 5.1. It can be observed that in few cases increasing the confidence level e.g., from 0.6 to 0.7 may decrease the flexibility requirements due to the occurrence of rare events.

Table 5.1: Comparison of probabilistic confidence level $(1-\epsilon)$ and the number of scenarios requirements. The confidence in result $(1-\beta)$ is set at 0.9999 for all cases.

$1-\epsilon$	N	$1-\epsilon$	N
0.5	33	0.6	41
0.7	54	0.8	81
0.9	162	0.99	1616

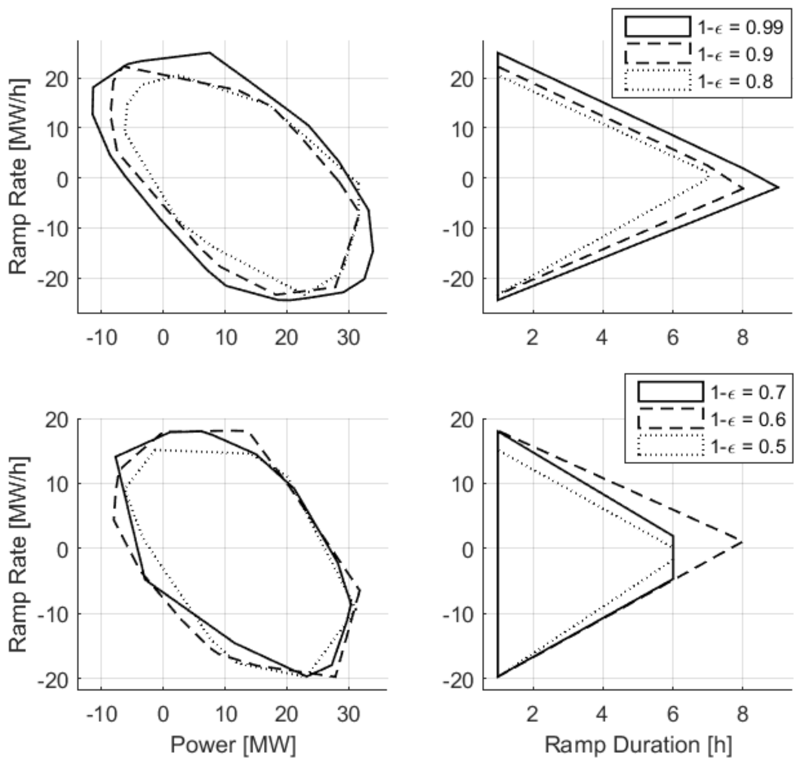

Figure 5.4: Impact of the desired probabilistic confidence against uncertainty $(1-\epsilon)$ on the size of the *net-demand* envelope in microgrid.

5.2.4 Flexibility Bid Formulation

Each resource can bid its flexibility based on the requirements and resource owner preferences. The flexibility bid structure can be based on the RFM presented in Section 4.2. It will be regulated by the structure of the local energy market. The objective in such a market can be to schedule the electricity supply from local resources and the grid to meet the local demand forecast. In any energy market setup, the two major role players are supply and demand parties that bid the prices as function of their energy offer. The supply side bid corresponds to the price charged for generating a specific quantity of power during a time interval e.g., hour. While the demand side bid represents price which the customers are willing to pay for a power level during a time interval. A simple bid format consists of pairs of quantity $(q,\ p)$ where, q is energy (MWh) and p is price (\$/MWh) value for each hour. Each participant can present several pairs (p, q) values for each hour. For each hour the supplier and consumers offer tuples of price and quantity value $((p_1, q_1), (p_2, q_2), \cdots, (p_T, q_T))$. The vectors of supply and demand are aggregated and the market clearing price is determined at their intersection points. The bids can be continuous curves or can be modeled as discrete steps. A demonstrative example of a simple auction is shown in Figure 5.5. The intersection of both the curves decides the market clearing price. In a day ahead market 24 hourly auctions are performed. For each hour, the supplier bids their offers. Based on the overall demand and supply curves the market clearing price is decided. The step-wise aggregate supply and demand curves as shown in Figure 5.5 intersect at a demonstrative value of 60 and at Market Clearing Price (MCP) of 23. The supplier bids whose price is less than or equal to the MCP are selected for the auction. During allocation the bids that are closest to the MCP are selected. Based on the demand forecast, each supplier designs its bidding strategy considering an expected revenue. Similar mechanisms are expected to evolve for the local energy market.

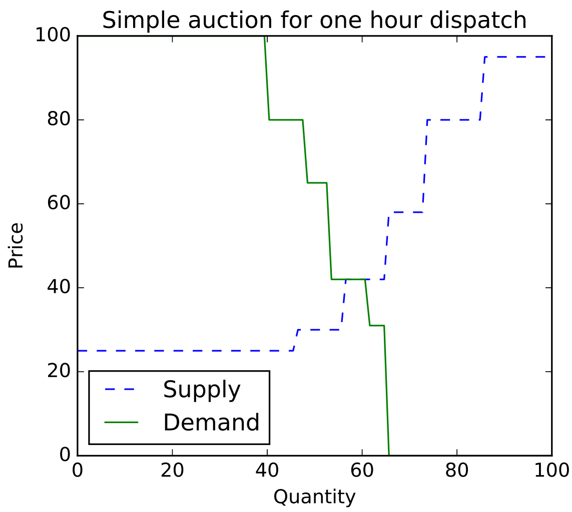

Figure 5.5: Illustration of simple auction in energy market where step-wise demand and supply are matched.

In addition to the simple price/quantity bids a supplier can add additional constraints [163],

- **Non-divisible quantity.** The cheapest bid can be designated as non-divisible. Such that if this bid is accepted the whole quantity should be accepted.

- **Minimum daily income amount.** This constraint specifies the minimum amount of income to the supplier that should be guaranteed by the market operator. The corresponding power quantity can vary based on the price dynamics.
- **Ramp-rate constraint.** The energy scheduling between consecutive time intervals need to consider the minimum ramp-up and ramp-down rates e.g., in MW/min of the participating suppliers.

These constraints can be handled as a single combinatorial optimization problem or a set of sub-problems in which the constraints are sequentially enforced. A detailed algorithm of market clearing can be found in [164]. Apart from the single round auction, the multiple round auction involves the update in bids as outcome of an iterative approach. The Resource Flexibility Model discussed in Section 4.2 provides a comprehensive representation of the capability of a resource. This information can be used in design of the bidding strategy as single period or multi-period bids. The amount of energy available at a resource can be divided into hours in the day e.g., in units of MWh and used in bidding process. The offered price can be determined using the generation cost obtained from the dynamic capability envelope and the market price. This price shall be greater than the sum of minimum revenue and generation cost at a supplier. Similarly, the demand side can bid its flexibility using RFM. In addition to the first order dynamics, the second order dynamic i.e., ramp acceleration can become part of demand and reserve market operations. In such a case ramp acceleration can be added to RFM. The control entity whether operating as a cell or microgrid controller shall be responsible for the flexibility aggregation from the resources.

5.2.5 Flexibility Aggregation

The role of aggregator is to combine the flexibility offered from distributed resources. This role can be performed by an independent organization or by a cell/microgrid controller. The flexibility of a resource can be modeled as envelope between the dynamics variables. Minkowski sum is used to add the geometric models of flexibility from resources. The Minkowski sum of two sets $S_1 \subset \mathbb{R}^2$ and $S_2 \subset \mathbb{R}^2$, denoted by $S_1 \oplus S_2$, is defined as,

$$S_1 \oplus S_2 = \{p + q \ : \ p \in S_1, q \in S_2\}, \tag{5.1}$$

where, $p + q$ denotes the vector sum of the vectors p and q i.e., if $p = (p_x, p_y)$ and $q = (q_x, q_y)$ then,

$$p + q = (p_x + q_x, p_y + q_y). \tag{5.2}$$

It is demonstrated in Figure 5.6. The minkowski sum can be used to aggregate the flexibility envelopes (Resource Capability Envelope (RCE)) from the resources. The allocation of demand flexibility envelope among the resources can be straight forward if the economics are not considered. The difference between demand envelope and the aggregate resource potential shall be imported or exported to the grid depending on the need or excess of the additional flexibility. As the economics of flexibility services offered by the resources greatly varies, therefore there is a need of an allocation method that optimizes the process with minimization of the costs. Such that the generation adequacy in the microgrid can be ensured within a budget specified by the microgrid operator.

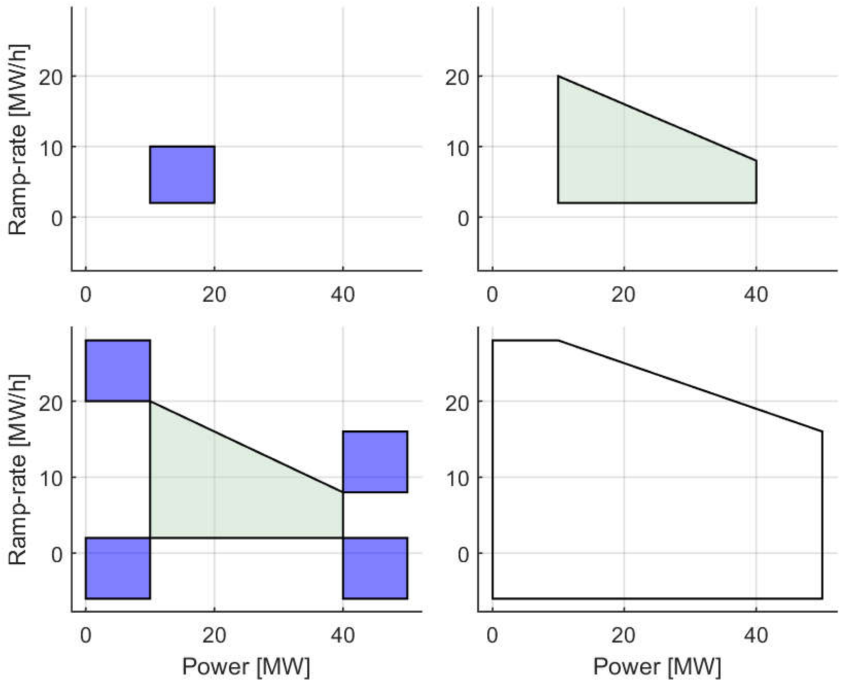

Figure 5.6: Flexibility aggregation using Minkowski sum.

5.3 Flexibility Allocation

Flexibility allocation is performed by the decomposition of uncertain demand envelope (Δ) among the generator capability envelopes (Δ_i). The area of computational geometry provides insights in the space allocation methods [165]. One of the method is to model the allocation process as an optimization problem with Δ defined in the hyper-plane representation. It is found that the corresponding allocation process involves non-convex scaling along ramp-rate and ramp duration axes. While, Minkowski sum can be relevant for the demand allocation process. In comparison, a vertex based allocation method is developed. It facilitates the modeling of constraints on individual variables. The allocation of Δ among resources is a deterministic process. During which, the power import from the main grid is used as a slack resource. Δ is decomposed in two steps, the demand and dynamics allocation.

5.3.1 Demand Allocation

The range of the Δ along power axis is divided into desired number of equidistant points C. Here, each point is a demand value termed x_j. Each x_j is dispatched among the resources by solving,

$$\begin{aligned} &\min \quad \sum_{i=1}^{N} \left[a_i P_i^j + b_i (P_i^j)^2 \right] \quad , \\ &\text{s.t.}: \quad \forall\, i = 1 \cdots N,\ j = 1 \cdots V_j \end{aligned} \tag{5.3}$$

power balance constraint,

$$\sum_{i=1}^{N} P_i^j \geq x_j \quad , \tag{5.4}$$

generator active power limits,

$$\underline{P_i} \leq P_i^j \leq \overline{P_i}, \quad i \in N \ , \tag{5.5}$$

generator reactive power limits,

$$\underline{Q_i} \leq Q_i^j \leq \overline{Q_i}, \quad i \in N \ , \tag{5.6}$$

power flow equations,

$$\begin{aligned}
&P_{Ga} - \sum_{b \in N_B} \left[e_a(e_b G_{ab} - f_a B_{ab}) + f_a(f_b G_{ab} + e_b B_{ab})\right] = P_{Da} \\
&Q_{Ga} - \sum_{b \in N_B} \left[f_a(e_b G_{ab} - f_a B_{ab}) - e_a(f_b^t G_{ab} + e_b B_{ab})\right] = Q_{Da} \\
&a \in N_B \ \ i.e., \ \ \forall a \notin N \implies P_{Ga}, \, Q_{Ga} = 0 \ ,
\end{aligned} \tag{5.7}$$

transmission line constraint,

$$\begin{aligned}
&\underline{P_{L_{ab}}} \leq P_{L_{ab}} \leq \overline{P_{L_{ab}}} \ , \\
&\text{where,} \\
&P_{L_{ab}} = \left[e_a^2 + f_a^2 - e_a e_b - f_a f_b\right] G_{ab} \\
&+ (e_a f_b - e_b f_a) B_{ab} \ , \ ab \in S_L \ ,
\end{aligned} \tag{5.8}$$

bus voltage limit constraint,

$$\underline{V_a}^2 \leq \left(e_a^2 + f_a^2\right) \leq \overline{V_a}^2, \quad a \in N_B \ . \tag{5.9}$$

The constraints in Equation 5.5 and 5.6 ensures the consideration of generator active and reactive power limits. While, the transmission line and voltage limit constraints in Equation 5.8 and 5.9 incorporates the location and operational aspects.

5.3.2 Dynamics Allocation

The polytope Δ is sectioned at each demand value x_j using Algorithm 3.2 resulting in C sub-polytopes ($S_j(\Delta)$). Here, the vertices of $S_j(\Delta)$ represents the ramp-rate and ramp duration. In the first step, the polytope of each generator Δ_i is sectioned at the assigned power P_i^j leading to the sub-polytopes $S_j(\Delta_i)$. The allocation is then performed for each vertex k of $S_j(\Delta)$, where $k = 1 \cdots V_j$. The k^{th} vertex of $S_j(\Delta)$ is given as $[y_j^k \ z_j^k]$. The corresponding generator vertices ($g_i^k = [r_i^k \ d_i^k]$) are found by solving,

$$\min \quad \sum_{i=1}^{N} \left[a_i(r_i^k d_i^k) + b_i(r_i^k d_i^k)^2\right] \ , \tag{5.10a}$$

$$\text{s.t.}: \quad \forall \, i = 1 \cdots N, \ k = 1 \cdots V_j \ ,$$

$$H_i^j \begin{bmatrix} g_i^k \\ -1 \end{bmatrix} \leq S_j(\Delta_i) \ , \tag{5.10b}$$

$$\sum_{i=1}^{N} r_i^k d_i^k \geq y_j^k z_j^k \ . \tag{5.10c}$$

Here, Equation 5.10a is the quadratic cost assigned to displacement in power of generator i. Equation 5.10b constrains the generator i variables to be within the sub-polytope space. While, Equation 5.10c is the power balance constraint. The result of the optimization problem are allocated vertices given as $[P_i^j \ r_i^k \ d_i^k]$. A polytope encloses the allocated vertices of each generator.

5.3.3 Scalability

The formulation in Section 5.3.1 is similar to that of the Optimal Power Flow (OPF) problem [166]. The time complexity in solving OPF can be attributed to the problem size and the solver used. Primal Dual Interior Point method is used to solve the demand allocation problem in Section 5.3.1. In Section 5.3.2, Equation 5.10 is the function of number of inputs (N) and the size of resource capability envelopes. An addition of a generator adds $\sum_{j=1}^{C} V_j$ constraints to the problem. Equation 5.10b restrict the vertex (g_i^k) assigned to a generator within its envelope. The size of $S_j(\Delta_i)$ defines the search space and influences the computational time. However, it is independently applied for each generator. Thus, the complexity of this equation increases linearly with N. The coupling between generators appears as a linear combination in Equation 5.10c and it scales accordingly. The structure of this constraint is bilinear, hence, branch and bound algorithm is used to solve Equation 5.10. Overall, the problem remains tractable as N increases.

5.4 Test Case of Flexibility Allocation

The flexibility aggregation and allocation method is demonstrated with a microgrid test-case which is based on International Council on Large Electric Systems (CIGRE) Medium Voltage (MV) benchmark [123, 124], European configuration. The details about network have been discussed in Section 3.4. The uncertain *net-demand* based demand envelope show in Figure 5.7 is to be allocated between resource envelopes. The resources considered here are the diesel generators. The dynamic ramp-rate of a generator is modeled using thermal stress model as discussed in Section 4.3.1. The result is a polytope Δ_i for each generator. The power import capability polytope has a cubic structure due to the consideration of static ramp-rate limits defined by the ratings of HV/MV transformer. After modeling of the resource envelopes, the next step is the allocation process.

5.4.1 Polytope Decomposition

An overview of the polytope decomposition process is show in Figure 5.7 where the *net-demand* envelope is allocated among the RCEs while optimizing for the generation cost. As discussed in Section 5.3, the decomposition of Δ is performed in two steps. In the first step, the demand x_j is dispatched by solving the demand allocation problem in Section 5.3.1. This process is repeated C times. In the second step, each vertex of the polygon $S_j(\Delta)$ for the j^{th} demand is allocated by solving optimization problem in Equation 5.10. The process results in the vertex assignment to generation resource i given as $[P_i^j \ r_i^k \ d_i^k]$. It is repeated for the j^{th} demand values and the k^{th} vertex of the polygon $S_j(\Delta)$. As a result of this process the spaces are allocated to each generation resource. Figure 5.8 shows the allocation among local generators in the microgrid test case. Figure 5.10 provides an insight in the capability utilization of generators 1 and 2. The projections of enclosed polytopes shows the comparative analysis of demand and reserve allocation among generators.

The optimization of individual polytope is based on the production cost while considering the operational constraints. Figure 5.9 shows the envelope assigned to the power import from the main grid. It can be used in the resource planning for the islanded-mode operation of microgrid. Such that the fast and slow ramping generators can be allocated with associated ramp duration

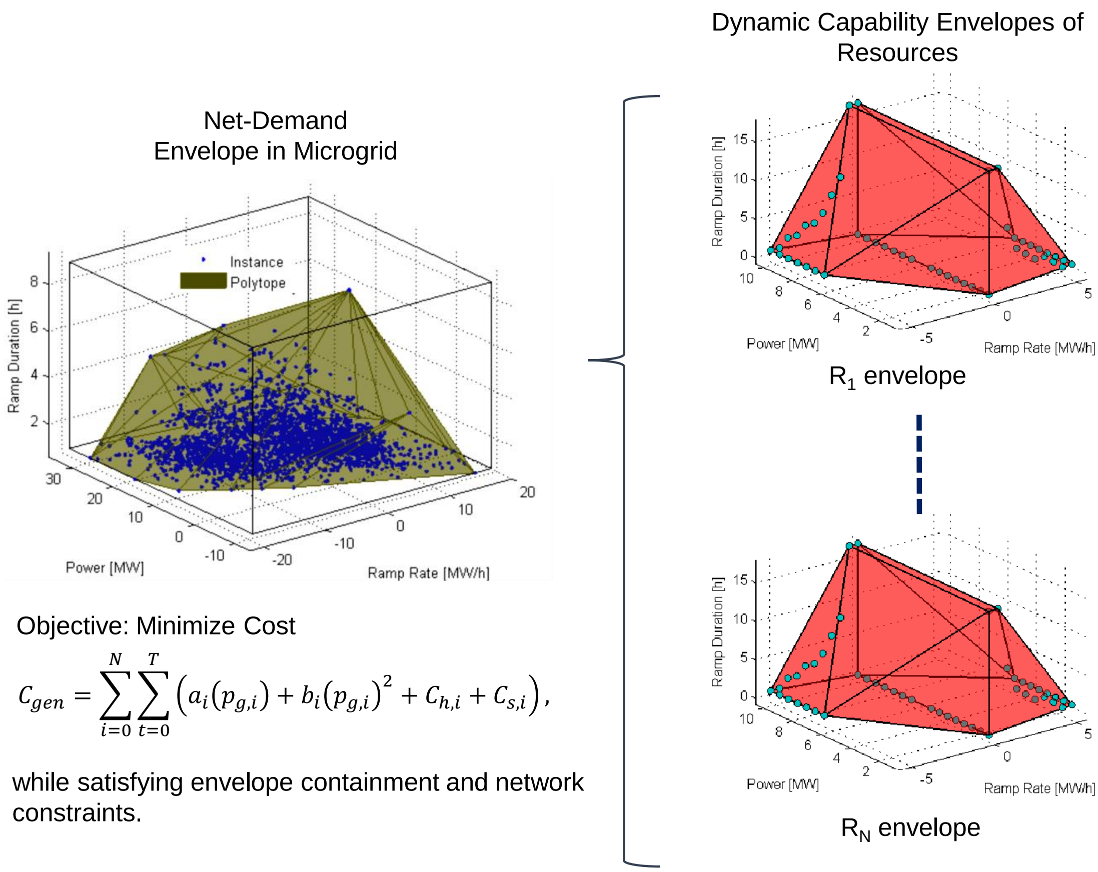

Figure 5.7: An illustration of the economic flexibility allocation process in which the *net-demand* and reserves are to be allocated between resources represented by envelopes.

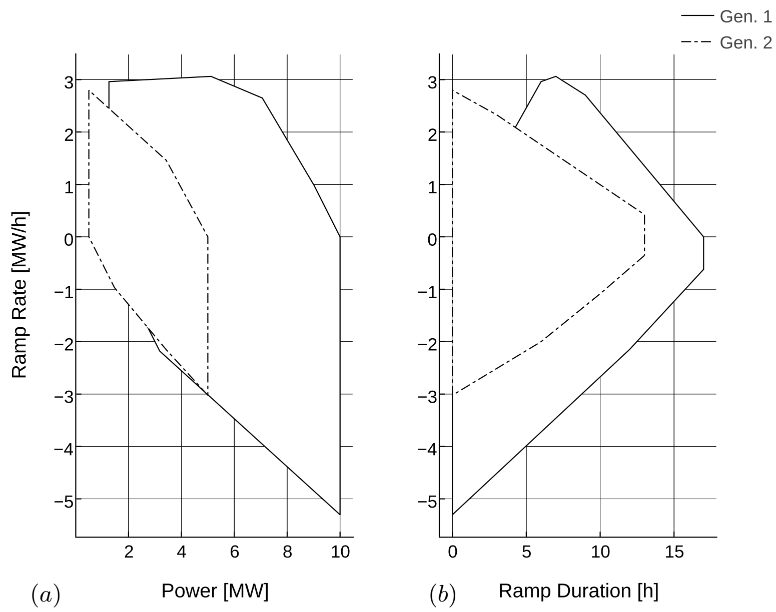

Figure 5.8: Figure (a) and (b) shows the $x-y$ and $y-z$ projections of the allocation of Δ among generator 1 and 2. The allocated capability is bounded by the operational constraints of each generator.

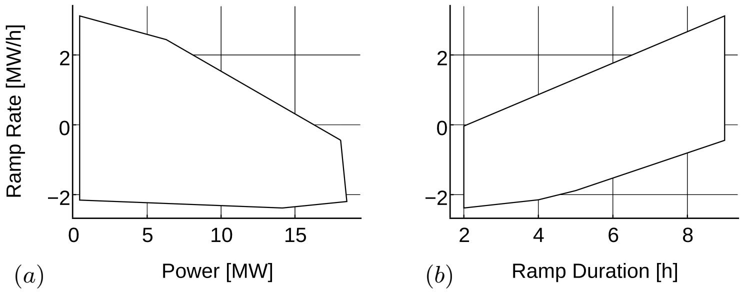

Figure 5.9: Figure (a) $x-y$ and (b) $y-z$ are projections of the polytope assigned to power import from grid. It provides a reference for the resource planning in the microgrid.

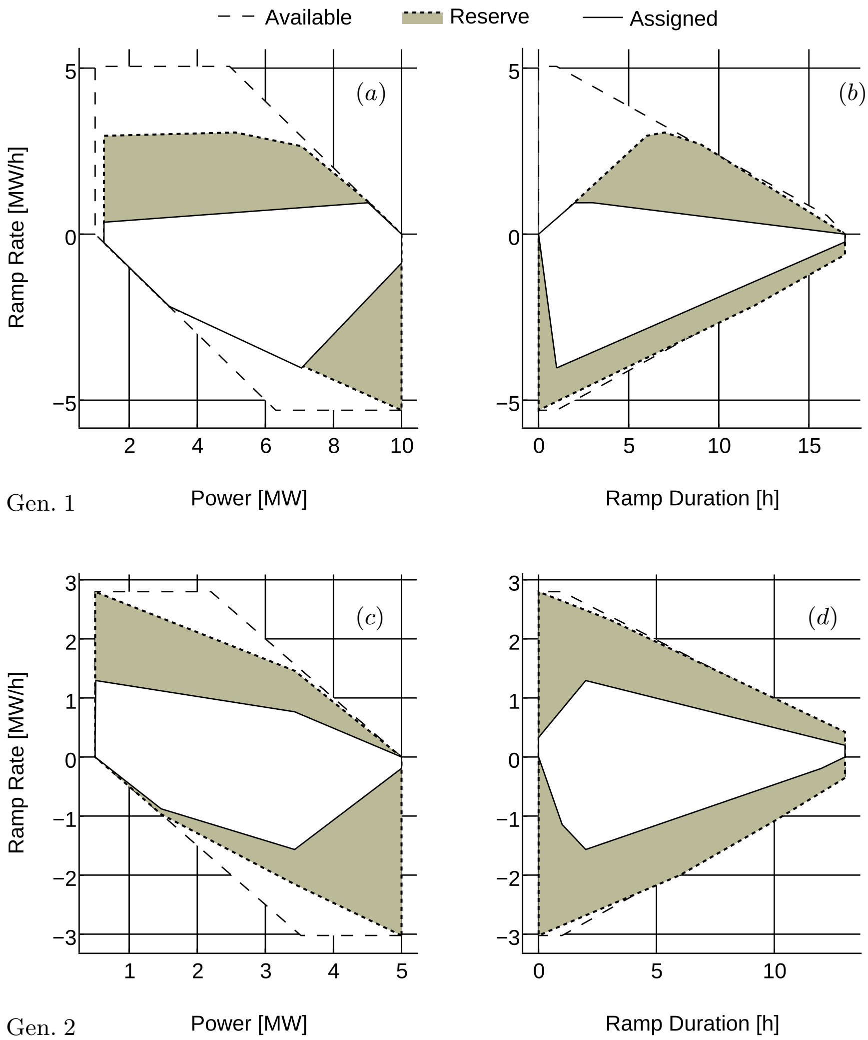

Figure 5.10: Projections of polytopes assigned to generator 1 and 2. The "assigned" areas are the generator polytopes against day-ahead demand forecast. The allocated polytopes Δ_i includes both the "assigned" and the "reserve" areas. While the "available" region shows the capability polytopes of generators. The space between "reserve" and "available" marks the un-used dynamic capability of a generator.

capability. The approach provides insights into the assigned, reserve and the available capabilities. It can be extended to the contingency reserve planning in microgrid. In case of a generator contingency, the respective capability envelope shall be allocated among the remaining resources in a similar way. The transmission line and bus contingencies can be incorporated during the allocation process as discussed in Section 5.3.1.

5.4.2 Cost Analysis

The maximum deviation from the day-ahead forecast as a reserve reference for the scheduling of up and down-spinning reserves has been discussed in [167]. This approach assumes fixed uncertainty at all power levels. However, the proposed approach allows for the consideration of dynamic value of the uncertainty. It is obtained from the worst case limits of the power balance scenarios generated by the Monte Carlo simulations. Figure 5.11 compares the limits associated with the fixed and dynamic reserve allocation approaches. The result shows 27% reserve requirement can be reduced by dynamic dispatch of reserves as compared to fixed percentage of load ramp-up/down reserve approach.

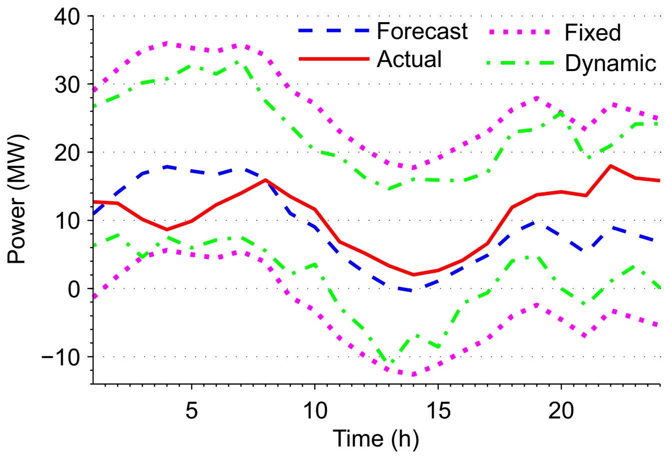

Figure 5.11: Comparison of the reserve requirements for the day-ahead fixed and the dynamic range based approaches. It shows that the reserve requirement can be decreased while still covering the uncertainty with a probability defined in Equation 3.8.

5.5 Flexibility in Operation

An important problem in the energy management of a microgrid is the operational schedule for generation resources. This needs to be decided ahead of time generators needs time for starting up. A day-ahead dispatch is performed to allocate these resources for meeting demand of the next day. The day-ahead operational planning needs to consider both the demand and generation uncertainty. For this purpose, a sufficient level of reserve is allocated for each time period. Here, these values are decided based on the results of flexibility assessment from Section 5.2. The reserve requirement is stochastic and is defined by the interval limits of the up and down spinning reserves. These values are incorporated in the day ahead planning by solving two problems i.e., the Unit Commitment and Economic Dispatch. In the next sections both of these problems are discussed.

The output of these algorithms is the operational schedule for the generators and dispatched value of the demand and reserve contributions.

5.5.1 Unit Commitment

The Unit Commitment (UC) problem is defined in [168] as, “Unit Commitment is an optimization problem of determining the operational status of generations for a given profile of energy demand. This problem is subject to generation and network operational constraints.” The objective of UC problem is generally the cost minimization but may include environmental, safety and/or market oriented objectives. Mathematically, UC is a large scale non-convex and nonlinear mixed integer problem [169]. Due to its importance in power system operation, the literature regarding solving and improving UC problem spans over four decades.

5.5.1.1 Mathematical Formulation

The objective of UC problem is the minimization of fuel cost given by,

$$\min\ C_T = \sum_{t=1}^{T}\sum_{i=1}^{N}\left[\rho_i^t C_F^i(P_i^t)\right] \quad , \tag{5.11}$$

where, ρ_i^t is the operational state of i^{th} generator at time t, C_T is the total cost, C_F is fuel cost, P_i^t is real power generated by i^{th} generator and value N is the total number of generators. The UC problem generally have following constraints [170],

Constraints.
1. Limits on the active power of generator i,

$$\rho_i^t \underline{P_i} \geq P_i^t \geq \rho_i^t \overline{P}_i \quad . \tag{5.12}$$

2. The power balance constraint,

$$\sum_{i=1}^{N} P_i^t \rho_i^t = P_D^t + \mathrm{SR}^t \quad . \tag{5.13}$$

Where P_D^t is the demand and SR^t is the spinning reserve requirements at time t. The spinning reserve requirement is obtained from the output of flexibility assessment discussed in Section 5.2.

3. Ramp-rate constraints on the generator,

$$P_i^t - P_i^{t-1} \leq \left[1-\rho_i^t(1-\rho_i^{t-1})\right]\overline{R_i^+} + \rho_i^t(1-\rho_i^{t-1})\underline{P_i} \quad , \tag{5.14}$$

$$P_i^{t-1} - P_i^t \leq \left[1-\rho_i^{t-1}(1-\rho_i^t)\right]\underline{R_i^-} + \rho_i^{t-1}(1-\rho_i^t)\underline{P_i} \quad . \tag{5.15}$$

4. Start-up and shut-down characteristics of generator,

$$\left(\rho_i^{t-1}-\rho_i^t\right)\left(X_i^{on}(t-1)-T_i^{on}\right) \geq 0 \quad , \tag{5.16}$$

$$\left(\rho_i^t-\rho_i^{t-1}\right)\left(-X_i^{off}(t-1)-T_i^{off}\right) \geq 0 \quad , \tag{5.17}$$

Here, T_i^{on} and T_i^{off} are minimum On and Off times of generator i. While, $X_i^{on}(t-1)$ and $X_i^{off}(t-1)$ are the duration of On and Off states of the generator i at time $(t-1)$.

The optimization in the UC problem is carried out over all the time steps in the horizon and can be termed as multi-period optimization. The hourly constraints in the UC problem includes the generator active power limit constraint (5.12), power balance constraints (5.13), ramp-rate limits on each generator (5.15) and (5.14), minimum On/Off times for a generator 5.16 and 5.17.

5.5.1.2 Test Case for Unit Commitment

The Unit Commitment optimization model is solved for a day ahead dispatch for the a Western System Coordinating Council (WSCC) 9 bus network presented in [171] and is shown in Figure 5.12. The test case data is also available as part of Matpower software [172].

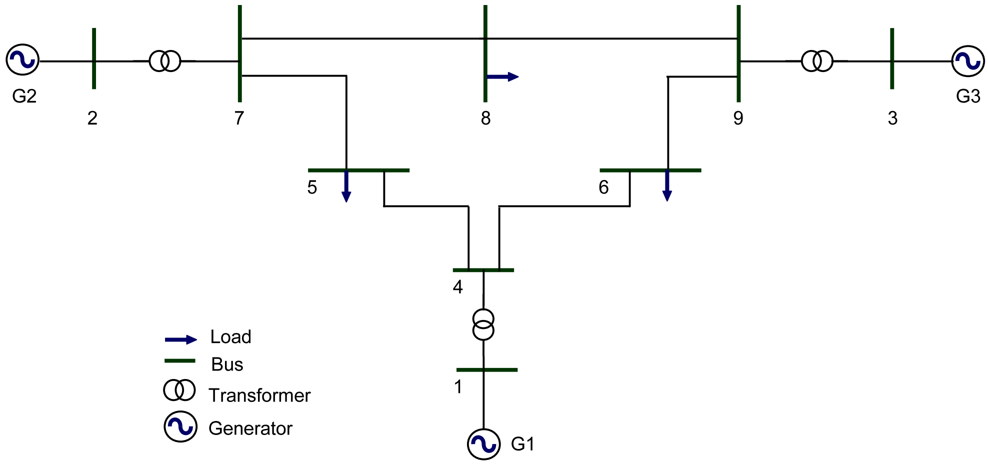

Figure 5.12: One-line diagram of 9 bus power system from [171].

Bus	Load		Bus	Load	
–	MW	Mvar	–	MW	Mvar
1	0	0	6	0	0
2	0	0	7	100	35
3	0	0	8	0	0
4	0	0	9	125	50
5	90	30	–	–	–

Table 5.2: Bus data.

Bus	Voltage	Generation	$\overline{P_i}$	$\underline{P_i}$	Fuel cost	Mvar Limits	
–	Mag.	MW	MW	MW	C_F (\$)	Min	Max
1	1	–	250	10	$0.11 \times P_i^2 + 5 \times P_i + 150$	-300	300
2	1	163	300	10	$0.085 \times P_i^2 + 1.2 \times P_i + 600$	-300	300
3	1	85	270	10	$0.1225 \times P_i^2 + P_i + 335$	-300	300

Table 5.3: Generator data.

Bus	Bus	R	X	$B/2$	Bus	Bus	R	X	$B/2$
–	–	p.u.	p.u.	p.u.	–	–	p.u.	p.u.	p.u.
1	4	0	0.0576	0	7	8	0.0085	0.072	0.074
4	5	0.017	0.092	0.079	8	2	0	0.0625	0
5	6	0.039	0.17	0.179	8	9	0.032	0.161	0.153
3	6	0	0.0586	0	9	4	0.01	0.085	0.088
6	7	0.0119	0.1008	0.104	–	–	–	–	–

Table 5.4: Line and transformer per-unit (p.u) data.

The problem is solved using MOSEK[1] optimization toolbox. Its dimensions are given in Table 5.5. The result of optimization process is shown in Figure 5.13. The previous status of the generators

Table 5.5: Optimization problem summary for the UC test case

Problem Type:	Quadratic Optimization Problem
Constraints:	1587
Scalar variables:	330
Integer variables:	120
Solver Used:	MOSEK
Platform:	Windows/64-X86

displayed at time 0. Upon solving UC problem the operational schedule of generators and the dispatched power level is obtained. The power flow evaluation at each hour results in the bus voltage dynamics shown in Figure 5.14. Generally, bus voltage limit constraints are not considered in the UC problem.

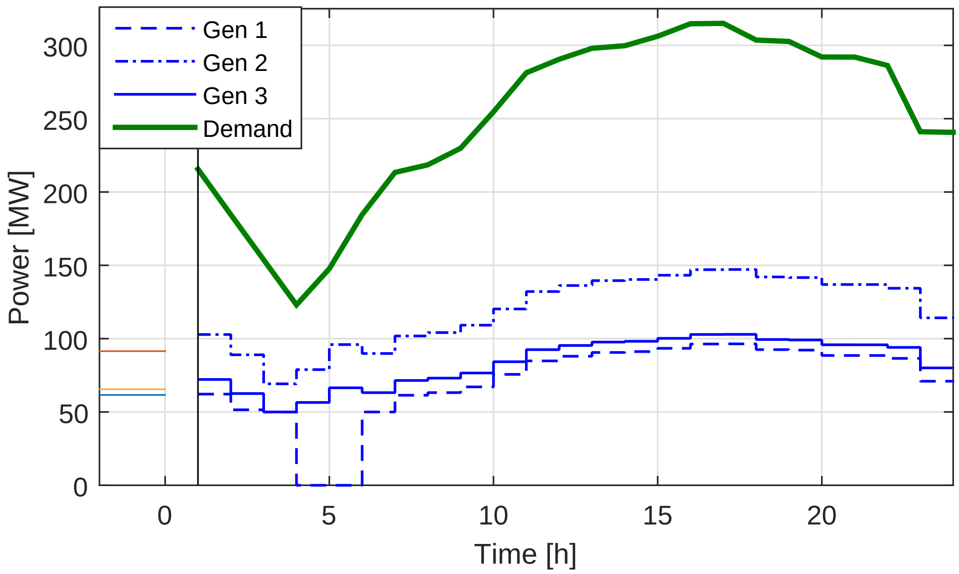

Figure 5.13: Generation allocation from the Unit Commitment problem for IEEE 9 bus system.

[1] https://www.mosek.com, MOSEK

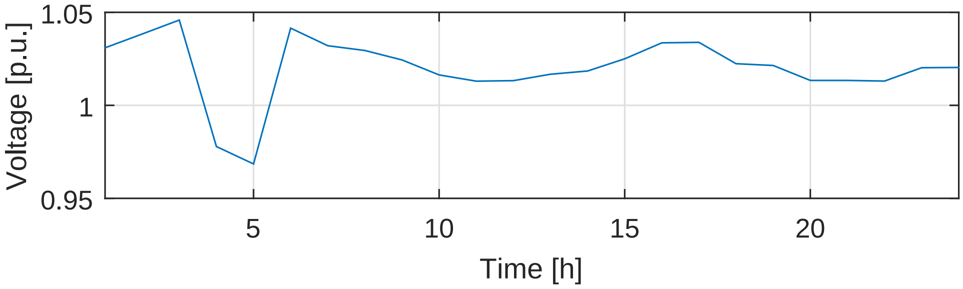

Figure 5.14: Voltage dynamics at bus 2 based from the Unit Commitment.

5.5.2 Economic Dispatch

Economic Dispatch (ED) is an optimization problem in which the set-points of the generating units are decided at each point in time. The objective is minimization of the total operational cost. There are two variants of this problem found in literature, the static and dynamic. The static ED solve the set-points of generator at a single time instant while dynamic ED is a multi-period optimization problem. A review of both approaches for ED is given in [173]. The dynamic ED considers the ramp-rate constraints of the generators inherently and optimizes the ramping effort as well as function of the ramp costs.

Here, static ED is discussed with the inclusion of stochastic reserve variable. The ramp-rate is taken into consideration by the dynamic upper/lower limits of the generators power ratings. Such that, the dispatched scheduled for i^{th} generator at time $(t-1)$ is used to set the $\overline{P_i}$ and $\underline{P_i}$ limits at time (t). The ED is different than UC as it involves the consideration of additional constraints of transmission line power carrying capability limits and the bus voltage limits.

5.5.2.1 Mathematical Formulation

The objective function of ED problem is,

$$\min \ C_F = \sum_{i=1}^{N} \left[a_i(P_i^t) + b_i(P_i^t)^2\right] \quad , \tag{5.18}$$

Constraints.
1. The power balance constraint from Equation 5.13,

$$\sum_{i=1}^{N} P_i^t = P_D^t + \mathrm{SR}^t \quad . \tag{5.19}$$

2. Limits on the active power of generator i,

$$\underline{P_i^t} \geq P_i^t \geq \overline{P_i^t} \;\; \text{where,} \;\; \overline{P_i^t} = P_i^{t-1} + \overline{R_i^+} \;\; \text{and} \;\; \underline{P_i^t} = P_i^{t-1} - \underline{R_i^-} \quad . \tag{5.20}$$

3. The transmission flow constraints,

$$|S_f(V)| = \left|S_f\left(e_k^t, f_k^t\right)\right| \leq S_m^{max} \tag{5.21}$$

$$|S_t(V)| = \left|S_t\left(e_k^t, f_k^t\right)\right| \leq S_m^{max} \tag{5.22}$$

where,

$$S_f(V) = [C_f\, V]\, I_f^* = [C_f\, V]\, Y_f^* V^* \tag{5.23}$$

$$S_t(V) = [C_t\, V]\, I_t^* = [C_t\, V]\, Y_t^* V^* \tag{5.24}$$

The matrices C_f and C_t are $N_L \times N_B$ sparse coefficient matrices. Where $\left(i, j^{th}\right)$ element of C_f and $\left(i, k^{th}\right)$ element of C_t are equal to 1 for each branch i connecting bus j to k. The N_L and N_B are number of lines and buses respectively. All other elements are equal to zero. The matrices Y_f and Y_t are given by,

$$Y_f = [Y_{ff}]\, C_f + [Y_{ft}]\, C_t \tag{5.25}$$

$$Y_t = [Y_{tf}]\, C_f + [Y_{tt}]\, C_t \tag{5.26}$$

Here the four $N_L \times 1$ vectors Y_{ff}, Y_{ft}, Y_{tf} and Y_{tt} are constructed in such a way that i^{th} element of each comes from corresponding element of Branch model [172].

4. The voltage limit constraint on buses,

$$\left(e_k^{min}\right)^2 \leq \left(\left(e_k^t\right)^2 + \left(f_k^t\right)^2\right) \leq \left(e_k^{max}\right)^2 \tag{5.27}$$

The bus voltages are influenced by the power consumed/generated at the connected buses in the network. It is incorporated in the power balance equations as,

$$P_{Gk}^t - P_{Dk}^t = e_k^t \sum_{j=1}^{N_B} \left(\mathbf{G}_{jk}\, e_j^t - \mathbf{B}_{jk} f_j^t\right) + f_k^t \sum_{j=1}^{N_B} \left(\mathbf{B}_{jk}\, e_j^t + \mathbf{G}_{jk} f_j^t\right) \tag{5.28}$$

$$Q_{Gk}^t - Q_{Dk}^t = e_k^t \sum_{j=1}^{N_B} \left(-\mathbf{B}_{jk}\, e_j^t - \mathbf{G}_{jk} f_j^t\right) + f_k^t \sum_{j=1}^{N_B} \left(\mathbf{G}_{jk}\, e_j^t - \mathbf{B}_{jk} f_j^t\right) \tag{5.29}$$

N-1 contingency. The outage of a network element that can be a generator, bus, load or a transmission line is termed as contingency in power system. The objective of contingency analysis is to make sure that there is enough generation capability in the system to meet the demand. In literature, the consideration of contingency requirements adds a preamble of security constrained to ED and UC problems. The commonly considered contingency includes generator, transmission line and loads in the system. Total number of possible outages can be denoted by $N_{out} = N_l + N_G + N_L$. There are two aspects necessary to consider while operating the system compliant with $N-1$ contingency criteria. The first is availability of generation potential, it can be achieved by the assessment of largest generator/load maximum power ratings and adding the respective value to the spinning reserve requirement for all times.

The total up-spinning reserve are given as

$$\mathrm{TR}_{\mathrm{up}}^t = \mathrm{SR}_{\mathrm{up}}^t + \max_{\forall\, i=1 \ldots N} \overline{P}_i^t \tag{5.30}$$

The down-spinning reserves are similarly formulated as,

$$\mathrm{TR}_{down}^t = \mathrm{SR}_{down}^t + \max_{\forall\, j=1 \ldots B} P_{Dj}^t \tag{5.31}$$

The consideration of generator and load contingency shall revise Equation 5.19 as,

$$\sum_{i=1}^{N} P_i^t = P_D^t + \mathrm{TR}_{\mathrm{up}}^t \ . \tag{5.32}$$

$$\sum_{i=1}^{N} \underline{P_i^t} \leq P_D^t - \mathrm{TR}_{down}^t \ . \tag{5.33}$$

Equation 5.32 and 5.33 are considered as part of Security Constrained Economic Dispatch (SCED) problem. For each time period the process is repeated for each line contingency to check the $(N-1)$ compliance of the dispatch. Normally DC power flow is performed while considering the $(N-1)$ security constraint as it simplifies the process [167].

5.5.2.2 Test Case for Economic Dispatch

The test case for the ED is based on IEEE 30 bus system. A wind farm is connected at bus 22 of the network as shown in Figure 5.15. The test case data can be also be accessed from the Matpower software [172]

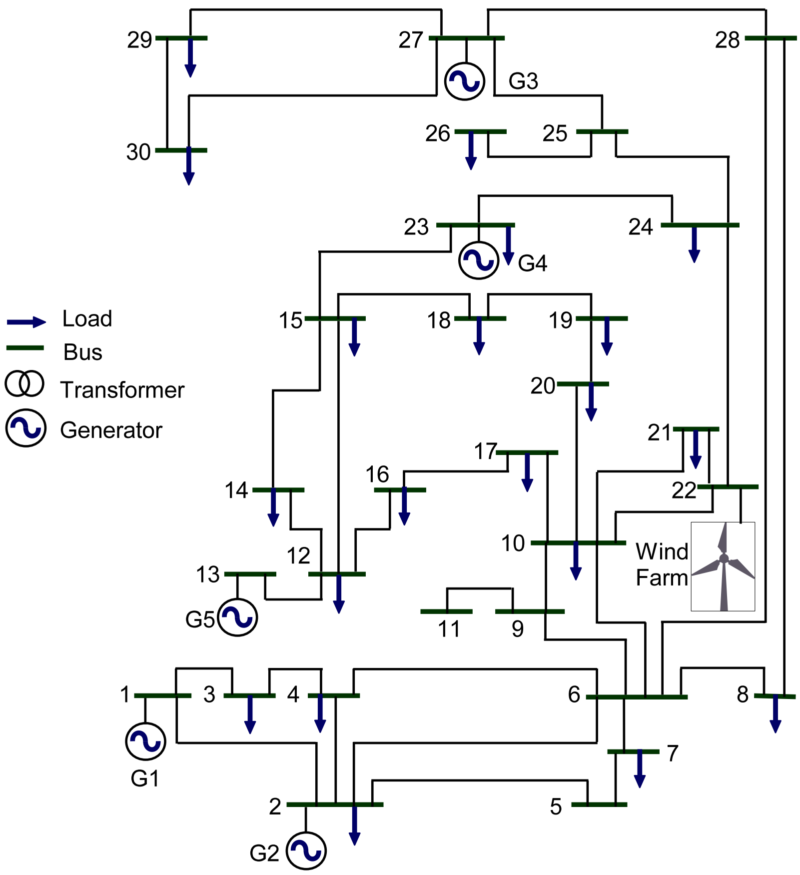

Figure 5.15: One-line diagram of 30 bus power system.

Bus	Load		B_s	$e^{\max}$	$e^{\min}$	Bus	Load		B_s	$e^{\max}$	$e^{\min}$
–	MW	Mvar	Siemens	p.u.	p.u.	–	MW	Mvar	Siemens	p.u.	p.u.
1	0	0	0	1.05	0.95	16	3.5	1.8	0	1.05	0.95
2	21.7	12.7	0	1.1	0.95	17	9	5.8	0	1.05	0.95
3	2.4	1.2	0	1.05	0.95	18	3.2	0.9	0	1.05	0.95
4	7.6	1.6	0	1.05	0.95	19	9.5	3.4	0	1.05	0.95
5	0	0	0.19	1.05	0.95	20	2.2	0.7	0	1.05	0.95
6	0	0	0	1.05	0.95	21	17.5	11.2	0	1.05	0.95
7	22.8	10.9	0	1.05	0.95	22	0	0	0	1.1	0.95
8	30	30	0	1.05	0.95	23	3.2	1.6	0	1.1	0.95
9	0	0	0	1.05	0.95	24	8.7	6.7	0.04	1.05	0.95
10	5.8	2	0	1.05	0.95	25	0	0	0	1.05	0.95
11	0	0	0	1.05	0.95	26	3.5	2.3	0	1.05	0.95
12	11.2	7.5	0	1.05	0.95	27	0	0	0	1.1	0.95
13	0	0	0	1.1	0.95	28	0	0	0	1.05	0.95
14	6.2	1.6	0	1.05	0.95	29	2.4	0.9	0	1.05	0.95
15	8.2	2.5	0	1.05	0.95	30	10.6	1.9	0	1.05	0.95

Table 5.6: Bus data.

Bus	Voltage	Generation	$\overline{P}_i$	$\underline{P}_i$	Fuel cost	Mvar Limits	
–	Mag.	MW	MW	MW	C_F (\$)	Min	Max
1	1	23.54	80	0	$0.02 \times P_i^2 + 2 \times P_i$	-20	150
2	1	60.97	80	0	$0.0175 \times P_i^2 + 1.75 \times P_i$	-20	60
3	1	26.91	55	0	$0.00834 \times P_i^2 + 3.25 \times P_i$	-15	48.7
3	1	19.2	30	0	$0.025 \times P_i^2 + 3 \times P_i$	-10	40
3	1	37	40	0	$0.025 \times P_i^2 + 3 \times P_i$	-15	44.7

Table 5.7: Generator data.

Two formulations of ED are considered,

- The AC OPF based ED considering the bus voltage and transmission line constraints. The reserves are allocated as fixed percentage of load and the uncertainty in the wind power.
- The DC OPF based ED considering the $N-1$ security constraints. The total reserve requirement includes reserves as fixed percentage of load, wind power uncertainty and the necessary reserve for satisfying the $N-1$ security criteria.

The first formulation is the static ED discussed from Equation 5.18 to 5.29 with the bus voltage and transmission line constraints. While the second formulation adds the constraints from equations 5.32 and 5.33 in the place of Equation 5.19. The results of SCED are studied to assess the impact of the reserve requirements on the dispatch of generation.

The demand profile in the network is shown in Figure 5.16. Demand uncertainty is taken as fixed percentage (20%) of total demand. The wind power forecast is shown in Figure 5.17. The flexibility assessment method is used to find the probabilistic maximum and minimum of the results. The difference between forecast and the extreme limits is used to define the ramp-up and

Bus	Bus	R	X	$B/2$	$S_m^{\max}$	Bus	Bus	R	X	$B/2$	$S_m^{\max}$
–	–	p.u.	p.u.	p.u.	MVA	–	–	p.u.	p.u.	p.u.	MVA
1	2	0.02	0.06	0.015	130	15	18	0.11	0.22	0	16
1	3	0.05	0.19	0.01	130	18	19	0.06	0.13	0	16
2	4	0.06	0.17	0.01	65	19	20	0.03	0.07	0	32
3	4	0.01	0.04	0	130	10	20	0.09	0.21	0	32
2	5	0.05	0.2	0.01	130	10	17	0.03	0.08	0	32
2	6	0.06	0.18	0.01	65	10	21	0.03	0.07	0	32
4	6	0.01	0.04	0	90	10	22	0.07	0.15	0	32
5	7	0.05	0.12	0.005	70	21	22	0.01	0.02	0	32
6	7	0.03	0.08	0.005	130	15	23	0.1	0.2	0	16
6	8	0.01	0.04	0	32	22	24	0.12	0.18	0	16
6	9	0	0.21	0	65	23	24	0.13	0.27	0	16
6	10	0	0.56	0	32	24	25	0.19	0.33	0	16
9	11	0	0.21	0	65	25	26	0.25	0.38	0	16
9	10	0	0.11	0	65	25	27	0.11	0.21	0	16
4	12	0	0.26	0	65	28	27	0	0.4	0	65
12	13	0	0.14	0	65	27	29	0.22	0.42	0	16
12	14	0.12	0.26	0	32	27	30	0.32	0.6	0	16
12	15	0.07	0.13	0	32	29	30	0.24	0.45	0	16
12	16	0.09	0.2	0	32	8	28	0.06	0.2	0.01	32
14	15	0.22	0.2	0	16	6	28	0.02	0.06	0.005	32
16	17	0.08	0.19	0	16	–	–	–	–	–	–

Table 5.8: Line and transformer data.

ramp-down reserve requirements corresponding to the wind power in the system. The consideration of voltage constraint during the process is validated by the Figure 5.18. The tightening of lower voltage limit from 0.99 to 0.95 is observed during the simulations. A demonstration of the total up and down spinning reserve requirements is shown in Figure 5.19. The total up and down spinning reserves are allocated among the generators. The Figures 5.20 and 5.21 shows the allocation results. If a fixed reserve margin is applied then the total reserve requirements can be set at 60 MW for the up and 55 MW for the down-spinning reserves. The reserve requirements related to the contingency cases is fixed for all time values as the contingency can happen at any time. The load forecast uncertainty is a fixed percentage of the load and hence impacts the reserve requirements for each time differently. The variable reserve requirements also emerges from the polytopic model based approach discussed in Section 5.2.3 which is used for modeling the wind forecast uncertainty.

5.5.3 Unit Commitment using Population Game Theory

The generators participating in the UC problem selects a bidding strategy based on their objectives. Environmental variables and the bidding strategies of other generators can influence this process. The strategic interaction between generators can be modeled using Game Theory. An interesting application from this theory is called Replicator Dynamics (RD). RD is a population game theory based method that is characterized by the reduced complexity and a support for parallel computation. As an outcome of the strategic game, the players (generators) can select

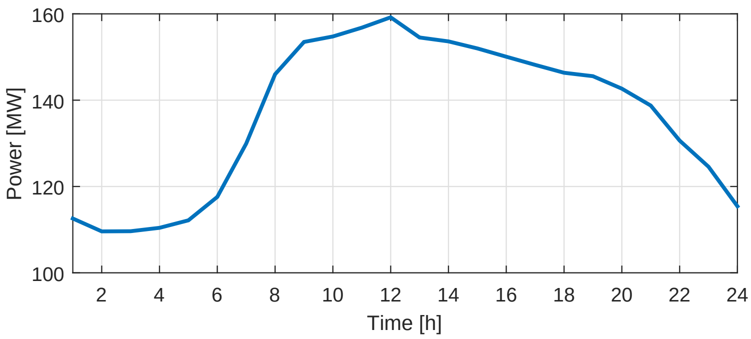

Figure 5.16: Real power demand to be dispatched among generators for the Security Constrained Economic Dispatch problem.

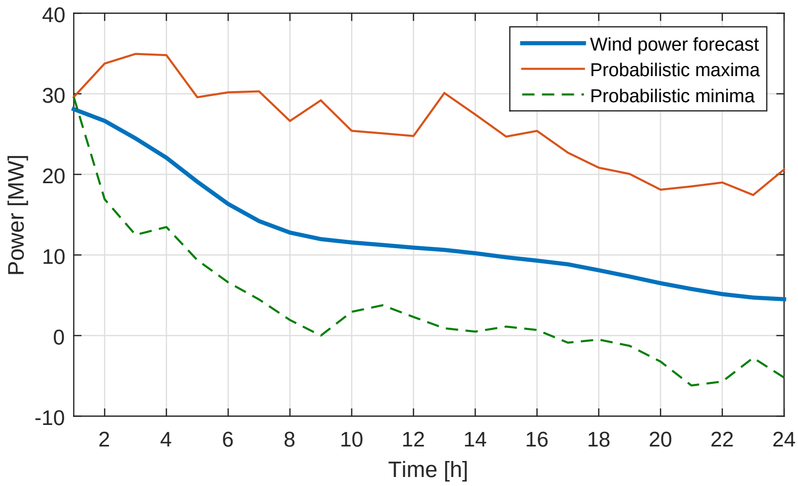

Figure 5.17: Wind power forecast with the probabilistic bounds obtained using Monte Carlo simulations.

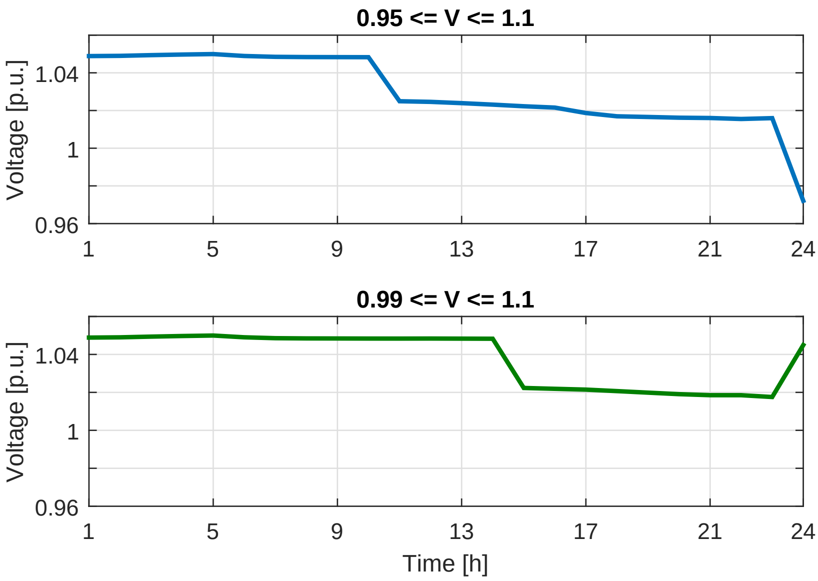

Figure 5.18: Enforcement of voltage constraint in the SCED problem.

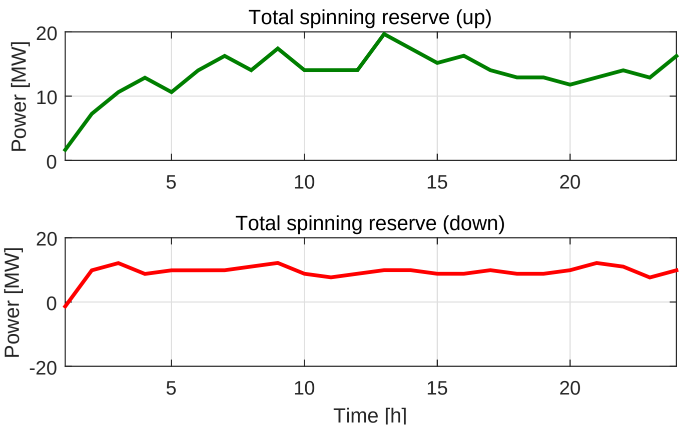

Figure 5.19: Total up and down spinning reserve requirements.

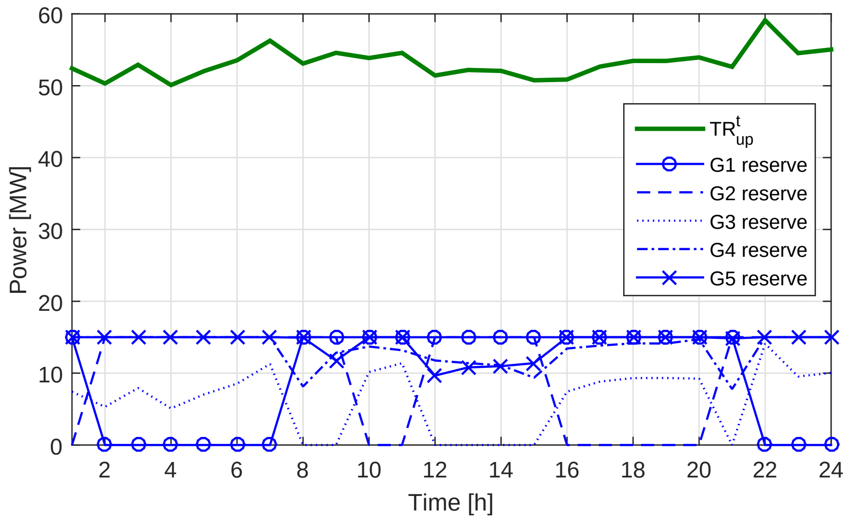

Figure 5.20: Up spinning reserve allocation among generators in the SCED problem.

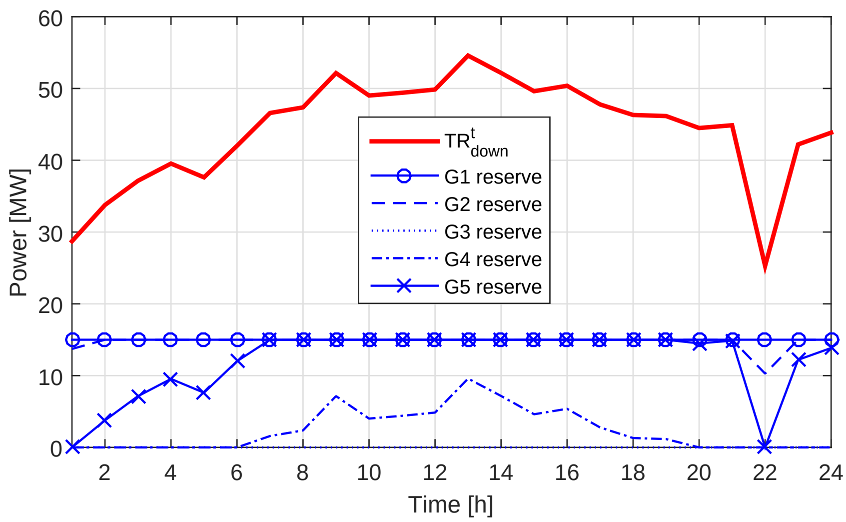

Figure 5.21: Down spinning reserve allocation among generators in the SCED problem.

best strategies based on the strategy of other players. The operator on other hand can observe and potentially influence the interaction in a broader perspective. The RD based economic dispatch has been explored in [174]. Here, this method is extended for the UC problem. RD models the strategy growth rate of a player in a population based on its payoff. Mathematically, it equals the difference between the strategy payoff and the average payoff of a population, given as [175],

$$\dot{x}_i = x_i\left[(Ax)_i - (x.Ax)\right] \quad , \tag{5.34}$$

where, the strategy state of the population is x_i and the payoff matrix is given by A. Based on the dynamic equation, most successful strategy prevails during the selection process. The RD based resource allocation method can be compared with the UC problem i.e., the generators corresponds to habitats with each one having a fitness (objective) function, The net power demand can be related to a population of values searching for a habitat (generators). The Population dynamics within a habitat can be described similar to Equation 5.34 as follows,

$$\dot{p}_i = p_i\left(f_i(p_i) - \overline{f}\right) \quad , \tag{5.35}$$

where, $\overline{f}$ and $f_i(p_i)$ represents the average fitness and i^{th} generator fitness value, respectively. The generator fitness function can be obtained from a quadratic cost function [174] that can be related to cost of generation. The discrete time version of Equation 5.35 is given as,

$$p_i[k+1] = p_i[k]\frac{1/T_s + f_i[k]}{1/T_s + \overline{f}[k]} \quad , \tag{5.36}$$

$$f_i\left[k+1\right] = \frac{1}{c_i}\left(1 - \frac{p_i\left[k+1\right]}{p_i^{\text{nom}'}}\right) \quad , \tag{5.37}$$

$$\overline{f}\left[k\right] = \frac{1}{P_d'}\sum_{j=1}^{N} p_j[k]\, f_j[k] \quad , \tag{5.38}$$

here, $k = 1, 2, 3, \ldots$ is the iteration count for each time instance, c_i is the cost associated with each generator and N is the number of generators. The local controller at each generator performs calculations based on Equations 5.36 and 5.37, while the central control implements Equation 5.38. The iterative process continues till the individual fitness functions are equal to the average fitness value, given as,

$$f_i(p_i) = \overline{f} \quad , \tag{5.39}$$

The result of the process is an optimal solution as commented in [174] and [176]. RD have similarities with the Newton's Approach (NA) for the optimal power flow [177]. The constraints are augmented to the cost function using the Lagrange multipliers given as,

$$\mathcal{L} = C_{\text{total}} + \lambda\left(P_d' - \sum_{i=1}^{N} p_i\right) , \tag{5.40}$$

Here, C_{total} is the total cost and P_d' is the demand. The function is minimized for the following condition,

$$\frac{\partial C_i}{\partial P_i} = \lambda \quad , \tag{5.41}$$

This is similar to Equation 5.39, i.e., generation dispatch is optimal if each generator operates at same incremental cost [100].

In Newtons method the value of λ is calculated using iterative procedure which involves the computation and inversion of Hessian matrix. The process is computationally intensive. Therefore, quasi-Newton approaches have been developed. They have good performance but poor accuracy due to approximations [178]. In comparison, RD has simple structure and can be suitable for on-line computation for UC problem.

In the Newton's method, the λ is calculated by an iterative process that involves the calculation of a Hessian matrix, resulting in computational complexity. Quasi-Newton methods have been developed to address this issue but lacks accuracy due to approximations [178]. In comparison, RD has a simpler structure and can be used for the UC problem.

5.5.3.1 Replicator Dynamics and Unit Commitment

The objective of UC problem is generally to minimize the total cost due to fuel (F), maintenance (M), start-up (U) and shut-down (D) costs by scheduling resources over a time horizon [168], given as,

$$C_{\text{total}} = \sum_{i=1}^{N}\sum_{k=1}^{T} F_i[k] + M_i[k] + U_i[k] + D_i[k] \ , \tag{5.42}$$

The fuel and maintenance costs can be combined to form a quadratic cost function, represented by the cost factor c_i in (5.37). The objective function in Equation 5.42 is subject to the following constraints [179]: (i) System power balance; (ii) System reserve requirement, namely p^{reserve}; (iii) Unit maximum (resp. minimum) operating limits, denoted p^{nom} (resp. p^{min}); (iv) Unit minimum-up (resp. down) time, $T^{\text{up}}_{\text{min}}$ (resp. $T^{\text{down}}_{\text{min}}$); (v) Unit status restrictions (must run, unavailable, fixed production) and others.

Several binary logic states of the generator are defined to facilitate the handling of constraints: (i) $I_i[k]$: Commitment state of generator i at k^{th} hour; (ii) $I_i^{\text{start/stop}}[k]$: Transition start-up (resp. shut-down); (iii) $X_{\text{i}}^{\text{off}}[k]$: time duration for which generator i has been switched off; These states are subsequently used in calculation of fitness function values.

The equality constraint can be given as,

$$\sum_{i=1}^{N} p_i - \sum_{i=1}^{N} p_i^{\text{reserve}} = P_d + P_L = P_d' \ , \tag{5.43}$$

This constraint is directly incorporated by the design of Equation 5.38 as commented in [174]. Here, the power loss (P_L) is calculated using the B-coefficient method [100]. The reserve power requirement from a generator impacts its nominal rating as,

$$p_i^{\text{nom}'} = p_i^{\text{nom}} - p_i^{\text{reserve}} \ , \tag{5.44}$$

The reserve power can be made available by a generator if required using this nominal power margin. Generator power limits can be transformed to constraints on the fitness function, given as,

$$f_i^{\text{min}} \leq f_i \leq f_i^{\text{max}} \ . \tag{5.45}$$

The f_i^{max} corresponds to p_i^{min}, see Equation 5.37. The shut-down or start-up conditions can be obtained by considering the minimum up and down time constraints of a generator and the fitness function values. It is given as, For shut-down:

$$\left(f_i > f_i^{\max}\right) \wedge \left(\overline{f} > f_i^{\max}\right) \wedge \left(I_i[k-1] = 1\right) \\ \wedge \left(\sum_{\alpha=k-T_{\text{min}}^{\text{up}}}^{k-1} I_i[\alpha] = T_{\text{min}}^{\text{up}} \right) . \tag{5.46}$$

For start-up:

$$\left(f_i \leq f_i^{\max}\right) \wedge \left(\overline{f} \leq f_i^{\max}\right) \wedge \left(I_i[k-1] = 0\right) \\ \wedge \left(\sum_{\alpha=k-T_{\text{min}}^{\text{down}}}^{k-1} I_i(\alpha) = T_{\text{min}}^{\text{down}} \right) , \tag{5.47}$$

where, $\wedge$ symbolizes the logical *&* operator. If the conditions in Equations 5.46 / 5.47 are met, then the shut-down/start-up costs are considered in the fitness function values as,

$$f_i' = f_i - I_i^{\text{start}}[k] D_i^{\text{marg}} + I_i^{\text{stop}}[k] U_i^{\text{marg}}, \tag{5.48}$$

here, D_i^{marg} and U_i^{marg} stands for marginal shut-down cost and start-up costs, respectively. The start-up cost is modeled as,

$$U_i[k] = \left(1 - e^{-X_{\text{i}}^{\text{off}}[k]/\tau}\right) U_i^{\text{marg}}, \tag{5.49}$$

where, τ is the time constant of generator start-up function. The economic feasibility to shut-down or start-up the generator can be performed by following inequality conditions,

$$f_i' > f_i^{\max} , \; f_i' \leq f_i^{\max}. \tag{5.50}$$

The resulting algorithm is a bounded form of the original RD algorithm, thus it retains the optimality characteristics.

5.5.3.2 Stability of Equilibrium

A strategy i is said to be evolutionary stable if it is robust against the opposing strategies. According to the dynamical-systems theory, a steady state is reached when the condition $\dot{x}_i = 0$ is satisfied. In the context of RD, the right-hand side of Equation 5.34 give us the stable vector field of the evolutionary game. It facilitates in turn the definition of the equilibrium. For RD model used for UC problem, the equilibrium is reached when each player plays reaches the stable equilibrium with the average fitness function given by Equation 5.39. This equilibrium condition is asymptotically stable i.e., the solution path that starts close to equilibrium as result of minimal perturbation remain arbitrarily close and converges to the equilibrium in steady sate [100].

5.5.3.3 Test Case of Replicator Dynamics for UC

The proposed algorithm for UC has been applied for the 26-bus power system from [100]. One-line diagram of the network is shown in Figure 5.22. For this use-case, the load, generator, shunt capacitor sizing, transformer tap settings and line data are tabulated from Tables 5.9 to 5.12, on a 100 MVA base, respectively.

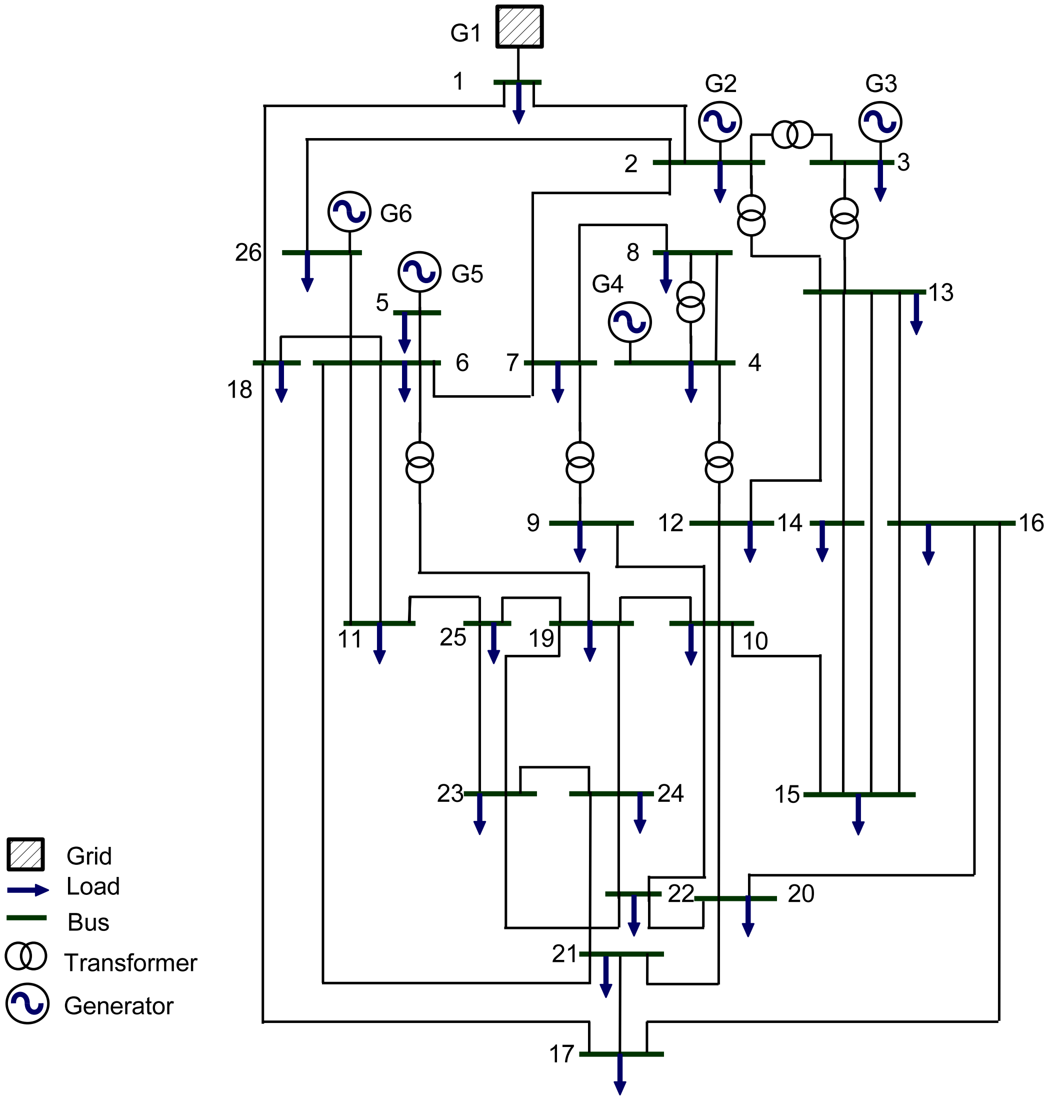

Figure 5.22: One-line diagram of 26 bus power system from [100].

Bus	Voltage	Generation	Mvar Limits	
–	Mag.	MW	Min	Max
1	1.025			
2	1.02	79	40	250
3	1.025	50	40	150
4	1.05	100	40	80
5	1.045	300	40	160
26	1.015	60	15	50

Table 5.9: Generator data.

The slack bus voltage is given as, $1.025\angle 0°$. Furthermore, generator parameter details are described in Table 5.13. The spinning reserve requirement is set as 5% of total load for each time period.

Bus	Load		Bus	Load	
–	MW	Mvar	–	MW	Mvar
1	51	41	14	24	12
2	22	15	15	70	31
3	64	50	16	55	27
4	25	10	17	78	38
5	50	30	18	153	67
6	76	29	19	75	15
7	0	0	20	48	27
8	0	0	21	46	23
9	89	50	22	45	22
10	0	0	23	25	12
11	25	15	24	54	27
12	89	48	25	28	13
13	31	15	26	40	20

Table 5.10: Bus data.

Shunt Capacitors		Transformer Taps	
Bus	Mvar	Designation	Tap Setting
1	4	02-03	0.96
4	2	02-13	0.96
5	5	03-13	1.017
6	2	04-08	1.05
11	1.5	04-12	1.05
12	2	06-19	0.95
15	0.5	07-09	0.95
19	5	–	–

Table 5.11: Shunt capacity and transformer taps settings.

	p^{nom}	p^{min}	$T^{\text{up}}_{\text{min}}$	$T^{\text{down}}_{\text{min}}$	Cost factor (c_i)	D_i^{marg}	U_i^{marg}	(τ)
Gen.	MW	MW	$Hours$	$Hours$	$per-unit$	$per-unit$	$per-unit$	$Hours$
G1	850	100	6	5	0.143	0.14	0.2	4
G2	500	50	5	5	0.100	0.12	0.18	3
G3	300	50	5	4	0.117	0.10	0.16	3
G4	180	100	3	2	0.090	0.09	0.13	2
G5	320	50	4	4	0.095	0.11	0.15	3
G6	100	62	3	2	0.083	0.08	0.10	2

Table 5.13: Generator data for the Replicator Dynamics based UC test case.

The power allocated to the generators as a result of UC process performed by RD is shown in Figure 5.23. It can be observed that, (i) The shut-down (resp. start-up) of G4 and G6 occurs after the minimum up-time constraint (resp. minimum down-time constraint) are satisfied. It is discussed in Equation 5.46 (resp. equation 5.47); (ii) G4 is shut-down at 140 hours due to low demand of energy. After this event, it remains off despite satisfying the minimum down-time

Bus	Bus	R	X	$B/2$	Bus	Bus	R	X	$B/2$
–	–	p.u.	p.u.	p.u.	–	–	p.u.	p.u.	p.u.
1	2	0.0005	0.0048	0.03	10	22	0.0069	0.0298	0.005
1	18	0.0013	0.011	0.06	11	25	0.096	0.27	0.01
2	3	0.0014	0.0513	0.05	11	26	0.0165	0.097	0.004
2	7	0.0103	0.0586	0.018	12	14	0.0327	0.0802	0
2	8	0.0074	0.0321	0.039	12	15	0.018	0.0598	0
2	13	0.0035	0.0967	0.025	13	14	0.0046	0.0271	0.001
2	26	0.0323	0.1967	0	13	15	0.0116	0.061	0
3	13	0.0007	0.0054	0.0005	13	16	0.0179	0.0888	0.001
4	8	0.0008	0.024	0.0001	14	15	0.0069	0.0382	0
4	12	0.0016	0.0207	0.015	15	16	0.0209	0.0512	0
5	6	0.0069	0.03	0.099	16	17	0.099	0.06	0
6	7	0.0053	0.0306	0.001	16	20	0.0239	0.0585	0
6	11	0.0097	0.057	0.0001	17	18	0.0032	0.06	0.038
6	18	0.0037	0.0222	0.0012	17	21	0.229	0.445	0
6	19	0.0035	0.066	0.045	19	23	0.03	0.131	0
6	21	0.005	0.09	0.0226	19	24	0.03	0.125	0.002
7	8	0.0012	0.0069	0.0001	19	25	0.119	0.2249	0.004
7	9	0.0009	0.0429	0.025	20	21	0.0657	0.157	0
8	12	0.002	0.018	0.02	20	22	0.015	0.0366	0
9	10	0.001	0.0493	0.001	21	24	0.0476	0.151	0
10	12	0.0024	0.0132	0.01	22	23	0.029	0.099	0
10	19	0.0547	0.236	0	22	24	0.031	0.088	0
10	20	0.0066	0.016	0.001	23	25	0.0987	0.1168	0

Table 5.12: Line and transformer per-unit (p.u) data.

requirements. This behavior is caused by the start-up cost; (iii) The power allocated to the slack bus is compared with that of the power flow result for each time. If it does-not matches sufficiently (here, tolerance is set to 0.001) then the convergence process is repeated. It can be observed in Figure 5.24-(a) that RD based results satisfy the equality constraint explained in Equation 5.43. For this use-case, the RD based results have been compared with NA and the error was found out to be less than 1.12%.

The convergence accuracy has been set to $1e-005$ during course of simulation for both RD and NA algorithms. The system had been simulated using Matlab[2]. In Figure 5.24-(c), the fitness function dynamics of generator G2 is shown for the whole duration. It satisfies the limits set due to operating limits of the generator as discussed in Equation 5.45. As an outlook, the ramp-rate limits of the generator can be modeled as limits on the fitness function dynamics.

Figure 5.25-(a) shows the dynamics of fitness functions of the generators and their convergence to a common average value. The convergence rate can be adjusted by controlling the sampling time T_s from Equation 5.36. Here, it has been fixed at $0.16sec$. Increasing this time can potentially decreases the number of iterations required for convergence. However, it has been observed that if it increased beyond a threshold, the fitness value starts to oscillate around a solution and may not satisfy the convergence accuracy criteria. Here, this threshold has been obtained

[2] `http://www.mathworks.com`, MathWorks

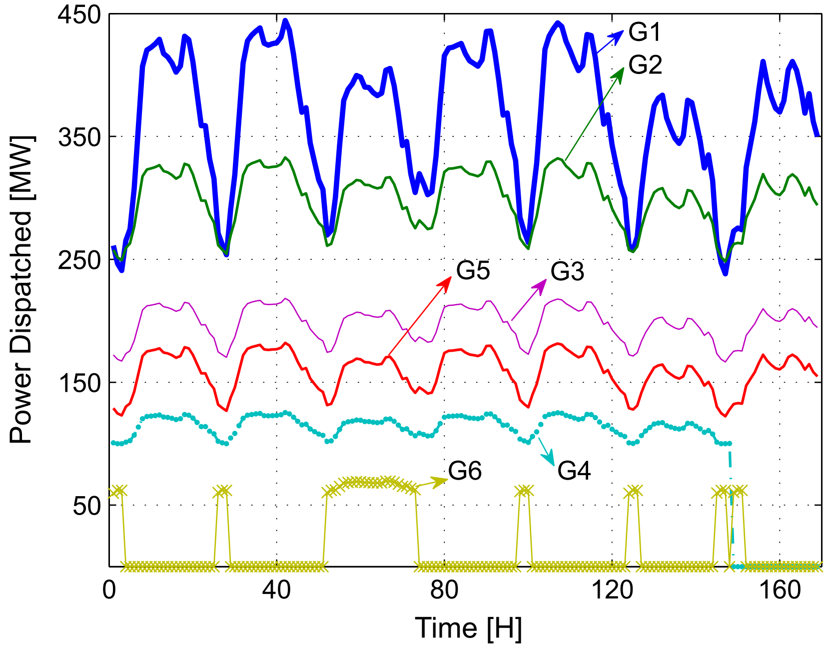

Figure 5.23: Power dispatch dynamics for 26-bus power system using RD algorithm, where G1 is the slack generator.

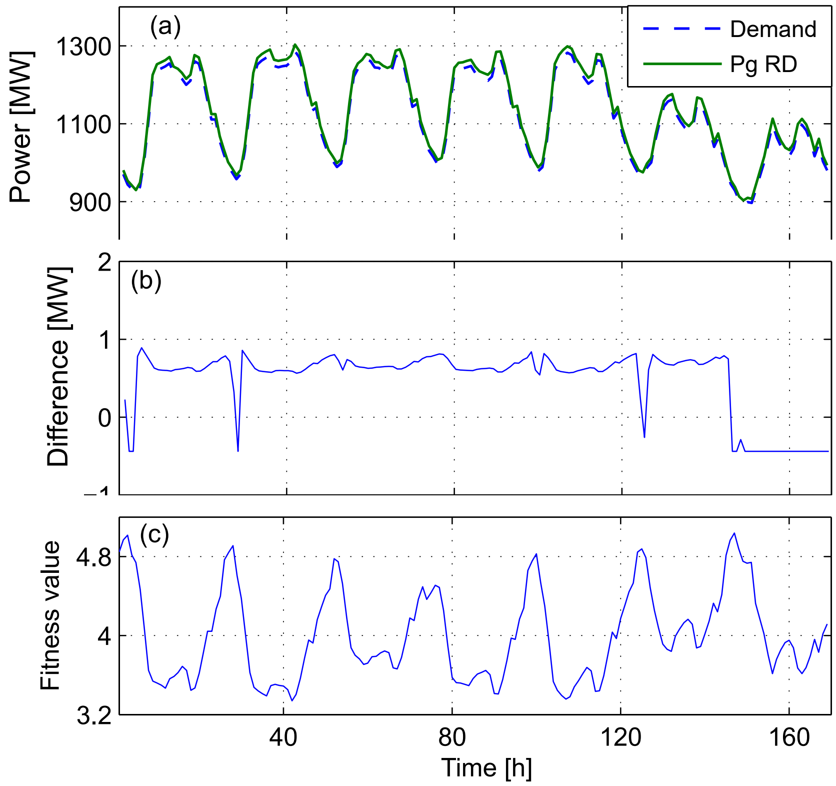

Figure 5.24: (a) Comparison of the total power dispatched using RD Vs the total demand, Equation 5.43. (b) Difference between results of RD and NA algorithms for generator 4. (c) Fitness function dynamics of generator 2 for the whole demand profile.

experimentally. Figure 5.25-(b) shows the robustness of RD approach when the process starts for a range of initial conditions. It is however required that the equality constraint is satisfied at initial condition [174]. The simulation results demonstrate the effectiveness of RD method in solving the UC problem. It has been observed that the convergence of fitness function is independent of initial conditions. The cost functions considered have a quadratic structure. However, the approach can be extended to other piece-wise and other polynomial functions. The structure of problems has a resemblance towards the secondary control approach in microgrid. There, a centralized control coordinates with local controlled in maintaining frequency and voltage in the network. The RD based implementation shall require dedicated communication links between the nodes. For the convergence at each time instance, the data needs to be transferred multiple times. This aspect can be a limiting factor for the applications have uncertain and relatively high communication latency. As an outlook, the generator specific constraints can be directly modeled on the fitness function and can reduce the problem complexity. In addition, the convergence towards the solution can be improved by introducing a gain multiplier to Equation 5.35.

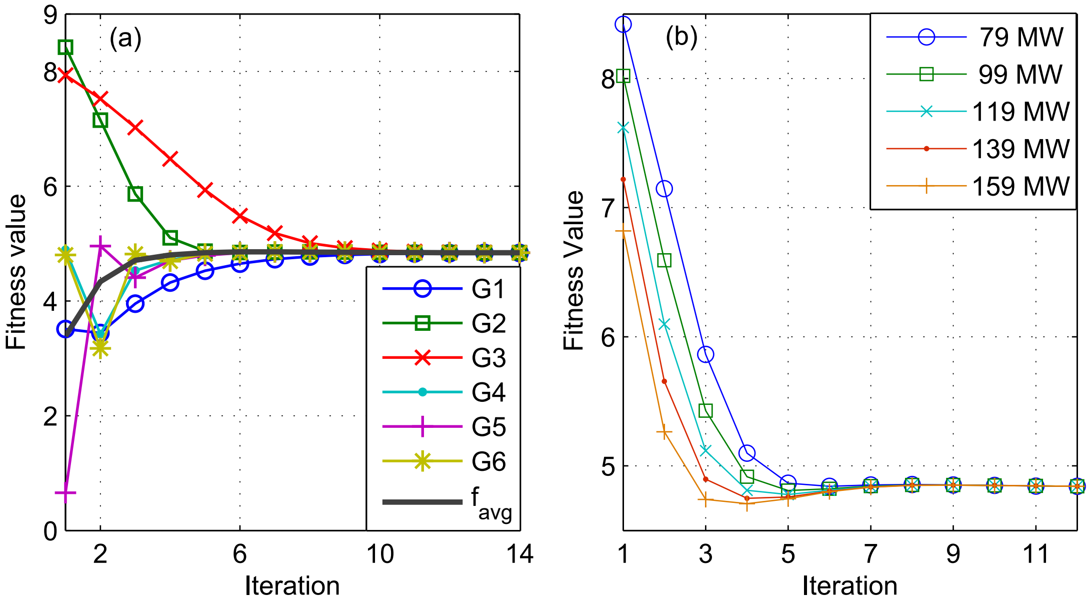

Figure 5.25: For single instance [k]: (a) Evolution of fitness function of generators and average fitness value (where, f_{avg} is the average fitness value). (b) The convergence of fitness function of G2 to average fitness function value for different initial conditions.

5.5.3.4 Game Theory and Optimization

From a conceptual point of view, game theory with an exception of mean field game theory is an iterative process of reaching towards a solution or equilibrium. The limitations of the convergences are similar to that encountered during optimization applications. The RD method explored here for the ED problem is a gradient based approach. Thus the applicability of this method is limited to the problems having a single solution or a single local extremum point. This may not be the case for a general ED or UC problem.

Game theory can be highly relevant for the applications involving a high level of strategic interactions where it can be used to solve the conflicts. For example, if the players or participants have multiple strategies that are function of other players strategies and/or system wide variables. Game theory has been used for numerous energy market applications [180]. In the electric distribution systems, the game theory has been applied to study the behavior of thermostatically controlled loads based demand response application [147].

In microgrid, a prosumer may have an incentive to maximize its benefit and/or the social welfare. Game theory can provide an elaborate analysis of the underlying optimization problem, where, it can be used to select an optimal or preferred strategy. However, the optimization applications such as ED or UC generally require fixed strategies (objective functions) from the stakeholders. The results of optimization process are set-points for the participating players. These set-points can be used by a player to fine tune its strategy relying on possibly game theory based algorithm. It is inferred that game theory can potentially contribute in the energy domain during the selection of the best strategy, and when selected, state of the art optimization processes can be applied.

6 Demand Side Flexibility as Frequency Reserve

6.1 Introduction

A critical requirement in the power system operation is to match the generation with demand, which happens continuously and instantaneously. The power system operators counter the generation-load imbalance by activating control reserves. These reserves can be differentiated based on the type of events causing the imbalance, time-scale requirements and the direction (upward/downward) of the response. A comparison of the different types of reserves as function of the time-scale is shown in the Figure 6.1.

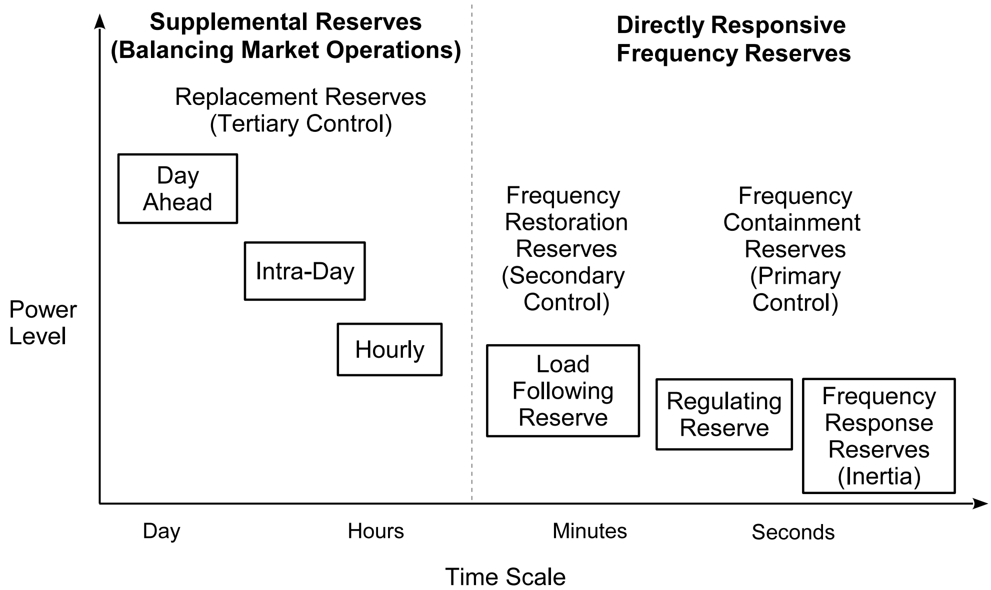

Figure 6.1: Reserve types as function of response time and power level.

When the generation is less than the demand there is an immediate impact on the generators output frequency. It can be understood by the study of a generator operation. As the demand increases, rotors of the generators tends to slow down due to increase in load. The angular speed of the generator's rotor has a direct relationship with the output frequency. A decrease in the angular speed droops down the output frequency. In order to maintain the frequency within permissible limits, the generators normally have governors. A governor implements droop control mechanism i.e., the generator output power is increased and the drooping frequency is recovered to the nominal value. This action of the governor is a primary reserve that provides an immediate relief to the system. The frequency compensation capability of the generators is normally termed as Frequency Response Reserve (FRR). Additionally, the frequency deviations in an interconnected system are countered by the Frequency Containment Reserve (FCR) that are activated automatically. Both the frequency response and containment reserves are triggered in the time scale of seconds to minutes and can be categorized as primary reserves. The compensation level provided by the primary reserves is limited and in general a steady state frequency error may be maintained in case of imbalance situation. This imbalance is adjusted by a secondary mechanism called load following reserves termed as Frequency Restoration Reserve (FRR). The time scale of FRR ranges from seconds to minutes. Generators have traditionally participated in this type of reserve. Along with it, demand response also posses a potential in contributing to this resource. Finally, the large scale reserve requirements are met by a tertiary level control as part of balancing market operations and are termed as Replacement Reserve (RR).

Generally, the activation of reserves from generators keep the frequency stable in the classical power system operation. However, the increasing share of renewables in the power system shall require a high level of reserves to cater for the associated forecast uncertainty. The high ramp-rate requirements from the reserve resources makes the traditional approach an expensive choice for providing reserves, therefore, the alternate sources of reserves are highly sought after. A number of studies have shown that the responsive loads in the distribution network can play an important role in contributing to the load following secondary reserves. International Energy Agency (IEA) estimates that every 1$ investment in Demand Side Management (DSM) is equivalent to 2$ investments in upgrading generation capabilities [25]. Among the potential demand response resources, the refrigeration, heating and air-conditioning loads amounts to more than 40% of total load in both residential and commercial sectors [181]. Such loads can be classified as Thermostatically Controlled Load (TCL) and they possess common working principle. These devices are thermostatically controlled and aim to maintain temperature within a dead-band around a set-point. A general objective of a TCL is to regulate specific level (set-point) of the temperature by maintaining it within a dead-band (interval) around the set-point. A TCL undergoes a cycling process in order to maintain temperature within this interval as shown in Figure 6.2.

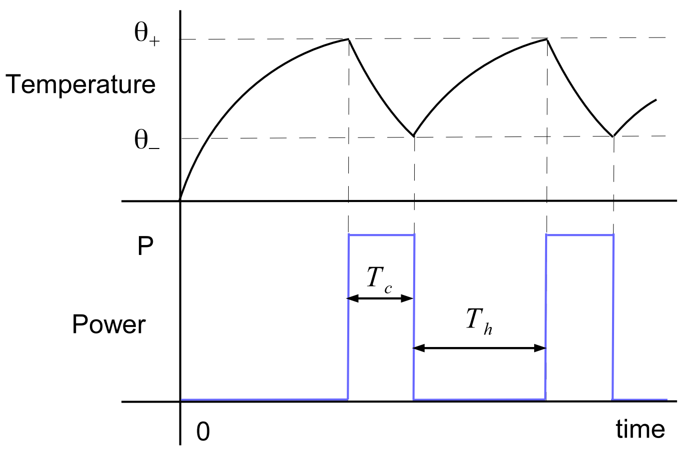

Figure 6.2: Cycling operation of a Thermostatically Controlled Load.

Consider an air-conditioning unit that is performing cooling to maintain the room temperature. It can be assumed that the output temperature is higher than the set-point. The TCL consumes power till temperature reaches minimum threshold, after that it is turned Off. The temperature of room rises due to the high outside temperature until it reaches maximum threshold, which triggers the air-conditioning unit On. The On and Off states of a TCL completes one cycle and the ongoing process is called "cycling", as shown in Figure 6.2.

The load of TCL can be changed while operating it within the dead-band. Such a control effort results in a non-disruptive operation towards the customer as temperature remain within the dead-band. Similarly, the power demand of a TCL aggregation can be changed during the cycling process and can be used to track a reference active power signal [144]. The potential of the TCL aggregation can be viewed as an energy storage. This chapter discusses the application of the flexibility model discussed in Section 4.4for tracking of a frequency regulation signal. It provides a proof of concept of using this resource for frequency regulation and validates the proposed stochastic battery mode. The contents of this chapter are partly published in [131] and accepted to be published in [182], where the energy storage model and a test cases are discussed.

6.1.1 TCL as frequency reserve

Frequency regulation is a process to maintain the instantaneous balance between demand and supply. Any imbalance effects the frequency of the system that is to be kept within permissible limits. It is achieved the frequency regulation process, the time scale for which ranges between seconds to minutes. This limits the maximum allowable delay in the response of reserve resources. An aggregation of the TCLs can be used as a reserve resource in supporting frequency regulation process [149]. The ability of TCL aggregation in responding to a real-time frequency adjustment signal has been reported in [142, 143] The application of this technology has also led to regional studies. For example, the ability to use TCLs as the storage capacity in Switzerland has been discussed in [183]. Potentially it is interesting, but to enable this technology, suitable communication infrastructure is the limiting factor.

The aggregate behavior of the TCLs can generally be modeled using two approaches. First approach is based on differential equation based model and had been presented in [150]. It is composed of a continuous temperature state dynamics model and a discrete switching state of the input power. It models the change in internal temperature of a thermal load while considering the thermal resistance, capacitance, ambient temperature and temperature gain due to power consumption [184, 185]. Due to the simplicity of this model, it is well suited for the application in simple control strategies applied to large number of TCLs [186]. This model has been verified for the real population of TCLs in [187]. The other approach is to use state space model to represent the TCL aggregation. It has received considerable interest in literature due to the inherent support for the controller design. Among state space methods, the partial differential equation based model in combination with sliding mode control has been used for TCL aggregation in [188]. Similarly, a three state model has been presented in [189] for a TCL aggregation. An advanced model has been presented in [190], that aims to model the TCL dynamics accurately. The implementation aspects of TCL based demand side management have also been explored in number of studies. Authors in [191] and [192] have proposed a direct control mechanism for the Distribution Network Operator (DNO). It allows the DNO to change the active power set points continuously. Similarly, an intelligent control based on the real time data of electricity price has been proposed in [147].

A battery model representing TCLs has been presented in [144], where the battery parameters of power and energy capacity are calculated. Similarly, a stochastic modeling approach for the calculation of battery parameters has been discussed in [130]. This paper presents the maximum ramp-up/down rate and the charging/discharging potential of the battery. Each TCL communicates its status, temperature distance to switching boundary and power level to central control. The requirement of power measurements adds additional expense and introduce measurement uncertainty to the process. In addition, the stochastic battery parameters are calculated using historical data of previous switching status and time since a switching state. The measurement uncertainty can adversely effect this process and the problem can become computationally complex for large number of TCLs. Here, these two aspects of the stochastic battery model are improved. A novel mathematical functions are presented for the calculation of battery parameters that does not need the historical information. This has been achieved by assuming that the TCL rated power is already known to the central control as part of the contractual agreement and each TCL only communicates its availability binary signal. On one hand it prevents the requirement of power measurement and in addition, it helps in the calculation of battery parameters. The main contributions can be summarized as,

- A mechanism where each TCL transmits the status $u^i[k]$, relative temperature distance to switching boundary $\pi^i[k]$ and the availability $\lambda^i[k]$ to the central control.
- Analytic expressions for calculating the stochastic ramp-up/down rate and State of Charge (SoC) of the battery. Validation of this model by tracking a realistic frequency regulation signal.
- The impact of communication delay on the tracking performance is studied.

6.1.2 System Model

Figure 6.3 shows an overview of control mechanism for the TCLs. The central control models aggregation of TCLs by a Resource Flexibility Model (RFM) discussed in Section 4.4 of Chapter 4. A frequency regulation signal ($r[k]$) corresponding to the imbalance between demand and supply is input to central control. The central control algorithm decides the activation/deactivation of suitable number of TCLs that can track the frequency regulation signal with sufficient accuracy. The operational state changes are sent to TCLs by the central control using dedicated communication channels. The tracking error is sent back for the monitoring purpose.

6.1.3 Regulatory Requirements

Each system operator has specific regulatory requirements for the demand side participation in the reserve market. For example, California Independent System Operator (CAISO) has defined the non-generator resources to provide power bid on the basis of their 15-minute energy capacity [143]. Alongside, strict requirements have been placed on the telemetry of TCL data. The TCLs are required to update their SoC and instantaneous power status every 4 seconds. In addition, the minimum TCL size that can participate is restricted to 0.5 MW. However, the results of this Chapter have complimented the findings in [130] that suggest a viable potential from a large number of residential TCLs. However, the uncertainties associated with such an application and the communication needs are required to be taken in account. This is essential for ensuring the resource availability that can make it a candidate of meeting the regulatory requirements. An

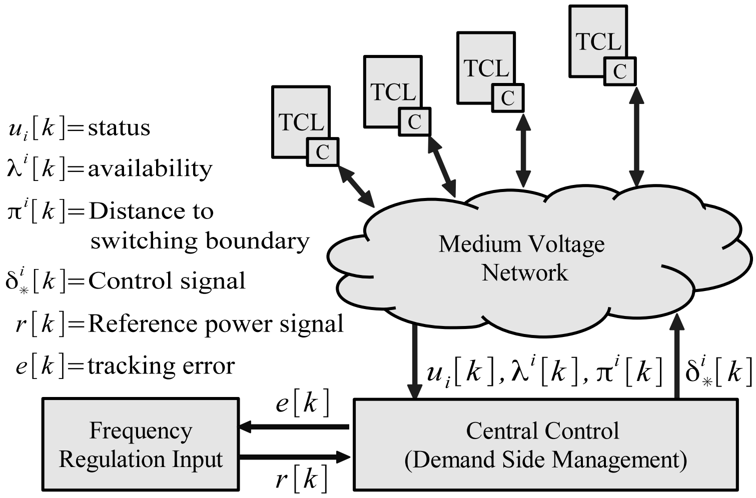

Figure 6.3: Overview of the control mechanism for TCL aggregation.

appropriate approach for modeling the uncertainties associated within the process is to model it in the equivalent battery model. In this way, a probabilistic approximation of the availability and potential of the resource can be made.

6.2 Control Scheme

Various control mechanisms have been studied in the literature for the control of TCLs, e.g., in [189, 193, 142, 188]. A predictive controller for controlling the TCL aggregation has been used in [142]. While in [193], the load control is achieved using minimum variance control law. These approaches have advantages but can be complex for the implementation of a large number of TCLs. In [143], a direct control mechanism of the TCL aggregation using priority stack based control has been proposed. In this method, the relative temperature distance ($\pi^i(t)$) of a TCL from its switching boundary is sent by each TCL to the central control. The central control then prioritizes to turn On/Off the TCLs that have the least distance to the switching boundary. The benefit of this method is that it reduces the overall number of forced cycling of the TCLs. This approach has been selected for the work in this Chapter.

6.2.1 Central Control Algorithm

The central control receives the flexibility information from each TCL in the form of its operational status ($u_i[k]$), availability ($\lambda_i[k]$) and temperature distance from the switching boundary ($\pi^i[k]$). It then performs a merit order to sort the TCLs based on value of $\pi^i[k]$. Such that, the TCLs having lesser distance to switching boundary are given preference. This schemes decreases the overall number of switching requirements. A frequency regulation signal from energy market is fed to the central control. It is followed by the difference between aggregate and baseline power consumption of the TCL aggregation. The difference from Equation 4.25 is given as,

$$\psi[k] = P_{\text{agg}}[k] - P_{\text{base}}[k] \ . \tag{6.1}$$

The objective of tracking the regulation signal is satisfied if $\psi[k]$ is equal to frequency regulation signal, $r[k]$. Without the regulation process ($r[k] = 0$)) and in the steady state, The $\psi[k] = 0$ as the TCL aggregation is consuming power equivalent to the base power. If $r[k] > \psi[k]$, then the algorithms at the central control turns On sufficient number of TCLs till the inequality $\psi[k] \geq r[k]$ becomes true. This process can be termed as charging of the battery. Similarly, for $r[k] < \psi[k]$, the battery shall be discharged to track the reference signal. The maximum charging potential of the battery is achieved when all the TCLs are turned On. It is given by,

$$\bar{\psi}[k] = \sum_{i} P^i - P_{\text{base}}[k] \ , \tag{6.2}$$

while, the maximum discharge potential can be obtained by setting $P_{\text{agg}} = 0$, resulting in $\underline{\psi}[k] = -P_{\text{base}}[k]$. If the base power consumption changes, then it shall impact the regulation limits. Considering this requirement, the base power consumption information shall be required from TCLs. However, this work assumes that the temperature set-points are static. The control scheme at the central control is described in Algorithm 6.1. The central control transmits the forced state

Algorithm 6.1: Priority stack algorithm at central controller.

Input : TCL i data ($u_i[k]$, $\lambda^i[k]$, $\pi^i[k]$)
Output: Forced state of the TCL δ^i_*

Calculate battery parameters (C, n_+, n_-);
for $t := 1 \cdots T$ **do** *(Time iteration loop)*
  Sample input frequency regulation signal $r[k]$;
  for $i := 1 \cdots N$ **do** *(TCL iteration loop)*
    Sort priority list of available On/Off TCLs;
  end
end
Update stochastic battery limits (C', n'_+, n'_-);
if ($R'_+ \leq r[k] \leq R'_-$) **then**
  $\xi = r[k] - \psi[k]$;
  if $r[k] < \psi[k]$ **then** *(Priority list based control)*
    Turn Off available TCLs till $\delta P < \xi$;
  end
  else
    Turn On available TCLs till $\delta P < -\xi$;
  end
end
else
  Regulation not possible;
end

change signals $\delta^i_*[k]$ to the TCLs. This algorithm also facilitate the addition or removal of TCLs dynamically to the system. In this case, the stochastic battery limits are updated dynamically. The stochastic battery model derived in Chapter 4 is shown in Figure 6.4 for reference. The

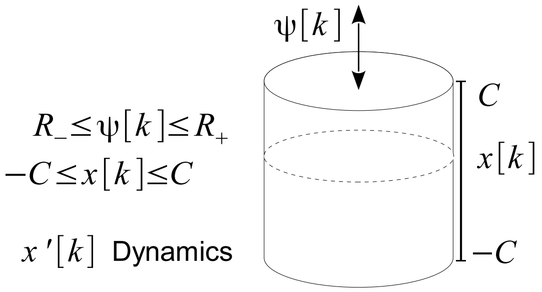

Figure 6.4: Stochastic battery model representing the TCL aggregation.

battery parameters have been discussed in Equation 4.27 are given as,

$$\begin{aligned} C &= \sum_i \lambda^i[k] \left(1 + \left|1 - \frac{a_i}{\alpha}\right|\right) \frac{\Delta_i}{b_i} \\ R_+ &= R'_+ - \sum_i (1 - \lambda^i[k]) P_i \\ R_- &= R'_- + \sum_i (1 - \lambda^i[k]) P_i \end{aligned} \quad . \tag{6.3}$$

The reference signal is compared to the stochastic limits given as,

$$R_- \leq r[k] \leq R_+ \ . \tag{6.4}$$

These limits can be used as a filter to guarantee the tracking of reference signal. If violated, the residual can be allocated to the other resources in the network e.g., distributed generators and the battery storage who are participating in the reserve service. Furthermore, the stochastic energy state of the TCLs aggregation can be observed at the central control.

6.2.2 Control at Thermostatically Controlled Load

The TCL dynamical model discussed in Equation 4.20 is given as,

$$\theta^i[k+1] = g^i \theta^i[k] + (1 - g^i)(\theta^i_a[k] - \delta^i[k]\theta^i_g) + \epsilon^i[k] \ , \tag{6.5}$$

The availability signal of a TCL has been introduced in Equation 4.28. A TCL is available if the temperature lies within the dead-band region and the short cycling constraint is fulfilled. The short cycling constraint ($\overline{\rho^i}[k]$) is the minimum time duration for which TCL must remain in a state after a state transition. The violation of this constraint or the operation of the TCL outside dead-band implies the non-availability. It is given as,

$$\lambda^i[k] = \begin{cases} 1 & \rho^i[k] > \overline{\rho^i} \ \& \ \underline{\theta^i} \leq \theta^i[k] \leq \overline{\theta^i} \\ 0 & \text{otherwise} \end{cases} \quad . \tag{6.6}$$

The temperature distance of the TCL from switching boundary is normalized with respect to the dead-band width before it is transmitted to the central control. The control strategy at a TCL is presented in Algorithm 6.2.

Algorithm 6.2: Algorithm at TCL.

Input: Control signal $\delta_*^i[k]$
Output: $(u_i[k+1],\ \lambda^i[k+1],\ \pi^i[k+1])$

$(\theta^i[k+1], \delta^i[k+1], \lambda^i[k+1]) = 0;$
if $\rho^i[k] > \overline{\rho^i}$ **then**
  $\lambda^i[k+1] \ = \ 1;$
  if $\delta_*^i[k]$ *is received* **then**
    $\delta^i[k] = \delta_*^i[k];$
    $\rho^i[k] = 0;$
  end
end
$\rho^i[k+1] = \rho^i[k] + 1;$
$\theta^i[k+1] = g^i\theta^i[k] + (1-g^i)(\theta_a^i[k] - \delta^i[k]\theta_g^i) + \epsilon^i[k];$
if $\underline{\theta}^i \leq \theta^i[k+1] \leq \bar{\theta}^i$ **then**
  $\delta^i[k+1] = \delta^i[k];$
end
else
  $\lambda^i[k+1] = 0;$
  if $\theta^i[k+1] < \underline{\theta}^i$ **then**
    $\delta^i[k+1] = 0;$
    if $\delta^i[k] = 1$ **then**
      $\rho^i[k+1] = 0$
    end
  end
  if $\theta^i[k+1] > \underline{\theta}^i$ **then**
    $\delta^i[k+1] = 1;$
    if $\delta^i[k] = 0$ **then**
      $\rho^i[k+1] = 0$
    end
  end
end
if $\delta^i[k+1] = 1$ **then** $\pi^i[k] \ = \ \left(\theta^i[k+1] - \underline{\theta}^i\right)/\Delta^i;$
if $\delta^i[k+1] = 0$ **then** $\pi^i[k] \ = \ \left(\underline{\theta}^i - \theta^i[k+1]\right)/\Delta^i;$

6.3 Test Cases of Demand Response Flexibility

Two test cases are presented for simulating the demand response flexibility from TCLs. In the first test case a large number of residential TCLs are simulated. The TCL aggregation is represented by an equivalent stochastic battery model and is used for tracking the reference frequency regulation signal. The objective of this test case has been to validate the hysteresis based control scheme and the proposed battery model. The regulation performance validates that a violation of the stochastic battery limits results in the loss of tracking. In the second model, a relatively small number of comparatively higher rating TCLs demonstrates the demand response scheme in a combined simulation environment. The individual TCL model and the distribution network are simulated in a power system simulation software, PowerFactory[1], while the control algorithm is programmed in Python[2]. The objective of this test case has been to develop a platform to assess the impact of the demand response activation on the distribution system.

6.3.1 Test Case for Residential Thermostatically Controlled Loads

The general specifications of a residential TCL is shown in Table 6.1. An aggregation of 1000 residential TCLs are modeled based on this generic data. The parameters of each TCL are obtained by sampling the normal distribution around these values with the heterogeneity of 30%. Here, the limits are taken as the percentage deviation from the mentioned quantity. These limits can be controlled to alter the heterogeneity in the aggregation. The TCL model time step is set at 10.02 seconds and the TCLs are initialized at steady state temperature condition $\theta^i[k] = \theta^i_{ref}$. The reference signal is a normalized scaled down version of the frequency regulation signal from the Pennsylvania-New Jersey-Maryland (PJM) market [194] in United States and is used to test the tracking performance of the stochastic battery model.

Table 6.1: Parameters of a typical residential air-conditioning TCL [149].

Parameter	Description	Value	Unit
C^i	Thermal capacitance	2	kWh/°C
R^i	Thermal resistance	2	°C/kW
θ^i_{ref}	Temperature	22.5	°C
Δ	dead-band length	2.5	°C
P^i	Nominal power	5.6	kW
η	Coefficient of performance	0.3	

6.3.1.1 Simulation Results

The temperature dynamics of a TCL is shown in Figure 6.5. It provides an insight into the temperature dynamics of the TCL when actively controlled by an external signal. It can be observed that the temperature evolves within the dead-band while state transition occurs at boundaries. The external signal can change the operational state while temperature is in limits, provided that the short cycling constraint is fulfilled. From results, it is observed that TCL experiences repeated activation between 780 to 950 seconds. This happens when the reference signal continues to force the state of TCL. Technically, it can cause damage to the device and hence a short cycling constraint is required. It sets a minimum time for turning On/Off a TCL after a state transition. The impact of this constraint can be seen in Figure 6.6, where the short cycling duration is increased from 2 to 6 seconds. The short cycling duration values are selected for the proof of concept here and can be conveniently changed to represent the actual requirements. The repeated activation phenomenon can also be observed by analysis of the regulation signal dynamics.

[1] `www.digsilent.de/index.php/products-powerfactory.html`, DIgSILENT PowerFactory
[2] `http://www.python.org`, Python

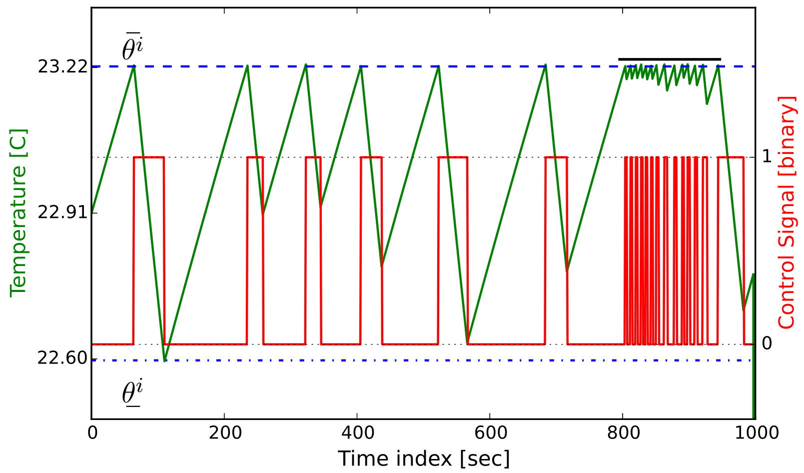

Figure 6.5: TCL state transition dynamics for short-cycle duration of 2 seconds.

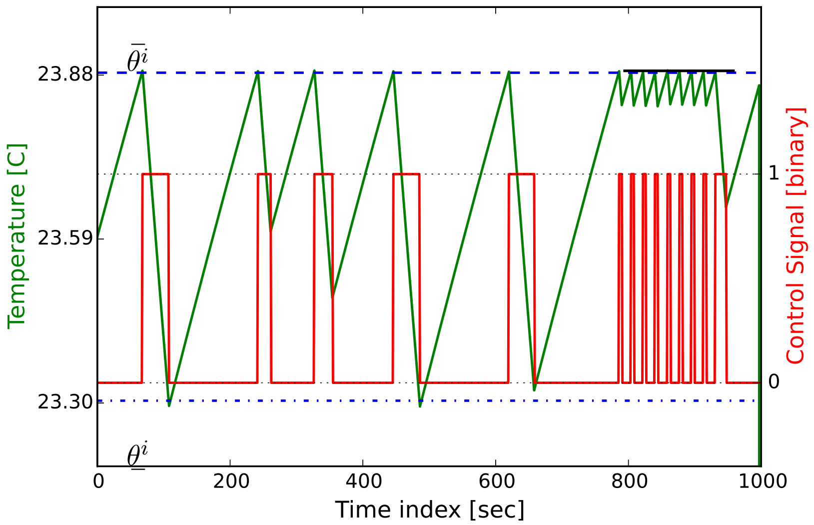

Figure 6.6: TCL state transition dynamics for short-cycle duration of 6 seconds.

Tracking performance for the test case is shown in Figure 6.7. It can be observed that the TCL aggregation successfully tracks the regulation signal till $k = 780$ seconds. The tracking is lost onward despite the reference signal occurring within the static regulation bounds (shown by the dotted lines and corresponds to the limits from Equation 4.26). It is due to the violation of dynamic limits discussed in Equation 6.3. The tracking error as result of the violation of this constraint can be seen in Figure 6.8. While, the stochastic regulation limits are shown in Figure 6.9. It can be observed that the reference signal violates the stochastic ramp-rate limits. The decrease in the permissible ramp-rate limits is due to the unavailability of TCLs as shown in Figure 6.10. Furthermore, the stochastic SoC limit of the battery given as C' from Equation 6.3 is dynamic and shown in Figure 6.11. These limits provides dynamic bounds and the tracking of regulation signal can be ensured if the stochastic SoC and ramp-rate limits are satisfied.

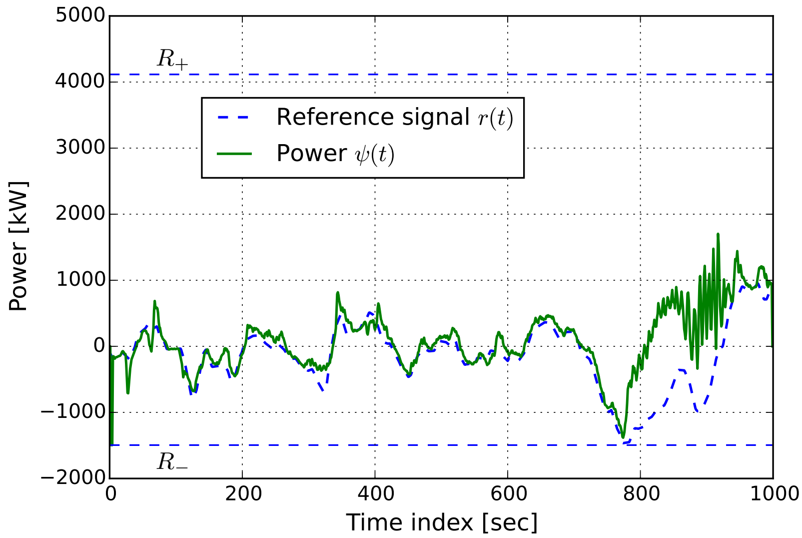

Figure 6.7: Tracking performance of TCL aggregation in responding to the regulation signal.

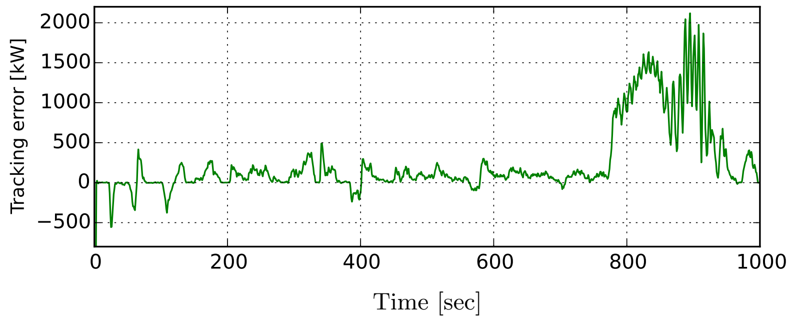

Figure 6.8: Tracking error in the regulation process.

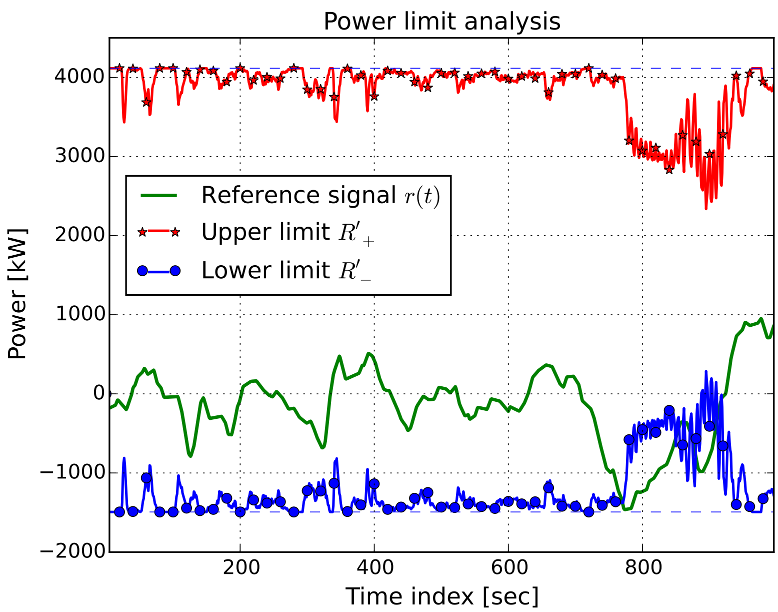

Figure 6.9: Tracking performance comparison with stochastic regulation limits.

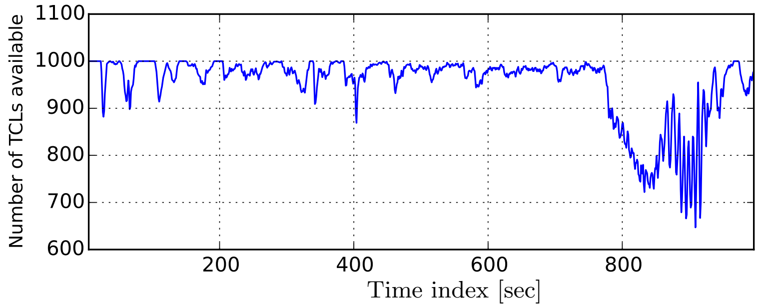

Figure 6.10: TCL availability dynamics.

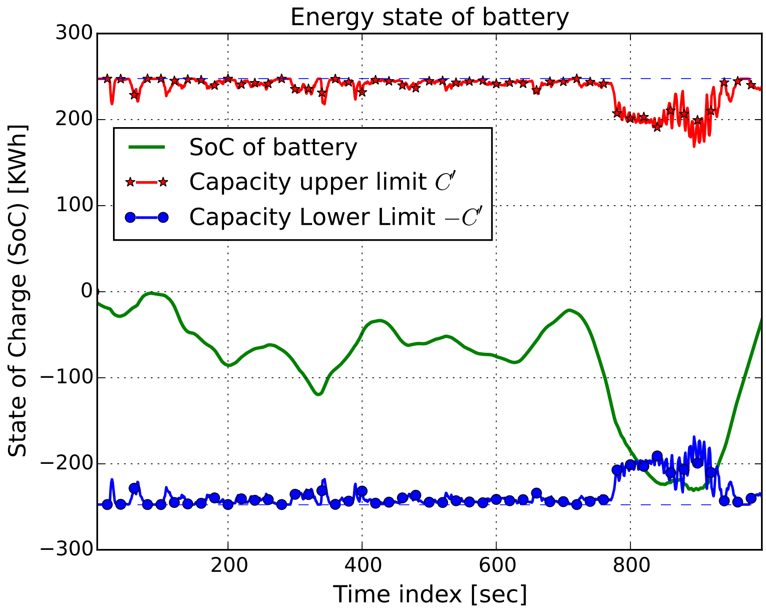

Figure 6.11: State of charge dynamics of the stochastic battery model.

6.3.1.2 Communication Delay Impact Analysis

The impact of communication delay on the tracking performance is shown in Figure 6.12. The communication delay is applied to all the TCLs equally. However, it can be sampled from a probability distribution without the loss of generality. It can be observed that with the communication delay of 10 seconds impacting all the TCLs, the tracking performance remains more than 50%. The impact of cycling duration on the tracking performance decreases with increase in the delay. It can be observed that the communication delay becomes a dominant factor in deciding the regulation performance.

6.3.2 Combined Simulation Test Case for Thermostatically Controlled Loads

This test case focuses on the development of a platform that facilitates the analysis of impact of demand side flexibility on the distribution network. The objective has been to study the impact on bus voltage in the network. For this study, it is assumed that the voltage decreases as the distance from feeder increases. Thus, the bus that is farthest from the main feeder is selected for the analysis.

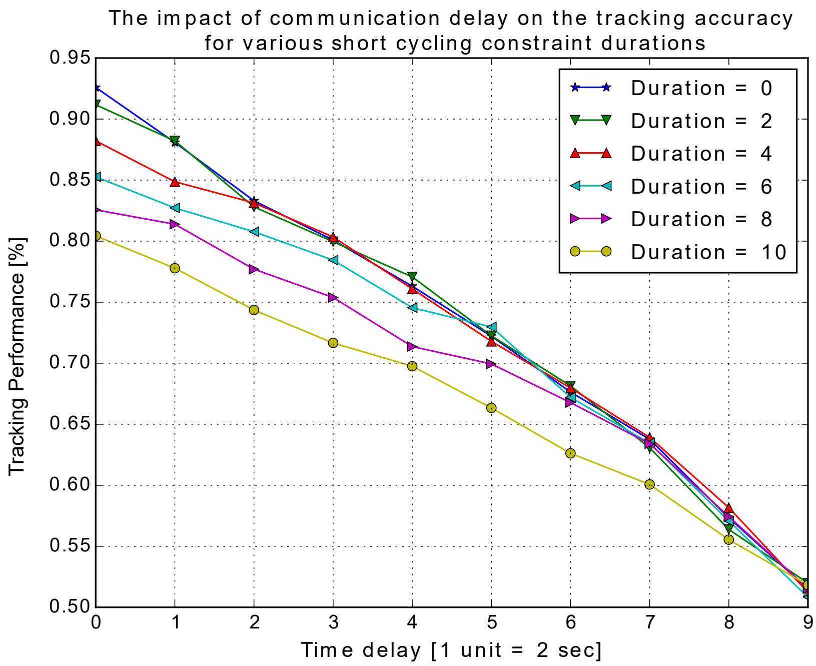

Figure 6.12: Impact of communication delay and the cycling duration on the tracking performance of TCL aggregation.

6.3.2.1 Simulation Setup

This section discusses the simulation tool selection and is followed by the description of power network and the combined simulation setup.

PowerFactory as power system simulation tool. PowerFactory is a domain specific tool for simulating, analysing and understanding power systems. The software package supports a programming language called DIgSILENT Simulation Language (DSL) which is used for implementing simulation models. DSL however does not support matrices, which are required for implementing of the central controller. Therefore, a combined simulation approach is selected where the power network and the local controllers for the TCLs have been simulated in PowerFactory and the central controller has been simulated in Python.

Python as control environment. Python is an open source high level scripting language with a large number of interdisciplinary toolboxes for optimization, signal processing, statistics, matrix calculations etc. This makes it an ideal candidate for programming control algorithms. Python is a high level language with comprehensive libraries that can be used for facilitating the computational and connectivity requirements. In combined simulation environment, python can be used to extend the capabilities of PowerFactory.

Power system network. The network chosen for this work is a Medium Voltage (MV) distribution system test case from Institute of Electrical and Electronics Engineers (IEEE) comprising of 119 nodes [195]. It consists of with 116 loads and 15 tie lines. This work defines the TCL aggregation at a bus as a percentage of the rated load. It is given as,

$$P_{TCL}^{i,rated} = 0.2 \times P_{load}^{i,rated} \times [U[0,1] + 1] \ , \tag{6.7}$$

where, $U[0,1]$ is a uniform number between 0 and 1.

Co-simulation Setup. Figure 6.13 provides a graphical overview of the co-simulation setup used in the test case. PowerFactory supports a number of external interfaces covered in [196] that can be used for data exchange with external software. Here, the PowerFactoy had been coupled with Python using sockets. DSL models are capable of making function calls to external C++ libraries. This ability has been used to provide socket communication support for local TCL controllers simulated within PowerFactory. Ease of implementation, re-usability and the ability to incorporate additional simulators for future work have been the main driving factors in selection of the simulation tools and the coupling scheme.

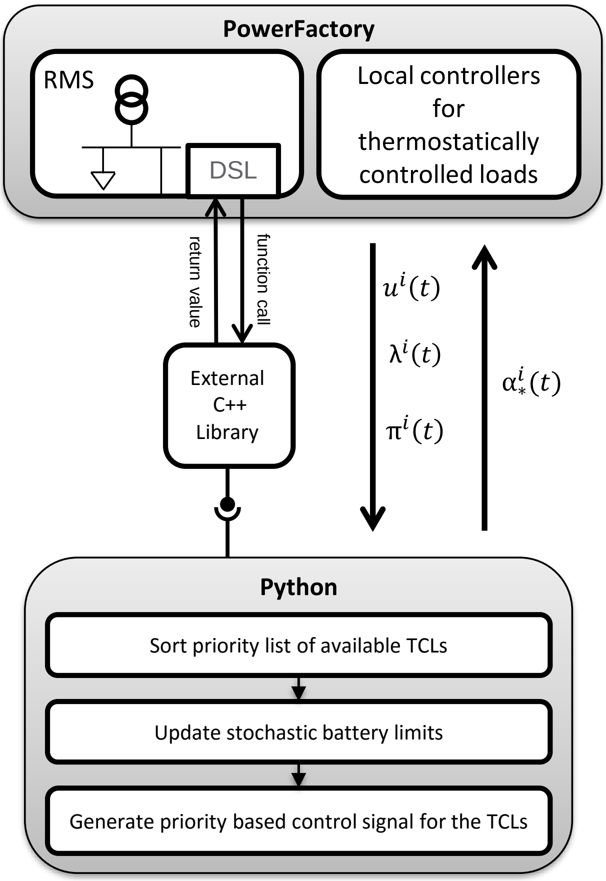

Figure 6.13: Overview of the co-simulation setup.

6.3.2.2 Simulation Results

Figure 6.14 shows the temperature dynamics of a TCL around the reference value for a limited time interval of simulation. The control signal influences the operation while temperate remains within the dead-band. In relation, Figure 6.15 shows how the temperature distance varies as function of the switching status. The state transition results in the temperature distance reaching to its maximum value as expected.

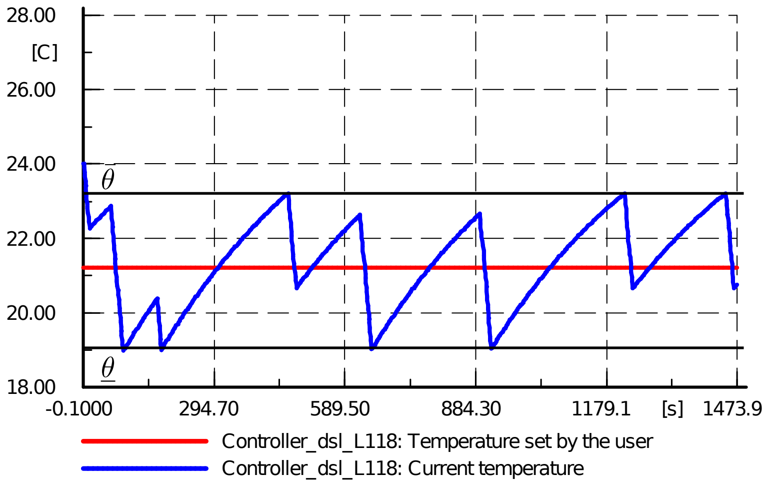

Figure 6.14: TCL temperature dynamics.

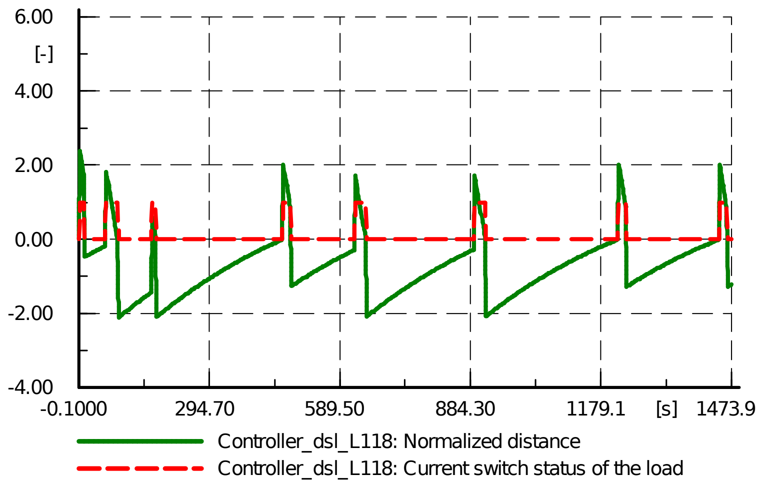

Figure 6.15: TCL temperature distance from the switching boundary.

The tracking performance of proposed control scheme is shown in Figure 6.16. It is observed that the TCL aggregation tend to follow the regulation signal dynamics. The precise regulation is not possible in this case. The main reason are the limited number of TCLs e.g., 116 in this case. The state transition triggers the cycling constraints which decreases the number of available TCLs. The higher ratings of the TCLs also hiders the precise tracking performance.

In order to observe the impact of frequency regulation on the network, a 24-hour simulation is simulated. This study aims to understand the impact of ambient temperature and the load forecast profiles on the frequency regulation. Some of the loads are considered residential and others commercial. The profiles of both are shown in Figure 6.17.

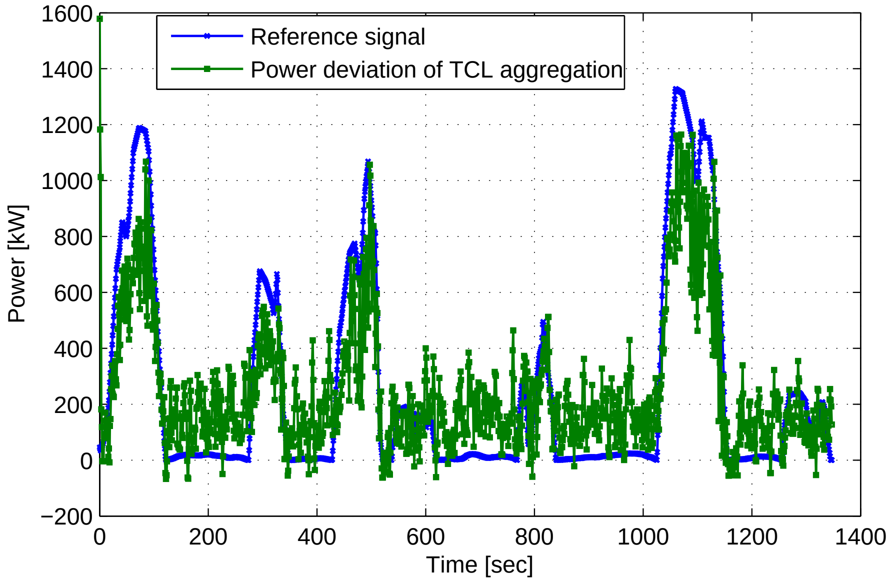

Figure 6.16: Regulation signal tracking performance.

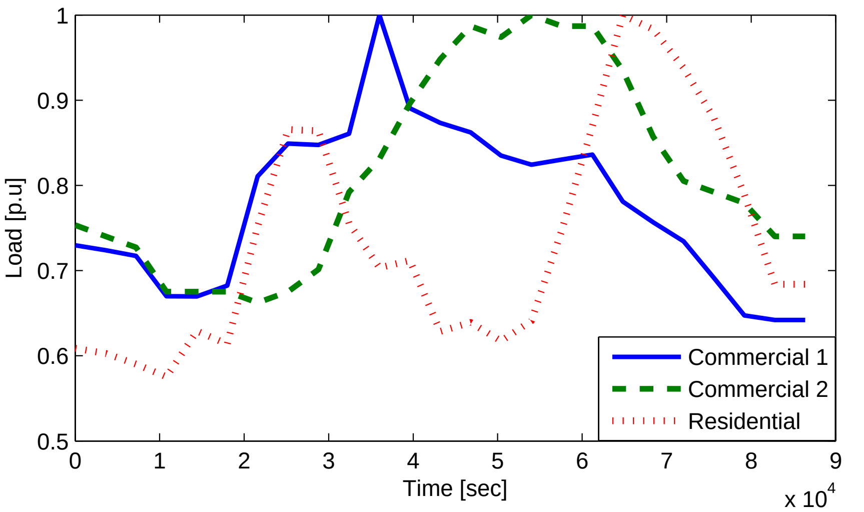

Figure 6.17: Load profiles for co-simulation test case.

Figure 6.18 shown the TCL dynamics in relation with the ambient temperature. It can be observed that despite the ambient temperature change the local TCL controller is able to keep the temperature within the limits along with providing serving for the frequency regulation. However, the availability of TCLs has a strong correlation with the difference between ambient

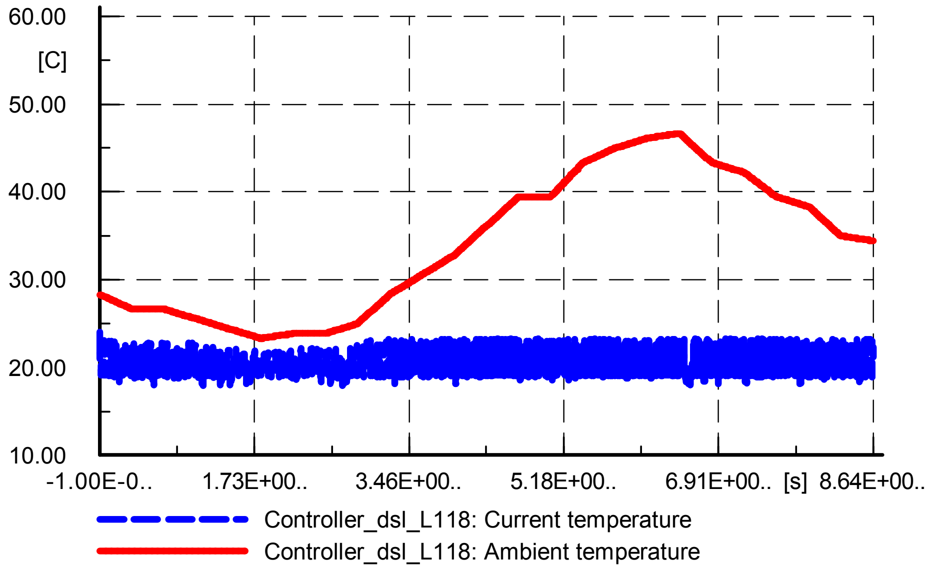

Figure 6.18: TCL switching as a function of ambient temperature.

and the internal temperature as shown in Figure 6.19. Such that, when the temperature is high, the frequency of air-conditioning loads being turned On/Off increase. This triggers the cycling constraints more frequently thus the number of available TCLs decreases. The impact of frequency regulation and the ambient temperature at the end of a feeder (bus 80 in the network) can be seen in Figure 6.20. The simulation platform facilitates the design of control schemes that can take the voltage limits at the end of the feeder as constraints. Thus the control methods in Python can be developed that can consider or contribute to avoiding the network constraint violations.

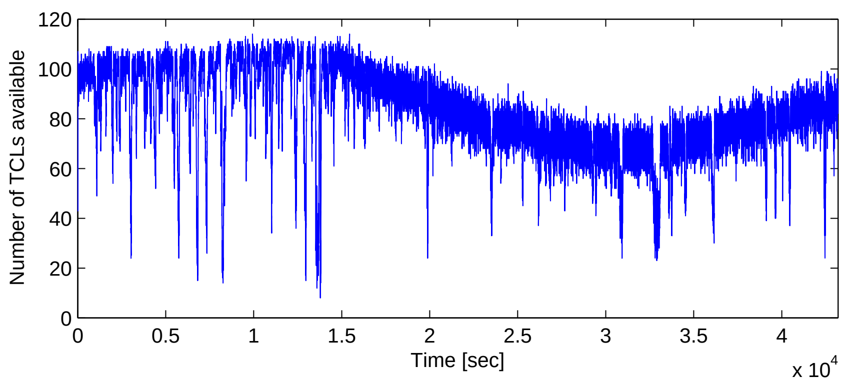

Figure 6.19: TCL availability.

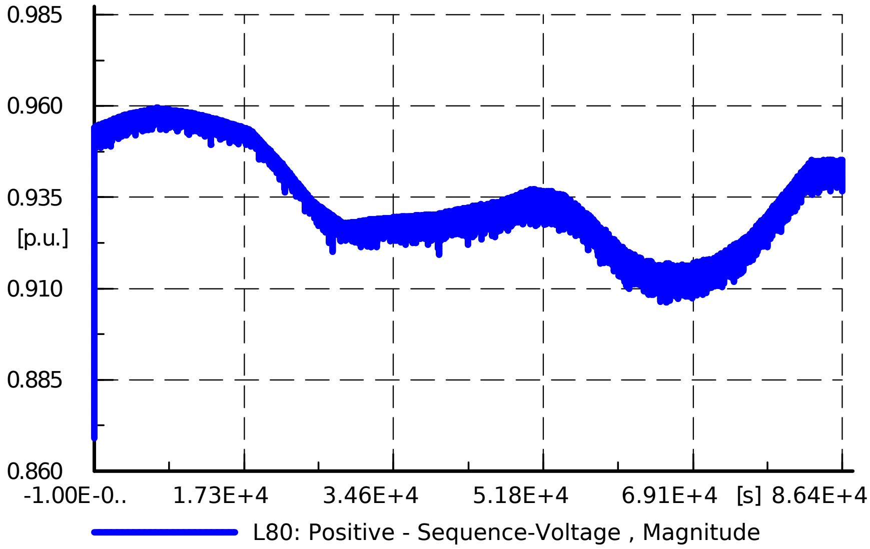

Figure 6.20: Impact of TCLs activation on the voltage at a selected bus.

7 Conclusion and Outlook

7.1 Conclusion

A resource in an electric distribution system had been defined as a power generating or consuming entity that possess operational flexibility. This study presented a Resource Flexibility Model (RFM) for representing the flexibility potential of a resource. Incorporation of flexibility from diverse resource types such as demand response, generators, storage etc., motivated the need for a common modeling approach in order to facilitate the flexibility aggregation and allocation processes. The proposed RFM had been designed to represent the storage and dynamic capability of a resource by an Energy Storage Model (ESM) and a Resource Capability Envelope (RCE). The ESM had been discussed based on the model proposed in [133]. The novel RCE as the second part of the RFM, models the capability constraints (e.g., ramp-rate and associated cost or response time) of the resource. The ability to represent cost as function of dynamic capability provided a mechanism for modeling the *over-drive* potential of the resource. It enables a resource to bid with more diverse offers that can potentially improve the energy efficiency and economics. Another variable proposed as part of RCE is the "response time". The applications responsible for the flexibility activation can make use of this information in planning and optimization of the operations. The RFM provides a holistic mechanism of flexibility modeling that can be adapted to represent a diverse range of resources. A resource can use it for the self-optimization and for making flexibility bids in energy market. The analysis performed based on the flexibility models assumes the availability of a suitable communication infrastructure for the transfer of flexibility bids/activation signals between resources and the central controller.

The distribution network of future is assumed to have Cells or microgrids that aims to facilitate the reliable operation in presence of a high distributed generation. The resource adequacy in a microgrid has been defined by a flexibility assessment problem. The objective had been to assess the *net-demand* forecast while considering the ramp-rate and ramp duration requirements as function of power values. The triad variables represents the first order dynamics [15]. The historical data of the demand and generation forecasts had been used to develop the uncertainty models for the flexibility assessment. Both clustering and probabilistic models had been used to model the spatial diversity of the uncertainty while temporal correlation was modeled using Markov chain. The results had been the models that captures both the temporal and spatial aspects of uncertainty. The uncertainty models were then sampled using Monte Carlo simulations resulting in *net-demand* scenarios for the microgrid. These scenarios were then transformed to instances in a three dimensional space spanned by the first order dynamics variables by the application of a compression algorithm. The compact representation of the enclosing envelope by a polytope resulted in an economic approach towards the flexibility assessment. The result had been compared to the bounding box approach presented in [14]. The polytope based envelope requires vertices or hyper plane information for its representation. This in comparison with the bounding box approach requires more storage However, the economic advantage can be much significant than additional information storage cost.

The *net-demand* dynamics and associated uncertainty represented by a polytope had been allocated among the generators, the capability of which was modeled using RCE. The flexibility allocation algorithm had resulted in the demand and reserve allocation among generators and the power import/export envelope related to the connected grid. A comparative analysis of a fixed reserve (percentage of the demand) and the polytope based reserve levels showed the economic advantage of the proposed method. Computational complexity of the proposed vertex based geometric allocation algorithm had been discussed. The flexibility allocation problem remains tractable as the number of resources increases. The reserve requirements as a result of flexibility assessment had been incorporated in the Economic Dispatch (ED) and Unit Commitment (UC) applications for a day-ahead dispatch.

The polytope representation of RCE is a convex bounding surface enclosing points in the space that are defined by the capability of a resource. Similarly, the *net-demand* envelope had been modeled using a convex envelope approach. The formulation also benefited the application of deterministic optimization methods applied during flexibility allocation process. However, further improvement can be made by fitting a non-convex envelope on the points in the space. Such an approach on one end can further reduce the reserve requirements (*net-demand* polytope) in the microgrid and on the other hand improves the accuracy of modeling the resource capability. Two approaches can be used to perform operation with non-convex envelope. The resource capability can be represented by multiple convex envelopes that approximately represent the non-convex capability envelope. In this case, the resource allocation shall require to switch between convex envelopes while performing optimization. This step shall add to the computational complexity of the problem. The second approach can be a heuristic based optimization method that can directly operate with the non-convex envelopes. Such an approach may be suitable as the flexibility planning problem is performed off-line and the convergence of the solution in polynomial time may not be a stringent requirement.

Demand response shall be an important player as a flexibility resource in maintaining an instantaneous balance between demand and supply. The flexibility offered by an aggregation of Thermostatically Controlled Loads (TCLs) in the distribution network had been modeled as a stochastic battery. The parameters of battery model (charge/discharge capacity and ramp-rate limits) were calculated using the information of status and availability (binary signals) from TCLs. The rated value of TCLs were assumed as known values to the central control as part of the contract with each TCL. If this assumption is not valid, then the proposed model can be extended with out the loss of generality. In such a case the power measurements shall be calculated at each TCL and communicated to the central control. For this scenario, the availability information may not be required as it will be inherently represented by the power value. The studies in [130] had used historical and cycling constraint (minimum time to stay off/on after a state transition) information from TCLs for the stochastic limits. The consideration of availability signal from each TCL had made it possible to compute the stochastic limits of the battery parameters directly using the present data only. The proposed battery model has been validated for two test cases. The tracking performance in first test case showed that the stochastic battery model for the TCL aggregation can be used to model the dynamic capability as a secondary frequency reserve resource. The results showed that the satisfaction of stochastic limits is important for successful tracking of regulation signal. The residual flexibility that is not tracked by the TCLs can be used to operate alternate resources. The proposed approach requires dedicated communication links between TCLs and the central control. It may required for meeting the regulatory requirements of guaranteed availability of the demand response resource. However, the process has to deal with the measurement uncertainty and the communication delays. The smart meter technology can facilitate future efforts in this direction.

The activation of flexibility from the demand response impacts the network and may lead to constraint violations. These violations can be related to voltage levels at critical buses, overloading the distribution lines or false triggering of protection devices. Therefore, it is highly likely that the central control performing the demand response shall require to perform the state estimation. This process leads to the network awareness and can be used to control the flexibility activation in the network. In the second test case, a combined simulation approach had been presented to assess the impact of TCLs activation on the network. The distribution network had been simulated using a dedicated power system modeling and simulation software (DIgSILENT PowerFactory) and the control scheme was programmed in Python. The Root Mean Square (RMS) simulation [197] of the network at each time instance had been used to study the impact of demand response service on voltage in the network. While, the control mechanism can be improved by using open source optimization toolboxes and methods in Python. The proposed platform enables to use the features of PowerFactory in the control scheme, thus opening new areas of research and possibilities. The consideration of the communication delays, accuracy of the communicated data due to measurement uncertainty at the local control shall further influence the tracking performance.

The flexibility in a distribution system that is aggregated using a microgrid or cell based approach requires a suitable retail market model. The technical and commercial activities at Distribution Network Operator (DNO) are challenged in dealing with distributed generation, a need to maintain local reserves and the uncertainties associated with renewables and consumption. The study in [198] presents a participation model of the microgrid in market clearing optimization model. The nodal prices at the distribution level can provide basis for remuneration of the flexibility offered by Distributed Generators (DGs).

The need for monitoring and control in the distribution network shall become inevitable to realize a high share of Renewable Energy Sources (RES) and increasing level of loads such as Electric Vehicle (EV). The enormous challenge posed to the DNOs encourage the role of microgrids or cells in managing the flexibility locally and appearing to the DNO as lumped loads with the flexibility offers. Th contribution from this thesis can be summarized as,

- Methods for assessing the flexibility requirements considering the *spatio-temporal* characteristics of uncertainty. Modeling the uncertainty scenario set as a space between first order dynamic variables and enclosing it with a compact geometric structure. It results in a representation of the uncertainty dynamics that can be used to plan reserve resources.
- A common flexibility model for distributed resources that captures both the storage and dynamic capability using a RFM. The reserve potential of distributed generation and the responsive thermostatically controlled loads was modeled using proposed RFM.
- Geometric methods for aggregating the flexibility offered by distributed resources. Optimization methods for allocating the uncertain demand space between generators capability envelopes.

- Using the demand response flexibility defined by RFM in a frequency regulation process.

7.2 Outlook

The emphasis during flexibility assessment had been on modeling the dynamics of the *net-demand* in microgrid. These includes the ramp-rate and corresponding ramp duration requirements as function of the power level. This approach can be extended to the second order dynamic variables involving ramp acceleration. This step can further improve an assessment of the ramp acceleration requirements in microgrid and the available potential within the microgrid. The results can be used to assess the transformer ratings at the point of common coupling with the distribution network.

The demand response potential in the distribution network can be modeled as a stochastic battery. The envelope representation of the dynamic capability of the battery can makes it visually appealing in comparing it with other resources that can participate as secondary frequency reserve. Apart from the direct control of the loads, the price based and incentive based approach can be used. These approaches may lead to less probabilistic confidence on the available demand response potential but can subside the requirement of communication with the TCLs. However, for such an application the demand flexibility estimation and activation needs to be assessed for a large range of possible scenarios. Reliance on the price/incentive based approach may lead to a high stochastic variation that may not be able to meet the regulatory requirements.

In order to decrease the communication requirements associated with the proposed method of flexibility exchange, a control mechanism in a Medium Voltage (MV) distribution network is shown in Figure 7.1. Here, the Resource Control Unit (RCU) between bus 8 and 14 can be a phase shifting transformer, Thyristor-Controlled Series Compensation or any other apparatus to control the flow in the tie line.

Each resource can optimize its portfolio based on the resource specific constraints and preferences. The resources can be TCLs, shift-able loads, generators, Photo Voltaic (PV), storage, domestic microgrid and any combination. The objective of the resource optimization can be to fulfill its energy demand and to meet any committed and/or offered flexibility. The proposed RFM can be used by a resource to model its flexibility. The model can be influenced by the electricity price, environment and external variables. The complexity of the local portfolio optimization shall be responsibility of the resource. Each resource may generate two flexibility offers. The first offer can be for the frequency regulation process. For a TCL, it can be composed of the status/power, temperature distance from the switching boundary and the availability signal as discussed in Chapter 4. This approach assumes that rated power of TCL is already known to the controller. On the contrary if this is not the case, then the availability signal shall be replaced by the available power signal. This shall require the installation of sensors for measuring the power. But this approach can facilitate the addition of additional resources in the frequency regulation service. The second offer can be a flexibility schedule and associated cost. The flexibility related to the loads can be managed by a dedicated load controller. The resources shall require to design algorithm on making flexibility bids while optimizing their portfolio. These flexibility bids can have a stochastic component as well, the availability of which can be a probabilistic value.

The algorithm at Feeder Control Unit (FCU) will have a responsibility to aggregate the flexibility bids and to define a stochastic battery model. The battery parameters shall be calculated from the flexibility offers from the RCUs and may have an associated probability of availability. The

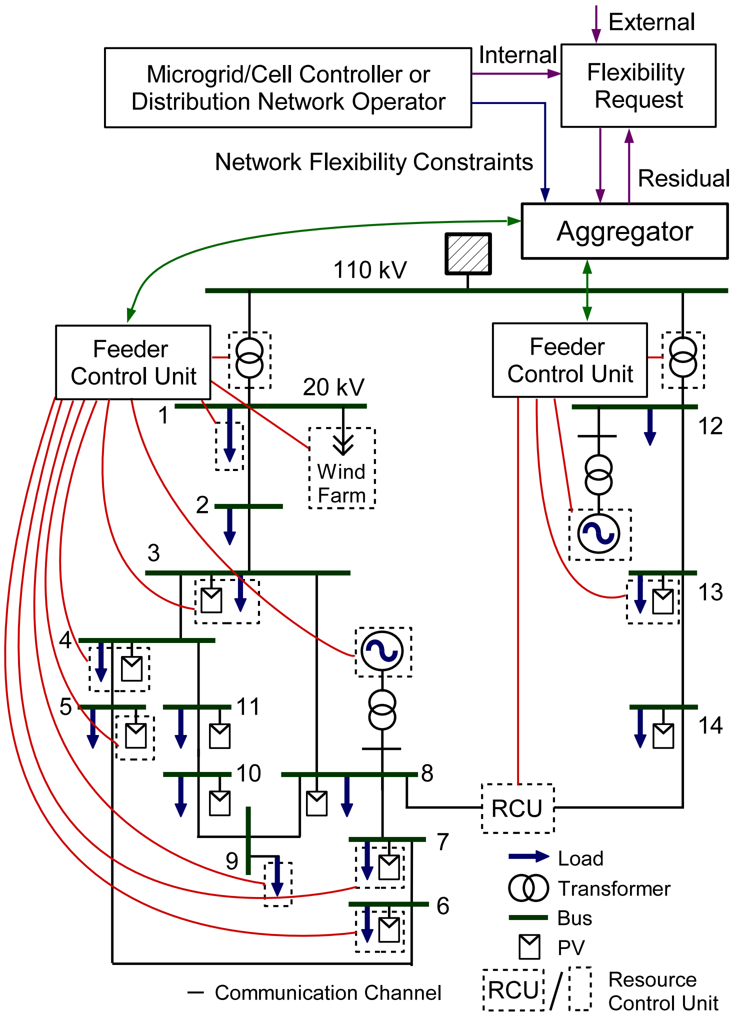

Figure 7.1: MV network with proposed controllers for controlling flexibility in the distribution network.

measurements errors and uncertainties associated with the resource data needs to be taken into account at this stage. The FCU shall also implement two stages of aggregation. First stage shall be to aggregate the TCL flexibility and formulate a priority stack. This stack shall be used to turn On/Off TCLs locally. The second aggregation effort shall be to calculate the parameters of the stochastic battery parameters of the equivalent energy storage model and the resource capability envelope. This information is communicated to the aggregator.

The aggregator responsibility is to aggregate the flexibility offers from the Load Control Units (LCUs). The battery parameters can be represented by the State of Charge (SoC), ramp-up and ramp-down limits while the capability envelope can be in the form of a polytope. This approach decreases the computational complexity of the aggregator in dealing with all the potential flexibility resources by a need to communicate to FCUs only. The aggregator communicates the maximum flexibility activation limits based on the overall system analysis to the FCUs. The microgrid/cell controller or the DNO shall assess the activation limits at each feeder by analyzing the network constraints. Such an approach can lead to realistic flexibility offers from FCU that can be activated based on prevailing network conditions. A limiting factor towards the consideration of flexibility from a far-end resource in the network can be a voltage issue. The frequency regulation signal is received from the microgrid/cell based control, DNO or externally from the energy market.

The flexibility of energy exchange between multiple areas in power system is discussed in [118]. This study defines the reserves that can be shared in the inter-area energy transfer by the polytopic projections of the flexibility on the desired bus. This method can be used to identify the flexibility that can be made available in the distribution network at a bus. It can be a useful resource for avoiding congestion in the distribution network.

The reserve requirement that is obtained as a result of the *net-demand* assessment in the microgrid has been used for scheduling generators using a DC Optimal Power Flow (OPF) based Security Constrained Economic Dispatch (SCED). The implementation of multi-period SCED involving AC OPF introduces quadratic equations in the optimization problem in terms of network matrices which should be positive semi-definite [199]. But the negative sign with the matrices is encountered, thus making the quadratic function non-convex [200]. The convex relaxation can be applied for making it a convex problem. The result will be a better schedule that considers the reactive power flows and impedance in the network.

Bibliography

[1] N. Jenkins, J. Ekanayake, and G. Strbac, *Distributed generation and future network architectures.* Energy Engineering, Institution of Engineering and Technology, 2010.

[2] J. Buchner, J. Katzfey, O. Florcken, A. Moser, H. Schuster, S. Dierkes, T. van Leeuwen, L. Verheggen, M. van Amelsvoort, and M. Uslar, “Smart grids in germany: How much costs do distribution grids cause at planning time?,” in *Smart Electric Distribution Systems and Technologies (EDST), 2015 International Symposium on*, pp. 224–229, Sept 2015.

[3] ENTSO-E, “Entso-e scenario outlook & adequacy forecast (so&af) 2015,” tech. rep., 2015.

[4] F. F. Wu, K. Moslehi, and A. Bose, “Power system control centers: Past, present, and future,” *Proceedings of the IEEE*, vol. 93, pp. 1890–1908, Nov 2005.

[5] M. Milligan, B. Frew, E. Zhou, and D. J. Arent, “Advancing system flexibility for high penetration renewable integration,” tech. rep., NREL (National Renewable Energy Laboratory (NREL), 2015.

[6] P. Lund, S. Cherian, and T. Ackermann, “A cell controller for autonomous operation of a 60 kv distribution area,” *International Journal of Distributed Energy Resources*, vol. 2, no. 2, pp. 83–100, 2005.

[7] M. Heleno, R. Soares, J. Sumaili, R. J. Bessa, L. Seca, and M. A. Matos, “Estimation of the flexibility range in the transmission-distribution boundary,” in *PowerTech, 2015 IEEE Eindhoven*, pp. 1–6, June 2015.

[8] H. Hooshyar, F. Mahmood, and L. Vanfretti, “Specification and implementation of a reference grid for distribution network dynamics studies,” in *PES General Meeting — Conference Exposition, 2014 IEEE*, pp. 1–5, July 2014.

[9] E. Vanet, G. Lebel, R. Caire, N. Hadjsaid, S. Bediou, and A. Glatigny, “Lv4mv: A concept for optimal power flow management in distribution grids, using der flexibility,” in *CIRED 2015-The 23nd International Conference on Electricity Distribution*, 2015.

[10] D. Bozalakov, T. Vandoorn, B. Meersman, and L. Vandevelde, “Overview of increasing the penetration of renewable energy sources in the distribution grid by developing control strategies and using ancillary services,” in *IEEE Young Researchers Symposium*, EESA, 2014.

[11] R. Santodomingo, M. Uslar, A. Göring, M. Gottschalk, L. Nordström, A. Saleem, and M. Chenine, "Sgam-based methodology to analyse smart grid solutions in discern european research project," in *Energy Conference (ENERGYCON), 2014 IEEE International*, pp. 751–758, May 2014.

[12] S. Henein, A. Zegers, and S. Übermasser, "Gap analysis of future energy grids," in *European Energy Market (EEM), 2015 12th International Conference on the*, pp. 1–4, May 2015.

[13] B. Klebow, A. Purvins, K. Piira, V. Lappalainen, and F. Judex, "Eepos automation and energy management system for neighbourhoods with high penetration of distributed renewable energy sources: A concept," in *Intelligent Energy Systems (IWIES), 2013 IEEE International Workshop on*, pp. 89–94, Nov 2013.

[14] Y. Makarov, P. Etingov, Z. Huang, J. Ma, B. Chakrabarti, K. Subbarao, C. Loutan, and R. Guttromson, "Integration of wind generation and load forecast uncertainties into power grid operations," in *Transmission and Distribution Conference and Exposition, 2010 IEEE PES*, pp. 1–8, April 2010.

[15] Y. Dvorkin, D. S. Kirschen, and M. A. Ortega-Vazquez, "Assessing flexibility requirements in power systems," *IET Generation, Transmission & Distribution*, vol. 8, pp. 1820–1830(10), November 2014.

[16] M. Petersen, K. Edlund, L. Hansen, J. Bendtsen, and J. Stoustrup, "A taxonomy for modeling flexibility and a computationally efficient algorithm for dispatch in smart grids," in *American Control Conference (ACC), 2013*, pp. 1150–1156, June 2013.

[17] L. Martini, "Trends of smart grids development as fostered by european research coordination: The contribution by the eera jp on smart grids and the electra irp," in *Power Engineering, Energy and Electrical Drives (POWERENG), 2015 IEEE 5th International Conference on*, pp. 23–30, May 2015.

[18] R. D'hulst, J. Merino Fernandez, E. Rikos, D. Kolodziej, K. Heussen, D. Geibelk, A. Temiz, and C. Caerts, "Voltage and frequency control for future power systems: the electra irp proposal," in *Smart Electric Distribution Systems and Technologies (EDST), 2015 International Symposium on*, pp. 245–250, Sept 2015.

[19] W. H. Kersting, *Distribution System Modeling and Analysis, Third Edition.* CRC Press, 3 ed., 1 2012.

[20] J. Ekanayake, N. Jenkins, K. Liyanage, J. Wu, and A. Yokoyama, *Smart grid: technology and applications.* John Wiley & Sons, 2012.

[21] E. Vaahedi, *Practical Power System Operation.* John Wiley & Sons, 2014.

[22] E. Wuppertal Institute for Climate and Energy, "Technical analysis and comparison of underlying scenarios for the forthcoming european commission white paper on a 2030 framework for climate and energy policies," tech. rep., 2014.

[23] G. Resch, C. Panzer, and A. Ortner, "2030 res targets for europe: a brief pre-assessment of feasibility and impact," *Intelligent Energy Europe Programme*, 2014.

[24] C. Lyons, "Guide to procurement of flexible peaking capacity: energy storage or combustion turbines," tech. rep., Enegy Strategies Group, 2014.

[25] IEA, "World energy outlook 2015," tech. rep., OECD Publishing, Paris, 2014.

[26] Frits Bliek; Arnoud Backers; Milo Broekmans; Claire Groosman; Hans de Heer; Marten van der Laan; Marijn de Koning; Jan Nijtmans; Phuong Nuygen; Tjerk Sanberg; Berry Staring; Marcel Volkerts; Eric Woittiez; , "An introduction to the universal smart energy framework," tech. rep., 2014.

[27] S. H. Widder, G. B. Parker, J. M. Petersen, and M. C. Baechler, *Demand Response Performance of GE Hybrid Heat Pump Water Heater*. Pacific Northwest National Laboratory, 2013.

[28] U. Foundation, "Usef: The framework explained," report, December 2015.

[29] IEEE, "Ieee guide for design, operation, and integration of distributed resource island systems with electric power systems," *IEEE Std 1547.4-2011*, pp. 1–54, 2011.

[30] C. W. Group, "Microgrids evolution roadmap - working group c6.22," tech. rep., 2012.

[31] P. Lund, "The danish cell project - part 1: Background and general approach," in *Power Engineering Society General Meeting, 2007. IEEE*, pp. 1–6, June 2007.

[32] S. Cherian and V. Knazkins, "The danish cell project - part 2: Verification of control approach via modeling and laboratory tests," in *Power Engineering Society General Meeting, 2007. IEEE*, pp. 1–5, June 2007.

[33] P. Piagi and R. Lasseter, "Autonomous control of microgrids," in *Power Engineering Society General Meeting, 2006. IEEE*, pp. 8 pp.–, 2006.

[34] C. Schwaegerl, L. Tao, J. P. Lopes, A. Madureira, P. Mancarella, A. Anastasiadis, N. Hatziargyriou, and A. Krkoleva, "Report on the technical, social, economic, and environmental benefits provided by microgrids on power system operation," tech. rep., 2009.

[35] A. Bidram and A. Davoudi, "Hierarchical structure of microgrids control system," *Smart Grid, IEEE Transactions on*, vol. 3, no. 4, pp. 1963–1976, 2012.

[36] T. Vandoorn, J. Vasquez, J. De Kooning, J. Guerrero, and L. Vandevelde, "Microgrids: Hierarchical control and an overview of the control and reserve management strategies," *Industrial Electronics Magazine, IEEE*, vol. 7, no. 4, pp. 42–55, 2013.

[37] J. Guerrero, M. Chandorkar, T. Lee, and P. Loh, "Advanced control architectures for intelligent microgrids part i: Decentralized and hierarchical control," *Industrial Electronics, IEEE Transactions on*, vol. 60, no. 4, pp. 1254–1262, 2013.

[38] H. Laaksonen, P. Saari, and R. Komulainen, "Voltage and frequency control of inverter based weak lv network microgrid," in *Future Power Systems, 2005 International Conference on*, pp. 6 pp.–6, 2005.

[39] M. Chandorkar, D. Divan, and R. Adapa, "Control of parallel connected inverters in standalone ac supply systems," *Industry Applications, IEEE Transactions on*, vol. 29, no. 1, pp. 136–143, 1993.

[40] F. Katiraei and M. Iravani, "Power management strategies for a microgrid with multiple distributed generation units," *Power Systems, IEEE Transactions on*, vol. 21, no. 4, pp. 1821–1831, 2006.

[41] A. Tuladhar, K. Jin, T. Unger, and K. Mauch, "Parallel operation of single phase inverter modules with no control interconnections," in *Applied Power Electronics Conference and Exposition, 1997. APEC '97 Conference Proceedings 1997., Twelfth Annual*, vol. 1, pp. 94–100 vol.1, 1997.

[42] A. Tuladhar, H. Jin, T. Unger, and K. Mauch, "Control of parallel inverters in distributed ac power systems with consideration of line impedance effect," *Industry Applications, IEEE Transactions on*, vol. 36, no. 1, pp. 131–138, 2000.

[43] C. Sao and P. Lehn, "Autonomous load sharing of voltage source converters," *Power Delivery, IEEE Transactions on*, vol. 20, no. 2, pp. 1009–1016, 2005.

[44] C. Sao and P. Lehn, "Control and power management of converter fed microgrids," *Power Systems, IEEE Transactions on*, vol. 23, no. 3, pp. 1088–1098, 2008.

[45] E. Rokrok and M. Golshan, "Adaptive voltage droop scheme for voltage source converters in an islanded multibus microgrid," *IET Generation, Transmission and Distribution*, vol. 4, no. 5, p. 562, 2010.

[46] J. Vasquez, J. Guerrero, A. Luna, P. Rodriguez, and R. Teodorescu, "Adaptive droop control applied to voltage-source inverters operating in grid-connected and islanded modes," *Industrial Electronics, IEEE Transactions on*, vol. 56, no. 10, pp. 4088–4096, 2009.

[47] Y. Li and Y. W. Li, "Power management of inverter interfaced autonomous microgrid based on virtual frequency-voltage frame," *Smart Grid, IEEE Transactions on*, vol. 2, no. 1, pp. 30–40, 2011.

[48] U. Borup, F. Blaabjerg, and P. Enjeti, "Sharing of nonlinear load in parallel-connected three-phase converters," *Industry Applications, IEEE Transactions on*, vol. 37, no. 6, pp. 1817–1823, 2001.

[49] Q.-C. Zhong, "Harmonic droop controller to reduce the voltage harmonics of inverters," *Industrial Electronics, IEEE Transactions on*, vol. 60, no. 3, pp. 936–945, 2013.

[50] W. Yao, M. Chen, J. Matas, J. Guerrero, and Z. ming Qian, "Design and analysis of the droop control method for parallel inverters considering the impact of the complex impedance on the power sharing," *Industrial Electronics, IEEE Transactions on*, vol. 58, no. 2, pp. 576–588, 2011.

[51] M. Savaghebi, A. Jalilian, J. Vasquez, and J. Guerrero, "Autonomous voltage unbalance compensation in an islanded droop-controlled microgrid," *Industrial Electronics, IEEE Transactions on*, vol. 60, no. 4, pp. 1390–1402, 2013.

[52] J. Guerrero, J. Vasquez, J. Matas, L. de Vicuña, and M. Castilla, "Hierarchical control of droop-controlled ac and dc microgrids a general approach toward standardization," *Industrial Electronics, IEEE Transactions on*, vol. 58, no. 1, pp. 158–172, 2011.

[53] M. Savaghebi, A. Jalilian, J. Vasquez, and J. Guerrero, "Secondary control scheme for voltage unbalance compensation in an islanded droop-controlled microgrid," *Smart Grid, IEEE Transactions on*, vol. 3, no. 2, pp. 797–807, 2012.

[54] M. Savaghebi, A. Jalilian, J. Vasquez, and J. Guerrero, "Secondary control for voltage quality enhancement in microgrids," *Smart Grid, IEEE Transactions on*, vol. 3, no. 4, pp. 1893–1902, 2012.

[55] Q. Shafiee, J. Guerrero, and J. Vasquez, "Distributed secondary control for islanded microgrids - a novel approach," *Power Electronics, IEEE Transactions on*, vol. 29, no. 2, pp. 1018–1031, 2014.

[56] F. Dorfler, J. Simpson-Porco, and F. Bullo, "Breaking the hierarchy: Distributed control amp; economic optimality in microgrids," *IEEE Transactions on Control of Network Systems*, vol. PP, no. 99, pp. 1–1, 2015.

[57] T. Kawabata and S. Higashino, "Parallel operation of voltage source inverters," *Industry Applications, IEEE Transactions on*, vol. 24, no. 2, pp. 281–287, 1988.

[58] P. Dobrovolny, J. Woods, and P. Ziogas, "A phase-locked-loop synchronization scheme for parallel operation of modular power supplies," in *Power Electronics Specialists Conference, 1989. PESC '89 Record., 20th Annual IEEE*, pp. 861–869 vol.2, 1989.

[59] J.-F. Chen and C.-L. Chu, "Combination voltage-controlled and current-controlled pwm inverters for ups parallel operation," *Power Electronics, IEEE Transactions on*, vol. 10, no. 5, pp. 547–558, 1995.

[60] T.-F. Wu, Y.-K. Chen, and Y.-H. Huang, "3c strategy for inverters in parallel operation achieving an equal current distribution," *Industrial Electronics, IEEE Transactions on*, vol. 47, no. 2, pp. 273–281, 2000.

[61] W.-C. Lee, T.-K. Lee, S.-H. Lee, K.-H. Kim, D.-S. Hyun, and I.-Y. Suh, "A master and slave control strategy for parallel operation of three-phase ups systems with different ratings," in *Applied Power Electronics Conference and Exposition, 2004. APEC '04. Nineteenth Annual IEEE*, vol. 1, pp. 456–462 Vol.1, 2004.

[62] J. Guerrero, L. Hang, and J. Uceda, "Control of distributed uninterruptible power supply systems," *Industrial Electronics, IEEE Transactions on*, vol. 55, no. 8, pp. 2845–2859, 2008.

[63] C.-L. Chen, Y. Wang, J.-S. Lai, Y.-S. Lee, and D. Martin, "Design of parallel inverters for smooth mode transfer microgrid applications," *Power Electronics, IEEE Transactions on*, vol. 25, no. 1, pp. 6–15, 2010.

[64] R. Majumder, B. Chaudhuri, A. Ghosh, R. Majumder, G. Ledwich, and F. Zare, "Improvement of stability and load sharing in an autonomous microgrid using supplementary droop control loop," *Power Systems, IEEE Transactions on*, vol. 25, no. 2, pp. 796–808, 2010.

[65] Q. Shafiee, J. Vasquez, and J. Guerrero, "Distributed secondary control for islanded microgrids - a networked control systems approach," in *IECON 2012 - 38th Annual Conference on IEEE Industrial Electronics Society*, pp. 5637–5642, 2012.

[66] A. Bidram, A. Davoudi, F. Lewis, and J. Guerrero, "Distributed cooperative secondary control of microgrids using feedback linearization," *Power Systems, IEEE Transactions on*, vol. 28, no. 3, pp. 3462–3470, 2013.

[67] H. Bouattour, F. Dörfler, and F. Bullo, *Distributed Secondary Control in Microgrids*. Phd thesis, University of California, Santa Barbara, 2013.

[68] E. Barklund, N. Pogaku, M. Prodanovic, C. Hernandez-Aramburo, and T. Green, "Energy management in autonomous microgrid using stability-constrained droop control of inverters," *Power Electronics, IEEE Transactions on*, vol. 23, no. 5, pp. 2346–2352, 2008.

[69] A. Hawkes and M. Leach, "Modelling high level system design and unit commitment for a microgrid," *Applied Energy*, vol. 86, no. 78, pp. 1253 – 1265, 2009.

[70] A. Chaouachi, R. Kamel, R. Andoulsi, and K. Nagasaka, "Multiobjective intelligent energy management for a microgrid," *Industrial Electronics, IEEE Transactions on*, vol. 60, no. 4, pp. 1688–1699, 2013.

[71] A. Brooks, E. Lu, D. Reicher, C. Spirakis, and B. Weihl, "Demand dispatch," *Power and Energy Magazine, IEEE*, vol. 8, no. 3, pp. 20–29, 2010.

[72] R. Zamora and A. K. Srivastava, "Controls for microgrids with storage: Review, challenges, and research needs," *Renewable and Sustainable Energy Reviews*, vol. 14, no. 7, pp. 2009 – 2018, 2010.

[73] F. Katiraei, R. Iravani, N. Hatziargyriou, and A. Dimeas, "Microgrids management," *Power and Energy Magazine, IEEE*, vol. 6, no. 3, pp. 54–65, 2008.

[74] C. Colson and M. Nehrir, "A review of challenges to real-time power management of microgrids," in *Power Energy Society General Meeting, 2009. PES '09. IEEE*, pp. 1–8, 2009.

[75] A. Tsikalakis and N. Hatziargyriou, "Centralized control for optimizing microgrids operation," in *Power and Energy Society General Meeting, 2011 IEEE*, pp. 1–8, 2011.

[76] M. Shahidehpour, M. Khodayar, and M. Barati, "Campus microgrid: High reliability for active distribution systems," in *Power and Energy Society General Meeting, 2012 IEEE*, pp. 1–2, 2012.

[77] M. Shahidehpour and M. Khodayar, "Cutting campus energy costs with hierarchical control: The economical and reliable operation of a microgrid," *Electrification Magazine, IEEE*, vol. 1, no. 1, pp. 40–56, 2013.

[78] NERC, "Reliability standards for the bulk electric systems of north america," tech. rep., North American Electric Reliability Corporation, November 2009.

[79] L. S. Vargas, F. A. Larrain, and H. Verdejo, "Operating reserves assessment in isolated power systems with high wind power penetration," in *Probabilistic Methods Applied to Power Systems (PMAPS), 2014 International Conference on*, pp. 1–6, July 2014.

[80] J. P. Lopes, S. A. Polenz, C. Moreira, and R. Cherkaoui, "Identification of control and management strategies for lv unbalanced microgrids with plugged-in electric vehicles," *Electric Power Systems Research*, vol. 80, no. 8, pp. 898 – 906, 2010.

[81] N. Hatziargyriou, ed., *Microgrids: Architectures and Control.* Wiley-IEEE Press, 1 ed., 3 2014.

[82] M. Nehrir, C. Wang, K. Strunz, H. Aki, R. Ramakumar, J. Bing, Z. Miao, and Z. Salameh, "A review of hybrid renewable/alternative energy systems for electric power generation: Configurations, control, and applications," *Sustainable Energy, IEEE Transactions on*, vol. 2, pp. 392–403, Oct 2011.

[83] S. Khan, W. Gawlik, and P. Palensky, "Reserve capability assessment considering correlated uncertainty in microgrid," *IEEE Transactions on Sustainable Energy*, vol. 7, pp. 637–646, April 2016.

[84] M. Aien, A. Hajebrahimi, and M. Fotuhi-Firuzabad, "A comprehensive review on uncertainty modeling techniques in power system studies," *Renewable and Sustainable Energy Reviews*, vol. 57, pp. 1077 – 1089, 2016.

[85] J. A. Taylor and J. L. Mathieu, *Uncertainty in Demand Response - Identification, Estimation, and Learning.* 2015.

[86] F. Alvarado, Y. Hu, and R. Adapa, "Uncertainty in power system modeling and computation," in *Systems, Man and Cybernetics, 1992., IEEE International Conference on*, pp. 754–760 vol.1, Oct 1992.

[87] M. Aien, M. Rashidinejad, and M. Fotuhi-Firuzabad, "On possibilistic and probabilistic uncertainty assessment of power flow problem: A review and a new approach," *Renewable and Sustainable Energy Reviews*, vol. 37, pp. 883 – 895, 2014.

[88] A. Douglas, A. Breipohl, F. Lee, and R. Adapa, "Risk due to load forecast uncertainty in short term power system planning," *Power Systems, IEEE Transactions on*, vol. 13, pp. 1493–1499, Nov 1998.

[89] G. Li, P. Zhang, P. Luh, W. Li, Z. Bie, C. Serna, and Z. Zhao, "Risk analysis for distribution systems in the northeast u.s. under wind storms," *Power Systems, IEEE Transactions on*, vol. 29, pp. 889–898, March 2014.

[90] G. J. Anders, *Probability concepts in electric power systems.* New York, NY; John Wiley and Sons Inc., 1989.

[91] A. Schellenberg, W. Rosehart, and J. Aguado, "Cumulant-based probabilistic optimal power flow (p-opf) with gaussian and gamma distributions," *Power Systems, IEEE Transactions on*, vol. 20, pp. 773–781, May 2005.

[92] L. Zadeh, "Fuzzy sets as a basis for a theory of possibility," *Fuzzy Sets and Systems*, vol. 100, Supplement 1, pp. 9 – 34, 1999.

[93] I. Ramirez-Rosado and J. Dominguez-Navarro, "Possibilistic model based on fuzzy sets for the multiobjective optimal planning of electric power distribution networks," *Power Systems, IEEE Transactions on*, vol. 19, pp. 1801–1810, Nov 2004.

[94] A. Soroudi, M. Ehsan, R. Caire, and N. Hadjsaid, "Possibilistic evaluation of distributed generations impacts on distribution networks," *Power Systems, IEEE Transactions on*, vol. 26, pp. 2293–2301, Nov 2011.

[95] A. Soroudi and M. Ehsan, "Igdt based robust decision making tool for dnos in load procurement under severe uncertainty," *Smart Grid, IEEE Transactions on*, vol. 4, pp. 886–895, June 2013.

[96] A. Rabiee, A. Soroudi, and A. Keane, "Information gap decision theory based opf with hvdc connected wind farms," *Power Systems, IEEE Transactions on*, vol. 30, pp. 3396–3406, Nov 2015.

[97] A. Chaturvedi, K. Prasad, and R. Ranjan, "Use of interval arithmetic to incorporate the uncertainty of load demand for radial distribution system analysis," *Power Delivery, IEEE Transactions on*, vol. 21, pp. 1019–1021, April 2006.

[98] D. Bertsimas, E. Litvinov, X. Sun, J. Zhao, and T. Zheng, "Adaptive robust optimization for the security constrained unit commitment problem," *Power Systems, IEEE Transactions on*, vol. 28, pp. 52–63, Feb 2013.

[99] A. Lorca and X. Sun, "Adaptive robust optimization with dynamic uncertainty sets for multi-period economic dispatch under significant wind," *Power Systems, IEEE Transactions on*, vol. 30, pp. 1702–1713, July 2015.

[100] H. Saadat, *Power System Analysis*. McGraw-Hill Higher Education, 2010.

[101] B. Borkowska, "Probabilistic load flow," *IEEE Transactions on Power Apparatus and Systems*, vol. 93, no. 3, pp. 752–759, 1974.

[102] J. Zhu, *Optimization of power system operation*, vol. 47. John Wiley & Sons, 2015.

[103] M. P. Nowak and W. Römisch, "Stochastic lagrangian relaxation applied to power scheduling in a hydro-thermal system under uncertainty," *Annals of Operations Research*, vol. 100, no. 1, pp. 251–272, 2000.

[104] L. Wang and C. Singh, "Balancing risk and cost in fuzzy economic dispatch including wind power penetration based on particle swarm optimization," *Electric Power Systems Research*, vol. 78, no. 8, pp. 1361 – 1368, 2008.

[105] K. Abdul-Rahman, S. Shahidehpour, and M. Daneshdoost, "Ai approach to optimal var control with fuzzy reactive loads," *Power Systems, IEEE Transactions on*, vol. 10, pp. 88–97, Feb 1995.

[106] B. Ummels, M. Gibescu, E. Pelgrum, W. Kling, and A. Brand, "Impacts of wind power on thermal generation unit commitment and dispatch," *Energy Conversion, IEEE Transactions on*, vol. 22, pp. 44–51, March 2007.

[107] J. Wang, M. Shahidehpour, and Z. Li, "Security-constrained unit commitment with volatile wind power generation," *Power Systems, IEEE Transactions on*, vol. 23, pp. 1319–1327, Aug 2008.

[108] D. Bertsimas, E. Litvinov, X. A. Sun, J. Zhao, and T. Zheng, "Adaptive robust optimization for the security constrained unit commitment problem," *Power Systems, IEEE Transactions on*, vol. 28, no. 1, pp. 52–63, 2013.

[109] X. Chen, M. Sim, and P. Sun, "A robust optimization perspective on stochastic programming," *Operations Research*, vol. 55, no. 6, pp. 1058–1071, 2007.

[110] M. Vrakopoulou, S. Chatzivasileiadis, E. Iggland, M. Imhof, T. Krause, O. Makela, J. L. Mathieu, L. Roald, R. Wiget, and G. Andersson, "A unified analysis of security-constrained opf formulations considering uncertainty, risk, and controllability in single and multi-area systems," in *Bulk Power System Dynamics and Control-IX Optimization, Security and Control of the Emerging Power Grid (IREP), 2013 IREP Symposium*, pp. 1–19, IEEE, 2013.

[111] C. Bandi and D. Bertsimas, "Tractable stochastic analysis in high dimensions via robust optimization," *Mathematical programming*, vol. 134, no. 1, pp. 23–70, 2012.

[112] R. Zorgati and W. van Ackooij, "Optimizing financial and physical assets with chance-constrained programming in the electrical industry," *Optimization and Engineering*, vol. 12, no. 1-2, pp. 237–255, 2011.

[113] W. Van Ackooij, R. Henrion, A. Möller, and R. Zorgati, "Joint chance constrained programming for hydro reservoir management," *Optimization and Engineering*, pp. 1–23, 2012.

[114] M. Milligan, P. Donohoo, D. Lew, E. Ela, B. Kirby, H. Holttinen, E. Lannoye, D. Flynn, M. O Malley, N. Miller, *et al.*, "Operating reserves and wind power integration: an international comparison," in *Proc. 9th International Workshop on large-scale integration of wind power into power systems*, pp. 18–29, 2010.

[115] Y. Rebours, D. Kirschen, M. Trotignon, and S. Rossignol, "A survey of frequency and voltage control ancillary services mdash;part ii: Economic features," *Power Systems, IEEE Transactions on*, vol. 22, pp. 358–366, Feb 2007.

[116] K. Margellos, P. Goulart, and J. Lygeros, "On the road between robust optimization and the scenario approach for chance constrained optimization problems," *Automatic Control, IEEE Transactions on*, vol. 59, pp. 2258–2263, Aug 2014.

[117] G. Papaefthymiou and B. Klockl, "Mcmc for wind power simulation," *Energy Conversion, IEEE Transactions on*, vol. 23, pp. 234–240, March 2008.

[118] M. Bucher, S. Chatzivasileiadis, and G. Andersson, "Managing flexibility in multi-area power systems," *Power Systems, IEEE Transactions on*, vol. PP, no. 99, pp. 1–9, 2015.

[119] W. Wei, F. Liu, and S. Mei, "Real-time dispatchability of bulk power systems with volatile renewable generations," *Sustainable Energy, IEEE Transactions on*, vol. 6, pp. 738–747, July 2015.

[120] D. Barr, "The use of a data historian to extend plant life," *IET Conference Proceedings*, pp. 35–39(4), January 1994.

[121] F. Chernousko, "What is Ellipsoidal Modelling and How to Use It for Control and State Estimation?," in *Whys and Hows in Uncertainty Modelling* (I. Elishakoff, ed.), vol. 388 of *CISM Courses and Lectures*, pp. 127–188, Springer Vienna, 1999.

[122] G. M. Ziegler, *Lectures on polytopes*, vol. 152. Springer, 1995.

[123] K. Strunz *et al.*, "Benchmark systems for network integration of renewable and distributed energy resources," *Preliminary version, Cigre Task Force C*, vol. 6, 2009.

[124] D. Olivares, C. Canizares, and M. Kazerani, "A centralized energy management system for isolated microgrids," *Smart Grid, IEEE Transactions on*, vol. 5, pp. 1864–1875, July 2014.

[125] K. Skaloumpakas, "Response of low voltage networks with high photovoltaic systems penetration to transmission network faults," Master's thesis, Intelligent Electrical Power Grids, Delft University of Technology, Delft, The Netherlands, 2014.

[126] TenneT-TSO, "Network data for 2013 and 2014." http://www.tennettso.de archived at http://dx.doi.org/10.13140/RG.2.1.2973.5281, 2015.

[127] 50-Hertz, "Forecast data of control area load for 2013 and 2014." http://www.50hertz.com archived at http://dx.doi.org/10.13140/RG.2.1.3170.1366, 2015.

[128] A. M.Annaswamy and M. Amin, "Ieee vision for smart grid controls: 2030 and beyond," *IEEE Vision for Smart Grid Controls: 2030 and Beyond*, pp. 1–168, June 2013.

[129] C. I. S. Operator, "Demand response and energy efficiency roadmap: Maximizing preferred resources caiso," tech. rep., CAISO, Folsom, CA, USA, Dec. 2013.

[130] B. Sanandaji, T. Vincent, and K. Poolla, "Ramping rate flexibility of residential hvac loads," *Sustainable Energy, IEEE Transactions on*, vol. PP, no. 99, pp. 1–10, 2015.

[131] S. Khan, M. Shahzad, U. Habib, W. Gawlik, and P. Palensky, "Stochastic battery model for aggregation of thermostatically controlled loads," in *2016 IEEE International Conference on Industrial Technology (ICIT)*, pp. 570–575, March 2016.

[132] E. Valsomatzis, K. Hose, T. Pedersen, and L. Siksnys, "Measuring and comparing energy flexibilities," *CEUR Workshop Proceedings*, vol. 1330, pp. 78–85, 2015.

[133] A. Ulbig and G. Andersson, "Analyzing operational flexibility of electric power systems," *International Journal of Electrical Power & Energy Systems*, vol. 72, pp. 155 – 164, 2015. The Special Issue for 18th Power Systems Computation Conference.

[134] IEA, "Distributed generation in liberalised electricity markets," 2002.

[135] J. K. Delson, "Thermal stress computation for steam-electric generator dispatch," *Power Systems, IEEE Transactions on*, vol. 9, pp. 120–127, Feb 1994.

[136] Z. Li and M. Shahidehpour, "Generation scheduling with thermal stress constraints," *Power Systems, IEEE Transactions on*, vol. 18, pp. 1402–1409, Nov 2003.

[137] D. Nikolic, M. Negnevitsky, and M. de Groot, "Effect of the diesel engine delay on stability of isolated power systems with high levels of renewable energy penetration," in *Smart Electric Distribution Systems and Technologies (EDST), 2015 International Symposium on*, pp. 70–73, Sept 2015.

[138] A. Subramanian, M. Garcia, A. Dominguez-Garcia, D. Callaway, K. Poolla, and P. Varaiya, "Real-time scheduling of deferrable electric loads," in *American Control Conference (ACC), 2012*, pp. 3643–3650, June 2012.

[139] M. Rahmani-andebili, "Modeling nonlinear incentive-based and price-based demand response programs and implementing on real power markets," *Electric Power Systems Research*, vol. 132, pp. 115 – 124, 2016.

[140] J. L. Mathieu, *Modeling, Analysis, and Control of Demand Response Resources.* PhD thesis, University of California, Berkeley, 2012.

[141] N. Lu and D. Chassin, "A state-queueing model of thermostatically controlled appliances," *Power Systems, IEEE Transactions on*, vol. 19, pp. 1666–1673, Aug 2004.

[142] S. Koch, J. L. Mathieu, and D. S. Callaway, "Modeling and control of aggregated heterogeneous thermostatically controlled loads for ancillary services," in *Proc. PSCC*, pp. 1–7, 2011.

[143] H. Hao, B. Sanandaji, K. Poolla, and T. Vincent, "Frequency regulation from flexible loads: Potential, economics, and implementation," in *American Control Conference (ACC), 2014*, pp. 65–72, June 2014.

[144] J. Mathieu, M. Kamgarpour, J. Lygeros, and D. Callaway, "Energy arbitrage with thermostatically controlled loads," in *Control Conference (ECC), 2013 European*, pp. 2519–2526, July 2013.

[145] N. Lu, D. Chassin, and S. Widergren, "Modeling uncertainties in aggregated thermostatically controlled loads using a state queueing model," *Power Systems, IEEE Transactions on*, vol. 20, pp. 725–733, May 2005.

[146] V. Trovato, S. H. Tindemans, and G. Strbac, "Leaky storage model for optimal multi-service allocation of thermostatic loads," *IET Generation, Transmission & Distribution*, October 2015.

[147] S. Li, W. Zhang, J. Lian, and K. Kalsi, "Market-based coordination of thermostatically controlled loads –part i: A mechanism design formulation," *Power Systems, IEEE Transactions on*, vol. PP, no. 99, pp. 1–9, 2015.

[148] A. Jahromi and F. Bouffard, "Contingency-type reserve leveraged through aggregated thermostatically-controlled loads –part ii: Case studies," *Power Systems, IEEE Transactions on*, vol. PP, no. 99, pp. 1–9, 2015.

[149] H. Hao, B. Sanandaji, K. Poolla, and T. Vincent, "Aggregate flexibility of thermostatically controlled loads," *Power Systems, IEEE Transactions on*, vol. 30, pp. 189–198, Jan 2015.

[150] S. Ihara and F. Schweppe, "Physically based modeling of cold load pickup," *Power Apparatus and Systems, IEEE Transactions on*, vol. PAS-100, pp. 4142–4150, Sept 1981.

[151] R. Mortensen and K. Haggerty, "Dynamics of heating and cooling loads: models, simulation, and actual utility data," *Power Systems, IEEE Transactions on*, vol. 5, pp. 243–249, Feb 1990.

[152] S. Khan, H. Bosetti, P. Palensky, and W. Gawlik, "A replicator dynamics method for the unit commitment problem," in *Modeling and Simulation of Cyber-Physical Energy Systems (MSCPES), 2014 Workshop on*, pp. 1–4, April 2014.

[153] H. Bosetti, S. Khan, H. Aghaie, and P. Palensky, "Survey, illustrations and limits of game theory for cyber-physical energy systems," *at-Automatisierungstechnik*, vol. 62, no. 5, pp. 375–384, 2014.

[154] J. P. Pfeifenberger, K. Spees, K. Carden, and N. Wintermantel, "Resource adequacy requirements: Reliability and economic implications," *The Brattle Group*, 2013.

[155] E. Ibanez and M. Milligan, "Impact of transmission on resource adequacy in systems with wind and solar power," in *Power and Energy Society General Meeting, 2012 IEEE*, pp. 1–5, July 2012.

[156] J. Adams, M. O'Malley, K. Hanson, *et al.*, "Flexibility requirements and potential metrics for variable generation: Implications for system planning studies," tech. rep., NERC, 2010.

[157] A. Keane, M. Milligan, C. Dent, B. Hasche, C. D'Annunzio, K. Dragoon, H. Holttinen, N. Samaan, L. Soder, and M. O'Malley, "Capacity value of wind power," *Power Systems, IEEE Transactions on*, vol. 26, pp. 564–572, May 2011.

[158] R. Duignan, C. Dent, A. Mills, N. Samaan, M. Milligan, A. Keane, and M. O'Malley, "Capacity value of solar power," in *Power and Energy Society General Meeting, 2012 IEEE*, pp. 1–6, July 2012.

[159] T. Vandoorn, J. Vasquez, J. De Kooning, J. Guerrero, and L. Vandevelde, "Microgrids: Hierarchical control and an overview of the control and reserve management strategies," *Industrial Electronics Magazine, IEEE*, vol. 7, pp. 42–55, Dec 2013.

[160] A. Zakariazadeh, S. Jadid, and P. Siano, "Smart microgrid energy and reserve scheduling with demand response using stochastic optimization," *International Journal of Electrical Power & Energy Systems*, vol. 63, pp. 523 – 533, 2014.

[161] X. Yan, B. Francois, and D. Abbes, "Operating power reserve quantification through pv generation uncertainty analysis of a microgrid," in *PowerTech, 2015 IEEE Eindhoven*, pp. 1–6, 2015.

[162] A. Hoke, R. Butler, J. Hambrick, and B. Kroposki, "Steady-state analysis of maximum photovoltaic penetration levels on typical distribution feeders," *IEEE Transactions on Sustainable Energy*, vol. 4, pp. 350–357, April 2013.

[163] J. Contreras, O. Candiles, J. I. de la Fuente, and T. Gomez, "Auction design in day-ahead electricity markets," *Power Engineering Review, IEEE*, vol. 21, pp. 54–55, Feb 2001.

[164] J. Alonso, A. Trias, V. Gaitan, and J. Alba, "Thermal plant bids and market clearing in an electricity pool. minimization of costs vs. minimization of consumer payments," *Power Systems, IEEE Transactions on*, vol. 14, pp. 1327–1334, Nov 1999.

[165] M. De Berg, M. Van Kreveld, M. Overmars, and O. C. Schwarzkopf, *Computational geometry.* Springer, 2000.

[166] S. Frank, I. Steponavice, and S. Rebennack, "Optimal power flow: a bibliographic survey i," *Energy Systems*, vol. 3, no. 3, pp. 221–258, 2012.

[167] M. Vrakopoulou, K. Margellos, J. Lygeros, and G. Andersson, "A probabilistic framework for reserve scheduling and n-1 security assessment of systems with high wind power penetration," *Power Systems, IEEE Transactions on*, vol. 28, pp. 3885–3896, Nov 2013.

[168] N. Padhy, "Unit commitment-a bibliographical survey," *Power Systems, IEEE Transactions on*, vol. 19, no. 2, pp. 1196–1205, 2004.

[169] U. A. Oztürk, *The stochastic unit commitment problem: a chance constrained programming approach considering extreme multivariate tail probabilities.* PhD thesis, University of Pittsburgh, 2003.

[170] B. Lu and M. Shahidehpour, "Unit commitment with flexible generating units," *IEEE Transactions on Power Systems*, vol. 20, pp. 1022–1034, May 2005.

[171] P. M. Anderson and A. A. Fouad, *Power system control and stability.* John Wiley & Sons, 2008.

[172] R. D. Zimmerman, C. E. Murillo-Sánchez, and R. J. Thomas, "Matpower: Steady-state operations, planning, and analysis tools for power systems research and education," *Power Systems, IEEE Transactions on*, vol. 26, no. 1, pp. 12–19, 2011.

[173] X. Xia and A. Elaiw, "Optimal dynamic economic dispatch of generation: a review," *Electric Power Systems Research*, vol. 80, no. 8, pp. 975–986, 2010.

[174] A. Pantoja and N. Quijano, "A population dynamics approach for the dispatch of distributed generators," *Industrial Electronics, IEEE Transactions on*, vol. 58, no. 10, pp. 4559–4567, 2011.

[175] K. Sigmund, *The calculus of selfishness.* Princeton University Press, 2010.

[176] J. Hofbauer and K. Sigmund, "Evolutionary game dynamics," *Bulletin of the American Mathematical Society*, vol. 40, pp. 479–520, Oct 2003.

[177] D. Sun, B. Ashley, B. Brewer, A. Hughes, and W. F. Tinney, "Optimal power flow by newton approach," *Power Apparatus and Systems, IEEE Transactions on*, vol. PAS-103, no. 10, pp. 2864–2880, 1984.

[178] S. Frank, I. Steponavice, and S. Rebennack, "Optimal power flow: a bibliographic survey i," *Energy Systems*, vol. 3, no. 3, pp. 221–258, 2012.

[179] S. Kazarlis, A. Bakirtzis, and V. Petridis, "A genetic algorithm solution to the unit commitment problem," *Power Systems, IEEE Transactions on*, vol. 11, no. 1, pp. 83–92, 1996.

[180] S. P. Karthikeyan, I. J. Raglend, and D. P. Kothari, "A review on market power in deregulated electricity market," *International Journal of Electrical Power & Energy Systems*, vol. 48, pp. 139–147, 2013.

[181] L. Pérez-Lombard, J. Ortiz, and C. Pout, "A review on buildings energy consumption information," *Energy and buildings*, vol. 40, no. 3, pp. 394–398, 2008.

[182] A. Latif, S. Khan, U. Habib, W. Gawlik and P. Palensky, "Co-simulation based platform for thermostatically controlled loads as a frequency reserve." Accepted in IEEE workshop on Modeling and Simulation of Cyber-Physical Energy Systems (MSCPES), January 2016.

[183] G. Maitre, G. Basso, C. Steiner, D. Gabioud, and P. Roduit, "Distributed grid storage by ordinary house heating variations: A swiss case study," in *Digital System Design (DSD), 2015 Euromicro Conference on*, pp. 241–249, Aug 2015.

[184] M. Liu, Y. Shi, and X. Liu, "Distributed mpc of aggregated heterogeneous thermostatically controlled loads in smart grid," 2016.

[185] S. Esmaeil Zadeh Soudjani and A. Abate, "Aggregation and control of populations of thermostatically controlled loads by formal abstractions," *Control Systems Technology, IEEE Transactions on*, vol. 23, no. 3, pp. 975–990, 2015.

[186] S. Koch, M. Zima, and G. Andersson, "Active coordination of thermal household appliances for load management purposes," in *IFAC Symposium on Power Plants and Power Systems Control*, Citeseer, 2009.

[187] Molina, A., Gabaldón, A., Fuentes and J.A., Álvarez, "Implementation and assessment of physically based electrical load models: application to direct load control residential programmes," *IEE Proceedings - Generation, Transmission and Distribution*, vol. 150, pp. 61–66(5), January 2003.

[188] S. Bashash and H. Fathy, "Modeling and control of aggregate air conditioning loads for robust renewable power management," *Control Systems Technology, IEEE Transactions on*, vol. 21, pp. 1318–1327, July 2013.

[189] W. Zhang, J. Lian, C.-Y. Chang, and K. Kalsi, "Aggregated modeling and control of air conditioning loads for demand response," *Power Systems, IEEE Transactions on*, vol. 28, pp. 4655–4664, Nov 2013.

[190] K. Schneider, J. Fuller, and D. Chassin, "Multi-state load models for distribution system analysis," *Power Systems, IEEE Transactions on*, vol. 26, pp. 2425–2433, Nov 2011.

[191] S. Kundu, N. Sinitsyn, S. Backhaus, and I. Hiskens, "Modeling and control of thermostatically controlled loads," *arXiv preprint arXiv:1101.2157*, 2011.

[192] S. E. Z. Soudjani and A. Abate, "Aggregation of thermostatically controlled loads by formal abstractions," in *European Control Conference, Zurich, Switzerland*, 2013.

[193] D. S. Callaway, "Tapping the energy storage potential in electric loads to deliver load following and regulation, with application to wind energy," *Energy Conversion and Management*, vol. 50, no. 5, pp. 1389 – 1400, 2009.

[194] PJM, "RTO Regulation Signal Data." http://www.pjm.com archived at http://dx.doi.org/10.13140/RG.2.1.4218.7122.

[195] S. Ghasemi and J. Moshtagh, "Radial distribution systems reconfiguration considering power losses cost and damage cost due to power supply interruption of consumers," *International Journal on Electrical Engineering and Informatics*, vol. 5, no. 3, p. 297, 2013.

[196] A. Latif, M. Shahzad, P. Palensky, and W. Gawlik, "An alternate powerfactory matlab coupling approach," in *Smart Electric Distribution Systems and Technologies (EDST), 2015 International Symposium on*, pp. 486–491, IEEE, 2015.

[197] P. E. Sørensen, A. D. Hansen, P. Christensen, M. Mieritz, J. Bech, B. Bak-Jensen, and H. Nielsen, *Simulation and verification of transient events in large wind power installations.* 2003.

[198] J. Solanki, N. Venkatesan, and S. K. Solanki, "Market optimization for microgrid with demand response model," in *North American Power Symposium (NAPS), 2011*, pp. 1–6, Aug 2011.

[199] S. Boyd and L. Vandenberghe, *Convex optimization.* Cambridge university press, 2009.

[200] S. Low, "Convex relaxation of optimal power flow: A tutorial," in *Bulk Power System Dynamics and Control - IX Optimization, Security and Control of the Emerging Power Grid (IREP), 2013 IREP Symposium*, pp. 1–15, Aug 2013.

List of Symbols

sign	description	unit
a_i	Linear cost coefficients of generator i	—
b_i	Quadratic cost coefficients of generator i	—
B_{ab}	Susceptance of line between bus a and b	[μS]
$(1-\beta)$	Confidence in the probabilistic result	—
e_k^{max}	Bus maximum voltage level	[V]
e_k^{min}	Bus minimum voltage level	[V]
c_i	Generator i cost factor for Replicator Dynamics algorithm	—
C_F	Generator fuel cost	[$]
C_{OD}	Resource (e.g., generator) over-drive cost	[$]
C_{Rd}	Cost of down-spinning reserve	[$]
C_{Ru}	Cost of up-spinning reserve	[$]
C_{SU}	Resource (e.g., generator) start-up cost	[$]
C_T	Total operating cost	[$]
Δ	Demand envelope	—
Δ_i	Generator flexibility envelope	—
ΔP^t	Lumped uncertainty in microgrid during t^{th} hour	—
ΔP_{symb}^t	Uncertainty in the demand, wind and PV power for symb=D,w,PV during t^{th} hour	—
$\overline{\delta_u}$	Maximum value of uncertain variable u	—
$\underline{\delta_u}$	Minimum value of uncertain variable u	—
$d_{down,t}^c$	Distribution vector for down-spinning reserves for c^{th} contingency	—
$d_{up,t}^c$	Distribution vector for up-spinning reserves for c^{th} contingency	—
$X_i^{off}(t)$	Duration since state of generator i has been Off	[h]
$X_i^{on}(t)$	Duration since state of generator i has been On	[h]
e_i	Real value of i^{th} bus voltage	—
f_i	Imaginary value of i^{th} bus voltage	—
$(1-\epsilon)$	Probability of the constraint satisfaction	—
$\epsilon_{\Delta P}$	Minimum ramp-rate tolerance	[MW/h]

sign	**description**	**unit**
F	Number of forecast clusters	—
G_{ab}	Conductance of line between bus a and b	[μS]
T_i^{off}	Minimum Off time of generator i	[h]
T_i^{on}	Minimum On time of generator i	[h]
H_i	High thermal stress limit of generator i	[°F]
H_i^j	Half-space coefficients of $S_j(\Delta_i)$	—
k_i	Temperature power slope of generator i	[°F/kW]
L_f	Probabilistic limits on the f^{th} forecast cluster	—
L_i	Low thermal stress limit of generator i	[°F]
N_B	Number of buses	—
N_L	Number of transmission lines	—
$\mathbf{G}$	Network conductance matrix	—
$\mathbf{B}$	Network susceptance matrix	—
N	Number of generators	—
P_{Da}	Real power demand at bus a	[MW]
P_i^t	Active power of i^{th} generator at time t	—
$\overline{P_{L_{ab}}}$	Maximum active power capacity of line ab	[MW]
$\underline{P_{L_{ab}}}$	Minimum active power capacity of line ab	[MW]
P_{loss}	Transmission loss	[MW]
$\overline{P_i}$	Maximum active power rating of i^{th} generator	[MW]
$\underline{P_i}$	Minimum active power rating of i^{th} generator i	[MW]
P_i^j	Active power of i^{th} generator against j^{th} demand	[MW]
P_i^d	The d^{th} power of generator i	[MW]
Q_{Da}	Reactive power demand at bus a	[Mvar]
Q_i^t	Reactive power of i^{th} generator at time t	[Mvar]
$\overline{Q_i}$	Maximum reactive power rating of i^{th} generator	[Mvar]
$\underline{Q_i}$	Minimum reactive power rating of i^{th} generator	[Mvar]
R	Number of reactive power sources	—
$R_{i,n}^-$	The n^{th} ramp-down rate of generator i	[MW/h]
$\overline{R_-}$	Maximum ramp-down rate of generator i	[MW/h]
R_-	Ramp-down rate limit of the stochastic battery model	[MW/h]
$R_{i,m}^+$	The m^{th} ramp-up rate of generator i	[MW/h]
$\overline{R_i^+}$	Maximum ramp-up rate of i^{th} generator	[MW/h]
R_+	Ramp-up rate limit of the stochastic battery model	[MW/h]
SR_i^t	Contribution of i^{th} generator to the spinning reserve	[MW]
$\mathrm{SR}_{\mathrm{up}}^t$	Up spinning reserve requirement at time t	[MW]
$\mathrm{SR}_{\mathrm{down}}^t$	Down spinning reserve requirement at time t	[MW]
ρ_i^t	Status (On/Off) of generator i at time t	—
S_{symb}	Set of all the buses, generator buses and transmission lines for symb=B,G,L in the network	—
$S_j(\Delta)$	The j^{th} uncertainty sub-polytope of polytope Δ	—
S_i^t	Thermal stress state of generator i	—
S	Number of Monte Carlo scenarios	
τ_i	Thermal time constant of generator i	[min]
T	Number of time intervals	—

sign	description	unit
S_f^m	Apparent power flow 'from' end of a transmission line m	[kVA]
S_t^m	Apparent power flow 'to' end of a transmission line m	[kVA]
S_m^{max}	Maximum apparent power flow rating of a transmission line m	[kVA]
u_δ	Number of uncertain variables	—
V_j	Number of vertices of the j^{th} sub-polytope	—
V_j	Number of vertices of j^{th} sub-polytope	—
w	Duration of ramp	[min]
x_j	The j^{th} demand value in microgrid	[MW]

Definitions

Net-demand	The difference between total demand and total power generation from renewables
Over-drive	Operating a resource beyond its ratings
Spatial	Variation in the value of a variable as its state
Spatio-temporal	Variation in the value of a variable considering both its state and evolution with time
Temporal	Variation in the value of a variable as function of time

Curriculum Vitae

Personal Information

Name: Sohail KHAN
Date and Place of Birth: February 24th, 1986, Haripur, Pakistan
Nationality: Pakistani
Email: sohail.khan@gmx.net

Education

Since 2013	Doctoral student at Faculty of Electrical Engineering and Information Technology, Technische Universität Wien, Vienna, Austria, supervised by Prof. Wolfgang Gawlik.
2008 – 2010	M.S. Electrical Engineering at National University of Sciences and Technology, Islamabad, Pakistan.
2004 – 2008	B.S. Electronics Engineering at COMSATS Institute of Information Technology, Abbottabad, Pakistan.

Professional History

Since 2013	PhD Student at Complex Energy Systems, Energy Department, Austrian Institute of Technology GmbH, Vienna, Austria.
2012 – 2013	Lecturer at Department of Electrical Engineering, COMSATS Institute of Information Technology , Islamabad, Pakistan.
2010 – 2012	Lecturer at Department of Electrical Engineering, Heavy Industries Taxila Education City , Taxila, Pakistan.
2009 – 2010	Teaching Assistant at Department of Electrical Engineering, College of Electrical and Mechanical Engineering, National University of Sciences and Technology, Pakistan.
2008	Junior Engineer at Nautical Group, Islamabad, Pakistan.

Journal Articles

- S. Khan, W. Gawlik, and P. Palensky, "Reserve Capability Assessment Considering Correlated Uncertainty in Microgrid," *Sustainable Energy, IEEE Transactions on*, vol. 7, no. 2, pp. 637-646, April 2016.
- H. Bosetti, S. Khan, H. Aghaie, and P. Palensky, "Survey, Illustrations and Limits of Game Theory for Cyber-Physical Energy Systems," *at-Automatisierungstechnik*, 62.5, 375-384, 2014.

Proceedings

- S. Khan, M. Shahzad, P. Palensky, K. Jahangir, "Dynamics of wind-turbine driven Self-Excited Induction Generator with online parameter calculation," in *39th Annual Conference of the Industrial Electronics Society, IEEE, IECON 2013*, vol., no., pp.5271-5275, 10-13 Nov. 2013.
- S. Khan, H. Bosetti, P. Palensky, and W. Gawlik, "A Replicator Dynamics method for the Unit Commitment problem," in *Workshop on Modeling and Simulation of Cyber-Physical Energy Systems (MSCPES), Berlin*, pp. 1-4, 2014.
- S. Khan, M. Shahzad, U. Habib, W. Gawlik and P. Palensky, "Stochastic battery model for aggregation of thermostatically controlled loads," IEEE International Conference on Industrial Technology (ICIT), Taipei, Taiwan, pp. 570-575, 2016.
- A. Latif, S. Khan, U. Habib, W. Gawlik, and P. Palensky, "Co-simulation Based Platform for Thermostatically Controlled Loads as a Frequency Reserve," in *IEEE workshop on Modeling and Simulation of Cyber-Physical Energy Systems (MSCPES)*, 2016.

Monograph

S. Khan, "Nonlinear Adaptive Flight Control System for Unmanned Aerial Vehicle: A Nonlinear Dynamic Inversion Based Approach", LAP LAMBERT Academic Publishing, 2011.